AD_____

Award Number: DAMD17-03-1-0222

TITLE: Detection of Serum Lysophosphatidic Acids using Affinity Binding and Surface Enhanced Laser Deorption/Ionization (SELDI) Time of Flight Mass Spectrometry

PRINCIPAL INVESTIGATOR: Gordan B. Mills, M.D., Ph.D.

CONTRACTING ORGANIZATION: University of Texas M.D. Anderson Cancer Center
Houston, TX 77030

REPORT DATE: April 2006

TYPE OF REPORT: Final

PREPARED FOR: U.S. Army Medical Research and Materiel Command
Fort Detrick, Maryland 21702-5012

REPORT DOCUMENTATION PAGE

Form Approved
OMB No. 0704-0188

1. REPORT DATE *(DD-MM-YYYY)*	2. REPORT TYPE	3. DATES COVERED *(From - To)*
01-04-2006	Final	1 APR 2003 - 31 MAR 2006

4. TITLE AND SUBTITLE
Detection of Serum Lysophosphatidic Acids using Affinity Binding and Surface Enhanced Laser Deorption/Ionization (SELDI) Time of Flight Mass Spectrometry

5a. CONTRACT NUMBER

5b. GRANT NUMBER
DAMD17-03-1-0222

5c. PROGRAM ELEMENT NUMBER

6. AUTHOR(S)
Gordan B. Mills, M.D., Ph.D.

E-mail: Gmills@mdanderson.org

5d. PROJECT NUMBER

5e. TASK NUMBER

5f. WORK UNIT NUMBER

7. PERFORMING ORGANIZATION NAME(S) AND ADDRESS(ES)
University of Texas M.D. Anderson Cancer Center
Houston, TX 77030

8. PERFORMING ORGANIZATION REPORT NUMBER

9. SPONSORING / MONITORING AGENCY NAME(S) AND ADDRESS(ES)
U.S. Army Medical Research and Materiel Command
Fort Detrick, Maryland 21702-5012

10. SPONSOR/MONITOR'S ACRONYM(S)

11. SPONSOR/MONITOR'S REPORT NUMBER(S)

12. DISTRIBUTION / AVAILABILITY STATEMENT
Approved for Public Release; Distribution Unlimited

13. SUPPLEMENTARY NOTES
Original contains color plates: All DTIC reproductions will be in black and white.

14. ABSTRACT

We proposed to apply novel technologies to the development of an approach suitable to detect plasma and serum lipid levels for screening for ovarian cancer in high and low risk women. The first of these is a novel approach to the development of antibodies, which will recognize specific phospholipids and lysophospholipids present in ovarian cancer patients and the second of these is SELDI tof mass spectroscopy. These two technologies will be merged with powerful computing tools to develop approaches capable of detecting ovarian cancer at an early, curable stage. This approach will further benefit from the expertise of the Mills laboratory (LPA screening, SELDI tof) with that of the Prestwich laboratory (lipid synthesis and antibody development).

Results We have completed the studies proposed in the application. We have demonstrated that SELDI mass spectroscopy using nonspecific and affinity matrices has the ability to detect and characterize model lysopholipids including LPC, LPA, S1P and LPS present in plasma and serum. This assay is applicable to relatively large volumes of plasma and serum >2ml. We have also demonstrated that additional mass spectroscopy approaches have a greater degree of sensitivity and specificity when compared to SELDI mass spectroscopy. We proposed to develop and analyze lipid specific antibodies. We have analyzed anti-S1P antibodies as both a theragnostic and a diagnostic using a sensitive ELISA approach. LPA antibodies appear to block the growth of hybridomas due to blocking LPA-mediated survival. We thus took an interim step of identifying novel LPA binding proteins as alternative affinity reagents. We also developed novel LPA receptor selective agonists that would bypass the inhibitory activity of the LPA antibody. With these in hand, we have immunized mice with LPA constructs and have developed very high titer anti-LPA antibodies.

15. SUBJECT TERMS
ovarian cancer, LPA, SELDI, early diagnosis

16. SECURITY CLASSIFICATION OF:			17. LIMITATION OF ABSTRACT	18. NUMBER OF PAGES	19a. NAME OF RESPONSIBLE PERSON
					USAMRMC
a. REPORT	b. ABSTRACT	c. THIS PAGE			19b. TELEPHONE NUMBER *(include area code)*
U	U	U	UU	155	

Table of Contents

This is the final report for DAMD17-03-01-0222

Original background and Preliminary Data

Ovarian cancer remains the 5th most frequent cause of death from cancer in women. Indeed, the current cure rate for ovarian cancer is under 40%, not substantially different from that in the 1950s. This abysmal prognosis occurs, in most part, due to ovarian cancer being diagnosed at a late stage where current therapies are ineffective. Unfortunately more than 75% of patients are diagnosed when the disease has spread beyond the pelvis. Thus a method to detect ovarian cancer at an early curable stage has the potential to provide an immediate and major impact on this devastating disease. This is particularly important for individuals at high risk either because of a strong family history or proven abnormalities in BRCA1 or BRCA2.

The identification of secreted molecules, which contribute to the pathophysiology of ovarian cancer, provides a major opportunity to identify markers that could contribute to early diagnosis. We have demonstrated that the most potent growth factor activity in ascites of ovarian cancer patients consists of multiple forms of lysophosphatidic acid (LPA). LPA increases proliferation, prevents apoptosis and anoikis, increases invasiveness, decreases sensitivity to cisplatin (the most effective drug in ovarian cancer), and increases production and activity of multiple growth factors, proteases and mediators of angiogenesis. Thus LPA contributes to the pathophysiology of ovarian cancer. We and others have subsequently demonstrated that multiple additional bioactive lysophospholipids, including lysophosphatidylcholine (LPC), sphingosylphosphorylcholine (SPC), sphingosine 1 phosphate (S1P) and lysophosphatidylserine (LPS) exhibit pleiomorphic effects on ovarian cancer cells.

Ascites from ovarian cancer patients contains high levels of lysophospholipids including multiple forms of LPA, lysophosphatidylinositol (LPI), LPC, SPC and S1P. Reports from our and other laboratories indicate that plasma and sera from ovarian cancer patients contain aberrant levels of these lysophospholipids. This suggests that an efficient method to determine levels of lysophopholipids in serum or plasma could provide an effective method to screen for ovarian cancer.

Over 500 species of lysophospholipids are present in plasma and serum. Currently, lysophospholipids are quantified by lipid extraction of a serum sample followed by Mass spectrometry (MS). While MS analysis is highly accurate, the methodology has limited throughput for large-scale screening of patient samples. Further, the need to use organic solvents to prepare specimens for MS limits the quantitation and the applicability of the method. Surface-enhanced laser desorption and ionization time of flight (SELDI tof) mass spectroscopy analyses of “markers” diagnostic of ovarian cancer have identified a number of candidates with mass/charge ratios of under1000, suggestive that these could be lysophospholipids rather than peptides. Identification of these markers required the global unbiased analysis of many different molecules in serum combined with powerful algorithms designed to identify patterns indicative of the presence of cancer.

We propose to apply two novel technologies to the development of a high through-put technology suitable for screening for ovarian cancer in high and low risk women. The first of these is a novel approach to the development of antibodies to specific phospholipids and lysophospholipids and the second of these is SELDI tof mass spectroscopy. These two technologies will be merged with powerful bioinformatics tools to develop heuristic algorithms capable of detecting ovarian cancer at an early, curable stage. This approach will benefit from

the expertise of the Mills laboratory (LPA screening, SELDI tof) with that of the Prestwich laboratory (lipid synthesis and antibody development).

To develop efficient methods for analysis of lysophospholipids in ovarian cancer patients, we will:

1. **Assess the efficacy of novel LPA/PA lipid antibodies developed by our group in capture and analysis of LPA/PA directly in serum and plasma using SELDI-tof**
2. **Determine whether non-specific matrices (hydrophobic C16, anionic SAX2) can be used to directly determine phospholipid and lysophospholipid levels using SELDI-tof**
3. **Develop additional anti lysophospholipid antibodies and determine their utility in analysis in Seldi-tof**

Significance: Over 75% of ovarian cancer patients are diagnosed when the disease has spread beyond the pelvis. At this stage of disease, the cure rate is under 15%. This is in contrast to the cure rate for early stage ovarian cancer, which can approach 90%. Thus any approach that can allow diagnosis of ovarian cancer at an earlier curable stage has the potential to have a marked impact on this devastating disease.

RESULTS OF STUDIES

Task #1 Assess the efficacy of novel LPA/PA lipid antibodies developed by our group in capture and analysis of LPA/PA directly in serum and plasma using SELDI-tof This specific aim was dependent on the production of anti-lipid antibodies and identification of lysophospholipid binding proteins for selective capture of these ligands. The original antibodies produced in this application proved to have a number of unexpected problems. Indeed, we experienced difficulty in achieving selective lipid binding by anti-lipid antibodies, scale-up production issues, and problems in obtaining homogenous, healthy anti-lipid producing clones using the approaches proposed in the application. This appeared to be due to a need for LPA for the continued viability and growth of the hybridomas. The anti-LPA antibodies produced appeared to kill the hybridomas. We thus adopted two different approaches to bypass this problem: 1. Identification of additional lysophospholipid binding agents and 2. Development of LPA analogs that would allow growth of hybridomas producing lysophospholipid antibodies.

1. We broadened the initial aim to include discovery of additional lysophospholipid and lipid binding proteins that could be readily produced as recombinant proteins and engineered to have particular useful lipid binding characteristics. To this, end, we have employed our tethered LPA and PA reagents developed in the application for the generation of antibodies and used in the application for anti lipid antibody elicitation, to make affinity resins for identification of novel LPA binding proteins from fibroblasts and cancer cells. The same modifications are in process for LPC, PC, LPI, and PI lipids. To identify new lysophospholipid binding proteins, a MS proteomics collaboration was established with Drs. J. Gettemans and J. Vanderkerckhove at the University of Ghent (Belgium Appendix#4). This collaboration has the benefit of discovering novel proteins in the LPA signaling pathway, which are likely to be important as diagnostic markers in their own right, as well as being important reagents for the proposed SELDI-MS

capture method. As indicated in Appendix#4, pyruvate kinase was identified as an unexpected binding partner for LPA.

2. Development of LPA analogs that would allow growth of hybridomas producing lysophospholipid antibodies. As indicated above, we were unable to expand our initial hybridomas to produce large amounts of LPA antibodies. This appeared to be due to the hybridomas requiring LPA for continued proliferation and survival. As indicated in appendix #3 and #5, we developed a series of high affinity, long lived LPA structural analogs for this purpose. These analogs proved to be highly efficient at allowing the growth and survival of cells and may indeed by activating on a subset of LPA receptors prove to be critical reagents for the growth of hybridomas and potential other cell types.

3. Based on our collaboration with Dr. Sabadinni which resulted in the studies to characterize the anti S1P antibodies described in appendix #7 and the studies in aim 3 below. We have developed high titer LPA antibodies using novel immunization approaches that were successful for anti-S1P and the progress in this project. These have exceedingly high activity and are being evaluated as affinity reagents. A number of potential antibodies are indicated in the figure below based on a competitive ELISA approach. This suggests that we will be able

4.

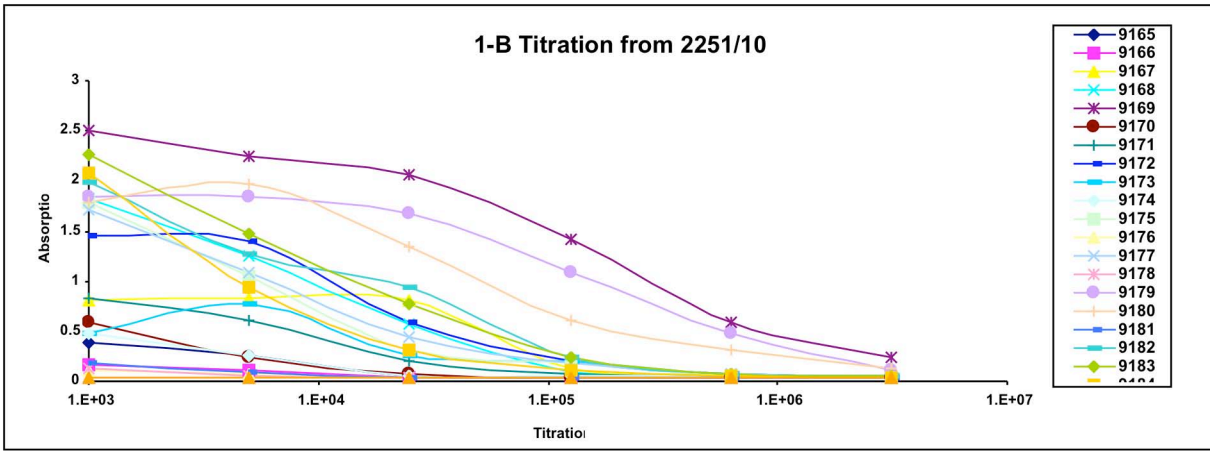

Task #2 Determine whether non-specific matrices (hydrophobic C16, anionic SAX2) can be used to directly determine phospholipid and lysophospholipid levels using SELDI-tof

As proposed in the application, we have applied model lysophospholipids to both non-specific and specific affinity matrices and demonstrated an ability to detect the model lysophospholipids. To determine whether there were different sensitivities for different lysophopholipids, we developed or purchased standard forms of each of the different LPA, S1P, LPS and LPC present in plasma. Using these standard lipid preparations, we have assessed different non-specific matrices as well as phospholipids specific capture matrices (3). We can readily detect 0.2nmol of LPA and other lysophospholipid isoforms in a single spot using SELDI-tof and MALDI approaches (we added this to the approaches proposed in the original application at no additional cost to the proposal). Indeed, in comparison, the MALDI technology was more stable than the SELDI technology. We have also compared both of these approaches to ESI mass spectroscopy using the model lysophospholipids. The ESI mass spectroscopy approaches are approximately 10-100 times more sensitive than the MALDI and SELDI-tof approaches.

The use of the SELDI-tof technology proposed in the application has a major rate-limiting factor. As noted above, the sensitivity of the SELDI-tof technology with both non-specific and specific affinity reagents is approximately 2nmol of model lipid. To determine the amount of LPA and other lipid isoforms in plasma as a prerequisite to determining the amount of plasma that would need to be loaded on the SELDI matrix, we assessed LPA and other lysophospholipid levels by ESI mass spectroscopy in plasma from control and normal individuals. This indicated that we would need to apply the equivalent of 7 ml of plasma to a single spot on the SELDI plate to assess levels of the more uncommon (such as unsaturated LPAs) and more important LPAs in plasma. We thus assessed multiple approaches to potentially bypass this problem.

1. We determined whether repeat administration of plasma with extensive washing would allow loading of sufficient material for detection. This approach was not successful with either non-specific or specific affinity reagents.
2. We then developed approaches to purify lipids from plasma. These approaches were highly successful and are now used in our standard approaches to lipid assessment using ESI-mass spectroscopy. These approaches are quite different from the current standard and greatly improve the sensitivity and specificity of the analysis. However, although this allows loading of additional material on the SELDI plate, this is still not sufficient for analysis of the rare lysopholipids present in plasma.

   The extraction approach consists of incubation with chloroform, methanol KCL and ammonia hydroxide. The liquids are then allowed to phase separate. Lysophospholipids such as LPA are moved from one phase to another using pH 2 HCL resulting in a high degree of purity.
3. The SELDI-tof approach has thus been validated as sufficiently sensitive enough for A.S1P, B. LPC and its isoforms C. Total PA, LPA, LPS, LPI and LPS. However, additional approaches are needed for isoforms of LPA and the other lysophospholipids with the exception of LPC, which are present in sufficient amounts.
4. Dr Tanaka and colleagues (Tanaka et al 2004 ref#3) demonstrated that a Maldi time of flight mass spec approach similar to that proposed in this application can detect LPA in egg white and further that it could be used to detect material in blood. The approach used a phosphate affinity matrices and a mass shift associated with a zinc complex. However, just as we have noted in the first report, the approach requires prepurification of LPA from the complex mixture in order to apply enough to the plate. The ability to detect LPA and also to determine the fatty acid chain mixture is compatible with an approach to make this an efficient method to detect and quantify LPA. The ability to quantify and characterize the various species of LPA showed acceptable CVs for development of a clinical grade assay. The detection approach of cocrystalizing LPA and Zn is an improvement of the approach proposed in the application and has been implemented into the approaches to determine lysophospholipid levels.
5. With this data in hand (ref#3), we recruited Dr. Tanaka from Japan to work as a Post Doctoral Fellow in this application. We have used these technologies to assay the samples proposed in the application. As previous studies have demonstrated, there is an increase in LPA particularly unsaturated LPA in plasma from cancer patients. However, there is insufficient separation between malignant, benign and control to function as a test

for the presence of ovarian cancer. In studies beyond the scope of this application, we will assess whether combined analysis of multiple markers including lysophospholipids will prove sufficiently sensitive for the detection of ovarian cancer.

6. The presence of the enzymes that produce LPA and other lysophospholipids in plasma suggested a novel approach to bypass the loading challenges for rare lysophospholipids. This suggests that the rate of production of different lysophospholipids may alter with time in culture. Indeed, the concentrations of rare lysophospholipids incubated in culture as compared to the control lipids prepared for application increases markedly into the range of sensitivity needed for the SELDI-tof assay. Based on this observation, we are currently assaying a series of samples (collected for this proposal) to determine differences in the generation of lysophospholipids over time of incubation. This observation may be important to early diagnosis as well as to the mechanisms resulting in altered levels of lysophospholipids in cancer.

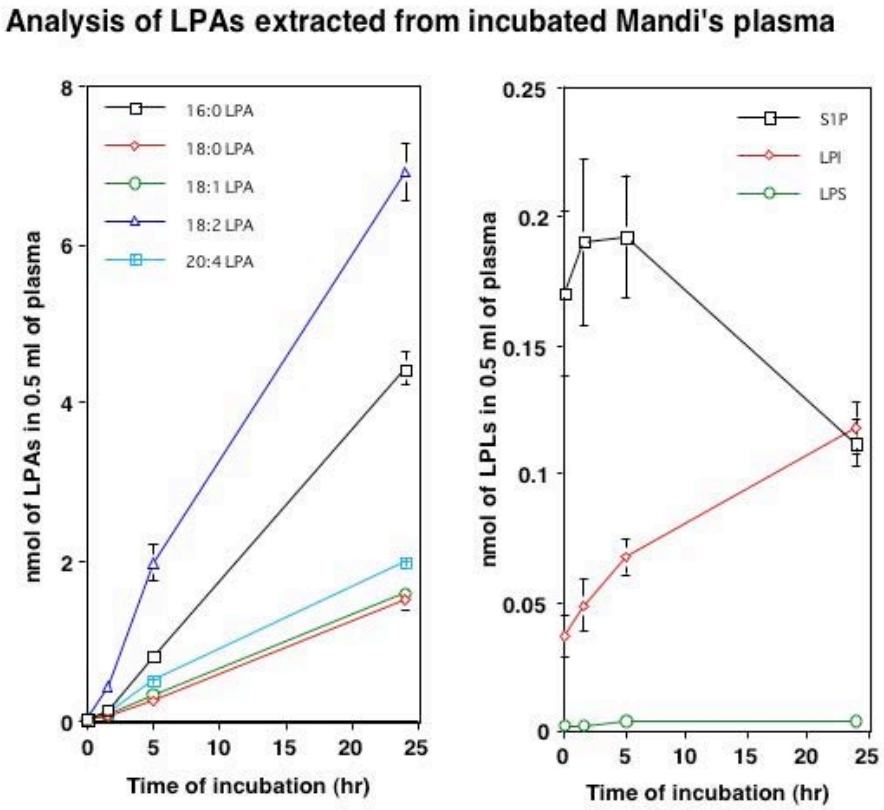

In summary, we have been able to validate SELDI tof as an approach for the sensitive measurement of prevalent lysophospholipids in plasma as isolated from the patient.

Specific Aim #1 and #2 are designed to combine affinity reagents with SELDI tof (see aim #1 and #3 for these approaches.

Task #3 Develop additional anti-lysophospholipid/lipid antibodies and determine their utility in analysis in Seldi-tof

Through an ongoing collaboration (see appendix #7), we have obtained a high affinity pan S1P antibody from Dr. Roger Sabadinni at UCSD. This antibody binds all forms of S1P and demonstrates efficacy in determining S1P levels using ELIZA. Our recent data indicates that there is only one major form of S1P in ovarian cancer patients. We have thus proceeded with the anti S1P antibodies as a first analysis.

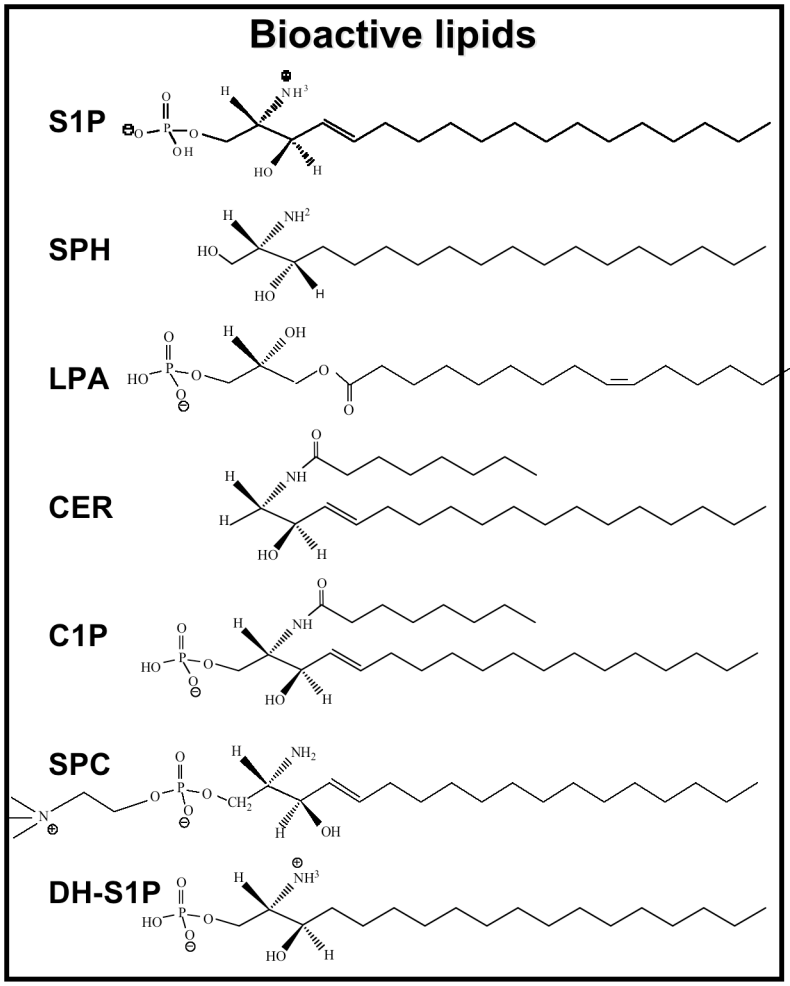

As can be seen from the competitive ELISA, the anti-S1P antibody interacts with S1P and dihydroS1P and modestly with SPC. It does not interact with other lysophospholipids. Given that the concentrations of SPC and dihydroS1P in plasma are low, the ELISA reliably measures S1P levels.

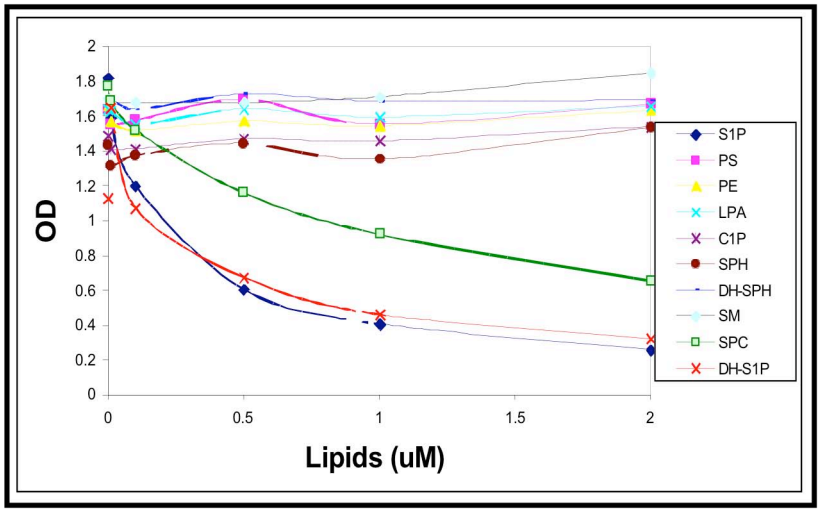

Above is a competition ELISA with known amounts of S1P demonstrating the linearity of the curve in phosphate buffered serum or human serum.

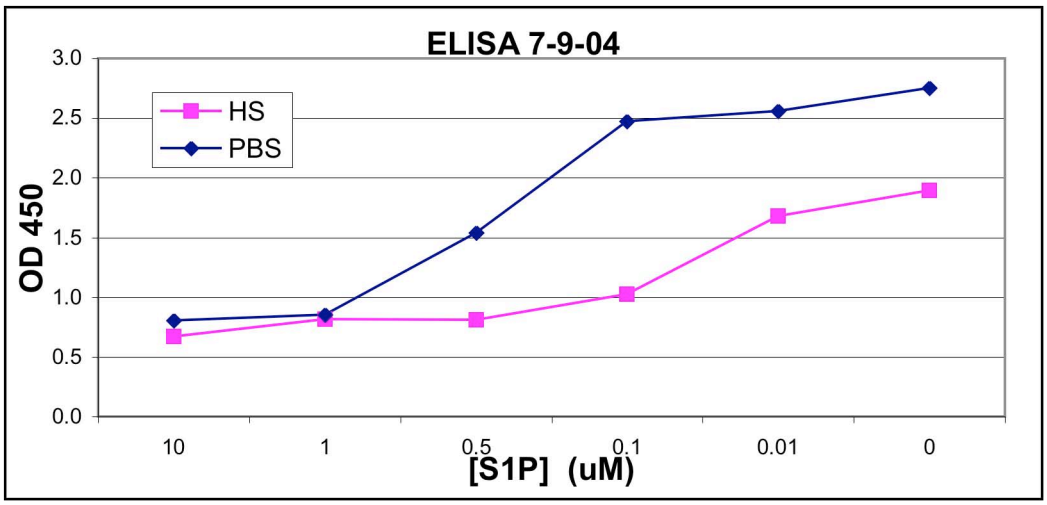

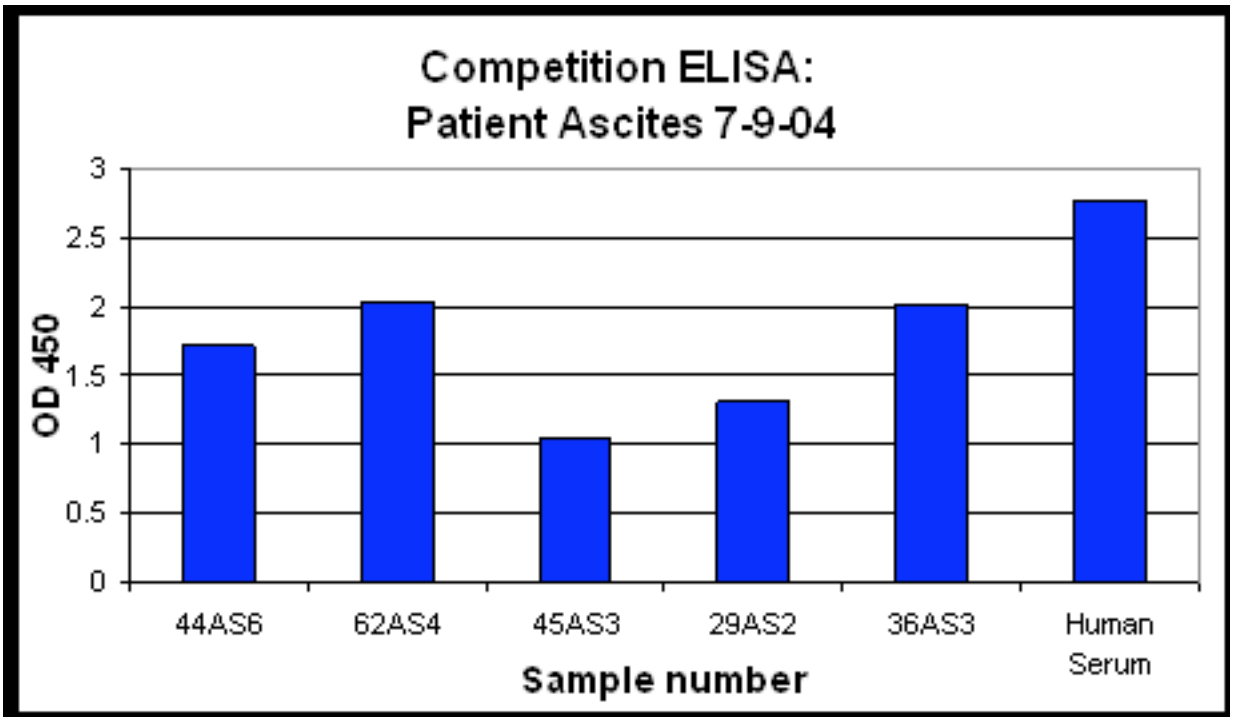

This is a competition ELISA with patient ascites samples as an example. Lower values represent higher amounts of S1P. Thus all of the model samples were elevated compared to human serum arguing that the approach will be able to detect and quantify S1P in serum and in ascites. Samples have been identified through this application and approved by the DoD and MDACC IRB. A final review is being conducted by the San Diego State University allowing these samples to be analyzed for S1P levels as described in the application.

Additional studies supported by the proposal not originally proposed in the application.

The overall goal of this application was to develop novel methods to assay for the presence of lysophospholipids in plasma from ovarian cancer patients. These approaches were to focus on affinity approaches using antibodies and binding proteins as well as on SELDI technology. As noted above, there were a number of unexpected challenges with the technologies. The resolution of the challenges and the application of additional approaches to the overall goal lead to a number of additional observations of importance.

1. Autotaxin activity

Contemporary with the submission of this application, the enzyme that produced LPA was identified in serum as Autotaxin but Makiko Goto who worked in this project. This suggested an alternative approach of measurement of autotaxin activity as a potential diagnostic approach. Workign with Dr. Prestwich, we developed a practical autotaxin assay. As indicated in appendix 2, autotaxin activity is increased in the plasma, serum and ascites of ovarian cancer patients. These levels are, however, not sufficient on their own to be diagnostic due to overlap between groups. Autotaxin levels will be assayed as part of a potential panel for the early detection of ovarian cancer.

2. LPA and lysolipid generation

As indicated above, we hypothesized that LPA and other lysophospholipids would be produced during incubation in culture. This indeed proves to be the case. The intriguing observation is that this does not appear to be solely due to the enzymes previously hypothesized to produce LPA in plasma. This indicates that there are additional LPA producing enzymes to be identified.

3. Selective LPA receptor agonists

In order to bypass the toxicity of LPA antibodies to hybridomas, we developed a series of LPA receptor selective analogs that could be used to culture hybridomas. Strikingly, not only are these molecules stable and highly receptor selective, they have unexpected properties. For example a number of these analogs are sufficient for the growth of hybridomas and potentially stem cells. This suggests that activation of different LPA receptors has markedly different biological consequences warranting further development and the development of receptor selective antagonists.

4. ELISA

With the challenge in loading sufficient lysophospholipids onto the SELDI and MALDI plates, we developed an ELISA to S1P and are currently developing ELISAs to LPA. These have the advantage of being a standard technology and widely applicable. The S1P ELISA appears to identify differences between plasma from normal and cancer patients providing a potentially important theragnostic or diagnostic approach.

5. ESI mass spec

In order to compare to the antibody and SELDI technologies in this application, we developed a number of improvements on the gold standard ESI mass spec procedures. Most important of these are a series of handling approaches to pre purify lysophospholipids from plasma and serum.

6. LPA binding molecules

As an alternative approach to affinity reagents, we identified novel LPA binding molecules, the most interesting of with is pyruvate kinase (Appendix 5). This provides a unique biological insight as well as a reagent for affinity capture of LPA.

7. Therapy approaches

As a consequence of these studies, we developed a number of collaborations with additional investigators. These led to the therapy studies described in appendix 7 and 8. The efficacy of therapy targeting SiP and autotaxin requires the development of further theragnostic agents allowing the selection of patients likely to respond to these therapies.

KEY RESEARCH ACCOMPLISHMENTS

Eight papers have been published or are in press as a result of the studies in this grant. Importantly, a new approach to the culture and growth of hybridomas has been developed. This required the development of LPA analogs that could maintain the growth of hybridomas

secreting LPA antibodies (the hybridomas required LPA) so these needed to be analogs of LPA that would not be blocked by the antibodies. Strikingly the LPA analogs developed and validated in this application not only evade the inhibition mediated by anti-LPA analogs but due to selective receptor activity.

1. Demonstrated that model lysophospholipids can be detected at concentrations present in patients by SELDI tof
2. Developed methods to prepurify lipids for attachment to SELDI plates
3. Obtained sufficient quantities of a high affinity S1P antibody
4. Demonstrated specificity of the anti S1P antibody
5. Demonstrated ability to quantitate S1P by competitive ELISA
6. Synthesized and characterized a large set of LPA analogs
7. Demonstrated selectivity of LPA analogs to specific receptors
8. Identified high affinity lysophospholipid binding proteins.
9. Demonstrated pyruvate kinase to be a LPA binding protein
9. Developed LPA specific antibodies
10. Compared affinity technologies developed in this proposal to phosphate capture methods developed by others (Tamotsu Tanaka who developed the approach was recruited to our laboratory for these studies).
11. Developed assays and assessed autotaxin activity in peripheral blood
12. Developed approaches to assess LPA generating activity in serum.

REPORTABLE OUTCOMES

APPENDICES* (Corrigendum's have been filed on several of the papers below to clarify the grant number as DAMD17-03-1-0222and to clarify training support to Drs. Goto, Liu and Tanyi from DAMD17-03-1-0409).

1. Mills G.B., and Moolenaar, WH. 2003 Emerging role of lysophosphatidic acid in cancer. Nature Cancer Reviews 3:582-591

This manuscript describes the importance of lysophospholipids in the initiation, progression and treatment of cancer. It describes the controversies around the differences in lysopholipids in the ascites, plasma and serum of patients. It also describes the differences in the levels of the enzymes producing and metabolizing lysophospholipids in cancer.

2. Umezu-Goto, M., Tanyi, J., Lahad, J., Liu, S., Yu, S., Lapushin, R., Hasegawa, Y., Lu, Y., Trost, R., Bevers, T., Jonasch, E., Aldape, K., Liu, J., James, R.A., Ferguson, C.G., Xu, Y., Prestwich, G.D., and Mills G.B., 2004 Lysophosphatidic acid production and action: Validated targets in cancer? J. Cellular Biochemistry 92:1115-40.

This manuscript describes the importance of lysophospholipids in the initiation, progression and treatment of cancer. It describes the controversies around the differences in lysopholipids in the ascites, plasma and serum of patients. It also describes the differences in the levels of the enzymes producing and metabolizing lysophospholipids in cancer. This manuscript describes the analysis of atutoaxin activity in the serum plasma and ascites of ovarian cancer patients.

3. Xu, Y., Aoki, J., Shimizu, K., Umezu- Goto, M., Hama, K., Takanezawa Y., Y, S., Mills, G.B., Arai H., Qian L., Prestwich G.D., 2005 Structure activity relationships of Fluorinated Lysophosphatidic Acid Analogues: Discovery of High-Affinity LPA3 receptor agonists J Med Chem. 48:3319-3327.

This manuscript describes the development of stable specific LPA3 receptor ligands. These ligands selectively allow the growth of hybridoma cells and are bind used to bypass the inhibitory activity of LPA antibodies on the growth of hybridomas. The enantiomers are particularly useful for the growth of hybridomas.

4. Desmaret S, Qian L, Vanloo B, Meerschaert K, Van Damme J, Grooten J, Vandekerckhove J, Prestwich GD, Gettemans J. Lysophosphatidic acid affinity chromatography reveals pyruvate kinase as a specific LPA-binding protein. Biol Chem. 2005 Nov;386(11):1137-47.

This manuscript describes the identification of high affinity LPA-binding proteins. Pyruvate kinase along with gelsolin identified by Dr. Goetzl are alternative affinity reagents for LPA as compared to antibodies for analysis.

5. Qian, L,, Xu, Y, Simper, T., Jian G., Aoki, A., Umezu-Goto, M., Arai, H., Yu, S., Mills G. B., Tsukahara, R., Makarova, N., Fujiwara, Y., Tigyi, G., and Prestwich, G. 2006 Phosphorothioate Analogues of Alkyl Lysophosphatidic Acid as LPA3 Receptor-Selective Agonists Chem Med Chem 1:376-383

This manuscript describes the development of stable specific LPA3 receptor ligands. These ligands selectively allow the growth of hybridoma cells and are bind used to bypass the inhibitory activity of LPA antibodies on the growth of hybridomas. The enantiomers are particularly useful for the growth of hybridomas.

6. Tanyi JL. Croetzer, D., Wolf, J., Yu, S., Hasegawa, Y., Lahad, J., Cheng, KW., Umezu-Goto, M., Prestwich, G.D., Morris A., Newman, R.A., Felix, EA., Lapis, R., and Mills G.B. 2006 Functional Lipidomics: Lysophosphatidic Acid as a Target for Molecular Diagnosis and Therapy of Ovarian Cancer Functional Lipidomics Prestwich and Feng Editors pp 101-124

This manuscript describes the importance of lysophospholipids in the initiation, progression and treatment of cancer. It describes the controversies around the differences in lysopholipids in the ascites, plasma and serum of patients. It also describes the differences in the levels of the enzymes producing and metabolizing lysophospholipids in cancer. This manuscript describes the analysis of atutoaxin activity in the serum plasma and ascites of ovarian cancer patients.

7. Visentin, B., Vekich J.A., Sibbald, B.J., Cavalli, A.L., Moreno, K.M., Matteo, R.G., Garland W.A., Lu, Y., Yu., S., Hall, H.S., Kundra V., Mills G.B., and Sabbadini R., 2006, Sphingosine-1-phosphate is required for tumor growth, invasion and angiogenesis mediated by bFGF and VEGF in multiple tumor lineages: Validation of an anti-S1P antibody as a potential therapeutic Cancer Cell: 9:225-238

This manuscript describes the characterization and utility as a therapeutic reagent of anti-S1P antibodies. These reagents are highly effective in blocking the growth of cancers in vivo. This emphasizes the need for a theragnostic to select patients for treatment with anti-S1P

antibodies. The theragnostic is described under Aim #3 above with a manuscript in preparation.

8. Baker, D.L., Fujiwara, Y., Pigg, K.R., Tsukahara, R., Kobayashi, S., Uchiyama, A., Murakami-Murofushi, K., Koh, E., Bandle, R.W., Byun H-S., Bittman R., Fan, D., Murph, M., Mills G.B., Tigyi G., 2006 Carba analogs of cyclic phosphatidic acid are selective inhibitors of autotaxin and cancer invasion and metastases. J. Biol Chem In Press

This manuscript describes an inhibitor of autotaxin, the enzyme that produces LPA. This study demonstrates the need for development of LPA assays as theragnostics.

CONCLUSIONS

This project has had a number of expected and unexpected consequences. The goal of this application was to determine whether SELDI-tof or SELDI-tof combined with novel affinity reagents could be used as the basis for a commercial assay for lysophospholipids. The rate limiting step in the analysis of lysophospholipids using SELDI-tof or MALDI mass spectroscopy approaches was unexpectedly the amount of material that could be loaded onto the SELDI or MALDI plates. This problem was alleviated slightly by the identification and validation of affinity reagents for lysophospholipids, however, this remains a rate limiting problem for rare lysophospholipids. However, the technology has been validated as a rapid and efficient method for the analysis of the more common lysophospholipids in plasma. This has been presented at several meetings and is in preparation as a manuscript.

Based on these challenges as proposed in the initial application, we have emphasized the development of affinity reagents for specific lysophopholipids. These consist of three different classes, affinity matrices for SELDI and MALDI plates, binding proteins and antibodies. The phospholipids binding agent identified and characterized by Tanaka et al, allowed the loading of additional material on the plates, however, this was still insufficient to detect the rare lysophospholipids present in plasma.

In order to develop LPA producing hybridomas, we produced and characterized a number of novel LPA analogs with high affinity, stability and selectivity for specific LPA receptors. These will not only be used to develop LPA antibodies but also to characterize the function of LPA receptors.

We have developed and validated a S1P ELISA and have reagents in hand for a similar process with LPA. These assays allow the use of larger amounts of plasma required for the characterization of rare lipids.

As a consequence of the collaborations developed as part of these studies, we have developed and evaluated therapeutic approaches to both LPA and S1P. Together, these results further emphasize the need to develop cost effective and robust methods to analyze lysophospholipids in patient plasma.

REFERENCES

1. Mills G.B., and Moolenaar, WH. 2003 Emerging role of lysophosphatidic acid in cancer. Nature Cancer Reviews 3:582-591
2. Umezu-Goto, M., Tanyi, J., Lahad, J., Liu, S., Yu, S., Lapushin, R., Hasegawa, Y., Lu, Y., Trost, R., Bevers, T., Jonasch, E., Aldape, K., Liu, J., James, R.A., Ferguson, C.G., Xu, Y., Prestwich, G.D., and Mills G.B., 2004 Lysophosphatidic acid production and action: Validated targets in cancer? J. Cellular Biochemistry 92:1115-40.
3. Tanaka T, Tsutsui H, Hirano K, Koike T, Tokumura A, Satouchi K. Quantitative analysis of lysophosphatidic acid by time-of-flight mass spectrometry using a phosphate-capture molecule.J Lipid Res. 2004 Nov;45(11):2145-50.
4. Xu, Y., Aoki, J., Shimizu, K., Umezu- Goto, M., Hama, K., Takanezawa Y., Y, S., Mills, G.B., Arai H., Qian L., Prestwich G.D., 2005 Structure activity relationships of Fluorinated Lysophosphatidic Acid Analogues: Discovery of High-Affinity LPA3 receptor agonists J Med Chem. 48:3319-3327.
5. Desmaret S, Qian L, Vanloo B, Meerschaert K, Van Damme J, Grooten J, Vandekerckhove J, Prestwich GD, Gettemans J. Lysophosphatidic acid affinity chromatography reveals pyruvate kinase as a specific LPA-binding protein. Biol Chem. 2005 Nov;386(11):1137-47.
6. Qian, L,, Xu, Y, Simper, T., Jian G., Aoki, A., Umezu-Goto, M., Arai, H., Yu, S., Mills G. B., Tsukahara, R., Makarova, N., Fujiwara, Y., Tigyi, G., and Prestwich, G. 2006 Phosphorothioate Analogues of Alkyl Lysophosphatidic Acid as LPA3 Receptor-Selective Agonists Chem Med Chem 1:376-383
7. Tanyi JL. Croetzer, D., Wolf, J., Yu, S., Hasegawa, Y., Lahad, J., Cheng, KW., Umezu-Goto, M., Prestwich, G.D., Morris A., Newman, R.A., Felix, EA., Lapis, R., and Mills G.B. 2006 Functional Lipidomics: Lysophosphatidic Acid as a Target for Molecular Diagnosis and Therapy of Ovarian Cancer Functional Lipidomics Prestwich and Feng Editors pp 101-124
8. Visentin, B., Vekich J.A., Sibbald, B.J., Cavalli, A.L., Moreno, K.M., Matteo, R.G., Garland W.A., Lu, Y., Yu., S., Hall, H.S., Kundra V., Mills G.B., and Sabbadini R., 2006, Sphingosine-1-phosphate is required for tumor growth, invasion and angiogenesis mediated by bFGF and VEGF in multiple tumor lineages: Validation of an anti-S1P antibody as a potential therapeutic Cancer Cell: 9:225-238

APPENDICES

1. Mills G.B., and Moolenaar, WH. 2003 Emerging role of lysophosphatidic acid in cancer. Nature Cancer Reviews 3:582-591
2. Umezu-Goto, M., Tanyi, J., Lahad, J., Liu, S., Yu, S., Lapushin, R., Hasegawa, Y., Lu, Y., Trost, R., Bevers, T., Jonasch, E., Aldape, K., Liu, J., James, R.A., Ferguson, C.G., Xu, Y., Prestwich, G.D., and Mills G.B., 2004 Lysophosphatidic acid production and action: Validated targets in cancer? J. Cellular Biochemistry 92:1115-40.
3. Xu, Y., Aoki, J., Shimizu, K., Umezu- Goto, M., Hama, K., Takanezawa Y., Y, S., Mills, G.B., Arai H., Qian L., Prestwich G.D., 2005 Structure activity relationships of Fluorinated Lysophosphatidic Acid Analogues: Discovery of High-Affinity LPA3 receptor agonists J Med Chem. 48:3319-3327.
4. Desmaret S, Qian L, Vanloo B, Meerschaert K, Van Damme J, Grooten J, Vandekerckhove J, Prestwich GD, Gettemans J. Lysophosphatidic acid affinity

chromatography reveals pyruvate kinase as a specific LPA-binding protein. Biol Chem. 2005 Nov;386(11):1137-47.

5. Qian, L,, Xu, Y, Simper, T., Jian G., Aoki, A., Umezu-Goto, M., Arai, H., Yu, S., Mills G. B., Tsukahara, R., Makarova, N., Fujiwara, Y., Tigyi, G., and Prestwich, G. 2006 Phosphorothioate Analogues of Alkyl Lysophosphatidic Acid as LPA3 Receptor-Selective Agonists Chem Med Chem 1:376-383
6. Tanyi JL. Croetzer, D., Wolf, J., Yu, S., Hasegawa, Y., Lahad, J., Cheng, KW., Umezu-Goto, M., Prestwich, G.D., Morris A., Newman, R.A., Felix, EA., Lapis, R., and Mills G.B. 2006 Functional Lipidomics: Lysophosphatidic Acid as a Target for Molecular Diagnosis and Therapy of Ovarian Cancer Functional Lipidomics Prestwich and Feng Editors pp 101-124
7. Visentin, B., Vekich J.A., Sibbald, B.J., Cavalli, A.L., Moreno, K.M., Matteo, R.G., Garland W.A., Lu, Y., Yu., S., Hall, H.S., Kundra V., Mills G.B., and Sabbadini R., 2006, Sphingosine-1-phosphate is required for tumor growth, invasion and angiogenesis mediated by bFGF and VEGF in multiple tumor lineages: Validation of an anti-S1P antibody as a potential therapeutic Cancer Cell: 9:225-238

THE EMERGING ROLE OF LYSOPHOSPHATIDIC ACID IN CANCER

Gordon B. Mills and Wouter H. Moolenaar‡*

The bioactive phospholipid lysophosphatidic acid (LPA) stimulates cell proliferation, migration and survival by acting on its cognate G-protein-coupled receptors. Aberrant LPA production, receptor expression and signalling probably contribute to cancer initiation, progression and metastasis. The recent identification of ecto-enzymes that mediate the production and degradation of LPA, as well as the development of receptor-selective analogues, indicate mechanisms by which LPA production or action could be modulated for cancer therapy.

PHOSPHOLIPID
A small molecule with one or two fatty acyl chains, a glycerol backbone, and a free or derivatized phosphate. Lysophospholipids only have a single fatty acyl chain (see figure 1).

SERUM
Fluid produced during blood coagulation. Many growth factors and mediators are released by platelets during clotting.

ECTO-ENZYME
An enzyme that is located on the outside of the cell. Primarily involved in metabolism of molecules in the interstitial space or bloodstream.

**MD Anderson Cancer Center, Houston 77030, Texas, USA.*
‡The Netherlands Cancer Institute, Amsterdam 1066CX, The Netherlands.
Correspondence to G. B. M.
e-mail: gmills@mdanderson.org
doi:10.1038/nrc1143

Lysophosphatidic acid (LPA) is one of the simplest natural PHOSPHOLIPIDS and, arguably, is also one of the most interesting. It consists of a single fatty acyl chain, a glycerol backbone and a free phosphate group, and unlike most other phospholipids, it is also water soluble (FIG. 1). Despite its simplicity, many structurally diverse forms of LPA exist, so it has the potential to contain a remarkable amount of informational content.

Although originally known for its rather unglamorous role as an intermediate in intracellular lipid metabolism, LPA is now recognized as an extracellular lipid mediator that evokes growth-factor-like responses in almost every cell type, both normal and transformed. The first indication that LPA was an important bioactive lipid came several decades ago, when it was found to induce smooth-muscle contraction, platelet aggregation and alterations in blood pressure, but the significance and physiological implications of those early findings remained obscure until the late 1980s and early 1990s. At this time, LPA was shown to have growth-factor-like activities, to signal through specific cell-surface receptors in a G-protein-dependent manner, and to be a major active constituent of SERUM. A new era of LPA research therefore began, and this has led to the unravelling and biochemical characterization of LPA's multiple signalling pathways and the discovery of new biological actions.

As an inducer of cell proliferation, migration and survival, LPA's actions are concordant with many of the 'hallmarks of cancer'[1], indicating a role for LPA in the initiation or progression of malignant disease. Indeed, LPA levels are significantly increased in malignant effusions, and its receptors are aberrantly expressed in several human cancers. The most noteworthy recent development underscoring the importance of LPA in cancer, however, is the discovery that a previously enigmatic ECTO-ENZYME that is involved in tumour invasion, neovascularization and metastasis — autotaxin (ATX) — acts by producing LPA in the cellular microenvironment, which indicates that LPA is a key contributor to the metastatic cascade.

Biological actions of LPA

The list of cellular responses to LPA is remarkably diverse (TABLE 1). Several of LPA's actions are rapid — for example, it affects morphological changes, motility, chemotaxis, invasion, gap-junction closure and tight-junction opening — and occur independently of new protein synthesis. Others are long-term and secondary to gene transcription, such as the stimulation of cell-cycle progression, increased cell viability, wound healing, the production of endothelin and pro-angiogenic factors (vascular endothelial growth factor (VEGF), interleukin (IL)-6, IL-8 and GRO1) — which can act as paracrine growth factors for malignant cells and can

Summary

- Lysophosphatidic acid (LPA) is a serum phospholipid with growth-factor-like activities for many cell types. It acts through specific G-protein-coupled receptors on the cell surface.
- LPA stimulates cell proliferation, migration and survival. In addition, LPA induces cellular shape changes, increases endothelial permeability and inhibits gap-junctional communication between adjacent cells. LPA promotes wound healing *in vivo* and suppresses intestinal damage following irradiation.
- LPA receptors couple to multiple signalling pathways that are now being clarified. These pathways include those initiated by the small GTPases RAS, RHO and RAC, with RAS controlling cell-cycle progression and RHO/RAC signalling having a dominant role in (tumour) cell migration and invasion.
- Significant levels (>1 μM) of bioactive LPA are detected in various body fluids, including serum (but not plasma), saliva, follicular fluid and malignant effusions. The mechanisms by which bioactive LPA is produced were unknown until recently.
- Recent evidence shows that LPA is produced extracellularly from lysophosphatidylcholine by 'autotaxin' (ATX/lysoPLD). ATX/lysoPLD is a ubiquitous exo-phosphodiesterase that was originally identified as an autocrine motility factor for melanoma cells and is implicated in tumour progression. Through local production of bioactive LPA, ATX/lysoPLD might support an invasive microenvironment for tumour cells and therefore contribute to the metastatic cascade.
- Both LPA receptors and ATX/lysoPLD are aberrantly expressed in several cancers.
- The use of inhibitory drugs directed against LPA receptors and/or ATX/lysoPLD could be effective in suppressing tumour metastasis.

also alter the *in vivo* environment by increasing neovascularization — and the production or activation of proteases such as urokinase plasminogen activator (uPA), METALLOPROTEINASES (such as MMP-2) and the metalloprotease-disintegrin tumour necrosis factor-α converting enzyme (TACE)[2–29].

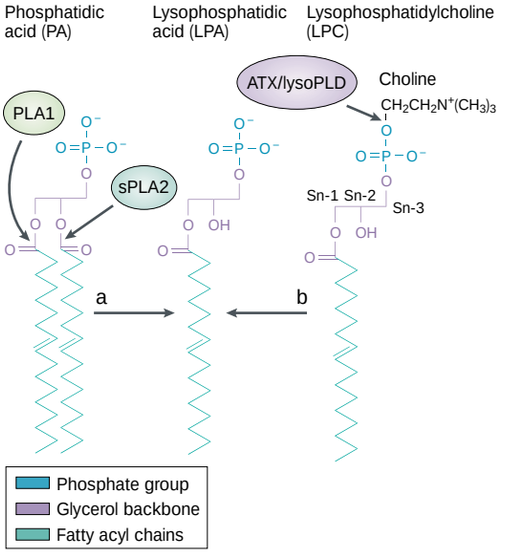

Figure 1 | **LPA metabolic pathways.** LPA can be produced by at least two distinct enzymatic mechanisms: **a** | hydrolysis of phosphatidic acid (PA) by soluble phospholipase A2 (sPLA2), which cleaves the fatty acyl chain at the sn-2 position, or hydrolysis by phospholipase A1 (PLA1), which cleaves the fatty acyl chain at the sn-1 position of the glycerol backbone; **b** | or hydrolysis of lysophosphatidylcholine (LPC) by ATX/lyso PLD, which liberates the hydrophilic headgroup (choline). LPC is produced by the action of PLA1 or PLA2 on membrane phosphatidylcholine.

In addition to transcriptional activation of growth factors, one mechanism by which LPA could indirectly regulate cellular function is through a G-PROTEIN-COUPLED RECEPTOR (GPCR)-regulated transmembrane metalloproteinase cleaving the precursor heparin-binding epidermal growth factor (HB-EGF) or amphiregulin protein at the cell surface, thereby allowing 'transactivation' of the EGF receptor in a classic autocrine manner[24,30,31]. Human EGF-receptor (HER) family members are frequently overexpressed in cancer. Indeed, LPA induces tyrosine phosphorylation of many intracellular proteins, including members of the HER family[5,16,30–33], which is compatible with the idea of LPA inducing a number of cellular responses through the release and action of ligands for the HER family and other tyrosine-kinase-linked receptors.

Although in most circumstances LPA seems to increase cell viability, LPA can induce NECROSIS and apoptosis in hippocampal neurons and neuronal PC12 cells[31–35]. Furthermore, renal ISCHAEMIA-REPERFUSION INJURY seems to be exacerbated by activation of LPA receptors, indicating that the effect of LPA on cellular viability *in vivo* could be cell or context dependent[36].

LPA also exerts diverse vascular effects: it alters attachment of monocytes to vascular endothelial cells, it increases endothelial permeability (decreased barrier function), and it alters the contractility, proliferation and differentiation of vascular smooth-muscle cells, potentially contributing to its effects on blood pressure[15,17,37–43]. These observations, together with the finding that LPA is an active ingredient of MILDLY OXIDIZED LOW DENSITY LIPOPROTEIN (LDL)[44–45], indicate that LPA might contribute to ATHEROSCLEROSIS.

As well as its role as an extracellular messenger, LPA has a well-established 'house-keeping' role inside the cell, namely as a precursor in the biosynthesis of more complex phospholipids. In addition, intracellular LPA

METALLOPROTEINASE
A class of metal-ion-requiring extracellular proteases.

G-PROTEIN-COUPLED RECEPTOR
A cell-surface receptor for small molecules, peptides and lipids that spans the plasma membrane seven times and signals via heterotrimeric G proteins.

NECROSIS
A form of cell death that is distinguished by autolysis.

ISCHAEMIA-REPERFUSION INJURY
Cellular injury that occurs when hypoxic tissue is reoxygenated. A significant problem in stroke, heart attacks and kidney injury.

MILDLY OXIDIZED LDL
Low-density lipoprotein (LDL) is present in plasma. It is a large spherical particle that is made up of cholesterol, cholesteryl esters, phospholipids and a single protein that organizes the particle. Under oxidative stress, LDLs become modified, resulting in alterations in lipid composition.

ATHEROSCLEROSIS
Narrowing of the blood vessels due to deposition of 'plaque' following injury. It is a frequent cause of cardiovascular disease, including heart attacks and stroke.

Table 1 | Main biological activities of LPA

Effect	Cell type/remarks	Major signalling pathway/effector
Cell proliferation	Many normal and transformed cell types	G_i–RAS–ERK1/2
Cell survival		G_i–PI3K–AKT(PKB)
Cell migration (random and directed)	Diverse normal and transformed cell types	G_i–PI3K–TIAM1–RAC (together with RHOA and CDC42 pathways)
Tumour-cell invasion *in vitro*	Hepatoma, T lymphoma, carcinoma cells	
Wound healing *in vivo*	Skin, intestinal epithelium	
Morphological changes	Cell rounding, neurite retraction Cell spreading, lamellipodia protrusion	$G_{12/13}$–RHO-GEF–RHOA G_i–P13K–TIAM1–RAC
Inhibition/reversal of differentiation	Neuroblastoma cells (suppression of neurite outgrowth) Astrocytes (reversal of stellation) Vascular smooth-muscle cells (conversion to fibroblast morphology; loss of contractility)	$G_{12/13}$–RHO-GEF–RHOA ERK and p38 MAPKs
Contraction	Smooth-muscle cells, myofibroblasts	$G_{12/13}$–RHO-GEF–RHOA
Increased endothelial permeability	Micro- and macrovascular endothelial cells	$G_{12/13}$–RHO-GEF–RHOA
Inhibition of gap-junctional communication	Fibroblasts, hepatoma cells, epithelial cells	G_q–PLC

ERK, extracellular signal-regulated kinase; PI3K, phosphatidylinositol 3-kinase; MAPK, mitogen-activated protein kinase; PLC, phospholipase C.

can, at least *in vitro*, serve as a substrate for 'endophilin' — a cytosolic protein that can convert LPA into phosphatidic acid by addition of an acyl chain — and so could influence membrane curvature and endocytosis[46]. Intriguingly, LPA has been reported to function as a high-affinity ligand for the transcription-factor perixosome proliferating activating receptor-γ (PPARγ)[47]. Exogenous LPA can induce PPARγ-mediated gene transcription, which supports the idea that this is a physiological role[47]. PPARγ normally binds fatty-acid derivatives and regulates genes that are involved in energy metabolism, cell differentiation, apoptosis and inflammation. As such, PPARγ has a central role in ADIPOGENESIS and insulin sensitization, but it can also affect cell proliferation and differentiation in various malignancies. It will be necessary to determine how a charged phospholipid such as LPA would cross the plasma membrane intact (without degradation) and in sufficient quantity to activate a nuclear transcription factor. The relative contribution, if any, of PPARγ activation to the physiological activities of extracellular LPA remains to be established.

G-protein signalling

The great variety of cellular and biological actions of LPA is explained by the fact that LPA receptors can couple to at least three distinct G proteins (G_q, G_i and $G_{12/13}$), which, in turn, feed into multiple effector systems[2,11,32,33,48–54] (FIG. 2). LPA activates G_q and thereby stimulates PHOSPHOLIPASE C (PLC), with subsequent phosphatidylinositol-bisphosphate hydrolysis and generation of multiple second messengers leading to protein kinase C activation and changes in cytosolic calcium[2]. LPA also activates G_i, which leads to at least three distinct signalling routes: inhibition of adenylyl cyclase with inhibition of cyclic AMP accumulation; stimulation of the mitogenic RAS–MAPK (mitogen-activated protein kinase) cascade; and activation of phosphatidylinositol 3-kinase (PI3K), leading to activation of the guanosine diphosphate/guanosine triphosphate (GDP/GTP) exchange factor TIAM1 and the downstream RAC GTPase, as well as to activation of the AKT/PKB anti-apoptotic pathway[2,48,51–54,56]. Finally, LPA activates $G_{12/13}$, leading to activation of the small GTPase RHOA, which drives cytoskeletal contraction and cell rounding[50,55]. So, LPA not only signals via classic second messengers such as calcium, diacylglycerol and cAMP, but it also activates RAS- and RHO-family GTPases — the master switches that control cell proliferation, migration and morphogenesis. The RAS- and RHO-GTPases cycle between GDP- and GTP-bound states, with GTP binding being promoted by specific GDP/GTP exchange factors (GEFs); the GTP-bound forms can interact with various downstream effectors (such as protein kinases and scaffold proteins) and thereby alter cell behaviour.

By activating G_i, LPA triggers the RAS-mediated MAPK cascade and thereby promotes cell-cycle progression and cell survival[2,51–53]. LPA-induced RAS activation presumably involves the RAS-specific GEF, SOS, and intermediate protein-tyrosine-kinase activity, but precisely how LPA activates RAS is still a matter of debate[2,32]. In addition to activating RAS, LPA activates the RAC GTPase — a key regulator of the actin cytoskeleton, cell morphology and motility[54]. LPA-induced RAC activation proceeds via a G_i-mediated pathway that involves enhanced PI3K activity and the RAC-specific GEF, TIAM1 (REF. 54). Interestingly, *Tiam1*-knockout mice are resistant to skin carcinogenesis, indicating that LPA-induced Tiam1 activation could have a role in tumour initiation[57]. Furthermore, LPA activates the RHOA GTPase via $G_{12/13}$ and one or more specific RHO-GEFs, thereby inducing cytoskeletal contraction and cell rounding[12,49,50]. So, the RHO-family GTPases RHOA and RAC are activated through two separate

ADIPOGENESIS
Development of fat cells (adipocytes) and formation of lipid bodies in adipocytes.

PHOSPHOLIPASE
An enzyme that cleaves phospholipids.

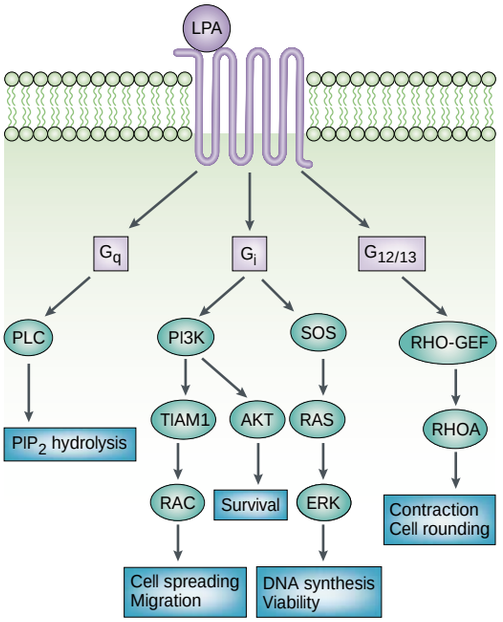

Figure 2 | **Major LPA signalling pathways.** LPA signals through its own G-protein-coupled receptors via at least three distinct classes of hetrotrimeric G proteins — G_q, G_i and $G_{12/13}$ — leading to activation of multiple downstream effector pathways. Among the main LPA-induced signalling pathways are: G_q (or/and G_i) -mediated activation of phospholipase C (PLC), which leads to the hydrolysis of phosphatidylinositol-bisphosphate (PIP_2), with consequent calcium mobilization and protein kinase C (PKC) activation; G_i-mediated activation of the RAS–ERK pathway, leading to cell proliferation; G_i-mediated activation of the PI3K–AKT (also known as PKB) 'survival' pathway, which suppresses apoptosis; and activation of the RHO and RAC GTPases via specific exchange factors, RHO-GEF and TIAM1, which leads to cytoskeletal remodelling (contraction and spreading), shape changes and cell migration.

G-protein pathways — $G_{12/13}$–RHO-GEF and G_i–PI3K–TIAM1 (REFS. 12,49,50,54). Their downstream effectors drive cell migration and invasion, but also impact on cell-cycle progression[33,55].

Finally, LPA induces cell-survival signalling through two pathways — via PI3K and AKT and through activation of the RAS/extracellular-signal-regulated kinase (ERK) pathway [33,51].

LPA receptors

Four mammalian cell-surface LPA receptors have been identified so far. The best known are LPA1, LPA2 and LPA3, which are all members of the so-called 'endothelial differentiation gene' (EDG) family of GPCRs and were formerly called EDG2, EDG4 and EDG7, respectively [58–62]. Five additional members of the EDG-receptor subfamily encode related GPCRs that are specific for the bioactive lysophospholipid SPHINGOSINE-1-PHOSPHATE (S1P)[63]. Recently, a fourth LPA receptor was identified (LPA4/GPR23/P2Y9), which shares no significant identity with the other LPA receptors[64]. LPA4 is more closely related to the purinergic (P2Y) GPCR family, yet does not bind nucleotides.

SPHINGOSINE-1-PHOSPHATE
A small lipid that is similar to LPA, but with a sphingosine rather than a glycerol backbone.

LPA1 is the most widely expressed receptor, with high mRNA levels in the colon, small intestine, placenta, brain and heart, and more modest expression in the pancreas, ovary and prostate[58]. Particularly high levels of LPA1 are present in the cerebral cortical ventricular zone during neurogenesis and in oligodendrocytes and Schwann cells in the adult. LPA2 and LPA3 have a more restricted distribution pattern compared with LPA1 (REFS. 58–62,65–66). Intriguingly, both LPA2 and LPA3 are aberrantly expressed in cancer cells, particularly in ovarian cancer cells, indicating a potential role in the pathophysiology of cancer[18,66–70]. LPA4 seems to be expressed at very low levels in most human tissues, although significant levels are found in the ovary[64].

Genetic studies with Lpa-receptor-null mice have shown the importance of LPA-receptor function for normal development. *Lpa1*-null mice show a failure to suckle, potentially due to decreased olfaction, leading to weight loss and partial neonatal mortality[71]. Cell migration, rounding and proliferation in response to LPA is decreased in embryonic fibroblasts from *Lpa1*-null mice, but is not absent, consistent with redundant signalling from LPA receptors. *Lpa2*-null mice show no obvious phenotypic aberrations[72] and, intriguingly, compound *Lpa1/Lpa2*-null mice do not show a phenotype different from that of *Lpa1*-null mice, except for a modest increase in frontal haematomas[72]. So, normal physiological functions either do not require LPA-receptor activation, or LPA3 and LPA4 (or other as yet unidentified LPA receptors) function redundantly. This also indicates that the main functions of the LPA receptors could become evident under pathophysiological conditions, such as wounding, inflammation or tumorigenesis, rather than during normal development. This further indicates that therapeutic modalities aimed at altering the function of specific LPA receptors might be well tolerated.

Nearly all mammalian cells, tissues and organs (except the liver) co-express several LPA-receptor subtypes of the EDG family, which strongly indicates that LPA receptors signal in a cooperative manner. However, which LPA receptor subtype couples to which G-protein-effector route(s) in a given cellular context is still not known. Heterologous expression studies have shown that each individual LPA receptor can mediate PLC activation, inhibition of cAMP accumulation and activation of the MAPK pathway, but there is considerable variation in the efficacy and potency that particular isoforms of LPA have for receptors, and the ability of receptors to link to particular downstream events. Indeed, in most systems LPA2 shows a higher affinity for LPA than for the other family members and couples more efficiently to production of neovascularizing factors (REF. 25 and E. Goetzl, personal communication). Similarly, LPA1 seems to be the main regulator of cellular motility[54,71,73].

Although a number of selective agonists and antagonists of the LPA receptors have been identified[52,61,62,74–81], their susceptibility to hydrolysis or the requirement for high concentrations of these inhibitors and lack of complete receptor specificity have hindered their use as therapeutic agents or probes of LPA-receptor function. The development of more selective inhibitors that cannot be

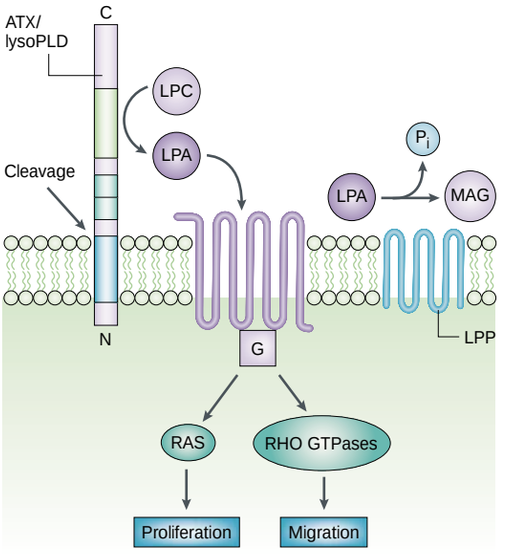

Figure 3 | **Regulation of bioactive LPA.** ATX/lysoPLD is synthesized as a large membrane-spanning glycoprotein that undergoes membrane-proximal proteolytic cleavage (not necessarily at the plasma membrane) to yield a secreted enzyme. Soluble ATX/lysoPLD hydrolyses LPC (and other lysophospholipids), which is abundantly present in the circulation, to generate LPA. Newly produced LPA acts on its own G-protein-coupled receptors to evoke its biological effects, including RAS-mediated cell proliferation and RHO/RAC-regulated cell migration. Excess LPA is converted into monoacylglycerol (MAG) by membrane-bound lipid phosphatases (LPPs) that remove the phosphate group from LPA.

hydrolysed is eagerly awaited. Nevertheless, the development of these molecules bodes well for the eventual ability to selectively target LPA receptors and functions.

The structural basis of receptor selectivity of LPA is beginning to be elucidated[52,61,62,74–82]. Molecular modelling could soon contribute to the development of receptor-selective agonists and antagonists that will both elucidate receptor function and serve as therapeutic mediators. For example, a single amino acid glutamine/glutamate exchange in transmembrane helix 3 between LPA1 and the S1P receptor S1P1 is sufficient to confer the ability to respond to the heterologous ligand[77], indicating that the binding specificity is probably conferred by modest structural changes in the receptors.

A number of important questions remain unanswered. For example, what is the nature of the signalling pathways that are activated by each individual LPA receptor, what are the downstream signal transducers and do distinct LPA receptors signal in a cooperative manner? Are the effects of activation of specific LPA receptors context dependent and altered by the particular intracellular machinery in the responding cell or by the cellular environment? How the diverse biochemical events activated by LPA are integrated into functional outcomes has remained particularly elusive. Future microarray studies, using specific LPA-receptor antagonists and agonists or cells in which LPA-receptor expression is selectively altered, might shed light on the unique gene-expression pattern that is induced by each LPA-receptor subtype in a given cellular context.

PLASMA
Fluid that is present in blood *in vivo*.

Extracellular metabolism of LPA

Physiologically significant concentrations of LPA are found not only in serum, but also in malignant effusions, saliva, follicular fluid, seminal plasma and in mildly oxidized LDL. In serum, and presumably in other body fluids, the main LPA-binding proteins/carriers are albumin and gelsolin[83–84]. One of the long-standing challenges has been to understand how bioactive LPA is produced and its level regulated in the cellular microenvironment. Emerging evidence indicates that bioactive LPA is generated extracellularly, rather than inside the cell, with subsequent secretion or release[85–87]. Indeed, a series of secreted and transmembrane ecto-enzymes are crucial for the production and metabolism of extracellular LPA[86–93] (FIGS 1,3). Steady-state PLASMA LPA levels are normally low (less than 100 nM)[86,87,94,95], representing the equilibrium between production, degradation and clearance. Unidentified factors in plasma and seminal fluid seem to inhibit LPA activity[87,96]. So, the effective levels of bioactive LPA in plasma are below those able to induce full activation of LPA receptors (usually observed at 100–200 nM LPA). Nevertheless, plasma contains both the enzymes and the lipid substrates that are required for LPA production. Incubation of plasma at 37°C, for example, results in an increase in LPA levels to those necessary to activate LPA receptors[86]. The mechanisms that restrict LPA production in plasma, as well as the triggers that increase LPA production during pathophysiological states, remain unclear. LPA is probably produced locally — following injury or stress such as wound healing — at the interface between cells and the interstitial fluid, and then migrates to plasma for degradation or clearance.

Whereas plasma levels of LPA are low, its concentration in serum is much higher at several micrometers (μM). LPA is produced following platelet activation[85,97], but the amount of LPA released is insufficient to explain LPA levels in serum[86,87]. Furthermore, the fatty acyl chain composition of LPA produced by platelets[85,97] differs from that in plasma or serum, which contains higher levels of LPA enriched with unsaturated fatty acids[87]. This indicates that different processes regulate production and degradation of LPA by platelets and in plasma, or following activation of the coagulation cascade.

LPA production

LPA can be produced by the sequential removal of a fatty acyl chain from phosphatidic acid by phospholipase A1 (PLA1) or phospholipase A2 (PLA2), or by the removal of choline from membrane phosphatidylcholine by ATX/lysoPLD (lyso phospholipase D)[86,87]. PLA1 releases fatty acids from the sn-1 position of membrane phospholipids (FIG. 1) that, when converted to LPA, produce sn-2 and polyunsaturated LPA isoforms that are selectively active on the LPA3 receptor[61,81]. Type-II secretory

Box 1 | Properties of ATX/lysoPLD

- Originally discovered as an autocrine motility factor (125 kDa) that is secreted by human melanoma cells and subsequently characterized as a transmembrane ecto-nucleotide phosphodiesterase (also termed NPP2).
- The soluble form is identical to plasma lysoPLD, which generates LPA from more complex lysophospholipids such as lysophosphatidylcholine (LPC).
- Widely expressed (highest expression in the brain, lung, ovary, kidney, intestine and testis).
- Upregulated in several cancers (including non-small-cell lung carcinoma, renal-cell carcinoma, mammary carcinoma, neuroblastoma and hepatocellular carcinoma).
- Upregulated by peptide growth factors (such as bFGF and BMP2), retinoic acid and WNT signalling (in mammary epithelial cells).
- Stimulates tumour aggressiveness, metastasis and angiogenesis in nude mice.
- ATX/lysoPLD-induced cell motility and proliferation are mediated by newly produced LPA.

phospholipase A2 (sPLA2), which cleaves fatty acyl chains from the sn-2 site (FIG. 1), has a limited ability to hydrolyse lipids in intact cell membranes, potentially contributing to the low levels of LPA in plasma. sPLA2 selectively hydrolyses lipids that are present in damaged membranes, membranes of activated cells, or microvesicles such as those released during apoptosis or that are produced by cancer cells[98,99]. Microvesicle numbers are particularly high in malignant fluids such as ASCITES, potentially contributing to the aberrant production of LPA in cancer patients[69,98,99,115–117].

The recent discovery that LPA is generated from lysophospholipids, particularly from lysophosphatidylcholine, by the previously enigmatic ATX/lysoPLD ecto-phosphodiesterase[90,91] (BOX 1; FIG. 3) — implicated in cell motility and tumour progression[100,102] — has shed light on how LPA is produced in the extracellular milieu. It has also provided impetus into studies of the role of ATX/lysoPLD and LPA in the metastatic cascade.

ATX was originally identified as an 'autocrine motility factor' secreted by melanoma cells[100] and was subsequently found to belong to the family of ecto-nucleotide phosphodiesterases (NPPs), which are capable of hydrolysing phosphodiester and pyrophosphate bonds that are typically found in ATP and ADP[101]. Therefore, ATX was previously thought to act via nucleotide (purinergic) receptor signalling. However, new work convincingly shows that ATX has lysoPLD activity and that the biological effects of ATX/lysoPLD can be attributed to the production of LPA and, potentially, S1P[90,91,103–105] (FIG. 3). Unexpectedly, it seems that ATX is a unique lysoPLD, in that its family members (NPP1 and NPP3) lack a similar phospholipase function[105].

ATX/lysoPLD is a transmembrane protein with a very short amino-terminal region, a single transmembrane domain, two cysteine-rich somatomedin-B-like domains — possibly involved in homodimerization — and a large catalytic ecto-domain[101]. Soluble ATX/lysoPLD is derived from the membrane-bound form by proteolytic cleavage, but details of ATX/lysoPLD biosynthesis and processing are still largely unknown. ATX/lysoPLD is widely expressed, with the highest mRNA levels in the brain, ovary, lung, intestine and kidney, and it is upregulated by certain peptide growth factors[106,107]. Targeted deletion and transgenic overexpression of ATX/lysoPLD in specific tissues should provide important insights into its (patho)physiological functions.

Outstanding questions concern the regulation of ATX/lysoPLD expression, activity and processing. Where is ATX/lysoPLD localized in cells? How and where is its proteolytic cleavage regulated? Does full-length ATX/lysoPLD exist on the cell surface? Is full-length ATX/lysoPLD catalytically active? What is the source of ATX/lysoPLD in plasma? How does ATX/lysoPLD participate in the development of pathophysiological states? Finally, how is its lipid substrate(s) locally produced? With regard to this last question, the main physiological substrate for ATX/lysoPLD is lysophosphatidylcholine (LPC) (FIG. 1). LPC is secreted by the liver and is abundantly present in plasma, where it is predominantly bound to albumin and, to a lesser extent, lipoproteins[108]. LPC is also found in the supernatant of cultured cells, presumably as a constituent of microvesicles that have been shed from the plasma membrane[92]. Interestingly, microvesicle shedding has been implicated in the metastatic cascade, with malignant body fluids (for example, ascites) containing large amounts of microvesicles[98,99]. So, ATX/lysoPLD could convert microvesicle-associated LPC into bioactive LPA, which would provide an explanation for the link between microvesicle shedding and metastasis.

The original identification of secreted ATX/lysoPLD as a tumour-motility factor indicates a link between ATX/lysoPLD and cancer, and strengthens the evidence for a role for LPA in the initiation and progression of cancer. Indeed, *ATX/lysoPLD* mRNA is upregulated in several human cancers, particularly melanoma, renal-cell carcinoma and glioma, and studies in nude mice have shown that ATX/lysoPLD enhances tumour aggressiveness[109]. Specifically, *Atx*-transfected, *Ras*-transformed NIH-3T3 cells are more invasive, tumorigenic and metastatic than *Ras*-transformed control cells. Further, the metastatic capability of breast cancer cells correlates with their ATX/lysoPLD levels[110]. These observations are compatible with the main activity of ATX/lysoPLD being due to production of LPA and its effects on protease production, cell motility, chemotaxis and invasion. Furthermore, ATX/lysoPLD can promote angiogenesis both *in vitro* and *in vivo*[102].

So, by generating LPA (and possibly other bioactive lysophospholipids), ATX/lysoPLD could contribute to tumour progression by providing an invasive and vasculogenic microenvironment for tumour cells. As a secreted or cell-surface enzyme, ATX/lysoPLD is a highly attractive pharmacological target for therapy and might be of diagnostic value.

ASCITES FLUID
Fluid that accumulates in the peritoneal cavity of ovarian cancer patients and occasionally in patients with other diseases, such as liver failure.

LPA inactivation

Production of bioactive LPA by ATX/lysoPLD is only half of the story: obviously, LPA accumulation must be counterbalanced by inactivation mechanisms. One possibility is that ATX/lysoPLD activity is tightly controlled by as-yet-unidentified cofactors or binding proteins. An alternative or additional mechanism is provided by inactivation of LPA itself. Indeed, exogenous LPA is rapidly dephosphorylated to yield biologically inactive monoacylglycerol. Recent advances have revealed that a family of lipid phosphate phosphohydrolases (LPPs), comprising at least four members, is responsible for the dephosphorylation of LPA and can therefore attenuate LPA signalling[79,88,89,93]. The LPPs are integral membrane ecto-enzymes, with six putative transmembrane domains[91]. Overexpression of LPPs in ovarian cancer cells decreases colony formation, increases apoptosis and decreases tumour growth *in vitro* and *in vivo*[93]. Interestingly, LPP activity can be increased by gonadotropin-releasing hormone analogues through recruitment of LPPs to the cell membrane[88]. So, LPA signal duration and strength is likely to depend, at least in part, on the expression level of LPPs, which are decreased in ovarian cancer[111], and their membrane localization relative to the LPA receptors. Pharmacological manipulation to increase LPP activity is an intriguing approach for cancer therapy.

LPA in the pathophysiology of cancer

The first indication that LPA could contribute to tumorigenesis came from studies showing that LPA increases motility and invasiveness of cells[3,9,21,22,24]. Studies from our groups, combined with the observation that ATX/lysoPLD mediates its effects through the production of LPA, have implicated LPA in the pathophysiology of ovarian cancer, and several studies have indicated a role for LPA in the initiation or progression of prostate, breast, melanoma, head and neck, bowel, thyroid and other cancers[5,23–25,52,66–70,73,99,101–104,109,111,112].

Ascites fluid in ovarian cancer patients provides a window on the cellular environment of the tumour, as well as on growth factors that are produced by tumour cells. Ascites fluid is a potent mitogen for ovarian cancer cells *in vitro* and *in vivo*[113–114]. A significant portion of this activity is mediated by LPA, which is present in ascites fluid at between 1 and 80 μM, exceeding levels required to optimally activate LPA receptors[70,95,115–117]. LPA is not produced at significant levels by normal ovarian epithelial cells, whereas ovarian cancer cells produce increased levels of LPA[69,118]. Prostate cancer cells also produce high levels of LPA and respond to LPA in an autocrine loop[112]. Surprisingly, LPA itself, as well as phorbol esters, are sufficient to increase production of LPA by some ovarian cancer cell lines, indicating the presence of autocrine networks[69,118]. Ovarian cancer cells do not express unusually high levels of *ATX/lysoPLD* mRNA; however, ATX/lysoPLD protein levels are increased in most ovarian cancers. Furthermore, as ovarian cancer patients present with large tumour masses, low-level production of ATX/lysoPLD or LPA by ovarian cancer cells might be sufficient to result in increased levels of LPA in ascites. Indeed, ATX/lysoPLD activity is increased in most ovarian cancer ascites. By contrast, *LPP1* mRNA levels are consistently decreased in ovarian cancer samples[110], indicating that LPA inactivation might be decreased, which would also contribute to the increased levels of LPA in ascites.

LPA2 and LPA3 are overexpressed by a significant fraction of ovarian cancer cells, contributing to the responsiveness of ovarian cancer cells to LPA[66–69]. LPA4 levels are particularly high in normal ovary[65], potentially contributing to the effects of LPA on ovarian cancer cells. Colorectal carcinoma cell lines show significant expression of *LPA1* mRNA and respond to LPA by cell migration and production of angiogenic factors[73]. It has been suggested that LPA2 overexpression has a role in the pathogenesis of thyroid cancer[70]. LPA3 was originally cloned from prostate cancer cells, concordant with the ability of LPA to induce autocrine proliferation of prostate cancer cells[62,112].

Lysophospholipids as tumour markers

The increased levels of LPA and vesicles in ascites from ovarian cancer patients indicated that, if LPA migrates from the peritoneal cavity into the circulation, it could be an early diagnostic marker, a prognostic indicator or an indicator of response to therapy. LPA levels are consistently higher in ascites samples than in matched plasma samples, which is compatible with this hypothesis[69]. Preliminary studies using purification followed by GAS CHROMATOGRAPHY (GC) indicated that levels of LPA or particular isoforms of LPA were increased in the plasma of approximately 90% of ovarian cancer patients[94,119]. LPA levels were not increased in samples from patients with breast cancer or leukaemia, but were increased in patients with myeloma, endometrial cancer and cervical cancer, as well as patients on renal dialysis[94,119–121]. A similar approach showed aberrations in particular LPC isoforms in plasma from ovarian cancer patients[122]. More recent studies using a mass-spectrometry approach failed to detect increased levels of LPA in plasma from ovarian cancer patients or alterations in levels of particular isoforms[95], although even this finding is controversial[12,124]. An analysis of ATX/lysoPLD activity failed to detect aberrant activity in blood samples from ovarian cancer patients[125]. The discrepancy between the results might represent differences in the technologies used or in the way in which the samples were collected or handled. It therefore remains possible that assessment of particular isoforms of the many different lysophospholipids present in plasma and ascites might provide diagnostic or prognostic information. Indeed, based on different backbones, fatty-acyl-chain linkage, location, length and saturation, and phosphate modification, several hundred different lysophospholipids could be present in plasma and ascites.

Prospects for the future

Almost half of all drugs in current use target members of the GPCR family, making LPA receptors attractive

LPPS
(Lipid phosphate phosphohydrolases). Cleave phosphate from LPA, sphingosine-1-phosphate, ceramide-1-phosphate and phosphatidic acid.

GAS CHROMATOGRAPHY
A method that is used to separate and identify small molecules.

targets for therapeutic development. As described above, LPA receptors are broadly expressed, including in the brain and vasculature, which has led to concerns about toxicity of inhibitors of LPA production or action. However, as compound *Lpa1/Lpa2*-null mice are viable and do not show marked functional aberrations in adult mice, it might be possible to target specific LPA receptors in tumour cells without undue systemic toxicity. LPA3 is particularly appealing as its expression is restricted and it is aberrantly expressed in multiple cancer lineages. Structure–function analysis, molecular modelling and studies of receptor structure are already contributing to the development of novel receptor-selective agonists and antagonists. However, as yet, therapeutically relevant LPA agonists and antagonists have not been developed. In addition to inhibition of receptor activation, LPA production and degradation could prove attractive targets for therapy. Both ATX/lysoPLD and LPPs are extracellular enzymes and are therefore readily available targets for therapy. In addition to its direct actions on tumour cells, LPA also prevents intestinal damage (epithelial apoptosis) in irradiated or chemotherapy-treated mice[126]. The latter finding indicates that diets that are rich in LPA or therapeutic modulation of LPA activity could be effective in reducing intestinal damage in patients undergoing cancer therapy. The development of selective LPA-receptor agonists and antagonists, as well as the identification of the pathways regulating LPA production and action, indicates that therapeutic approaches targeting the LPA cascade might be a realistic addition to the treatment of malignant disease in the near future. We look forward to the future, when the role of LPA and related lysophospholipids in the physiology, pathophysiology and management of cancer and other diseases is elucidated.

1. Hanahan, D. & Weinberg, R. A. The hallmarks of cancer. *Cell* **100**, 57–70 (2000).
2. van Corven, E. J., Groenink, A., Jalink, K., Eichholtz, T. & Moolenaar, W. H. Lysophosphatidate-induced cell proliferation: identification and dissection of signaling pathways mediated by G proteins. *Cell* **59**, 45–54 (1989).
   Seminal observation that LPA has growth-factor-like activities, and signals in a strictly G-protein-dependent manner.
3. Imamura, F. *et al.* Induction of *in vitro* tumour cell invasion of cellular monolayers by lysophosphatidic acid or phospholipase D. *Biochem. Biophys. Res. Commun.* **193**, 497–503 (1993).
4. Jalink, K., Hordijk, P. L. & Moolenaar, W. H. Growth factor-like effects of lysophosphatidic acid, a novel lipid mediator. *Biochim. Biophys. Acta* **1198**, 185–196 (1994).
5. Xu, Y., Fang, X. J., Casey, G. & Mills, G. B. Lysophospholipids activate ovarian and breast cancer cells. *Biochem. J.* **309**, 933–940 (1995).
6. Xu, Y., Casey, G. & Mills, G. B. Effect of lysophospholipids on signaling in the human Jurkat T cell line. *J. Cell Physiol.* **163**, 441–450 (1995).
7. Levine, J. S., Koh, J. S., Triaca, V. & Lieberthal, W. Lysophosphatidic acid: a novel growth and survival factor for renal proximal tubular cells. *Am. J. Physiol.* **273**, F575–F585 (1997).
8. Altun-Gultekin, Z. F. *et al.* Activation of Rho-dependent cell spreading and focal adhesion biogenesis by the v-Crk adaptor protein. *Mol. Cell Biol.* **18**, 3044–3058 (1998).
9. Stam, J. C., Michiels, F., van der Kammen, R. A., Moolenaar, W. H. & Collard, J. G. Invasion of T-lymphoma cells: cooperation between Rho family GTPases and lysophospholipid receptor signaling. *EMBO J.* **17**, 4066–4074 (1998).
10. Weiner, J. A. & Chun, J. Schwann cell survival mediated by the signaling phospholipid lysophosphatidic acid. *Proc. Natl Acad. Sci. USA* **96**, 5233–5238 (1999).
11. Jalink, K., Eichholtz, T., Postma, F. R., van Corven, E. J. & Moolenaar, W. H. Lysophosphatidic acid induces neuronal shape changes via a novel, receptor-mediated signaling pathway: similarity to thrombin action. *Cell Growth Differ.* **4**, 247–255 (1993).
    First demonstration that LPA induces neurite retraction in neuroblastoma cells.
12. Jalink, K., van Corven, E. J., Hengeveld, T., Morii, N., Narumiya, S. & Moolenaar, W. H. Inhibition of lysophosphatidate- and thrombin-induced neurite retraction and neuronal cell rounding by ADP ribosylation of the small GTP-binding protein *Rho*. *J. Cell Biol.* **126**, 801–810 (1994).
    First paper indicating a role for RHOA in LPA-induced 'dedifferentiation' of neuroblastoma cells, independently of classic second messengers.
13. Hill, C. S., Oh, S. Y., Schmidt, S. A., Clark, K. J. & Murray, A. W. Lysophosphatidic acid inhibits gap-junctional communication and stimulates phosphorylation of connexin-43 in WB cells: possible involvement of the mitogen-activated protein kinase cascade. *Biochem. J.* **303**, 475–479 (1994).
14. Tigyi, G. *et al.* Lysophosphatidic acid-induced neurite retraction in PC12 cells: control by phosphoinositide-Ca^{2+} signaling and Rho. *J. Neurochem.* **66**, 537–548 (1996).
15. Schulze, C., Smales, C., Rubin, L. L. & Staddon, J. M. Lysophosphatidic acid increases tight junction permeability in cultured brain endothelial cells. *J. Neurochem.* **68**, 991–1000 (1997).
16. Postma, F. R. *et al.* Acute loss of cell–cell communication caused by G protein-coupled receptors: a critical role for c-Src. *J. Cell Biol.* **140**, 1199–1209 (1998).
17. van Nieuw Amerongen, G. P., Vermeer, M. A. & van Hinsbergh, V. W. Role of RhoA and Rho kinase in lysophosphatidic acid-induced endothelial barrier dysfunction. *Arterioscler. Thromb. Vasc. Biol.* **20**, E127–E133 (2000).
18. Pustilnik, T. B. *et al.* Lysophosphatidic acid induces urokinase secretion by ovarian cancer cells. *Clin. Cancer Res.* **5**, 3704–3710 (1999).
19. Palmetshofer, A., Robson, S. C. & Nehls, V. Lysophosphatidic acid activates nuclear factor kappa B and induces proinflammatory gene expression in endothelial cells. *Thromb. Haemost.* **82**, 1532–1537 (1999).
20. Schwartz, B. M. *et al.* Lysophospholipids increase interleukin-8 expression in ovarian cancer cells. *Gynecol. Oncol.* **81**, 291–300 (2001).
21. Fishman, D. A., Liu, Y., Ellerbroek, S. M. & Stack, M. S. Lysophosphatidic acid promotes matrix metalloproteinase (MMP) activation and MMP-dependent invasion in ovarian cancer cells. *Cancer Res.* **61**, 3194–3199 (2001).
22. Zheng, Y., Kong, Y. & Goetzl, E. J. Lysophosphatidic acid receptor-selective effects on Jurkat T cell migration through a Matrigel model basement membrane. *J. Immunol.* **166**, 2317–2322 (2001).
23. Hu, Y. L. *et al.* Lysophosphatidic acid induction of vascular endothelial growth factor expression in human ovarian cancer cells. *J. Natl Cancer Inst.* **93**, 762–768 (2001).
24. Gschwind, A., Hart, S., Fischer, O. M. & Ullrich, A. TACE cleavage of proamphiregulin regulates GPCR-induced proliferation and motility of cancer cells. *EMBO J.* **22**, 2411–2421 (2003).
    Novel mechanism for transactivation of tyrosine-kinase receptors by G-protein-coupled receptors.
25. Fang, X. *et al.* Mechanisms of lysophosphatidic acid-induced cytokine production in ovarian cancer cells. *J. Biol. Chem.* (in the press).
26. Sturm, A., Sudermann, T., Schulte, K. M., Goebell, H. & Dignass, A. U. Modulation of intestinal epithelial wound healing *in vitro* and *in vivo* by lysophosphatidic acid. *Gastroenterology* **117**, 368–377 (1999).
27. Lee, H., Goetzl, E. J. & An, S. Lysophosphatidic acid and sphingosine 1-phosphate stimulate endothelial cell wound healing. *Am. J. Physiol. Cell Physiol.* **278**, C612–C618 (2000).
28. Watsky, M. A., Griffith, M., Wang, D. A. & Tigyi, G. J. Phospholipid growth factors and corneal wound healing. *Ann. NY Acad. Sci.* **905**,142–158 (2000).
29. Balazs, L., Okolicany, J., Ferrebee, M., Tolley, B. & Tigyi, G. Topical application of the phospholipid growth factor lysophosphatidic acid promotes wound healing *in vivo*. *Am. J. Physiol. Regul. Integr. Comp. Physiol.* **280**, R466–R472 (2001).
30. Daub, H., Weiss, F. U., Wallasch, C. & Ullrich, A. Role of transactivation of the EGF receptor in signalling by G-protein-coupled receptors. *Nature* **379**, 557–560 (1996).
    Demonstration of cross-talk between G-protein-coupled receptors and receptor protein tyrosine kinases.
31. Prenzel, N. *et al.* EGF receptor transactivation by G-protein-coupled receptors requires metalloproteinase cleavage of proHB-EGF. *Nature* **402**, 884–888 (1999).
32. Hordijk, P. L., Verlaan, I., van Corven, E. J. & Moolenaar, W. H. Protein tyrosine phosphorylation induced by lysophosphatidic acid in Rat-1 fibroblasts. Evidence that phosphorylation of map kinase is mediated by the G_i-p21ras pathway. *J. Biol. Chem.* **269**, 645–651 (1994).
33. Kumagai, N., Morii, N., Fujisawa, K., Nemoto, Y., & Narumiya, S. ADP-ribosylation of *rho* p21 inhibits lysophosphatidic acid-induced protein tyrosine phosphorylation and phosphatidylinositol 3-kinase activation. *J. Biol. Chem.* **268**, 24535–24538 (1993).
34. Holtsberg, F. W. *et al.* Lysophosphatidic acid induces necrosis and apoptosis in hippocampal neurons. *J. Neurochem.* **70**, 66–76 (1998).
35. Holtsberg, F. W. *et al.* Lysophosphatidic acid and apoptosis of nerve growth factor-differentiated PC12 cells. *J. Neurosci. Res.* **53**, 685–696 (1998).
36. Okusa, M. D. *et al.* Selective blockade of lysophosphatidic acid LPA3 receptors reduces murine renal ischemia-reperfusion injury. *Am. J. Physiol. Renal Physiol.* 27 May 2003 [epub ahead of print].
    Use of receptor-selective LPA agonists and antagonists *in vivo* to define the function and role of particular LPA receptors in ischaemia reperfusion.
37. Tokumura, A. *et al.* Lysophosphatidic acids induce proliferation of cultured vascular smooth muscle cells from rat aorta. *Am. J. Physiol.* **267**, C204–C210 (1994).
38. Tokumura, A., Yotsumoto, T., Masuda, Y. & Tanaka, S. Vasopressor effect of lysophosphatidic acid on spontaneously hypertensive rats and Wistar Kyoto rats. *Res. Commun. Mol. Pathol. Pharmacol.* **90**, 96–102 (1995).
39. Cerutis, D. R. *et al.* Lysophosphatidic acid and EGF stimulate mitogenesis in human airway smooth muscle cells. *Am. J. Physiol.* **273**, L10–L15 (1997).
40. Toews, M. L., Ustinova, E. E. & Schultz, H. D. Lysophosphatidic acid enhances contractility of isolated airway smooth muscle. *J. Appl. Physiol.* **83**, 1216–1222 (1997).
41. Rizza, C. *et al.* Lysophosphatidic acid as a regulator of endothelial/leukocyte interaction. *Lab. Invest.* **79**, 1227–1235 (1999).
42. Scalia, R., Pruefer, D. & Lefer, A. M. A novel lysophosphatidic acid analog, LXR-1035, inhibits leukocyte-endothelium interaction via inhibition of cell adhesion molecules. *J. Leukoc. Biol.* **67**, 26–33 (2000).
43. Hayashi, K. *et al.* Phenotypic modulation of vascular smooth muscle cells induced by unsaturated lysophosphatidic acids. *Circ. Res.* **89**, 251–258 (2001).

44. Natarajan, V., Scribner, W. M., Hart, C. M. & Parthasarathy, S. Oxidized low density lipoprotein-mediated activation of phospholipase D in smooth muscle cells: a possible role in cell proliferation and atherogenesis. *J. Lipid Res.* **36**, 2005–2016 (1995).
45. Siess, W. *et al.* Lysophosphatidic acid mediates the rapid activation of platelets and endothelial cells by mildly oxidized low density lipoprotein and accumulates in human atherosclerotic lesions. *Proc. Natl Acad. Sci. USA* **96**, 6931–6936 (1999).
Clear implication of LPA in atherosclerosis.
46. Schmidt, A. *et al.* Endophilin I mediates synaptic vesicle formation by transfer of arachidonate to lysophosphatidic acid. *Nature* **401**, 133–141 (1999).
Demonstration of a potential role for intracellular LPA in vesicle formation.
47. McIntyre, T. M. *et al.* Identification of an intracellular receptor for lysophosphatidic acid (LPA): LPA is a transcellular PPARgamma agonist. *Proc. Natl Acad. Sci. USA* **100**, 131–136 (2003).
Potential novel function for intracelullar LPA in the activation of the transcription factor PPARγ.
48. van Corven, E. J., Hordijk, P. L., Medema, R. H., Bos, J. L. & Moolenaar, W. H. Pertussis toxin-sensitive activation of p21ras by G protein-coupled receptor agonists in fibroblasts. *Proc. Natl Acad. Sci. USA* **90**, 1257–1261 (1993).
First paper showing that G-protein-coupled receptor ligands, including LPA, can activate RAS via pertussis-toxin-sensitive G_i and a putative protein tyrosine kinase.
49. van Dijk, M. C. *et al.* Exogenous phospholipase D generates lysophosphatidic acid and activates Ras, Rho and Ca^{2+} signaling pathways. *Curr. Biol.* **8**, 386–392 (1998).
First demonstration that a secreted phospholipase D (of bacterial origin) can generate LPA and activate LPA signalling pathways in mammalian cells.
50. Kranenburg, O. *et al.* Activation of RhoA by lysophosphatidic acid and $G_{12/13}$ subunits in neuronal cells: induction of neurite retraction. *Mol. Biol. Cell* **10**, 1851–1857 (1999).
51. Fang, X. *et al.* Lysophosphatidic acid prevents apoptosis in fibroblasts via G(i)-protein-mediated activation of mitogen-activated protein kinase. *Biochem. J.* **352**, 135–143 (2000).
52. Fang, X. *et al.* Lysophospholipid growth factors in the initiation, progression, metastases, and management of ovarian cancer. *Ann. NY Acad. Sci.* **905**, 188–208 (2000).
53. Kranenburg, O. & Moolenaar, W. H. Ras-MAP kinase signalling by lysophosphatidic acid and other G protein-coupled receptor agonists. *Oncogene* **20**, 1540–1546 (2001).
54. Van Leeuwen, F. N. *et al.* Rac activation by lysophosphatidic acid LPA1 receptors through the guanine nucleotide exchange factor Tiam1. *J. Biol. Chem.* **278**, 400–406 (2003).
Shows that LPA1 receptors signal RAC activation and cell migration via the invasion-inducing GDP/GTP exchange factor TIAM1.
55. Etienne-Manneville, S. & Hall, A. Rho GTPases in cell biology. *Nature* **420**, 629–635 (2002).
56. Takeda, H. *et al.* PI 3-kinase gamma and protein kinase C-zeta mediate RAS-independent activation of MAP kinase by a Gi protein-coupled receptor. *EMBO J.* **18**, 386–395 (1999).
57. Malliri A. *et al*. Mice deficient in the Rac activator Tiam1 are resistant to Ras-induced skin tumours. *Nature* **417**, 867–871 (2002).
58. Hecht, J. H., Weiner, J. A., Post, S. R. & Chun, J. Ventricular zone gene-1 (vzg-1) encodes a lysophosphatidic acid receptor expressed in neurogenic regions of the developing cerebral cortex. *J. Cell. Biol.* **135**, 1071–1083 (1996).
Identification and cloning of the first LPA receptor.
59. An, S., Dickens, M. A., Bleu, T., Hallmark, O. G. & Goetzl, E. J. Molecular cloning of the human Edg2 protein and its identification as a functional cellular receptor for lysophosphatidic acid. *Biochem. Biophys. Res. Commun.* **231**, 619–622 (1997).
60. An, S., Bleu, T., Hallmark, O. G. & Goetzl, E. J. Characterization of a novel subtype of human G protein-coupled receptor for lysophosphatidic acid. *J. Biol. Chem.* **273**, 7906–7910 (1998).
Identification and cloning of the second LPA receptor.
61. Bandoh, K. *et al.* Molecular cloning and characterization of a novel human G-protein-coupled receptor, EDG7, for lysophosphatidic acid. *J. Biol. Chem.* **274**, 27776–27785 (1999).
Cloning of *EDG7*/*LPA3*, the third LPA receptor.
62. Im, D. S. *et al.* Molecular cloning and characterization of a lysophosphatidic acid receptor, Edg-7, expressed in prostate. *Mol. Pharmacol.* **57**, 753–759 (2000).
Cloning of the third LPA receptor *EDG7*/*LPA3* from prostate cancer cells.
63. Hla, T., Lee, M. J., Ancellin, N., Paik, J. H. & Kluk, M. J. Lysophospholipids — receptor revelations. *Science* **294**, 1875–1878 (2001).
64. Noguchi, K., Ishii, S. & Shimizu, T. Identification of p2y9/GPR23 as a novel G protein-coupled receptor for lysophosphatidic acid, structurally distant from the Edg family. *J. Biol. Chem.* 30 Apr 2003 [epub ahead of print].
Identification of the fourth LPA receptor, *LPA4*.
65. Contos, J. J. & Chun, J. The mouse lp(A3)/Edg7 lysophosphatidic acid receptor gene: genomic structure, chromosomal localization, and expression pattern. *Gene* **267**, 243–253 (2001).
66. Fang, X. *et al.* Lysophosphatidic acid is a bioactive mediator in ovarian cancer. *Biochim. Biophys. Acta* **1582**, 257–264 (2002).
67. Goetzl, E. J. *et al.* Distinctive expression and functions of the type 4 endothelial differentiation gene-encoded G protein-coupled receptor for lysophosphatidic acid in ovarian cancer. *Cancer Res.* **59**, 5370–5375 (1999).
68. Furui, T. *et al.* Overexpression of edg-2/vzg-1 induces apoptosis and anoikis in ovarian cancer cells in a lysophosphatidic acid-independent manner. *Clin. Cancer Res.* **5**, 4308–4318 (1999).
69. Eder, A. M., Sasagawa, T., Mao, M., Aoki, J. & Mills, G. B. Constitutive and lysophosphatidic acid (LPA)-induced LPA production: role of phospholipase D and phospholipase A2. *Clin. Cancer Res.* **6**, 2482–2491 (2000).
70. Schulte, K. M., Beyer, A., Kohrer, K., Oberhauser, S. & Roher, H. D. Lysophosphatidic acid, a novel lipid growth factor for human thyroid cells: over-expression of the high-affinity receptor edg4 in differentiated thyroid cancer. *Int. J. Cancer* **92**, 249–256 (2001).
71. Contos, J. J., Fukushima, N., Weiner, J. A. & Kaushal, D. J. Requirement for the LPA1 lysophosphatidic acid receptor gene in normal suckling behavior. *Proc. Natl Acad. Sci. USA* **97**, 13384–13389 (2000).
Shows that *Lpa1*-knockout mice have reduced viability because of defects in suckling behaviour.
72. Contos, J. J. *et al.* Characterization of lpa(2) (Edg4) and lpa(1)/lpa(2) (Edg2/Edg4) lysophosphatidic acid receptor knockout mice: signaling deficits without obvious phenotypic abnormality attributable to lpa(2). *Mol. Cell Biol.* **22**, 6921–6929 (2002).
Shows that compound *Lpa1*/*Lpa2*-knockout mice have a phenotype that is not significantly different from *Lpa*1-knockout mice. This indicates redundancy in the system and strengthens the likelihood that drugs can be developed against LPA production or function.
73. Shida, D. *et al.* Lysophosphatidic acid (LPA) enhances the metastatic potential of human colon carcinoma DLD1 cells through LPA1. *Cancer Res.* **63**, 1706–1711 (2003).
74. Fischer, D. J. *et al.* Naturally occurring analogs of lysophosphatidic acid elicit different cellular responses through selective activation of multiple receptor subtypes. *Mol. Pharmacol.* **54**, 979–988 (1998).
75. Erickson, J. R., Espinal, G. & Mills, G. B. Analysis of the EDG2 receptor based on the structure/activity relationship of LPA. *Ann. N Y Acad. Sci.* **905**, 279–281 (2000).
76. Fischer, D. J. *et al.* Short-chain phosphatidates are subtype-selective antagonists of lysophosphatidic acid receptors. *Mol. Pharmacol.* **60**, 776–784 (2001).
Identification of a compound LPA1/LPA3 inhibitor. Low activity and stability limit use to *in vitro* studies.
77. Wang, D. A. *et al.* A single amino acid determines lysophospholipid specificity of the S1P1 (EDG1) and LPA1 (EDG2) phospholipid growth factor receptors. *J. Biol. Chem.* **276**, 49213–49220 (2001).
Definition of the structural characteristics that determine whether S1P1 and LPA1 will bind their respective ligands.
78. Heise, C. E. *et al.* Activity of 2-substituted lysophosphatidic acid (LPA) analogs at LPA receptors: discovery of a LPA1/LPA3 receptor antagonist. *Mol. Pharmacol.* **60**, 173–180 (2001).
Identification of a composite LPA1/LPA3 receptor antagonist with *in vivo* activity.
79. Hooks, S. B. *et al.* Lysophosphatidic acid-induced mitogenesis is regulated by lipid phosphate phosphatases and is Edg-receptor independent. *J. Biol. Chem.* **276**, 4611–4621 (2001).
80. Hasegawa, Y. *et al.* Identification of a phosphothionate analogue of lysophosphatidic acid (LPA) as a selective agonist of the LPA3 receptor. *J. Biol. Chem.* **278**, 11962–11969 (2003).
Identification of a stable agonist of LPA3 with *in vivo* applicability.
81. Bandoh, K. *et al*. Lysophosphatidic acid (LPA) receptors of the EDG family are differentially activated by LPA species. Structure–activity relationship of cloned LPA receptors. *FEBS Lett.* **478**,159–165 (2000).
82. Virag, T. *et al.* Fatty alcohol phosphates are subtype-selective agonists and antagonists of lysophosphatidic acid receptors. *Mol. Pharmacol.* **63**, 1032–1042 (2003).
Rational drug design identifies novel receptor-selective agonists and antagonists.
83. Tigyi, G. & Miledi, R. Lysophosphatidates bound to serum albumin activate membrane currents in *Xenopus* oocytes and neurite retraction in PC12 pheochromacytoma cells. *J. Biol. Chem.* **267**, 21360–21367 (1992).
84. Goetzl, E. J. *et al.* Gelsolin binding and cellular presentation of lysophosphatidic acid. *J. Biol. Chem.* **275**, 14573–14578 (2000).
85. Eichholtz, T., Jalink, K., Fahrenfort, I. & Moolenaar, W. H. The bioactive phospholipid lysophosphatidic acid is released from activated platelets. *Biochem. J.* **291**, 677–680 (1993).
86. Aoki, J. *et al.* Serum lysophosphatidic acid is produced through diverse phospholipase pathways. *J. Biol. Chem.* **277**, 48737–48744 (2002).
Describes the biochemical pathways regulating LPA production in plasma and serum.
87. Sano, T. *et al.* Multiple mechanisms linked to platelet activation result in lysophosphatidic acid and sphingosine 1-phosphate generation in blood. *J. Biol. Chem.* **277**, 21197–21206 (2002).
Elucidation of the mechanisms regulating the production of LPA in plasma and serum.
88. Imai, A., Furui, T., Tamaya, T. & Mills, G. B. A gonadotropin-releasing hormone-responsive phosphatase hydrolyses lysophosphatidic acid within the plasma membrane of ovarian cancer cells. *J. Clin. Endocrinol. Metab.* **85**, 3370–3375 (2000).
89. Xu, J. *et al.* Lipid phosphate phosphatase-1 and Ca^{2+} control lysophosphatidate signaling through EDG-2 receptors. *J. Biol. Chem.* **275**, 27520–27530 (2000).
Strong evidence implicating LPPs in the degradation of LPA and in limiting LPA signalling.
90. Tokumura, A. *et al.* Identification of human plasma lysophospholipase D, a lysophosphatidic acid-producing enzyme, as autotaxin, a multifunctional phosphodiesterase. *J. Biol. Chem.* **277**, 39436–39442 (2002a).
91. Umezu-Goto, M. *et al.* Autotaxin has lysophospholipase D activity leading to tumour cell growth and motility by lysophosphatidic acid production. *J. Cell Biol.* **158**, 227–233 (2002).
Shows that the long sought after lysoPLD was actually autotaxin. Opened a whole new era in LPA function and potential therapeutic application.
92. Sciorra, V. A. & Morris, A. J. Roles for lipid phosphate phosphatases in regulation of cellular signaling. *Biochim. Biophys. Acta* **1582**, 45–51 (2002).
93. Tanyi, J. L. *et al.* The human lipid phosphate phosphatase-3 decreases the growth, survival, and tumorigenesis of ovarian cancer cells: validation of the lysophosphatidic acid signaling cascade as a target for therapy in ovarian cancer. *Cancer Res.* **63**, 1073–1082 (2003).
Genetic validation of LPA production and action as a therapeutic target in ovarian cancer.
94. Xu, Y. *et al.* Lysophosphatidic acid as a potential biomarker for ovarian and other gynecologic cancers. *JAMA* **280**, 719–723 (1998).
Provocative preliminary data indicating that measurement of lysophospholipids might allow for early diagnosis of cancer.
95. Baker, D. L. *et al.* Plasma lysophosphatidic acid concentration and ovarian cancer. *JAMA* **287**, 3081–3082 (2002).
Careful analysis of the levels of LPA in plasma in ovarian cancer. Failed to confirm that plasma LPA levels are significantly increased in ovarian cancer patients.
96. Hama, K., Bandoh, K., Kakehi, Y., Aoki, J. & Arai, H. Lysophosphatidic acid (LPA) receptors are activated differentially by biological fluids: possible role of LPA-binding proteins in activation of LPA receptors. *FEBS Lett.* **523**, 187–192 (2002).
97. Gerrard, J. M. & Robinson, P. Identification of the molecular species of lysophosphatidic acid produced when platelets are stimulated by thrombin. *Biochim. Biophys. Acta* **1001**, 282–285 (1989).
98. Ginestra, A., Miceli, D., Dolo, V., Romano, F. M. & Vittorelli, M. L. Membrane vesicles in ovarian cancer fluids: a new potential marker. *Anticancer Res* **19**, 3439–3445 (1999).
99. Andre, F. *et al.* Malignant effusions and immunogenic tumour-derived exosomes. *Lancet* **360**, 295–305 (2002).
100. Stracke, M. L. *et al.* Identification, purification, and partial sequence analysis of autotaxin, a novel motility-stimulating protein. *J. Biol. Chem.* **267**, 2524–2529 (1992).

Identification of autotaxin as a motogen. Autotaxin would eventually be shown to be lysoPLD, the key enzyme regulating LPA production.
101. Murata, J. *et al.* cDNA cloning of the human tumour motility-stimulating protein, autotaxin, reveals a homology with phosphodiesterases. *J. Biol. Chem.* **269**, 30479–30484 (1994).
102. Nam, S. W. *et al.* Autotaxin (NPP-2), a metastasis-enhancing motogen, is an angiogenic factor. *Cancer Res.* **61**, 6938–6944 (2001).
Describes the role of autotaxin in neovascularization *in vivo*.
103. Koh, E. *et al.* Site-directed mutations in the tumor-associated cytokine, autotaxin, eliminate nucleotide phosphodiesterase, lysophospholipase D, and motogenic activities. *Cancer Res.* **63**, 2042–2045 (2003).
104. Clair, T. *et al.* Autotaxin hydrolyzes phospholipids to produce a migration stimulator, lysophosphatidic acid, or a migration inhibitor, sphingosine-1-phosphate. *Cancer Res.* (in the press).
105. Gijsbers, R., Aoki, J., Arai, H. & Bollen, M. The hydrolysis of lysophospholipids and nucleotides by autotaxin (NPP2) involves a single catalytic site. *FEBS Lett.* **538**, 60–64 (2003).
106. Bachner, D. *et al.* Bmp-2 downstream targets in mesenchymal development identified by subtractive cloning from recombinant mesenchymal progenitors (C3H10T1/2). *Dev. Dyn.* **213**, 398–411 (1998).
107. Tice, D. A. *et al.* Synergistic induction of tumour antigens by Wnt-1 signaling and retinoic acid revealed by gene expression profiling. *J. Biol. Chem.* **277**, 14329–14335 (2002).
108. Croset, M., Brossard, N., Polette, A. & Lagarde, M. Characterization of plasma unsaturated lysophosphatidylcholines in human and rat. *Biochem. J.* **345**, 61–67 (2000).
109. Nam, S. W. *et al.* Autotaxin (ATX), a potent tumour motogen, augments invasive and metastatic potential of ras-transformed cells. *Oncogene* **19**, 241–247 (2000).
Describes the role of autotaxin in the metastatic cascade *in vivo*.
110. Yang, S. Y. *et al.* Expression of autotaxin (NPP-2) is closely linked to invasiveness of breast cancer cells. *Clin. Exp. Metastasis* **19**, 603–608 (2002).
111. Tanyi, J. L. *et al.* 2003b Role of decreased levels of LPP-1 in accumulation of lysophosphatidic acid (LPA) in ovarian cancer. *Clinical Cancer Res.* (in the press).
112. Xie, Y., Gibbs, T. C., Mukhin, Y. V. & Meier, K. E. Role for 18:1 lysophosphatidic acid as an autocrine mediator in prostate cancer cells. *J. Biol. Chem.* **277**, 32516–32526 (2002).
Describes an autocrine LPA loop in the stimulation of prostate cancer cells.
113. Mills, G. B., May, C., McGill, M., Roifman, C. & Mellors, A. A putative new growth factor in ascitic fluid from ovarian cancer patients: identification, characterization and mechanism of action. *Cancer Res.* **48**, 1066–1071 (1988).
114. Mills, G. B. *et al.* Ascitic fluid from human ovarian cancer patients contains growth factors necessary for intraperitoneal growth of human ovarian cancer cells. *J. Clin. Invest.* **86**, 851–855 (1990).
115. Xu, Y. *et al.* Characterization of an ovarian cancer activating factor (OCAF) in ascites from ovarian cancer patients. *Clin. Cancer Res.* **1**, 1223–1232 (1995).
Shows that ascites from ovarian cancer patients contain high levels of bioactive LPA, including unusual LPA isoforms.
116. Westermann, A. M. *et al.* Malignant effusions contain lysophosphatidic acid (LPA)-like activity. *Ann. Oncol.* **9**, 437–442 (1998).
117. Xiao, Y. J. *et al.* Electrospray ionization mass spectrometry analysis of lysophospholipids in human ascitic fluids: comparison of the lysophospholipid contents in malignant vs nonmalignant ascitic fluids. *Anal. Biochem.* **290**, 302–313 (2001).
118. Shen, Z., Belinson, J., Morton, R. E., Xu, Y. & Xu, Y. Phorbol 12-myristate 13-acetate stimulates lysophosphatidic acid secretion from ovarian and cervical cancer cells but not from breast or leukemia cells. *Gynecol. Oncol.* **71**, 364–368 (1998).
119. Okita, M. Abnormal plasma lysophosphatidic acid level in ovarian cancer patients. *Bulletin of Faculty of Health and Welfare Science, Okayama Prefectural University* **1**, 29–35 (1994).
120. Sasagawa, T., Suzuki, K., Shiota, T., Kondo, T. & Okita, M. The significance of plasma lysophospholipids in patients with renal failure on hemodialysis. *J. Nutr. Sci. Vitaminol.* **44**, 809–818 (1998).
121. Sasagawa, T., Okita, M., Murakami, J., Kato, T. & Watanabe, A. Abnormal serum lysophospholipids in multiple myeloma patients. *Lipids* **34**, 17–21 (1999).
122. Okita, M., Gaudette, D. C., Mills, G. B. & Holub, B. J. Elevated levels and altered fatty acid composition of plasma lysophosphatidylcholine(lysoPC) in ovarian cancer patients. *Int. J. Cancer* **71**, 31–34 (1997).
123. Yoon, H. R., Kim, H. & Cho, S. H. Quantitative analysis of acyl-lysophosphatidic acid in plasma using negative ionization tandem mass spectrometry. *J. Chromatogr. B Analyt. Technol. Biomed. Life Sci.* **788**, 85–92 (2003).
124. Shen, Z. *et al.* Fatty acid composition of lysophosphatidic acid and lysophosphatidylinositol in plasma from patients with ovarian cancer and other gynecological diseases. *Gynecol. Oncol.* **83**, 25–30 (2001).
125. Tokumura, A. *et al.* Lack of significant differences in the corrected activity of lysophospholipase D, producer of phospholipid mediator lysophosphatidic acid, in incubated serum from women with and without ovarian tumors. *Cancer* **94**, 141–151 (2002).
126. Deng, W. *et al.* Lysophosphatidic acid protects and rescues intestinal epithelial cells from radiation- and chemotherapy-induced apoptosis. *Gastroenterology* **123**, 206–216 (2002).
Indicates that compounds that mimic LPA could decrease toxicity associated with cancer therapy under appropriate conditions.

Acknowledgements
We would like to thank E. Goetzl (University of California, San Fransisco) as well as members of our laboratories for allowing us to share unpublished data. This work is supported by grants from the National Cancer Institute (USA), Department of Defense (USA) and the Netherlands Cancer Institute (Holland).

Online links
DATABASES
The following terms in this article are linked online to:
Cancer.gov: http://www.cancer.gov/
breast cancer | cervical cancer | endometrial cancer | head and neck | melanoma | myeloma | ovarian cancer | prostate cancer
LocusLink: http://www.ncbi.nlm.nih.gov/LocusLink/
ATX | LPA1 | LPA2 | LPA3 | LPA4 | PLA1 | PLA2 | PLC | PPARγ | RAS | TIAM1

Journal of Cellular Biochemistry 92:1115–1140 (2004)

Lysophosphatidic Acid Production and Action: Validated Targets in Cancer?

Makiko Umezu-Goto,[1]* Janos Tanyi,[1] John Lahad,[1] Shuying Liu,[1] Shuangxing Yu,[1] Ruth Lapushin,[1] Yutaka Hasegawa,[1] Yiling Lu,[1] Rosanne Trost,[1] Therese Bevers,[1] Eric Jonasch,[1] Ken Aldape,[1] Jinsong Liu,[1] Robyn D. James,[2] Colin G. Ferguson,[3] Yong Xu,[4] Glenn D. Prestwich,[5] and Gordon B. Mills[6]

[1]Department of Molecular Therapeutics, MD Anderson Cancer Center, Houston Texas 77030
[2]Department of Pathology, MD Anderson Cancer Center, Houston Texas 77030
[3]Department of Clinical Cancer Prevention, MD Anderson Cancer Center, Houston Texas 77030
[4]Department of Genitourinary Medical Oncology, MD Anderson Cancer Center, Houston Texas 77030
[5]Department of Medicinal Chemistry, University of Utah, Salt Lake City, Utah 84108
[6]Echelon Biosciences, Salt Lake City, Utah 84108

Abstract The completion of the human genome project, the evolution of transcriptional profiling and the emergence of proteomics have focused attention on these areas in the pathophysiology and therapy of cancer. The role of lysophospholipids as potential mediators in cancer pathophysiology, screening and management has taken a major leap forward with the recent cloning of several enzymes involved in the metabolism of lysophospholipids. Lysophospholipids, although small molecules, contain a high ''informational'' content. Differences include the nature of the phosphate head group, the regiochemistry of the fatty acyl chain on the glyceryl backbone, the presence of ether versus ester linkages to the backbone, and the length and saturation of the fatty acyl or alkyl chain. This informational content is sufficient to result in a marked structure function activity relationship at their cognate receptors. Thus the emerging discipline of ''functional lipidomics'' is likely to prove as important as genomics and proteomics in terms of early diagnosis, prognosis, and therapy. Lysophospholipid levels are elevated in vivo in a number of pathophysiological states including ascitic fluid from ovarian cancer patients indicating a role in the pathophysiology of this devastating disease. Although controversial, levels of specific lysophospholipids may be altered in the blood of cancer patients providing a potential mechanism for early diagnosis. Several of the enzymes involved in the metabolism of lysophospholipids are aberrant in ovarian and other cancers. Further, the enzymes are active in the interstitial space, rendering them readily accessible to the effects of inhibitors including antibodies, proteins, and small molecules. In support of a role for lysophospholipids in the pathophysiology of cancer, expression of receptors for lysophospholipids is also aberrant in cancer cells from multiple different lineages. All of the cell surface receptors for lysophospholipids belong to the G protein coupled receptor family. As over 40% of all drugs in current use target this family of receptors, lysophospholipid receptors are highly ''druggable.'' Indeed, a number of highly specific agonists and antagonists of lysophospholipid receptors have been identified. A number are in preclinical evaluation as therapeutics. We look forward to the next several years when the role of lysophospholipids in physiology and the pathophysiology and management of cancer and other diseases are fully elucidated. J. Cell. Biochem. 92: 1115–1140, 2004.

Key words: lysophosphatidic acid; autotaxin; cancer; treatment

Overview

Lysophosphatidic acid, the simplest phospholipid, exhibits a broad spectrum of activity in many different cellular lineages and contributes to multiple physiological and likely to many pathophysiological processes in vivo [see Fang et al., 2002; Graler and Goetzl, 2002; Lynch and Macdonald, 2002; Mills et al., 2002; Yang et al., 2002a; Feng et al., 2003; Luquain et al., 2003a; Mills and Moolenaar, 2003; Tigyi and Parrill, 2003; Xu et al., 2003 for reviews and

Grant sponsor: NCI (to G.B.M.); Grant number: PO1 CA64602; Grant sponsor: DAMD (to G.B.M. and G.D.P.); Grant number: 17-02-1-0222; Grant sponsor: Cancer Center; Grant number: P30 CA16672.

*Correspondence to: Makiko Umezu-Goto, Graduate School of Pharmaceutical Sciences, the University of Tokyo, 7-3-1 Hongo, Bunkyo-ku, Japan. E-mail: mg@sendme.email.ne.jp

Makiko Umezu-Goto's current address is at the University of Tokyo.

Received 1 March 2004; Accepted 8 March 2004
DOI 10.1002/jcb.20113

elsewhere in this issue]. LPA mediates it effects by binding to G protein coupled receptors with subsequent activation of heterotrimeric G proteins and downstream events including increases in cytosolic calcium, alterations in cAMP levels, Rac and Rho small GTPases, activation of phospholipase C, protein kinase C, the phosphatidylinositol 3 kinase pathway, the RAS MAPK pathway, proteases and, by as yet somewhat unclear mechanisms, tyrosine kinases [Fang et al., 2002; Graler and Goetzl, 2002; Lynch and Macdonald, 2002; Mills et al., 2002; Yang et al., 2002a; Feng et al., 2003; Luquain et al., 2003a; Mills and Moolenaar, 2003; Tigyi and Parrill, 2003; Xu et al., 2003]. This latter effect is likely due, in part, to the activation of proteases and release of cell surface growth factors with subsequent activation of the epidermal growth factor receptor family [Prenzel et al., 1999; Gschwind et al., 2003]. There are four different LPA receptors so far characterized on the surface of mammalian cells, three members of the Edg family of receptors (LPA1, 2, 3 previously known as Edg 2, 4, 7, respectively), and a newly identified receptor LPA4 (previously GPR23/P2Y9) of the purinergic receptor family [Fang et al., 2002; Graler and Goetzl, 2002; Lynch and Macdonald, 2002; Mills et al., 2002; Yang et al., 2002a; Feng et al., 2003; Luquain et al., 2003a; Mills and Moolenaar, 2003; Noguchi et al., 2003; Tigyi and Parrill, 2003; Xu et al., 2003]. Through activation of these GPCR and subsequent downstream signaling, LPA induces cellular proliferation, cellular differentiation, regulates cell–cell interactions, inhibits cell death, increases cellular motility, increases invasiveness, increases the production of cytokines including those affecting formation and maintenance of new vessels, and increases the production and action of proteases [Fang et al., 2002; Graler and Goetzl, 2002; Lynch and Macdonald, 2002; Mills et al., 2002; Yang et al., 2002b; Feng et al., 2003; Luquain et al., 2003a; Mills and Moolenaar, 2003; Tigyi and Parrill, 2003; Xu et al., 2003]. On an organism level, LPA is implicated in complex physiological states such as immunological competence, brain development, wound healing, coagulation, and regulation of blood pressure [Fang et al., 2002; Graler and Goetzl, 2002; Lynch and Macdonald, 2002; Mills et al., 2002; Yang et al., 2002a; Feng et al., 2003; Luquain et al., 2003a; Mills and Moolenaar, 2003; Tigyi and Parrill, 2003; Xu et al., 2003]. LPA has recently been implicated as a physiological ligand for PPARγ, a member of the nuclear hormone receptor superfamily [McIntyre et al., 2002]. Recently, LPA was shown to induce neointima formation—a prelude to atherosclerosis in humans—by interaction with PPARγ in a rat carotid artery model [Zhang et al., 2004]. Importantly, LPA analogues that were inactive at the GPCRs were potent activators of PPARγ in this assay [Xu and Prestwich, 2002], demonstrating that LPA acting on this nuclear transcription factor was both necessary and sufficient for neointima formation.

As the effects of LPA are pleiomorphic and could potentially contribute to the development of multiple pathophysiological states, under normal circumstances the production and degradation of LPA is in a tight equilibrium with normal levels of LPA being in the 100–200 nM range or lower [Xu et al., 1998; Xiao et al., 2000; Shen et al., 2001; Aoki et al., 2002; Baker et al., 2002; Sano et al., 2002]. Levels of LPA are elevated during wound healing and in a number of physiological media such as saliva and ovarian cyst fluid [Westermann et al., 1998; Sugiura et al., 2002]. The physiological functions of LPA suggest that LPA could contribute to a number of pathophysiological states including cancer, autoimmune or immunodeficiency disease, atherosclerosis, and ischemia reperfusion injury [Fang et al., 2002; Graler and Goetzl, 2002; Mills et al., 2002; Yang et al., 2002a; Feng et al., 2003; Luquain et al., 2003a; Mills and Moolenaar, 2003; Okusa et al., 2003; Tigyi and Parrill, 2003; Xu et al., 2003]. Indeed as described above, the physiological responses to LPA parallel events, which must occur for the full expression of the malignant phenotype including the ability to invade and metastasize [Hanahan and Weinberg, 2000; Fidler, 2003]. Although the underlying mechanisms remain elusive, aberrations in production and degradation of LPA have been identified in cancer cells as well as in cancer patients, in particular in the markedly elevated levels of LPA in the ascitic fluid of ovarian cancer patients and in autocrine activation loops in ovarian and prostate cancer [Shen et al., 1998; Eder et al., 2000; Fang et al., 2002; Mills et al., 2002; Xie et al., 2002; Feng et al., 2003; Mills and Moolenaar, 2003; Sengupta et al., 2003]. In combination with alterations in LPA receptor expression and potentially receptor function in multiple cancer

lineages, this implicates LPA as an important mediator in the pathophysiology of cancer [Goetzl et al., 1999; Fang et al., 2002; Mills et al., 2002; Feng et al., 2003; Mills and Moolenaar, 2003]. As a corollary, LPA production and degradation, receptors and signaling are high quality targets for therapy [Feng et al., 2003; Mills and Moolenaar, 2003].

LPA Production

LPA is a critical component of the production and remodeling of lipids that occurs intracellularly. Both calcium-independent phospholipase A2 (iPLA2) and calcium-dependent PLA2 (cPLA2) contribute to this process intracellularly (Fig. 1). Intracellular LPA can activate the PPARγ receptor, however, the physiologic role of this process remains to be clarified [McIntyre et al., 2002; Zhang et al., 2004]. Through conversion to PA, LPA also regulates membrane curvature and formation of caveoli, which are critical to internalization and sorting of signaling complexes [Schmidt et al., 1999; Kooijman et al., 2003]. The unconventional lipid lysobisphosphatidic acid (LBPA) has recently been shown to induce the formation of multivesicular liposomes in vitro, and, with a protein partner Alix, the organization of endosomes in vivo [Matsuo et al., 2004]. Thus, by activating intracellular receptors and by serving as a substrate for enzymes such as endophilin and LCAT, LPA plays an important role in cellular functions (Fig. 1). Whether, under physiological conditions, extracellular LPA migrates to the cytosol in sufficient concentrations to contribute to these processes or whether intracellularly produced LPA is the only relevant source remains to be determined. Further, it is not clear that intracellular LPA is exported from the cell to participate in intercellular signaling. Indeed a series of secreted and ectoenzymes with their catalytic surface outside the cell appear critical to the production and metabolism of extracellular LPA.

As noted above, under physiological conditions, plasma LPA levels are maintained at low concentrations in the range of 100–200 nM [Xu et al., 1998; Xiao et al., 2000; Shen et al., 2001; Aoki et al., 2002; Baker et al., 2002; Sano et al., 2002]. LPA levels in plasma represent the steady state attained by separately regulated rates of production, degradation, and clearance. The removal of LPA from the bloodstream is extremely rapid, suggesting that degradation or clearance is very efficient. In addition to containing low levels of LPA, inhibitory factors in plasma limit LPA activity and production [Sano et al., 2002]. Thus the bioavailable levels of LPA in plasma may be below those able to optimally activate LPA receptors. Nevertheless, plasma contains both the enzymes and the substrates required for LPA production [Aoki et al., 2002; Sano et al., 2002]. Incubation of plasma at 37°C, e.g., results in an increase in LPC levels and a concomitant LPA increase resulting in the production of micromolar amounts of LPA [Aoki et al., 2002].

Cellular activation such as occurs during blood clotting, wound healing, or inflammation increases local production and action of LPA. Serum, in comparison to plasma, contains much higher levels of LPA with levels being between 1 and 5 μm [Aoki et al., 2002; Sano et al., 2002]. In tissue culture, it is likely that continuous production of LPC and LPA results in regeneration of LPA over time. Indeed, the regeneration of LPA, a potent growth and survival factor likely accounts for the quality of serum as a growth media. Platelets were initially proposed to be the main source of LPA in serum as they can produce LPA on activation [Gerrard and Robinson, 1989]. However, the amount of LPA released by activated platelets is insufficient to explain the increase in LPA levels that occur on blood clotting and likely accounts for only a small portion of the LPA present in serum [Aoki et al., 2002; Sano et al., 2002]. Further the fatty acyl chain composition of LPA produced by platelets [Gerrard and Robinson, 1989] 16:0 > 18:0 > 20:4 > 18:1 > 18:2 is markedly different from that present in plasma (18:2 > 18:1 = 18:0 > 16:0 > 20:4) or serum (20:4 > 18:2 > 16:0 = 18:1 > 18:0) [Sano et al., 2002]. This suggests that different molecular processes regulate production or degradation of LPA by platelets and the production and degradation of LPA that occurs in plasma or during the coagulation process that produces serum. LPA1 and -2 demonstrate selectivity towards saturated LPA as ligands, whereas LPA3 and -4 preferentially bind unsaturated versions of LPA [Bandoh et al., 1999; Yang et al., 2002a; Noguchi et al., 2003; Tigyi and Parrill, 2003]. Thus the different forms of LPA produced by platelets and during coagulation could activate different species of LPA receptors resulting in differential functions.

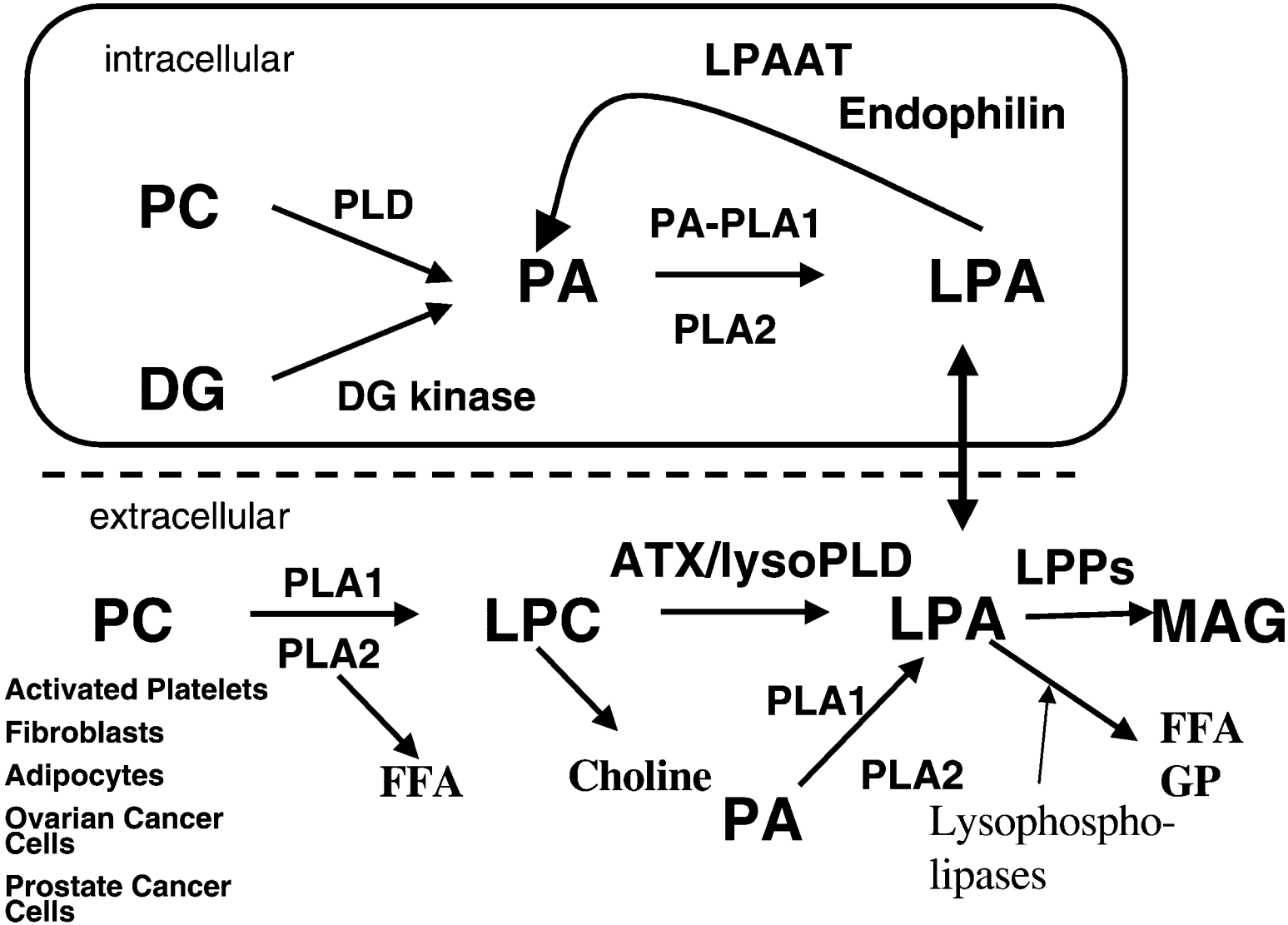

Fig. 1. LPA metabolism pathways the major intracellular and extracellular pathways of production and degradation of LPA are outlined. Whether intracellular and extracellular LPA are independent pools or whether there is exchange between these pools is unknown. Intracellular and extracellular LPA mediate different but important functions that could contribute to the pathophysiology of cancer. Cells known to produce LPA are indicated at the lower left.

Platelets contain high levels of phospholipases capable of cleaving phospholipids to produce lysophospholipids [Aoki et al., 2002; Sano et al., 2002]. Group IIA secretory phospholipase A2 (sPLA2, pancreatic) and phosphatidylserine-specific phospholipase A1 (PS-PLA1) are released from platelets activated by thrombin or calcium ionophores and likely contribute to the production of LPA by producing lysophosphatidylcholine (LPC), lysophosphatidylethanolamine (LPE), lysophosphatidylinositol (LPI), and lysophosphatidylserine (LPS) precursor molecules [Aoki et al., 2002; Sano et al., 2002]. PS-PLA1 produces *sn*-2 lysophospholipids with unsaturated fatty acyl chains. At either high or low pH, the *sn*-2 fatty acyl chain migrates to the *sn*-1 site with equilibrium favoring *sn*-1 lysophospholipids, however, at neutral pH *sn*-2 lysophospholipids are relatively stable. As noted above, these forms of LPA may selectively activate LPA3 and -4 [Bandoh et al., 1999; Noguchi et al., 2003]. In addition to sPLA2 IIA, it is also likely that several other isoforms of sPLA2 can contribute to LPA production following platelet activation or in serum as expression of sPLA2 isoforms in platelets is species dependent and also LPA production is not altered in mice genetically deficient in group IIA sPLA2 [Fourcade et al., 1998].

sPLA2 has limited ability to hydrolyze lipids in intact cell membranes [Kudo et al., 1993; Fourcade et al., 1995, 1998]. sPLA2 selectively hydrolyzes lipids present in damaged membranes, membranes of activated cells or microvesicles such as those released during apoptosis or produced by cancer cells to produce *sn*-1 lysophospholipids [Kudo et al., 1993; Fourcade et al., 1995, 1998]. Disruption of the membrane microenvironment by phosphatidic acid (PA) produced by the action of phospholipase (PLD) or activation of intracellular signaling pathways such as thrombin-induced increases in cytosolic calcium render cellular membranes more susceptible to the action of sPLA2 [Kudo et al., 1993; Fourcade et al., 1995, 1998; Kinkaid et al., 1998]. PLD also induces the production of extracellular microvesicles that are susceptible to the effects of sPLA2 [Morgan et al., 1997]. Strikingly, LPA induces the activation of PLD, increases cytosolic free calcium and increases PA levels compatible with LPA contributing to its own production [van der Bend et al., 1992; Kam and Exton, 2004]. The microenvironment wherein PS-PLA1 can hydrolyze lipids is not clear but it may also require access to substrates in particular structures limiting the production of LPA in plasma. Taken together, this suggests that LPA production likely occurs at sites of cellular injury or disruption. Further as tumors exhibit high levels of spontaneous apoptosis that produces vesicles, production of cellular vesicles and aberrations in membrane composition and symmetry [Fourcade et al., 1995; Ginestra et al., 1999; Andre, 2002], LPA may be produced at elevated levels in the tumor microenvironment.

In comparison to LPA, plasma contains high levels of phospholipids and lysophospholipids [LPC levels exceeding 100 μM and phosphatidylcholine (PC) levels approaching 1 mM]. Thus, precursors for LPA production are abundant. Indeed, incubation of plasma or serum at 37°C results in a time dependent increase in both LPC and LPA [Aoki et al., 2002]. However, despite the high concentrations of precursors, LPA levels are maintained at a low level. LPA production by plasma may be constrained in an inactive state by the presences of inhibitors [Sano et al., 2002]. This is consistent with a decreased rate of production of LPA in plasma as compared to serum [Aoki et al., 2002].

The source of phospholipids and lysophospholipids in plasma and sera that contribute to LPA production under physiological and pathophysiological conditions is not completely clear. Hepatocytes produce large amounts of lipids and lysophospholipids. LDL and HDL contain phospholipids, which can be converted to lysophospholipids by oxidation or by the action of sPLA2 or PS-PLA1 [Natarajan et al., 1995; Siess, 1999]. Indeed a number of responses to oxidized LDL or lysophospholipids such as LPC could potentially be mediated by conversion to LPA [Natarajan et al., 1995; Siess, 1999]. The still controversial suggestion that LPC-specific GPCRs exist [Kabarowski et al., 2001; Zhu et al., 2001; Bektas et al., 2003; Ludwig et al., 2003] suggests that LPC may mediate cellular signaling in addition to being a precursor for LPA.

A number of cell types produce lysophospholipids under physiological conditions. In blood cells, activation of platelets with thrombin or calcium ionophores results in the release of lysophospholipids [Aoki et al., 2002; Sano et al., 2002]. Erythrocytes can release small amounts of LPC. Both lecithin cholesterol acyltransferase

and platelet-activating factor acetylhydrolase (PAF-AH) have been implicated in production of LPC in plasma and sera. Studies by Aoki and colleagues using blood from patients deficient in LCAT and PAF-AH demonstrate that both LPC and LPA production is deficient in plasma from LCAT-deficient but not PAF-AH deficient patients [Aoki et al., 2002]. However, it is important to note that while basal LPC levels are slightly depressed in LCAT-deficient patients, they still are in the 100 μM range suggesting that plasma LPC originates from a source other than LCAT. Further the 100 μM of LPC present in plasma is far in excess of that required for the production of LPA. Patients with LCAT deficiency exhibit kidney dysfunction, anemia, and corneal opacification along with aberrations in plasma composition and amounts of cholesterol and other lipids [Gjone, 1982]. It is not clear whether LCAT-deficient patients exhibit decreased agonist induced LPA production in pathophysiological states and whether any of the consequences of the syndrome are due to LPA-deficiency. Indeed, these patients do not exhibit aberrations in processes proposed to be mediated by LPA such as wound healing or vessel development [Gjone, 1982].

In an independent pathway, PA produced by the action of PLD on cellular membranes can be hydrolyzed by sPLA2 or PA-specific PLA1 (PA-PLA1) to produce LPA [Hiramatsu et al., 2003]. The magnitude of the contribution of this pathway in physiologic or pathophysiologic conditions remains unknown (Fig. 1). A fluorogenic PLA1/2 assay using a PC analogue has been developed [Feng et al., 2002], and a fluorogenic substrate for PA-specific PLA activity has also been synthesized [Xu et al., 2004]. These assays can be used to determine activity or screen for inhibitors.

LysoPLD/Autotaxin

Plasma and sera contain a lysophospholipid specific PLD (lysoPLD), which cleaves lysophospholipids to produce LPA [Xu et al., 1998; Aoki et al., 2002]. LysoPLD exhibits a preference for lysophospholipids containing unsaturated fatty acyl chains and may thus contribute to the preferential increases in the unsaturated fatty acyl chain containing LPA present in plasma and sera. LysoPLD activity is increased in women in the third trimester of pregnancy and in women at risk for preterm labor suggesting that levels of lysoPLD can vary under physiological and pathophysiological conditions [Tokumura et al., 2002a]. LysoPLD activity is also increased in rabbits fed a high cholesterol diet [Tokumura et al., 2002b]. As LPA also increases attachment of monocytes to vascular endothelial cells, and alters proliferation, and differentiation, of vascular smooth muscle cells and is present in atherosclerotic plaques, lysoPLD with subsequent LPA production may contribute to atherosclerosis [Tokumura et al., 1994; Siess et al., 1999].

The cloning of LysoPLD and its identification as autotaxin (ATX, nucleotide phosphodiesterase/pyrophosphatase, NPP2, phosphodiesterase-Ialpha) by the Aoki and Tokumura groups [Tokumura et al., 2002c; Umezu-Goto et al., 2002] opened a new era in our understanding of the metabolism and, significantly, the function of LPA. ATX had been previously cloned from melanoma cells and studied by the Liotta group and others as autocrine motility factor, an inducer of cell motility, angiogenesis, invasiveness, metastasis, and tumor aggressiveness [Murata et al., 1994; Nam et al., 2000, 2001; Yang et al., 2002b]. Indeed, in retrospect, the actions and mechanisms of signaling of ATX and LPA demonstrated remarkable concordance suggesting an overlap in mechanisms. ATX is a member of the nucleotide phosphodiesterase/pyrophosphatase family, but in contrast to other members of the family, it exhibits the novel ability to hydrolyze LPC and sphingosylphosphorylcholine (SPC) to produce LPA and sphingosine 1-phosphate (S1P). All of the demonstrated activities of ATX appear to be related to its ability to hydrolyze lysophospholipids rather than to its nucleotide phosphodiesterase/pyrophosphatase activity [Koh et al., 2003]. At least in model systems, the relative production of S1P by ATX can inhibit the migratory effects of LPA suggesting that the outcome of autotaxin action may reflect the relative production of LPA and S1P [Clair et al., 2003].

ATX, a 125 kDa type II transmembrane protein, has a short intracellular domain and a large extracellular domain with the catalytic site localized near the membrane in the extracellular domain and thus readily accessible to extracellular LPA and S1P as well as to inhibitors and drugs (Fig. 2). While the mechanism of catalysis of ATX is well characterized [Koh et al., 2003], its post-translational processing, regulation of expression and mechanism of

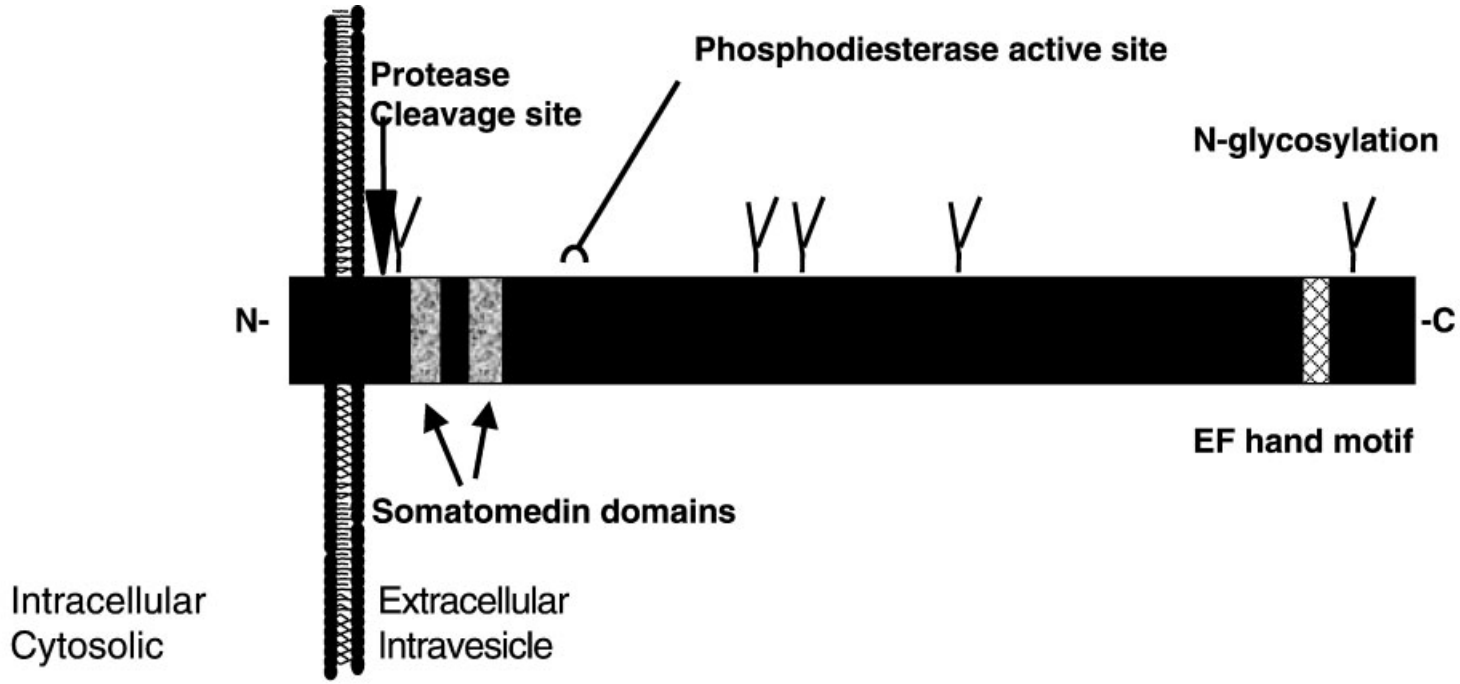

- 125 kDa type II membrane protein and released from membrane.
- 5'-nucleotide pyrophosphatase / phosphodiesterase family (NPP-2)
- Widely expressed
- Upregulated by bFGF, BMP-2, retinoic acid and Wnt-1signaling
- Stimulates tumor cell motility, metastasis and angiogenesis
- Metastatic capability relates to ATX levels in breast cancer
- Ectoenzyme Potential therapeutic target

Fig. 2. Characteristics of ATX/LysoPLD ATX is released from cells due to perimembrane cleavage. The mechanism and whether this happens intracellularly or at the cell surface is unknown as is the enzyme involved. The major action site of action of ATX is nevertheless extracellular.

release from cells are not well understood. Further, the relative activity of cell surface versus cleaved ATX is unknown. It is also not clear whether cleavage of ATX occurs in intracellular organelles or at the cell surface. Histochemical analysis suggests that that majority of ATX is localized in intracellular organelles rather than on the cell surface (not presented). However, as noted above, ATX and lysoPLD activity is found in bodily fluids and cell supernatants indicating that autotaxin is released from cells either following cleavage in organelles.

As assessed by SAGE analysis (http://cgap.nci.nih.gov/Sage/Viewer), levels of ATX are low in most cell lineages. Spinal cord has the highest level of expression of ATX suggesting a novel function in differentiated cells. Significant levels of ATX mRNA are also present in brain, breast, prostate, and hematopoietic cells. ATX can be upregulated by a number of cellular stimuli including growth factors such as bFGF and BMP2, retinoic acid and the WNT pathway [Bachner et al., 1998; Tice et al., 2002], however, the role of ATX and LPA in the function of these mediators is unknown. ATX can regulate proliferation of preadipocytes, and its production is increased during adipocyte differentiation and obesity implicating LPA production in obesity [Gesta et al., 2002; Ferry et al., 2003]. The mechanisms regulating ATX upregulation by these factors is unclear, however, MKK7, JNK, and Jun have been implicated in the process by several different approaches [Wolter et al., 2002; Black et al., 2004].

An analysis of ATX mRNA levels using a publicly available transcriptional profiling database (http://www.gnf.org/cancer/epican) indicates that levels of ATX mRNA are low in adult epithelial cells derived from a variety of tissues [Su et al., 2001]. As compared to the levels in normal epithelium, ATX mRNA levels are remarkably increased up to several thousand folds in kidney (renal cell carcinoma) tumors suggesting an important role in this tumor lineage (Fig. 3, Table I). Suppressed subtractive hybridization had previously demonstrated over expression of ATX in renal cell carcinoma [Stassar et al., 2001] compatible with these results. Renal cell carcinomas are amongst the most vascular tumors and contain high levels of angiogenic factors suggesting a potential role for LPA-mediated production of angiogenic factors such as VEGF, IL8, and IL6 in this disease [Takahashi et al., 1994]. This is compatible with our observations that LPA is a potent induced of angiogenic factors including VEGF, IL8, and IL6 and with the high levels of VEGF present in ovarian cancer ascites [Zebrowski et al., 1999; Hu et al., 2001; Schwartz et al., 2001; Fang et al., 2003]. According to the SAGE database, ATX mRNA levels are low to undetectable in normal kidney suggesting that the increased levels of autotaxin mRNA in renal cell carcinoma represent a novel acquisition of expression. ATX mRNA levels are more modestly but still markedly (100 fold) increased in a broad spectrum of cancers, including liver, gastric, ovary, lung, liver, prostate, and bowel (Fig. 3 and Table I). The modestly elevated levels in ovary and prostate may contribute to the autocrine LPA loops present in both of these tumors [Fang et al., 2002; Mills et al., 2002; Xie et al., 2002; Feng et al., 2003; Mills and Moolenaar, 2003]. It is important to note that within a given tumor type expression levels vary markedly with only modest or no increases in some tumors coupled with remarkable increases at least hundred fold in others. Transcriptional profiling data from Stanford [Schaner et al., 2003] and our own group indicates at least a 2 fold increase with a range of 1–12 in more that half of ovarian cancers as compared to normal ovarian epithelial cells. The discrepancy in relative increases between data sets likely arises from the low levels of ATX mRNA in normal tissues and need to use this as a comparator. Nevertheless, this confirms that ATX mRNA levels are increased in a number of cancer lineages.

We thus assessed ATX levels in a number of tumor cell lines using quantitative PCR. As indicated in Figure 4, ATX mRNA levels vary markedly among tumor cell lines [IOSE29 is used to represent a normal, non-transformed cell line, Auersperg et al., 1999]. However, compatible with the transcriptional profiling data, ATX levels were markedly elevated in a subset of tumor cell lines, particularly glioma and renal cell carcinomas. Even in these two cell lineages, some tumors show limited increases in ATX levels. More modest increases are observed in ovarian cancer cell lines with only limited changes in a subset of breast lines.

If the marked increase in mRNA levels of ATX in glioma and renal cell carcinoma (Figs. 3 and 4) results in release of active enzyme and diffusion into the plasma, ATX levels and ATX activity

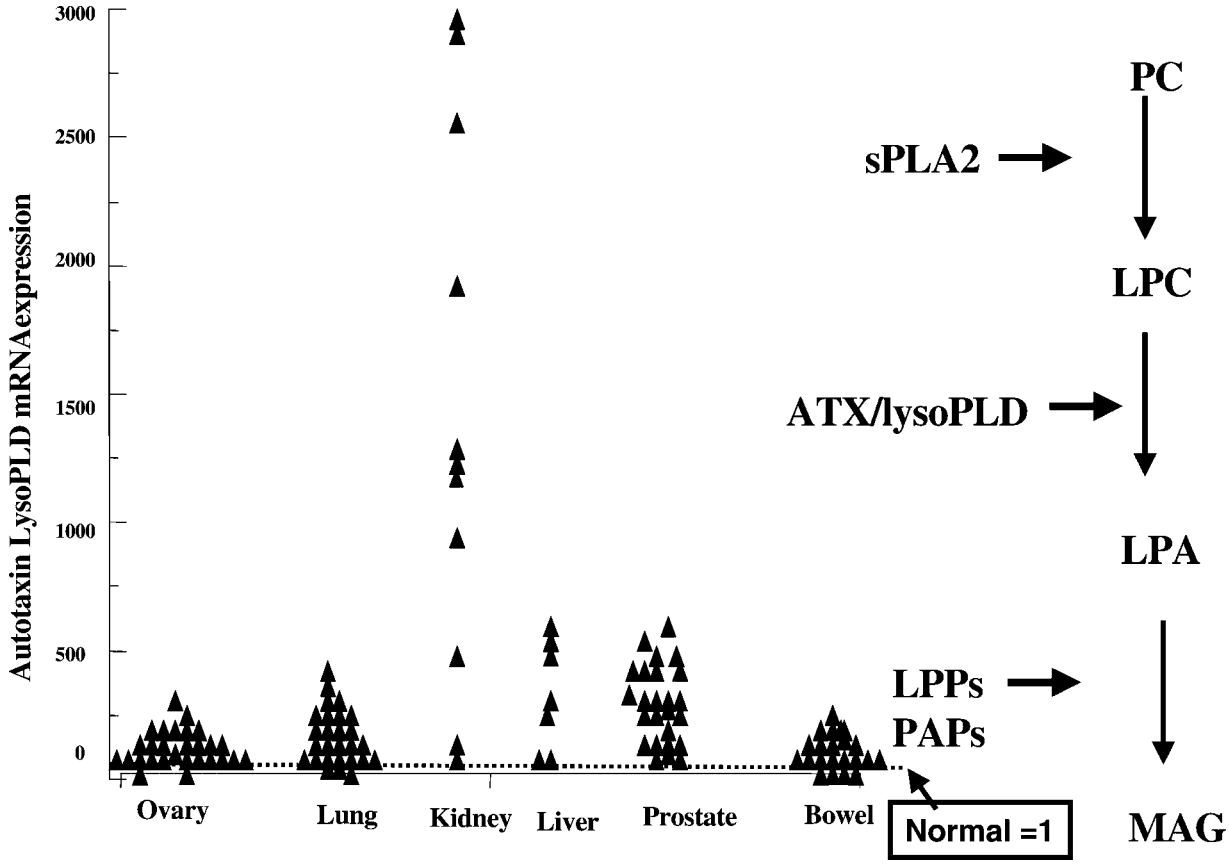

Fig. 3. ATX/LysoPLD mRNA levels are increased in cancer using a publicly available database of Affymetrix U95 arrays (http://www.gnf.org/cancer/epican 74), autotaxin mRNA levels are shown to be markedly aberrant in a number of tumor types. Data is expressed for each tumor relative to control values based on 36 normal adult epithelial tissues. As indicated in the figure, a number of tumors from each cell lineage express elevated levels of autotaxin mRNA.

could be markedly increased in a number of tumor types. To rapidly quantify the lysoPLD activity of ATX in patient samples, a novel fluorogenic assay was developed using the principles developed earlier for PLA activity measurement [Feng et al., 2002]. We thus evaluated ATX enzyme activity assay based on a quenched dye approach detecting the release of fluorescent ethanolamine from its quencher on a synthetic LPE [Drees et al., 2003; see Fig. 5 legend]. OVCAR3 express modest levels of ATX (Fig. 4) and also produces low levels of LPA in culture [Eder et al., 2000], compatible with the basal level of ATX activity. As indicated in Figure 6, cell supernatants from OVCAR3 cells induced a time dependent increase in fluorescence due to unquenching of the fluorescent dye. Further, fetal bovine serum, which contains high levels of ATX and supernatants from lysoPLD/ATX transfected OVCAR3 cells demonstrated increased lysoPLD activity (Fig. 6). This assay was used to assess the levels of ATX activity in plasma and sera samples from controls and patients. As indicated in Figure 7, levels of ATX activity in ovarian cancer ascites were markedly elevated as compared to plasma and sera. There was a statistically significant increase in ATX/lysoPLD activity in the plasma of patients at diagnosis with ovarian cancer and glioma but not in patients with breast cancer similar to the ATX mRNA levels in tumors and cell lines from these cancers (Fig. 7). Similar results were obtained for serum, which had modestly elevated activity as compared to plasma suggesting that ATX is activated (derepressed) or released from blood cells during the coagulation process. However, the increase in ATX activity in serum and plasma from cancer patients were modest as compared to normal controls and exhibited significant overlap

TABLE I. Analysis of Gene Expression Profiles of *LPP* Genes in Different Tumor Samples From Published Microarray Hybridization Data

	Type of cancer									
	Ovarian	Breast	Colon	Prostate	Kidney	Pancreas	Bladder	Liver	Gastric	Lung
Enzyme										
LPP-1	0.2 + 0.1	0.4 + 0.1	0.3 + 0.1	6.0 + 2.15	2.6 + 1.3	0.7 + 0.2	1.6 + 0.8	1.0 + 0.3	0.4 + 0.4	0.5 + 0.3
LPP-2	1.1 + 1.2	2.8 + 1.5	3.1 + 1.0	1.0 + 1.0	0.4 + 0.8	3.7 + 1.3	2.0 + 1.1	0.6 + 1.6	2.1 + 1.8	2.2 + 1.0
LPP-3	1.0 + 1.1	0.6 + 0.5	0.5 + 0.4	2.9 + 1.2	4.7 + 2.6	0.9 + 0.4	1.2 + 0.8	1.8 + 2.3	0.2 + 0.4	1.1 + 0.4
ATX	34.3 + 32	27.7 + 27	20.7 + 17	73.8 + 46	689 + 493	61.4 + 37	58.5 + 59	121 + 95	24.6 + 35	56.6 + 43.5

Affymetrix U95 array hybridization data are publicly available on 10 different primary human cancers and normal epithelial samples (http://www.gnf.org/cancer/epican 74). The control samples consisted of 36 normal adult epithelial tissues. To allow comparison across multiple tumor types, the mRNA expression data of each gene was normalized to the expression detected in normal epithelial cells. The data is expressed as average of expression ± standard deviation relative to normal epithelial cells. The sample numbers varied between from 6 to 28 for different tumor types.

with ATX levels in normal individuals (Fig. 7) suggesting that an analysis of ATX activity, at least by this approach, in serum or plasma would not provide clinically relevant data. This is in concordance with an earlier report on ovarian cancer sera that failed to detect clinically relevant increases in lysoPLD activity [Tokumura et al., 2002d].

Both LPA and ATX, through LPA production, have been implicated in the activation, proliferation and survival of several cancer cell lineages, but have not been assessed in the pathophysiology of renal cell carcinoma. As indicated above, the ability of ATX and LPA to induce the production of angiogenic factors combined with the high level of these factors produced by renal cell carcinoma cells suggested that ATX and LPA may be critical players in renal cell carcinoma. Given the high level of ATX mRNA in renal cell carcinomas and in the UM-RC-7 renal cell carcinoma cell line (Fig. 4), we explored the effects of decreasing ATX levels with siRNA on cellular signaling and on cell cycle progression and apoptosis in UM-RC-7 cells. As indicated in Figure 8, siRNA specific to autotaxin markedly downregulates ATX expression, an effect that persists for at least 72 h. Compatible with decreased endogenous LPA production, activated MAPK and AKT levels decreased, albeit with greater decreases at later time points (Fig. 8) (total AKT and total MAPK serve as loading controls indicating that equal amounts of proteins were assessed). The delayed decrease in cell signaling as compared to ATX levels may reflect persistence of extracellular ATX or of LPA in supernatants. Nevertheless, siRNA effectively downregulates ATX expression in UM-RC-7 cells and down regulation of ATX is associated with a marked decrease in cell signaling.

We thus explored the effects of down regulation of ATX on cell cycle progression and apoptosis as indicated by cells with a hypodiploid DNA content. In UM-RC-7 cells in both the presence and absence of sera, down regulation of ATX, resulted in an arrest of cells in S phase with an accumulation of apoptotic cells as indicated by an increase in hypodiploid (sub G0/G1) cells (Fig. 9). Similar increases in apoptosis and accumulation of cells in S phase were noted in both glioma and breast cancer cells (not presented). The marked accumulation of cells in S phase was unexpected and suggests activation of the intra-S cell cycle checkpoint, an enigmatic

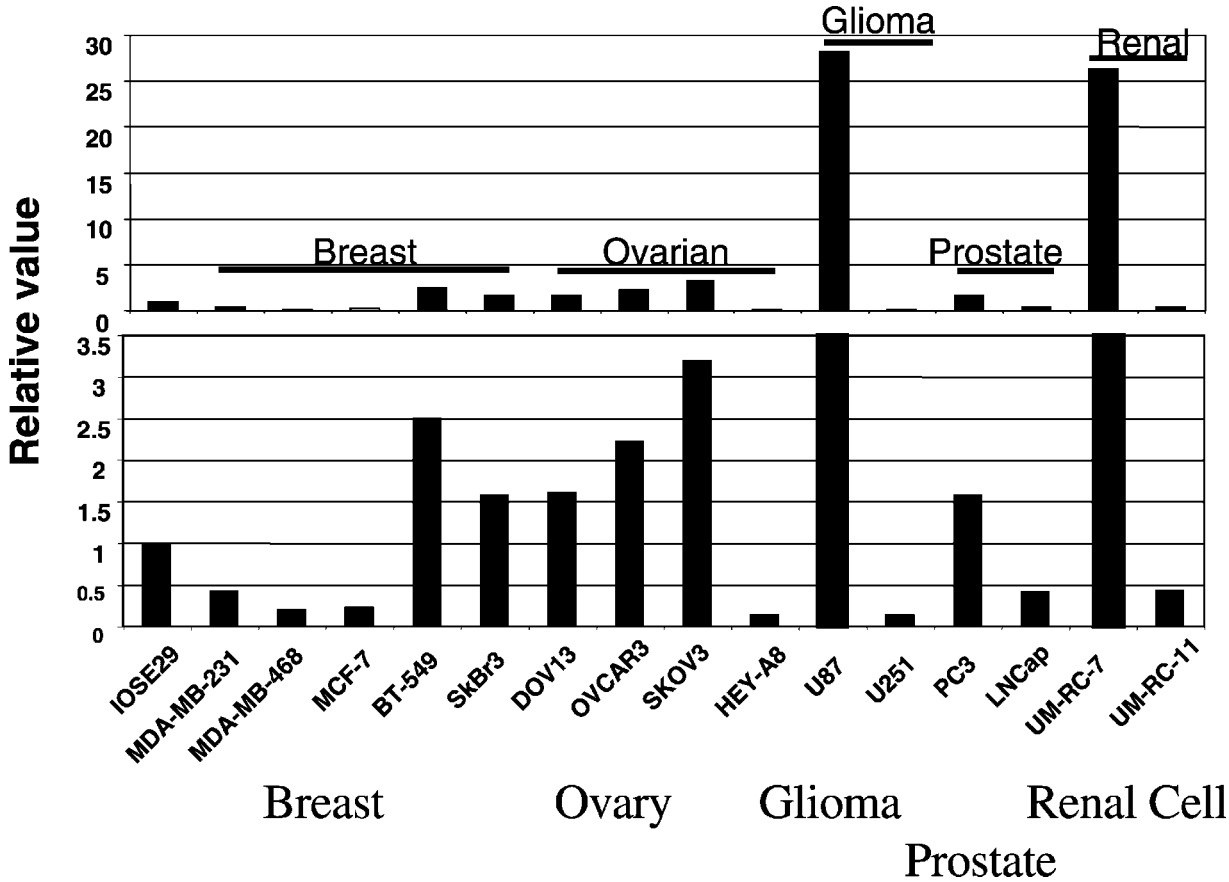

Fig. 4. LysoPLD/ATX RNA levels in tumor cell lines Quantitative PCR was performed on a series of breast, ovarian, glioma, prostate and renal cancer cell lines. Data is normalized to IOSE 29, a SV40 T antigen semi-immortalized cell line that is set to 1. As indicated in the figure, the levels of ATX/lysoPLD mRNA are variable between cell lines including within specific tumor types. U87, a glioma cell line, and UM-RC-7, a renal cell line, express markedly elevated levels of ATX/lysoPLD RNA levels.

check point previously implicated in repair of DNA damage. We have previously overexpressed LPA phosphatases (LPPs) in ovarian cancer cells [see below Tanyi et al., 2003a,b], which increase LPA hydrolysis and should thus have similar effects to autotaxin siRNA that decreases LPA production. Indeed, overexpression of LPPs resulted in an accumulation, albeit more modest that ATX siRNA, in cells in S phase as well as increased apoptosis. The mechanism leading to an increased in cells in S phase is unknown and the topic of ongoing studies.

Taken together, ATX mRNA levels are markedly elevated in a number of cancer cell lineages. Although ATX activity is increased in the plasma and serum from patients with particular types of cancer, the increases are modest and unlikely to be clinically or diagnostically relevant. However, increased autotaxin activity at the tumor cell interstitial fluid interface is likely to result in increased production of LPA. Indeed, in ovarian cancer patients, genes that are co-regulated with ATX comprise an LPA-dependent transcriptome (not presented), potentially providing a method to identify LPA-dependent tumors likely to be responsive to manipulation of ATX activity or LPA expression. In tumor cell lines over expressing ATX, silencing of ATX with siRNA to ATX results in decreased transmembrane signaling, S phase arrest, and accumulation of apoptotic cells. This combined with previous data implicating ATX in tumor proliferation, motility, aggressiveness, and metastases validates autotaxin and by implication LPA production and action as a target for tumor therapy. As ATX functions as an extracellular enzyme, it is highly accessible for inhibition by antibodies, peptides, pseudosubstrates, or small molecule drugs.

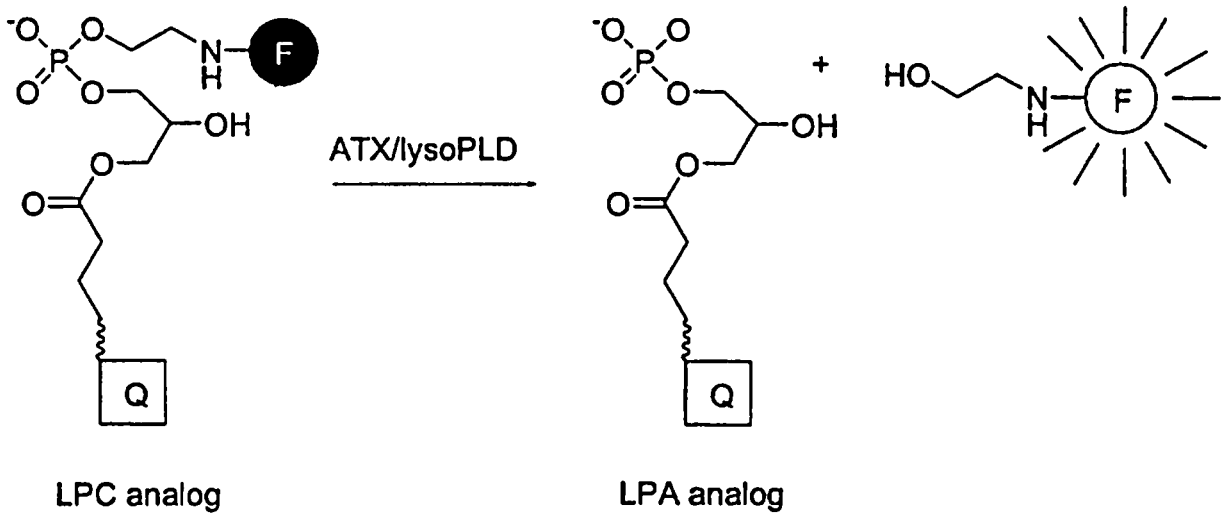

Fig. 5. Quenched fluorescence lysoPLD enzyme assay. A quenched cleavable substrate assay similar that developed for PLA2 [Feng et al., 2002] was established for LysoPLD. A doubly labeled substrate analog based on LPE was synthesized containing fluor and quencher moieties. The close intramolecular proximity of the quencher and fluorescent groups results in effective quenching of fluorescence by energy transfer in the substrate. Upon digestion by lysoPLD, the ethanolamine group containing the fluor is released, energy transfer is interrupted, and fluorescence increases as a function of the extent of lipase activity.

LPA Degradation

LPA can be removed by cleavage of the acyl chain by phospholipases, reacylation by LPAAT or endophilin, or by hydrolysis of the phosphate by lysophosphatidic acid phosphatases [LPP-1, -2, -3 also know and PAPs or PA phosphatases, Brindley et al., 2002; Mills et al., 2002; Tanyi et al., 2003a,b; see studies in this review]. LPPs are hexahelical transmembrane lysolipid phosphatases with an extracellular catalytic site, suggesting a role in hydrolysis of extracellular LPA. Although different LPPs demonstrate modest selectivity for lysophospholipid isoforms, each of the LPP isoforms can hydrolyze LPA, S1P or ceramide 1-phosphate and likely other lysophospholipids. They exhibit little activity however toward PA or other diacyl chain lipids. Over 95% of hydrolysis of LPA by cancer cells appears to be due a membrane associated LPP activity suggesting that LPPs are the major method for clearance of LPA in vivo [Imai et al., 2000]. As indicated in Table I (relative levels) and Figure 10 (absolute levels), LPP mRNA levels and in particular LPP-1 mRNA levels demonstrate marked variability in different tumor lineages. For example, LPP levels are elevated in prostate and kidney cancers whereas they are markedly decreased in ovary, lung, and breast cancer. Intriguingly, prostate and renal cell carcinomas, which have high levels of autotaxin mRNA (Table I, Fig. 3) also exhibit elevated levels of LPP-1 mRNA. Thus there is likely to be an increased production and hydrolysis of LPA in these tumor types with potentially increased information flow through the pathway. What the net effect of overexpression of both ATX and LPP-1 is on LPA production and degradation is remains to be assessed. LPP-1 levels are markedly decreased in ovarian cancer (Table I, Fig. 10), potentially contributing to the elevated levels of LPA present in ascites. We have explored the role of LPPs in ovarian cancer by increasing expression of LPP-1 and determining effects on cellular functions [Tanyi et al., 2003a,b]. In most ovarian cancer cells, overexpression of LPPs is incompatible with cell proliferation and survival. Overexpression of LPP-1 or LPP-3 in SKOV3 cells which have high levels of ATX (Fig. 4) and produce LPA spontaneously [Eder et al., 2000] is tolerated by the cells. Stable LPP overexpression decreases LPA levels, increases LPA hydrolyses, inhibits cell cycle progression resulting in an S phase arrest and accumulation of apoptotic cells and decreases growth subcutaneously and intraperitoneally [Tanyi et al., 2003a,b]. In a typical experiment (Fig. 11), transient overexpression of LPPs markedly decreases colony forming cell activity. Strikingly, this effect is reversed by addition of XY-13 (Fig. 11) and XY-14, two enantiomeric phosphonate analogues of PA [Xu and Prestwich, 2002], that act as potent inhibitors of the

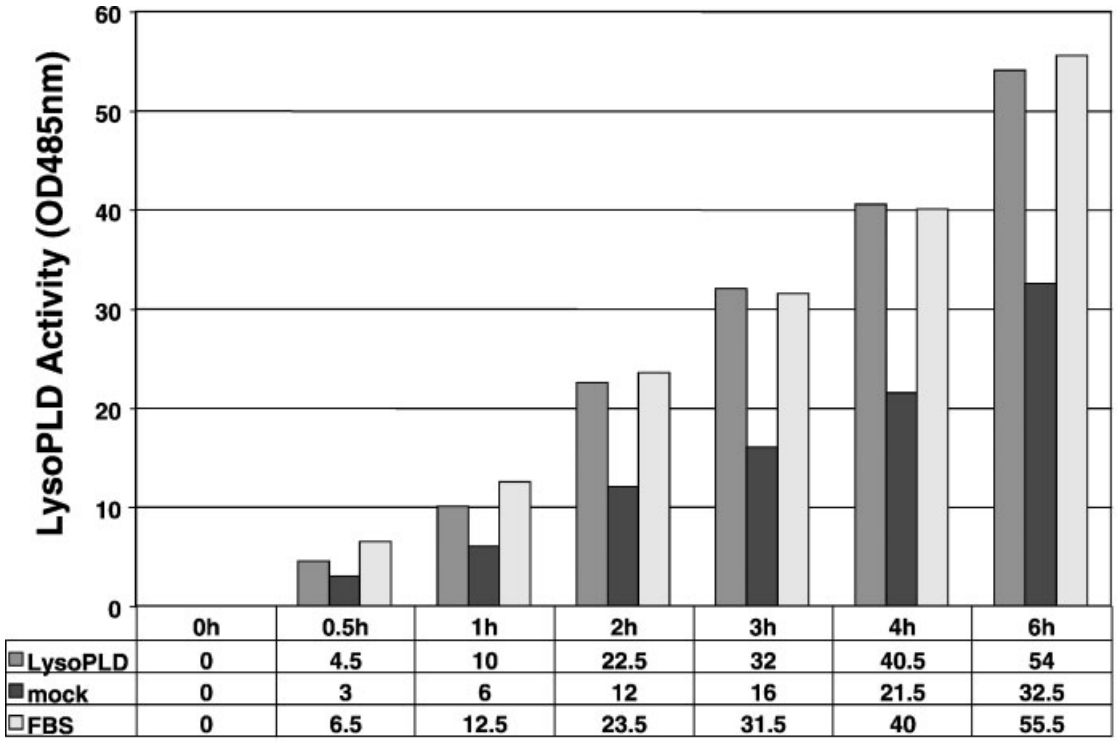

	0h	0.5h	1h	2h	3h	4h	6h
LysoPLD	0	4.5	10	22.5	32	40.5	54
mock	0	3	6	12	16	21.5	32.5
FBS	0	6.5	12.5	23.5	31.5	40	55.5

The culture media from ATX / LysoPLD or control vector transfected OVCAR3, and FBS were subjected to LysoPLD assay. They showed time-dependent increase in activity and an increase in transfected cells.

Fig. 6. Validation of the lysoPLD assay. The quenched cleavable lysoPLD assay described in Figure 1, was validated by incubation with supernatants from lysoPLD and mock transfected OVCAR3 cells (OVCAR3 cells have modest lysoPLD mRNA levels) as well as with fetal bovine serum, which has high levels of lysoPLD [Umezu-Goto et al., 2002]. As indicated in the figure, following background subtraction there is a linear time dependent increase in lysoPLD substrate cleavage.

LPPs [Smyth et al., 2003]. The effect is also reversed by OMPT an LPP-resistant LPA analog [Hasegawa et al., 2003] that shows enantioselective activation of LPA3 [Qian et al., 2003] confirming that the effect of the LPPs is through degradation of LPA (Fig. 11). In support of hydrolysis of LPA as a mechanism of action, overexpression of LPPs in SKOV3 cells resulted in a marked decrease in the proliferation and survival of non-transfected SKOV3 cells, a bystander effect. This extracellular mechanism of action and strong bystander effect is optimistic for potential gene therapy approaches to ovarian cancer, a process being explored by our group.

The combined studies with autotaxin siRNA and overexpression of LPPs provide strong evidence validating the LPA pathway as a target for therapy in cancer. This suggests that drugs targeting autotaxin, which is relatively specific for LPA production (SPC levels are low extracellularly compared to LPC), or specific LPA receptors or their downstream signaling pathways may have efficacy in the therapy of cancer [Tokumura et al., 2002c; Umezu-Goto et al., 2002; Clair et al., 2003]. As indicated above, LPA and autotaxin have pleiomorphic effects in multiple cell lineages, suggesting that inhibition of the LPA production or action may be toxic. However, knockouts of LPA1 and -2 and indeed combined LPA1 and -2 knockout mice are viable suggesting either that these pathways are not required for normal cellular physiology or that LPA3 and -4 exhibit redundant activities [Yang et al., 2002a]. These questions will be answered through the development

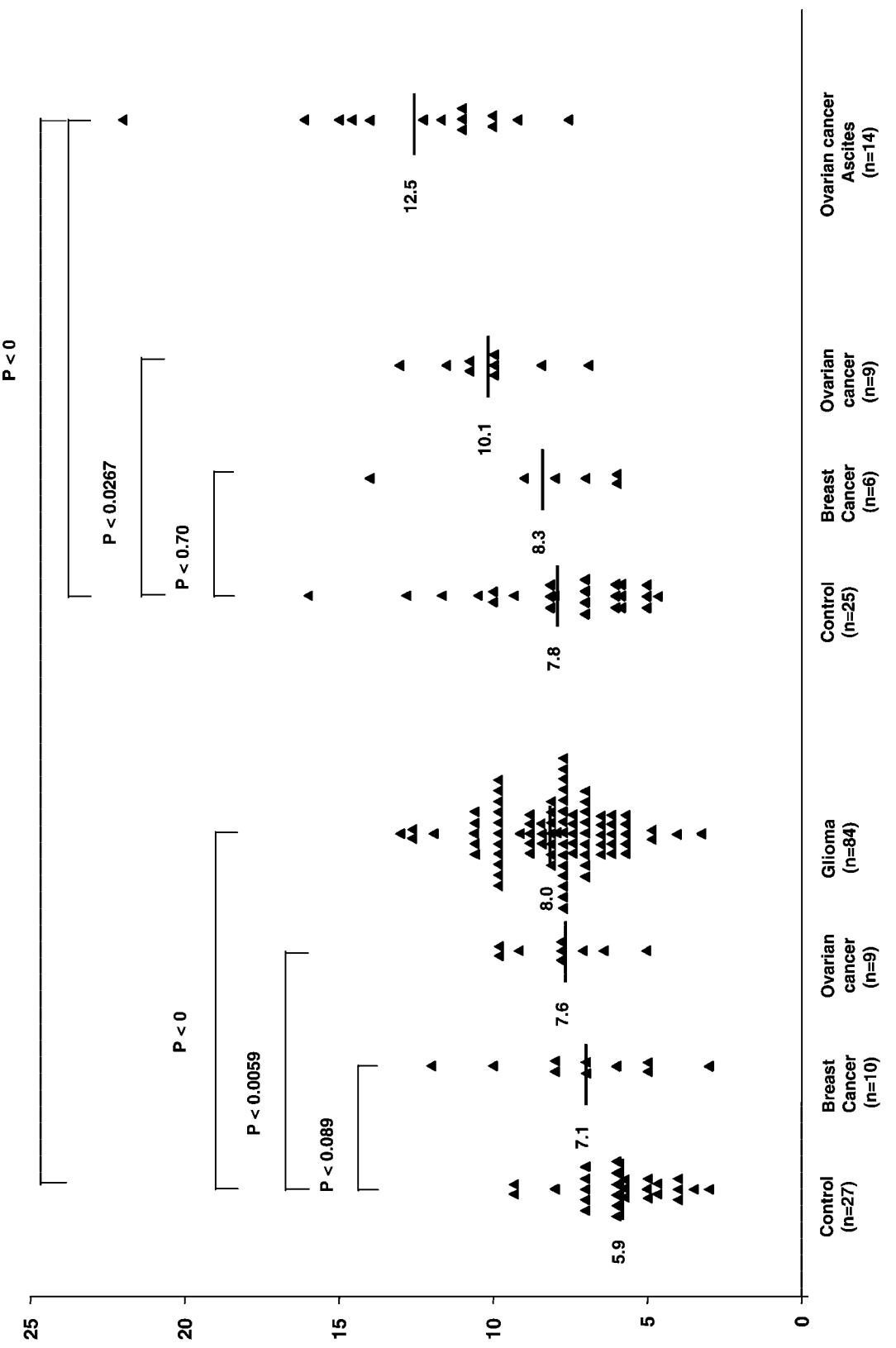

Fig. 7. LysoPLD activity in patient samples using the validated lysoPLD assay. lysoPLD enzyme activity was measured in serum and plasma of patients with glioma, ovarian cancer or breast cancer. Serum and plasma activity was assessed for breast and ovary and ascites levels for ovarian cancer. Mean levels are indicated by a bar for each set. Statistically different results (Student's *t*-test) are indicated in the figure.

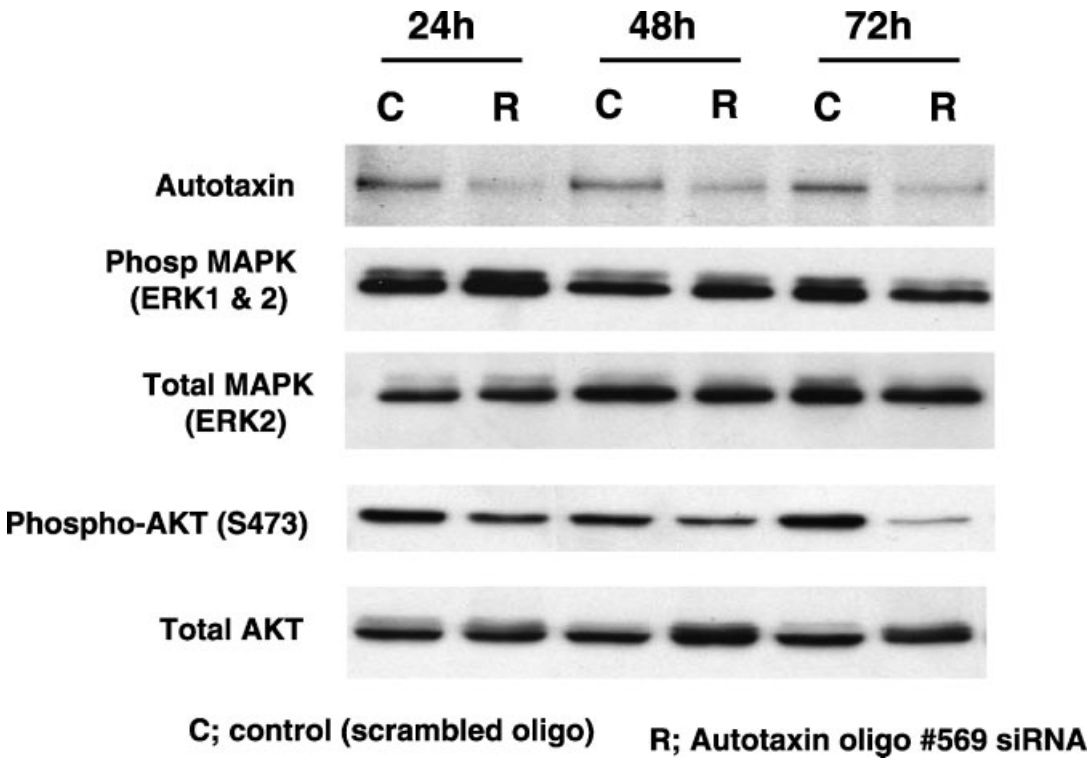

Fig. 8. RNAi to ATX /lysoPLD decreases ATX levels and decreases signaling to AKT and MAPK RNAi specific to autotaxin was introduced into UM-RC-7 renal cell carcinoma cells that overexpress autotaxin (Fig. 4). The RNAi induced a prolonged and significant downregulation of autotaxin protein levels in the cell line. This decrease was associated with decreased phosphorylation of both erk1 and erk2 as well as AKT. There was no decrease in total MAPK or AKT demonstrating equal loading and lack of non-specific effects.

and assessment of small molecule inhibitors and agonists of specific LPA receptors, a process which we have recently reviewed [Feng et al., 2003].

LPA in Ovarian Cancer

Ovarian cancer has been extensively explored as a model for aberrations in LPA production, metabolism and function [Xu et al., 1995, 1998, 2003; Shen et al., 1998, 2001; Westermann et al., 1998; Eder et al., 2000; Xiao et al., 2000, 2001; Hu et al., 2001; Schwartz et al., 2001; Baker et al., 2002; Fang et al., 2002, 2003; Mills et al., 2002; Feng et al., 2003; Luquain et al., 2003a; Mills and Moolenaar, 2003; Sengupta et al., 2003]. Although it is clear that LPA plays a major role in the pathophysiology of ovarian cancer, data is rapidly accumulating [see above Mills and Moolenaar, 2003], implicating LPA in the pathophysiology of multiple different cancers. Nevertheless, due to the wealth of data in ovarian cancer, the remainder of this review will concentrate on the unique aspects of ovarian cancer and what is known about LPA production, metabolism, and action in ovarian cancer.

LPA levels. It is difficult to determine the levels of LPA and indeed any growth factor in the interstitial fluid of tumors and thus we have been limited in our ability to assess whether cancer cells, in vivo, are stimulated by particular growth factors. The ascitic fluid that accumulates in ovarian cancer patients provides access to the distinctive ovarian cancer microenvironment. The growth factor composition of ascitic fluid reflects growth factor production, degradation and clearance from the local environment and also reflects the growth factor environment of the tumor cell. We have demonstrated that malignant ascites from ovarian cancer patients contain high levels of growth factor activity both in vitro and in vivo [Fang et al., 2002; Mills et al., 2002]. At least a portion of the growth factor activity in ascites can be attributed to the presence of high concentrations of LPA and LPA like molecules present

72h	0% FBS		10% FBS	
	control	siRNA	control	siRNA
Sub G0 / G1	4.27%	9.73%	1.21%	3.92%
G0 / G1	88.34%	58.99%	90.10%	41.95%
S	4.67%	27.10%	5.57%	54.83%
G2 / M	6.98%	13.91%	4.33%	3.22%

Fig. 9. RNAi to ATX induces a S phase arrest and apoptosis. RNAi specific to ATX was introduced into UM-RC-7 renal cell carcinoma cells that overexpress ATX. Seventy-two hours later adherent and floating cells were collected and analyzed for cell cycle and apoptosis (hypodiploid peak) using flow cytometry of propidium iodide labeled cells. RNAi induced a marked accumulation of cells in S phase as well as hypodiploid cells. Similar results were obtained at 48 h.

in ascites (1–80 μM) [Westermann et al., 1998; Eder et al., 2000; Xiao et al., 2001; Fang et al., 2002; Mills et al., 2002; Mills and Moolenaar, 2003; Xu et al., 2003]. Ovarian cancer ascites not only contains consistently elevated levels of LPA, but the LPA present contains a number of unusual forms, which may have novel mechanisms of production or action [Xiao et al., 2001].

Since LPA levels are elevated in ascites of ovarian cancer patients, if LPA migrates to the periphery, there is a potential that LPA levels could be elevated in the plasma of patients providing an early diagnostic marker or marker of disease behavior. Indeed, LPA levels are consistently higher in ascites samples than matched plasma samples suggesting that LPA produced in the peritoneal cavity migrates into the plasma [Eder et al., 2000]. In a preliminary analysis with a limited number of patients and controls, LPA levels were elevated in more than 80% of stage I ovarian cancer patients with a false positive rate of 5% [Xu et al., 1998, 2003]. LPA levels are not elevated in blood samples from patients with most other cancers, but are increased in patients with myeloma, endometrial cancer, cervical cancer, and renal dialysis [Sasagawa et al., 1998, 1999], all of which can be distinguished from ovarian cancer by medical assessment. Following the original publication, a number of reports have supported or refuted the potential utility of LPA levels in early diagnosis and prognosis of ovarian cancer [Xiao et al., 2000; Shen et al., 2001; Baker et al., 2002; Yoon et al., 2003; Xu et al., 2003]. As plasma contains enzymes required for the production and metabolism of LPA [Xu et al., 1998; Aoki et al., 2002], differences in the results from the groups likely arise from challenges in the collection and handling of plasma to prevent post collection production, metabolism or loss of LPA. An additional complication arises in the analysis of LPA, which requires purification, concentration and multiple handling steps, which could result in artifactual changes in LPA levels. Current studies have focused on total LPA levels and levels of LPA isoforms. It

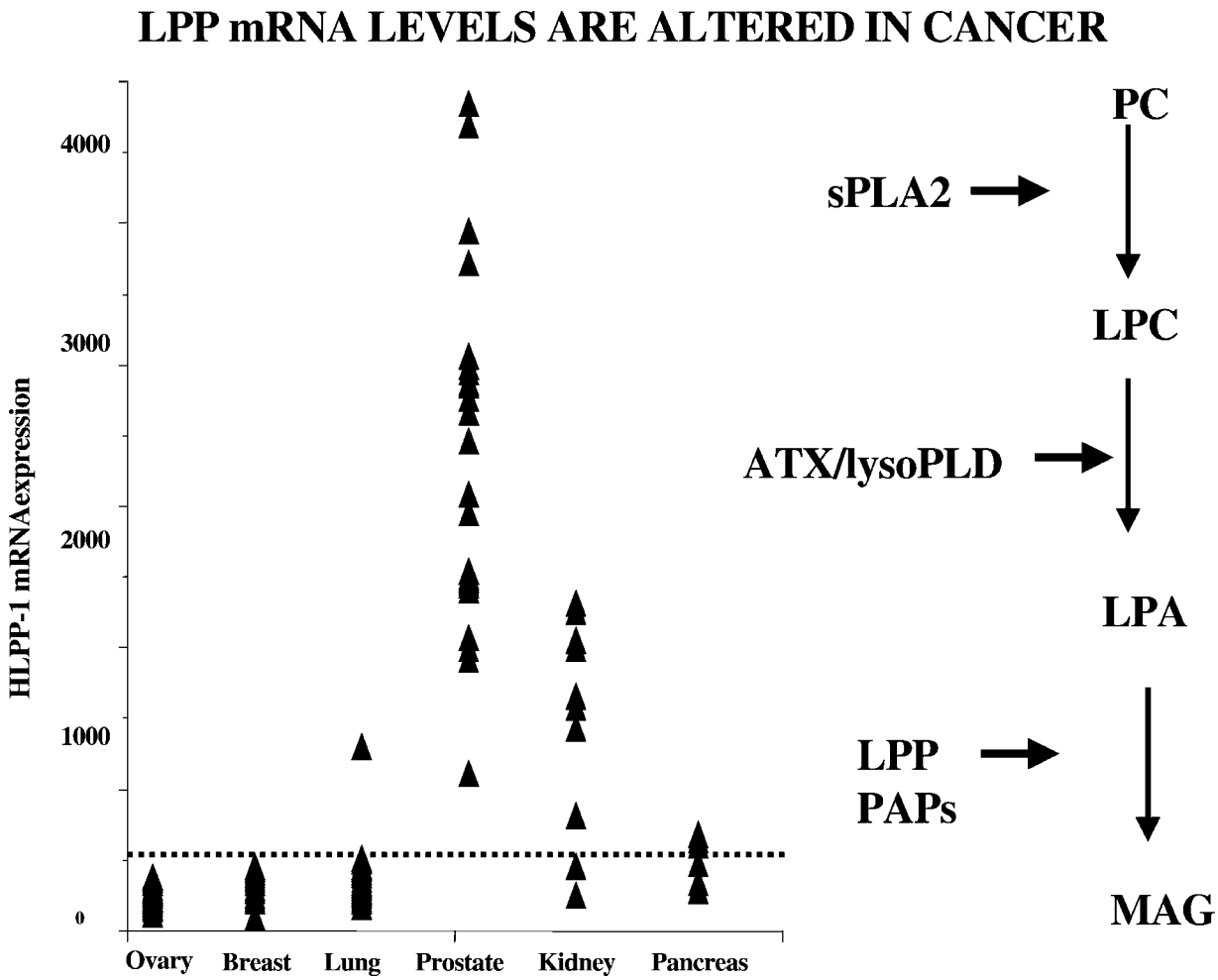

Fig. 10. LPP-1 mRNA levels are altered in cancer using a publicly available database of Affymetrix U95 arrays (http://www.gnf.org/cancer/epican), LPP-1 mRNA levels are shown to be markedly aberrant in a number of tumor types. Data is expressed for each tumor relative to control values based on 36 normal adult epithelial tissues. As indicated in the figure, LPP-1 mRNA levels are elevated in a number of tumor types, and decreased in others.

may, however, be necessary to assess the composition of particular isoforms of LPA or other lysophospholipids and related lipids precursors and breakdown products as part of a lipid profile to develop an algorithm able to detect clinically relevant changes in lipid levels or composition. Such approaches using global analysis of small molecules by mass spectroscopy has been designated metabolomics and a release of this technology as a clinically available "home brew" screening test for ovarian cancer is being proposed for early 2004. A reanalysis of data and follow up data from the original study describing the use of pattern recognition of small molecules by SELDI-TOF mass spectroscopy as a potential approach to detect ovarian cancer [Petricoin et al., 2002], suggested that a number of different molecules in the range of 200–800 Da had discriminatory power for the detection of ovarian cancer. A recent follow up study, indicates that the majority of these molecules are carried in the blood stream bound to albumin and other carrier proteins [Mehta et al., 2004]. LPA associates with albumin as well as with other carrier proteins such as gelsolin [Goetzl et al., 2000] suggesting that it may be in the carrier protein compartment. Combined with the observation that fatty acyl chains (200–300 Da), monoacylglycerols (300–400 Da), lysophospholipids (400–600 Da), and phospholipids (700–900 Da) fall into this range, it is possible that a

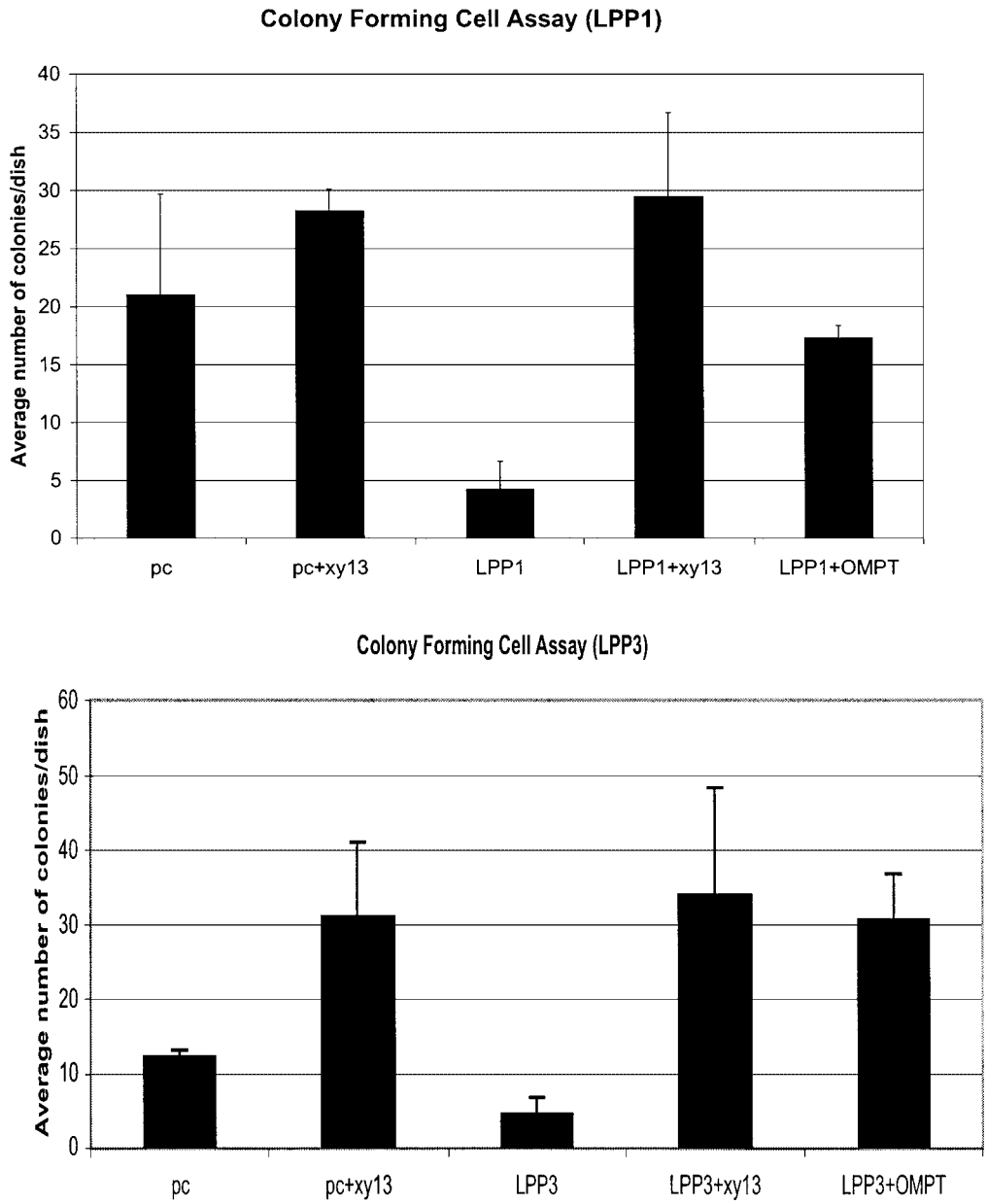

Fig. 11. LPP-1 and LPP-3 decrease colony forming cell activity of ovarian cancer cells through degradation of LPA. As indicated in Figure 10, LPP-1 levels are decreased in ovarian cancer (85). Transient transfection with LPP-1 or LPP-3 induces a marked decrease in colony forming cell activity in SKOV3 ovarian cancer cells, which express high levels of LysoPLD and produce LPA constitutively. Transfected cells were incubated with XY13 that inhibits LPPs and with OMPT, a LPP resistant LPA analog. Both XY-13 and OMPT reversed the effects of LPP on colony forming cell activity demonstrating that the effects of LPP-1 and LPP-3 were due to degradation of LPA.

global analysis of lipid patterns could prove diagnostic for particular cancers. We have demonstrated that model lipids bind with high affinity to the matrices used in SELDI, are excited by the laser and are easily visualized by SELDI-TOF. A prospective clinical trial to evaluate the utility of assessment of patterns of lipids in plasma measured by ESI (metabolomics), SELDI- or MALDI-TOF or other approaches as an ovarian cancer marker is clearly warranted.

Until recently the mechanisms resulting in high levels of LPA present in ovarian cancer ascites remained elusive. However, as indicated in Figure 12, a number of enzymes producing LPA including sPLA2 [Ben-Shlomo et al., 1997]

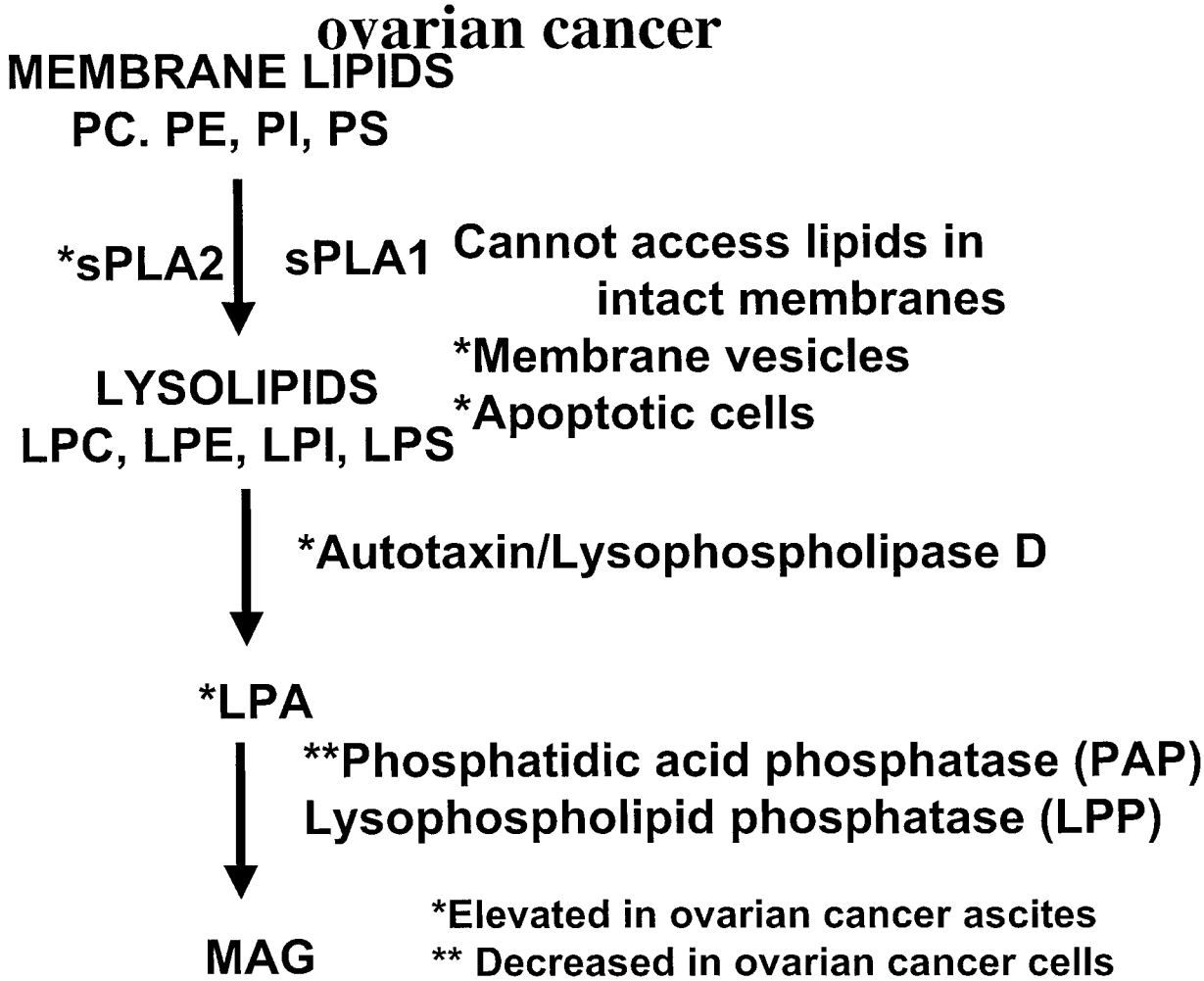

Fig. 12. Aberrations in lipid metabolism in ovarian cancer points of aberrations in lipid metabolism in ovarian cancer are indicated based on the major pathway of extracellular LPA production.

and autotaxin are increased in ovarian cancer patients (Fig. 3), and as noted above, LPP isoforms are decreased (Fig. 10) [Tanyi et al., 2003a,b]. Like many cancers, the number of apoptotic cells in ovarian cancers is high and membranes are accessible to the action of sPLA2 potentially resulting in increased production of substrates for ATX [Fourcade et al., 1995]. Ascites also contains markedly elevated levels of vesicles that are also accessible to sPLA2 [Ginestra et al., 1999; Andre, 2002]. Furthermore, ovarian cancer cells both constitutively and inducibly produce LPA [Shen et al., 1998; Eder et al., 2000; Sengupta et al., 2003]. As patients may have kilograms of tumor present when diagnosed, even a modest increment in production or decreased metabolism of LPA by ovarian cancer cells could result in marked accumulation of LPA in ascites. Indeed, ascites itself can contain up to 10^9 tumor cells per milliliter, which could result in release of high levels of LPA. Thus, there is a suite of aberrations in ovarian cancer that potentially contributes to the accumulation of LPA at the tumor interface and in ascites. Taken together, the data suggest that the increased levels of LPA in ovarian cancer ascites reflects both increased production and decreased hydrolysis.

LPA is not produced at significant levels by normal ovarian epithelial cells, whereas ovarian cancer cells both constitutively and inducibly produce elevated levels of LPA in response to phorbol esters, laminin and LPA itself [Shen et al., 1998; Eder et al., 2000; Sengupta et al., 2003], suggesting that ovarian cancer cells which present at great numbers in the peritoneal cavity could contribute to the elevated levels. The ability of ovarian cancer cells to

produce and respond to LPA suggests that ovarian cancer cells are likely regulated by autocrine LPA loops. A recent report confirms the presence of an autocrine LPA loop in prostate cancer [Xie et al., 2002] suggesting that LPA autocrine loops may contribute to the pathophysiology of multiple cancers.

In view of the higher levels of LPA in ascites from ovarian cancer patients and the ability of LPA to activate the pathways mediating LPA production, we assessed basal and LPA-induced LPA production by ovarian cancer cells. We found that ovarian cancer cells, in contrast to normal ovarian epithelial cells or breast cancer cells, produce LPA either constitutively or in response to LPA [Eder et al., 2000]. Both constitutive and LPA-induced LPA production exhibited PLD-dependent and -independent components. LPA has been demonstrated to activate PLD in a number of systems [van der Bend et al., 1992; Kam and Exton, 2004]. PLD can alter membrane composition and in particular induce production of membrane vesicles [Morgan et al., 1997; Kinkaid et al., 1998]. Indeed, ascites contains high levels of vesicles potentially due to PLD activation [Ginestra et al., 1999; Andre, 2002]. Constitutive LPA production was primarily dependent on group IB (pancreatic) sPLA2 and on cPLA2 and/or iPLA2, whereas LPA-induced LPA production was dependent on both group IB (pancreatic) and group IIA (synovial) sPLA2, but not cPLA2 or iPLA2 suggesting that LPA induces extracellular LPA production [Eder et al., 2000]. LPA is a potent activator of increases in cytosolic calcium and of MAPKs in ovarian cancer cells and both increases in cytosolic calcium and MAPK activity activate cPLA2 potentially contributing to the increases in LPA production. In contrast to LPA-induced LPA production, PMA-induced LPA production is dependent on cPLA2 or iPLA2 indicating effects on intracellular LPA production [Shen et al., 1998]. Laminin-induced LPA production by ovarian cancer cells is dependent on beta1 integrins and iPLA2 similar to PMA-induced LPA production [Sengupta et al., 2003]. Nucleotide agonists acting at the P2Y4 purinergic receptors on ovarian cancer cells also induce LPA production. Nucleotide induced LPA production is associated with an increase in PLD activity and PLD augments LPA production suggestion that it could be a major contributor to LPA production by ovarian cancers [Luquain et al., 2003b]. Ovarian cancer cells secrete PLA2. Indeed the increased concentration of vesicles in ascites that are accessible to sPLA could contribute to LPA production either by conversion of PA to LPA or through the production of LPC and other autotaxin substrates.

Aberrations in LPA Function in Ovarian Cancer

As noted above, the production of LPA is aberrant in ovarian cancer cells due to changes in the levels and activity of multiple different enzymes resulting in the accumulation of high concentrations of LPA in ascites fluid and likely in the interstitial space in the tumor. This accumulation of LPA would be sufficient to play a major role in the pathophysiology of ovarian cancer. However, the effects of the high levels of LPA present in ovarian cancer patients are amplified by aberrations in the response of ovarian cancer cells to LPA. The expression of LPA receptors on ovarian cancer cells is markedly different from that on normal ovarian epithelial cells resulting in increased responsiveness to LPA [Goetzl et al., 1999; Fang et al., 2002; Mills et al., 2002; Feng et al., 2003]. Further, unusual splice variants of LPA receptors, selectively linking to processes such as production of neovascularizing factors, may be present in ovarian cancer cells [Huang et al., 2004]. Finally, additional genetic aberrations in ovarian cancer cells such as amplification and mutation of multiple components of the phosphatidylinositol 3 kinase pathway sensitize ovarian cancer cells to downstream signaling effects of LPA [Fang et al., 2002; Mills et al., 2002; Feng et al., 2003]. As for changes in LPA production and metabolism, the genetic mechanisms underlying these processes remain to be determined. Nevertheless, taken together, LPA production or action appears well justified as a target for therapy in ovarian cancer.

Although freshly isolated ovarian cancer cell preparations and ovarian cancer cell lines are consistently responsive to LPA, normal ovarian surface epithelial cells (OSE) do not demonstrate significant responses to LPA [Goetzl et al., 1999; Eder et al., 2000; Fang et al., 2002; Mills et al., 2002; Feng et al., 2003]. In contrast, OSE demonstrate marked responses to S1P, whereas ovarian cancer cells demonstrate more limited responses to S1P [Goetzl et al., 1999]. Consistent with the shift from S1P-dependence to LPA-dependence, ovarian cancer cell lines express markedly increased levels of mRNA

and protein for the LPA2 and -3 receptors and decreased levels of mRNA and protein for S1P receptors [Goetzl et al., 1999] as compared to OSE which have very low levels of LPA2 and -3. There are no consistent changes in levels of LPA1 receptors between OSE and ovarian cancer cell lines. However, LPA1 may function as a negative LPA receptor, as overexpression of LPA1 results in decreased proliferation as a consequence of increased apoptosis [Furui et al., 1999]. Analysis of ovarian cancer cells directly from the patient paints a similar picture in that LPA1 levels are not different from those in normal epithelium and LPA2 and -3 are each elevated in approximately 40% of tumors with a significant overlap resulting in increased expression of LPA receptors in approximately 60% of ovarian cancers [Fang et al., 2002]. Thus acquisition of expression of LPA2 and -3 during transformation leads to increased responses to LPA potentially contributing to the pathophysiology of ovarian cancer. LPA4 receptors are reported to expressed in ovary, however, the initial report did not indicate whether this was in stroma or epithelium [Noguchi et al., 2003]. As assessed by QPCR, ovarian cancer cells have low to absent levels of LPA4.

Ovarian cancer cells contain an unusual variant of LPA2 with an intracellular extension [Huang et al., 2004]. This extension destroys the PDZ binding site in LPA2 that may have important functional consequences. The variant exhibits increased ability to link to production of active VEGF, an important permeability and neovascularizing factor [Hu et al., 2001; Huang et al., 2004]. LPA couples efficiently to VEGF production potentially contributing to the elevated VEGF levels in ovarian cancer ascites [Zebrowski et al., 1999; Hu et al., 2001]. Further, although LPA1 and -3 appear able to couple to the production of IL8 and IL6 neovasularization factors, LPA2 appears to most efficient in mediating production of these factors [Schwartz et al., 2001; Fang et al., 2003]. As IL8 production is dependent on NfκB mediated activation of the IL8 promoter, it appears likely that LPA2 couples most efficiently to activation of NfκB [Fang et al., 2003]. In ovarian cancer, VEGF appears to play a major role in the production of ascites whereas IL8 production appears to regulate aggressiveness and potentially neovascularization. The effects of the increased ability of LPA2 to couple to these pathways suggest that inhibitors targeting the LPA2 receptor may selectively alter neovascularization.

Expression of the ovarian cancer specific LPA2 variant in the stroma (the promoter used does not express or is expressed at low levels in the epithelial cells of the ovary, the most frequent precursor for ovarian cancer) of transgenic murine ovaries results in constitutive production of active VEGF-A again supportive a selective role of LPA2 in production of neovascularizing factors [Huang et al., 2004]. In addition expression of the ovarian cancer specific LPA2 variant increases the production of urokinase (uPA), compatible with previous reports showing that these factors are regulated by LPA in ovarian cancer cells [Pustilnik et al., 1999; Huang et al., 2004]. This was accompanied by increased expression of VEGF receptors and decreased production of type 2 PA inhibitor. Together, this suggests that activation of the LPA2 receptor aberrantly expressed in ovarian cancer cells may contribute to neovascularization and also result in ovarian cancer cells being responsive to VEGF. If similar processes affect other neovascularizing factors such as IL6 and IL8 activation of LPA receptors may stimulate a number of aberrant autocrine loops.

LPA appears to activate a number of additional feed-forward autocrine signaling loops. For example, LPA can induce the production of endothelin, a potent activator of ovarian cancer cells [Chua et al., 1998]. Indeed, endothelin receptor isoforms appear to be aberrantly expressed in ovarian cancer. Alternatively, the effects of LPA on ovarian cancer cells may be due to LPA-induced production or processing of growth factors, which in turn activate cognate cell surface receptors. As described above, LPA induces the activation of a number of tyrosine kinase linked growth factor receptors including multiple members of the human EGF receptor (HER) family, and the platelet-derived growth factor receptor. LPA-induced processing of HB-EGF and PDGF, which, in turn, activates members of the HER family and PDGFR respectively. LPA also induces activation of Src either through activation of tyrosine kinase linked receptors or through other as yet unclear mechanisms. As src and EGFR family members are overexpressed in ovarian cancers, this may amplify the effects of LPA. Indeed, we have demonstrated that LPA induces tyrosine-phosphorylation of multiple members of the HER family and of Src in ovarian cancer cells,

compatible with LPA inducing proliferation through the increased production or action of other growth factors which activate members of the HER or PDGFR family [Xu et al., 1995; Fang et al., 2002; Mills et al., 2002; Feng et al., 2003]. Nevertheless, the relative role of the direct and indirect activation of ovarian cancer cells by LPA in the pathophysiology of ovarian cancer remains to be elucidated.

Ovarian cancer cells may also have aberrant responses to other lysophospholipids. As indicated above, there are aberrations in the expression of both LPA and S1P receptors that could alter the responsiveness of ovarian cancer cells [Goetzl et al., 1999]. In at least one model system, S1P can transdominantly inhibit responses to LPA suggesting that the shift in receptor selectivity from S1P in normal ovarian epithelial cells to LPA in ovarian cancer cells may have functional consequences in addition to the effects of increased LPA receptor levels [Clair et al., 2003]. The OGR1 orphan GPCR, which is overexpressed in some ovarian cancer cell lines, has been demonstrated to be a specific receptor for SPC [Xu et al., 2003]. SPC increases cytosolic calcium in ovarian cancer cells but appears to decrease cellular proliferation, questioning the role of SPC and OGR1 in transformation of ovarian epithelium [Xu et al., 1995]. LPC, LPS, and PAF can activate ovarian cancer cells, but their effects on physiological responses are unclear [Xu et al., 1995]. PA, which is both a precursor and a product of LPA metabolism, can modestly increase proliferation of ovarian cancer cells [Xu et al., 1995]. The complete spectrum of responses to the different lipids, lysolipids, and isoforms in ovarian cancer will require a thorough evaluation of the levels and responses to these moieties. Several may prove both to be functionally important and optimal targets for therapy.

The responses of ovarian cancer cells to LPA have been extensively evaluated (see Fang et al., 2002; Mills et al., 2002 and references therein). At concentrations to which ovarian cancer cells are exposed, LPA can modestly increase the proliferation of ovarian cancer cells. Its pathophysiological role in ovarian cancer may link more tightly to the metastatic cascade than to cell growth as in addition to the effects on the production of neovascularizing factors described above, it increases invasiveness through altering cytosekeletal organization, increasing cellular motility, increasing production and action of urokinase plasminogen activator (uPA), and activity of metalloproteinases (MMP2 and MMP9), all critical components in the metastatic cascade. For cells to metastasize, they must detach from their underlying matrix and move to a new site. The vast majority of tumor cells die from anoikis, a form of apoptosis. LPA is highly protective from both apoptosis and anoikis. The ability of LPA to prevent apoptosis may also contribute to the poor outcome in the disease through induced resistance to the main drug used in ovarian cancer cisplatin [Fang et al., 2002; Mills et al., 2002].

The mechanisms by which LPA mediates it functional effects on ovarian cancer cells are only beginning to be delineated. In ovarian cancer cells, LPA through binding to its cognate receptors induces increases in cytosolic free calcium, Rac, Rho, and Rock activation, activation of phospholipase C and D, as well as activation of tyrosine kinases and the PI3K and Ras/MAP signaling cascades [Fang et al., 2002; Mills et al., 2002; Feng et al., 2003]. These in turn lead to activation of NFκB, AP1, and AP2. The roles of specific signaling pathways in specific responses to LPA remain to be delineated.

Almost half of all drugs in current use target members of the GPCR family of receptors making the Edg family of LPA receptors attractive targets for therapeutic development. By analyzing the structure–function relationships of the Edg receptors using yeast, insect and mammalian cells, we and others are beginning to develop receptor selective agonists and antagonists for LPA1, -2, and -3 [Fang et al., 2002; Lynch and Macdonald, 2002; Mills et al., 2002; Feng et al., 2003]. As LPA1 may be a negative growth regulator, agonists of LPA1 may decrease viability and growth of ovarian cancer cells. However, as LPA1 can mediate cellular motility, this could come at the consequence of increased tumor spread. In contrast, LPA2 and -3 can increase motility, production of neovascularizing factors and induce proliferation, respectively, suggesting that antagonists may demonstrate optimal activity. Further, LPA2 is implicated in the production of neovascularizing factors and in particular IL8, which may define the aggressiveness of ovarian cancer [Fang et al., 2003]. LPA3 is particularly appealing as it is selectively activated by the subtype of LPA (with unsaturated fatty acyl chains) that

are found at high levels in ascites from ovarian cancer patients [Bandoh et al., 1999; Xiao et al., 2001; Fang et al., 2002; Mills et al., 2002; Feng et al., 2003]. Indeed, LPA subtypes with unsaturated fatty acyl chains are highly active on ovarian cancer cells. LPA receptors are expressed by multiple cell lineages including fibroblasts, platelets, and brain cells [Fang et al., 2002]. However, the observation that LPA3 is selectively elevated in ovarian cancer cells and that ovarian cancer cells are particularly responsive to specific species of LPA (polyunsaturated fatty acyl chains) suggests that inhibitors based on these forms of LPA may demonstrate specificity for ovarian cancer cells. Taken together, ovarian cancer appears to be driven through the production and action of LPA. Thus inhibitors of LPA production or action may provide an effective approach to the therapy of this disease.

REFERENCES

Andre F, Schartz NE, Movassagh M, Flament C, Pautier P, Morice P, Pomel C, Lhomme C, Escudier B, Le Chevalier T, Tursz T, Amigorena S, Raposo G, Angevin E, Zitvogel L. 2002. Malignant effusions and immunogenic tumour-derived exosomes. Lancet 369:295–305.

Aoki J, Taira A, Takanezawa Y, Kishi Y, Hama K, Kishimoto T, Mizuno K, Saku K, Taguchi R, Arai H. 2002. Serum lysophosphatidic acid is produced through diverse phospholipase pathways. J Biol Chem 277: 48737–48744.

Auersperg N, Pan J, Grove BD, Peterson T, Fisher J, Maines-Bandiera S, Somasiri A, Roskelley CD. 1999. E-cadherin induces mesenchymal-to-epithelial transition in human ovarian surface epithelium. Proc Natl Acad Sci USA 96:6249–6254.

Bachner D, Ahrens M, Schroder D, Hoffmann A, Lauber J, Betat N, Steinert P, Flohe L, Gross G. 1998. Bmp-2 downstream targets in mesenchymal development identified by subtractive cloning from recombinant mesenchymal progenitors (C3H10T1/2). Dev Dyn 213:398–411.

Baker DL, Morrison P, Miller B, Riely CA, Tolley B, Westermann AM, Bonfrer JM, Bais E, Moolenaar WH, Tigyi G. 2002. Plasma lysophosphatidic acid concentration and ovarian cancer. JAMA 287:3081–3082.

Bandoh K, Aoki J, Hosono H, Kobayashi S, Kobayashi T, Murakami-Murofushi K, Tsujimoto M, Arai H, Inoue K. 1999. Molecular cloning and characterization of a novel human G-protein-coupled receptor, EDG7, for lysophosphatidic acid. J Biol Chem 274:27776–27785.

Bektas M, Barak LS, Jolly PS, Liu H, Lynch KR, Lacana E, Suhr KB, Milstien S, Spiegel S. 2003. The G protein-coupled receptor GPR4 suppresses ERK activation in a ligand-independent manner. Biochemistry 42:12181–12191.

Ben-Shlomo I, Kol S, Ando M, Altman KR, Putowski LT, Rohan RM, Adashi EY. 1997. Ovarian expression, cellular localization, and hormonal regulation of rat secretory phospholipase A2: increased expression by interleukin-1 and by gonadotropins. Biol Reprod 57: 217–225.

Black EJ, Clair T, Delrow J, Neiman P, Gillespie DA. 2004. Microarray analysis identifies Autotaxin, a tumour cell motility and angiogenic factor with lysophospholipase D activity, as a specific target of cell transformation by v-Jun. Oncogene, in press.

Brindley DN, English D, Pilquil C, Buri K, Ling ZC. 2002. Lipid phosphate phosphatases regulate signal transduction through glycerolipids and sphingolipids. Biochim Biophys Acta 1582:33–44.

Chua CC, Hamdy RC, Chua BH. 1998. Upregulation of endothelin-1 production by lysophosphatidic acid in rat aortic endothelial cells. Biochim Biophys Acta 1405: 29–34.

Clair T, Aoki J, Nam SW, Bandle R, Woodhouse E, Ptaszynska M, Koh EJ, Braverman R, Mills G.B, Schiffman E, Liotta L.A, Stracke ML. 2003. Autotaxin hydrolyzes phospholipids to produce a migration stimulator, lysophosphatidic acid, or a migration inhibitor, sphingosine-1-phosphate. Cancer Res 63:5446–5453.

Drees BE, Weipert A, Hudson H, Ferguson CG, Chakravarty L, Prestwich GD. 2003. Competitive fluorescent polarization assay for detection of phosphoinositide kinase and phosphatase activity. Comb Chem High Throughput Screen 6:321–330.

Eder AM, Sasagawa T, Mao M, Aoki J, Mills GB. 2000. Constitutive and lysophosphatidic acid (LPA)-induced LPA production: Role of phospholipase D and phospholipase A2. Clin Cancer Res 6:2482–2491.

Fang X, Schummer M, Mao M, Yu S, Tabassam FH, Swaby R, Hasegawa Y, Tanyi JL, LaPushin R, Eder A, Jaffe R, Erickson J, Mills GB. 2002. Lysophosphatidic acid is a bioactive mediator in ovarian cancer. Biochim Biophys Acta 1582:257–264.

Fang X, Yu S, Bast RC, Liu S, Xu HJ, Hu SX, LaPushin R, Claret FX, Aggarwal BB, Lu Y, Mills GB. 2004. Mechanisms for lysophosphatidic acid-induced cytokine production in ovarian cancer cells. J Biol Chem 279: 9653–9661.

Feng L, Manabe K, Shope JC, Widmer S, DeWald DB, Prestwich GD. 2002. A Real–time fluorogenic phospholipase A_2 assay for biochemical and cellular activity measurements. Chem Biol 9:795–803.

Feng L, Mills GB, Prestwich GD. 2003. Modulators of lysophosphatidic acid signaling, Expert Opin. Therapeut Pat 13:1619–1634.

Ferry G, Tellier E, Try A, Gres S, Naime I, Simon MF, Rodriguez M, Boucher J, Tack I, Gesta S, Chomarat P, Dieu M, Raes M, Galizzi JP, Valet P, Boutin JA, Saulnier-Blache JS. 2003. Autotaxin is released from adipocytes, catalyzes lysophosphatidic acid synthesis, and activates preadipocyte proliferation. Up-regulated expression with adipocyte differentiation and obesity. J Biol Chem 278:18162–18169.

Fidler IJ. 2003. The pathogenesis of cancer metastasis: The 'seed and soil' hypothesis revisited. Nat Rev Cancer 3: 453–458.

Fourcade O, Simon MF, Viode C, Rugani N, Leballe F, Ragab A, Fournie B, Sarda L, Chap H. 1995. Secretory phospholipase A2 generates the novel lipid mediator lysophosphatidic acid in membrane microvesicles shed from activated cells. Cell 80:919–927.

Fourcade O, Le Balle F, Fauvel J, Simon MF, Chap H. 1998. Regulation of secretory type-II phospholipase A2 and of lysophosphatidic acid synthesis. Adv Enzyme Regul 38: 99–107.

Furui T, LaPushin R, Mao M, Kahn H, Watt SR, Watt MV, Lu Y, Fang XJ, Tsutusi S, Siddik Z, Bast R, Mills GB. 1999. Overexpression of Edg-2/vzg-1 induces apoptosis and anoikis in ovarian cancer cells in a lysophosphatidic acid independent manner. Clin Cancer Res 5:4308–4318.

Gerrard JM, Robinson P. 1989. Identification of the molecular species of lysophosphatidic acid produced when platelets are stimulated by thrombin. Biochim Biophys Acta 1001:282–285.

Gesta S, Simon MF, Rey A, Sibrac D, Girard A, Lafontan M, Valet P, Saulnier-Blache JS. 2002. Secretion of a lysophospholipase D activity by adipocytes: Involvement in lysophosphatidic acid synthesis. J Lipid Res 43:904–910.

Ginestra A, Miceli D, Dolo V, Romano FM, Vittorelli ML. 1999. Membrane vesicles in ovarian cancer fluids: A new potential marker. Anticancer Res 19:3439–3445.

Gjone E. 1982. Familial lecithin cholesterol acyltransferase (LCAT) deficiency. Birth Defects Orig Artic Ser 18:423–431.

Goetzl EJ, Dolezalova H, Kong Y, Hu YL, Jaffe RB, Kalli KR, Conover CA. 1999. Distinctive expression and functions of the type 4 endothelial differentiation gene-encoded G protein-coupled receptor for lysophosphatidic acid in ovarian cancer. Cancer Res 59:5370–5375.

Goetzl EJ, Lee H, Azuma T, Stossel TP, Turck CW, Karliner JS. 2000. Gelsolin binding and cellular presentation of lysophosphatidic acid. J Biol Chem 275:14573–14578.

Graler MH, Goetzl EJ. 2002. Lysophospholipids and their G protein-coupled receptors in inflammation and immunity. Biochim Biophys Acta 1582:168–174.

Gschwind A, Hart S, Fischer OM, Ullrich A. 2003. TACE cleavage of proamphiregulin regulates GPCR-induced proliferation and motility of cancer cells. EMBO J 22: 2411–2421.

Hanahan D, Weinberg RA. 2000. The hallmarks of cancer. Cell 100(1):57–70.

Hasegawa Y, Erickson JR, Goddard GJ, Yu S, Liu S, Cheng KW, Eder A, Bandoh K, Aoki J, Jarosz R, Schrier AD, Lynch KR, Mills GB, Fang X. 2003. Identification of a phosphothionate analogue of lysophosphatidic acid as a selective agonist of the LPA3 receptor. J Biol Chem 278: 11962–11969.

Hiramatsu T, Sonoda H, Takanezawa Y, Morikawa R, Ishida M, Kasahara K, Sanai Y, Taguchi R, Aoki J, Arai H. 2003. Biochemical and molecular characterization of two phosphatidic acid-selective phospholipase A1s, mPA-PLA1alpha and mPA-PLA1beta. J Biol Chem 278:49438–49447.

Hu Y-L, Goetzl EJ, Mills GB, Ferrara N, Jaffe RB. 2001. Induction of vascular endothelial growth factor expression by lysophosphatidic acid in normal and neoplastic human ovarian epithelial cells. J Natl Cancer Institute 93:762–767.

Huang MC, Lee HY, Yeh CC, Kong Y, Zaloudek CJ, Goetzl EJ. 2004. Induction of protein growth factor systems in the ovaries of transgenic mice overexpressing human type 2 lysophosphatidic acid G protein-coupled receptor (LPA2). Oncogene 23:122–129.

Imai A, Furui T, Tamaya T, Mills GB. 2000. A gonadotropin-releasing hormone-responsive phosphatase hydrolyses lysophosphatidic acid within the plasma membrane of ovarian cancer cells. J Clin Endrocrinol Metab 85: 3370–3375.

Kabarowski JH, Zhu K, Le LQ, Witte ON, Xu Y. 2001. Lysophosphatidylcholine as a ligand for the immunoregulatory receptor G2A. Science 293:702–705.

Kam Y, Exton JH. 2004. Role of phospholipase D1 in the regulation of mTOR activity by lysophosphatidic acid. FASEB J 18:311–319.

Kinkaid AR, Othman R, Voysey J, Wilton DC. 1998. Phospholipase D and phosphatidic acid enhance the hydrolysis of phospholipids in vesicles and in cell membranes by human secreted phospholipase A2. Biochim Biophys Acta 1390:173–185.

Koh E, Clair T, Woodhouse EC, Schiffmann E, Liotta L, Stracke M. 2003. Site-directed mutations in the tumor-associated cytokine, autotaxin, eliminate nucleotide phosphodiesterase, lysophospholipase D, and motogenic activities. Cancer Res 63:2042–2045.

Kooijman EE, Chupin V, de Kruijff B, Burger KN. 2003. Modulation of membrane curvature by phosphatidic acid and lysophosphatidic acid. Traffic 4:162–174.

Kudo I, Murakami M, Hara S, Inoue K. 1993. Mammalian non-pancreatic phospholipases A2. Biochim Biophys Acta 1170:217–231.

Ludwig MG, Vanek M, Guerini D, Gasser JA, Jones CE, Junker U, Hofstetter H, Wolf RM, Seuwen K. 2003. Proton-sensing G-protein-coupled receptors. Nature 425: 93–98.

Luquain C, Sciorra VA, Morris AJ. 2003a. Lysophosphatidic acid signaling: How a small lipid does big things. Trends Biochem Sci 28:377–383.

Luquain C, Singh A, Wang L, Natarajan V, Morris AJ. 2003b. Role of phospholipase D in agonist-stimulated lysophosphatidic acid synthesis by ovarian cancer cells. J Lipid Res 44:1963–1975.

Lynch KR, Macdonald TL. 2002. Structure–activity relationships of lysophosphatidic acid analogs. Biochim Biophys Acta 1582:289–294.

Matsuo H, Chevallier J, Mayran N, LeBlanc I, Ferguson C, Faure J, Blanc NS, Matile S, Dubochet J, Sadoul R, Parton RG, Vilbois R, Gruenberg J. 2004. Role of LBPA and Alix in multivesicular liposome formation and endosome organization. Science 303:531–534.

McIntyre TM, Pontstler AV, Silva AR, St Hilaire A, Xu Y, Hinshaw JC, Zimmerman GA, Hama K, Aoki J, Arai H, Prestwich GD. 2002. Identification of an intracellular receptor for lysophosphatidic acid (LPA): LPA is a transcellular pparγ agonist. Proc Natl Acad Sci USA 100:131–136.

Mehta AI, Ross S, Lowenthal MS, Fusaro V, Fishman DA, Petricoin EF, Liotta LA. 2004. Biomarker amplification by serum carrier protein binding. Dis Markers 19:1–10.

Mills GB, Moolenaar WH. 2003. The emerging role of lysophosphatidic acid in cancer. Nat Rev Cancer 8:582–591.

Mills GB, Eder A, Fang X, Hasegawa Y, Mao M, Lu Y, Tanyi J, Tabassam FH, Wiener J, Lapushin R, Yu S, Parrott JA, Compton T, Tribley W, Fishman D, Stack MS, Gaudette D, Jaffe R, Furui T, Aoki J, Erickson JR. 2002. Critical role of lysophospholipids in the pathophysiology, diagnosis, and management of ovarian cancer. Cancer Treat Res 107:259–283.

Morgan CP, Sengelov H, Whatmore J, Borregaard N, Cockcroft S. 1997. ADP-ribosylation-factor-regulated phospholipase D activity localizes to secretory vesicles and mobilizes to the plasma membrane following *N*-formylmethionyl-leucyl-phenylalanine stimulation of human neutrophils. Biochem J 325:581–585.

Murata J, Lee HY, Clair T, Krutzsch HC, Arestad AA, Sobel ME, Liotta LA, Stracke ML. 1994. Cloning of the human tumor motility-stimulating protein, autotaxin, reveals a homology with phosphodiesterases. J Biol Chem 269: 30479–30484.

Nam SW, Clair T, Campo CK, Lee HY, Liotta LA, Stracke ML. 2000. Autotaxin (ATX), a potent tumor motogen, augments invasive and metastatic potential of ras-transformed cells. Oncogene 19:241–247.

Nam SW, Clair T, Kim YS, McMarlin A, Schiffmann E, Liotta LA, Stracke ML. 2001. Autotaxin (NPP-2), a metastasis-enhancing motogen, is an angiogenic factor. Cancer Res 61:6938–6944.

Natarajan V, Scribner WM, Hart CM, Parthasarathy S. 1995. Oxidized low density lipoprotein-mediated activation of phospholipase D in smooth muscle cells: A possible role in cell proliferation and atherogenesis. J Lipid Res 36:2005–2016.

Noguchi K, Ishii S, Shimizu T. 2003. Identification of p2y9/GPR23 as a novel G protein-coupled receptor for lysophosphatidic acid, structurally distant from the Edg family. J Biol Chem 278:25600–25606.

Okusa MD, Ye H, Huang L, Sigismund L, Macdonald T, Lynch KR. 2003. Selective blockade of lysophosphatidic acid LPA3 receptors reduces murine renal ischemia-reperfusion injury. Am J Physiol Renal Physiol 285: F565–F574.

Petricoin EF, Ardekani AM, Hitt BA, Levine PJ, Fusaro VA, Steinberg SM, Mills GB, Simone C, Fishman DA, Kohn EC, Liotta LA. 2002. Use of proteomic patterns in serum to identify ovarian cancer. Lancet 359:572–577.

Prenzel N, Zwick E, Daub H, Leserer M, Abraham R, Wallasch C, Ullrich A. 1999. EGF receptor transactivation by G-protein-coupled receptors requires metalloproteinase cleavage of proHB-EGF. Nature 402:884–888.

Pustilnik TB, Estrella V, Wiener JR, Mao M, Eder A, Watt MA, Bast RC, Jr,, Mills GB. 1999. Lysophosphatidic acid induces urokinase secretion by ovarian cancer cells. Clin Cancer Res 5:3704–3710.

Qian L, Xu Y, Hasegawa Y, Aoki J, Mills GB, Prestwich GD. 2003. Enantioselective responses to a phosphorothioate analogue of lysophosphatidic acid with LPA_3 receptor-selective agonist activity. J Med Chem 46:5575–5578.

Sano T, Baker D, Virag T, Wada A, Yatomi Y, Kobayashi T, Igarashi Y, Tigyi G. 2002. Multiple mechanisms linked to platelet activation result in lysophosphatidic acid and sphingosine 1-phosphate generation in blood. J Biol Chem 277:21197–22206.

Sasagawa T, Suzuki K, Shiota T, Kondo T, Okita M. 1998. The significance of plasma lysophospholipids in patients with renal failure on hemodialysis. J Nutr Sci Vitaminol (Tokyo) 44:809–818.

Sasagawa T, Okita M, Murakami J, Kato T, Watanabe A. 1999. Abnormal serum lysophospholipids in multiple myeloma patients. Lipids 34(1):17–21.

Schaner ME, Ross DT, Ciaravino G, Sorlie T, Troyanskaya O, Diehn M, Wang YC, Duran GE, Sikic TL, Caldeira S, Skomedal H, Tu IP, Hernandez-Boussard T, Johnson SW, O'Dwyer PJ, Fero MJ, Kristensen GB, Borresen-Dale AL, Hastie T, Tibshirani R, van de Rijn M, Teng NN, Longacre TA, Botstein D, Brown PO, Sikic BI. 2003. Gene expression patterns in ovarian carcinomas. Mol Biol Cell 14:4376–4386.

Schmidt A, Wolde M, Thiele C, Fest W, Kratzin H, Podtelejnikov AV, Witke W, Huttner WB, Soling HD. 1999. Endophilin I mediates synaptic vesicle formation by transfer of arachidonate to lysophosphatidic acid. Nature 401:133–141.

Schwartz BM, Hong G, Morrison BH, Wu W, Baudhuin LM, Xiao YJ, Mok SC, Xu Y. 2001. Lysophospholipids increase interleukin-8 expression in ovarian cancer cells. Gynecol Oncol 81:291–300.

Sengupta S, Xiao YJ, Xu Y. 2003. A novel laminin-induced LPA autocrine loop in the migration of ovarian cancer cells. FASEB J 17:1570–1572.

Shen Z, Belinson J, Morton RE, Xu Y, Xu Y. 1998. Phorbol 12-myristate 13-acetate stimulates lysophosphatidic acid secretion from ovarian and cervical cancer cells but not from breast or leukemia cells. Gynecol Oncol 71:364–368.

Shen Z, Wu M, Elson P, Kennedy AW, Belinson J, Casey G, Xu Y. 2001. Fatty acid composition of lysophosphatidic acid and lysophosphatidylinositol in plasma from patients with ovarian cancer and other gynecological diseases. Gynecol Oncol 83:25–30.

Siess W, Zangl KJ, Essler M, Bauer M, Brandl R, Corrinth C, Bittman R, Tigyi G, Aepfelbacher M. 1999. Lysophosphatidic acid mediates the rapid activation of platelets and endothelial cells by mildly oxidized low density lipoprotein and accumulates in human atherosclerotic lesions. Proc Natl Acad Sci USA 96:6931–6936.

Siess W, Zangl KJ, Essler M, Bauer M, Brandl R, Corrinth C, Bittman R, Tigyi G, Aepfelbacher M. 1999. Lysophosphatidic acid mediates the rapid activation of platelets and endothelial cells by mildly oxidized low density lipoprotein and accumulates in human atherosclerotic lesions. Proc Natl Acad Sci USA 96:6931–6936.

Smyth SS, Sciorra VA, Sigal YA, Wang Z, Xu Y, Prestwich GD, Morris AJ. 2003. Lipid phosphate phosphatase 1 (LPP1) regulates lysophosphatidic acid signaling in platelets. J Biol Chem 278:43214–43223.

Stassar MJ, Devitt G, Brosius M, Rinnab L, Prang J, Schradin T, Simon J, Petersen S, Kopp-Schneider A, Zoller M. 2001. Identification of human renal cell carcinoma associated genes by suppression subtractive hybridization. Br J Cancer 85:1372–1382.

Su AI, Welsh JB, Sapinoso LM, Kern SG, Dimitrov P, Lapp H, Schultz PG, Powell SM, Moskaluk CA, Frierson HF, Jr., Hampton GM. 2001. Molecular classification of human carcinomas by use of gene expression signatures. Cancer Res 61:7388–7393.

Sugiura T, Nakane S, Kishimoto S, Waku K, Yoshioka Y, Tokumura A. 2002. Lysophosphatidic acid, a growth factor-like lipid, in the saliva. J Lipid Res 43:2049–2055.

Takahashi A, Sasaki H, Kim SJ, Tobisu K, Kakizoe T, Tsukamoto T, Kumamoto Y, Sugimura T, Terada M. 1994. Markedly increased amounts of messenger RNAs for vascular endothelial growth factor and placenta growth factor in renal cell carcinoma associated with angiogenesis. Cancer Res 54:4233–4237.

Tanyi JL, Morris AJ, Wolf JK, Fang X, Hasegawa Y, Lapushin R, Auersperg N, Sigal YJ, Newman RA, Felix EA, Atkinson EN, Mills GB. 2003a. The human lipid

phosphate phosphatase-3 decreases the growth, survival, and tumorigenesis of ovarian cancer cells: Validation of the lysophosphatidic acid signaling cascade as a target for therapy in ovarian cancer. Cancer Res 63:1073–1082.

Tanyi JL, Morris AM, Wolf JK, Bast RC, Lu K, Smith D, Kalli K, Hartmann L, McCune K, Lu K, Broaddus R, Cheng KW, Atkinson EN, Yamal JM, Lapushin R, Mills GB. 2003b. Role of decreased levels of LPP-1 in accumulation of lysophosphatidic acid (LPA) in ovarian cancer. Clinical Cancer Res 9:3534–3545.

Tice DA, Szeto W, Soloviev I, Rubinfeld B, Fong SE, Dugger DL, Winer J, Williams PM, Wieand D, Smith V, Schwall RH, Pennica D, Polakis P. 2002. Synergistic induction of tumor antigens by Wnt-1 signaling and retinoic acid revealed by gene expression profiling. J Biol Chem 277: 14329–14335.

Tigyi G, Parrill AL. 2003. Molecular mechanisms of lysophosphatidic acid action. Prog Lipid Res 42:498–526.

Tokumura A, Iimori M, Nishioka Y, Kitahara M, Sakashita M, Tanaka S. 1994. Lysophosphatidic acids induce proliferation of cultured vascular smooth muscle cells from rat aorta. Am J Physiol 267:C204–C210.

Tokumura A, Kanaya Y, Miyake M, Yamano S, Irahara M, Fukuzawa K. 2002a. Increased production of bioactive lysophosphatidic acid by serum lysophospholipase D in human pregnancy. Biol Reprod 67:1386–1392.

Tokumura A, Kanaya Y, Kitahara M, Miyake M, Yoshioka Y, Fukuzawa K. 2002b. Increased formation of lysophosphatidic acids by lysophospholipase D in serum of hypercholesterolemic rabbits. J Lipid Res 43:307–315.

Tokumura A, Majima E, Kariya Y, Tominaga K, Kogure K, Yasuda K, Fukuzawa K. 2002c. Identification of human plasma lysophospholipase D, a lysophosphatidic acid-producing enzyme, as autotaxin, a multifunctional phosphodiesterase. J Biol Chem 277:39436–39442.

Tokumura A, Tominaga K, Yasuda K, Kanzaki H, Kogure K, Fukuzawa K. 2002d. Lack of significant differences in the corrected activity of lysophospholipase D, producer of phospholipid mediator lysophosphatidic acid, in incubated serum from women with and without ovarian tumors. Cancer 94(1):141–151.

Umezu-Goto M, Kishi Y, Taira A, Hama K, Dohmae N, Takio K, Yamori T, Mills GB, Inoue K, Aoki J, Arai H. 2002. Autotaxin has lysophospholipase D activity leading to tumor cell growth and motility by lysophosphatidic acid production. J Cell Biol 158:227–233.

van der Bend RL, de Widt J, van Corven EJ, Moolenaar WH, van Blitterswijk WJ. 1992. The biologically active phospholipid, lysophosphatidic acid, induces phosphatidylcholine breakdown in fibroblasts via activation of phospholipase D. Comparison with the response to endothelin. Biochem J 285:235–240.

Westermann AM, Havik E, Postma FR, Beijnen JH, Dalesio O, Moolenaar WH, Rodenhuis S. 1998. Malignant effusions contain lysophosphatidic acid (LPA)-like activity. Ann Oncol 9:437–442.

Wolter S, Mushinski JF, Saboori AM, Resch K, Kracht M. 2002. Inducible expression of a constitutively active mutant of mitogen-activated protein kinase kinase 7 specifically activates c-JUN NH2-terminal protein kinase, alters expression of at least nine genes, and inhibits cell proliferation. J Biol Chem 277:3576–3584.

Xiao Y, Chen Y, Kennedy AW, Belinson J, Xu Y. 2000. Evaluation of plasma lysophospholipids for diagnostic significance using electrospray ionization mass spectrometry (ESI-MS) analyses. Ann NY Acad Sci 905:242–259.

Xiao YJ, Schwartz B, Washington M, Kennedy A, Webster K, Belinson J, Xu Y. 2001. Electrospray ionization mass spectrometry analysis of lysophospholipids in human ascitic fluids: Comparison of the lysophospholipid contents in malignant vs nonmalignant ascitic fluids. Anal Biochem 290:302–313.

Xie Y, Gibbs TC, Mukhin YV, Meier KE. 2002. Role for 18:1 lysophosphatidic acid as an autocrine mediator in prostate cancer cells. J Biol Chem 277:32516–32526.

Xu Y, Prestwich GD. 2002. Synthesis of chiral (α,α-Difluoroalkyl)phosphonate analogues of (Lyso)phosphatidic acid via hydrolytic kinetic resolution. Organic Lett 4:4021–4024.

Xu Y, Fang XF, Casey G, Mills GB. 1995. Lysophospholipids activate ovarian and breast cancer cells. Biochem J 309:933–940.

Xu Y, Shen Z, Wiper DW, Wu M, Morton RE, Elson P, Kennedy AW, Belinson J, Markman M, Casey G. 1998. Lysophosphatidic acid as a potential biomarker for ovarian and other gynecologic cancers. JAMA 280:719–723.

Xu Y, Xiao YJ, Zhu K, Baudhuin LM, Lu J, Hong G, Kim KS, Cristina KL, Song L, S Williams F, Elson P, Markman M, Belinson J. 2003. Unfolding the pathophysiological role of bioactive lysophospholipids. Curr Drug Targets Immune Endocr Metabol Disord 3:23–32.

Xu Y, Fang Y, Chen J, Prestwich GD. 2004. Activation of mTOR signaling by novel fluoromethylene phosphonate analogues of phosphatidic acid. Bioorg Med Chem Lett 14:1461–1464.

Yang AH, Ishii I, Chun J. 2002a. In vivo roles of lysophospholipid receptors revealed by gene targeting studies in mice. Biochim Biophys Acta 1582:197–203.

Yang SY, Lee J, Park CG, Kim S, Hong S, Chung HC, Min SK, Han JW, Lee HW, Lee HY. 2002b. Expression of autotaxin (NPP-2) is closely linked to invasiveness of breast cancer cells. Clin Exp Metastasis 19:603–608.

Yoon HR, Kim H, Cho SH. 2003. Quantitative analysis of acyl-lysophosphatidic acid in plasma using negative ionization tandem mass spectrometry. J Chromatogr B Analyt Technol Biomed Life Sci 788:85–92.

Zebrowski B.K, Liu W, Ramirez K, Akagi MD, Mills G.B, Ellis LM. 1999. Markedly elevated levels of vascular endothelial growth factor in malignant ascites. Ann Surg Oncol 6:373–378.

Zhang C, Baker DL, Yasuda S, Makarova N, Balazs L, Johnson LR, Marathe GK, McIntyre TM, Xu Y, Prestwich GD, Byun HS, Bittman R, Tigyi G. 2004. Lysophosphatidic acid induces neointima formation through PPARγ activation. J Exp. Med 199:763–774.

Zhu K, Baudhuin LM, Hong G, Williams FS, Cristina KL, Kabarowski JH, Witte ON, Xu Y. 2001. Sphingosylphosphorylcholine and lysophosphatidylcholine are ligands for the G protein-coupled receptor GPR4. J Biol Chem 276:41325–41335.

Structure−Activity Relationships of Fluorinated Lysophosphatidic Acid Analogues

Yong Xu,[†] Junken Aoki,[‡] Kumiko Shimizu,[‡] Makiko Umezu-Goto,[‡] Kotaro Hama,[‡] Yasukazu Takanezawa,[‡] Shuangxing Yu,[§] Gordon B. Mills,[§] Hiroyuki Arai,[‡] Lian Qian,[†] and Glenn D. Prestwich*,[†]

Department of Medicinal Chemistry and The Center for Cell Signaling, The University of Utah, 419 Wakara Way, Suite 205, Salt Lake City, Utah 84108-1257, Graduate School of Pharmaceutical Sciences, The University of Tokyo, 7-3-1, Hongo, Bunkyo-ku, Tokyo, 113-0033, Japan, and Department of Molecular Therapeutics, M. D. Anderson Cancer Center, 1515 Holcombe Boulevard, Houston, Texas 77030

Received October 12, 2004

Lysophosphatidic acid (LPA, 1- or 2-acyl-*sn*-glycerol 3-phosphate) displays an intriguing cell biology that is mediated via interactions with seven-transmembrane G-protein-coupled receptors (GPCRs) and the nuclear hormone receptor PPARγ. To identify receptor-selective LPA analogues, we describe a series of fluorinated LPA analogues in which either the *sn*-1 or *sn*-2 hydroxyl group was replaced by a fluoro or fluoromethyl substituent. We also describe stabilized phosphonate analogues in which the bridging oxygen of the monophosphate was replaced by an α-monofluoromethylene (−CHF−) or α-difluoromethylene (−CF_2−) moiety. The *sn*-2- and *sn*-1-fluoro-LPA analogues were unable to undergo acyl migration, effectively "freezing" them in the *sn*-1-*O*-acyl or *sn*-2-*O*-acyl forms, respectively. We first tested these LPA analogues on insect Sf9 cells induced to express human LPA_1, LPA_2, and LPA_3 receptors. While none of the analogues were found to be more potent than 1-oleoyl-LPA at LPA_1 and LPA_2, several LPA analogues were potent LPA_3-selective agonists. In contrast, 1-oleoyl-LPA had similar activity at all three receptors. The α-fluoromethylene phosphonate analogue **15** activated calcium release in LPA_3-transfected insect Sf9 cells at a concentration 100-fold lower than that of 1-oleoyl-LPA. This activation was enantioselective, with the (2*S*)-enantiomer showing 1000-fold more activity than the (2*R*)-enantiomer. Similar results were found for calcium release in HT-29 and OVCAR8 cells. Analogue **15** was also more effective than 1-oleoyl-LPA in activating MAPK and AKT in cells expressing high levels of LPA_3. The α-fluoromethylene phosphonate moiety greatly increased the half-life of **15** in cell culture. Thus, α-fluoromethylene LPA analogues are unique new phosphatase-resistant ligands that provide enantiospecific and receptor-specific biological readouts.

Introduction

Lysophosphatidic acid (LPA, 1- or 2-acyl-*sn*-glycerol 3-phosphate) (Figure 1) is a naturally occurring phospholipid with a deceptively simple structure. It has received increasing attention because of the variety of biological responses that it evokes, including platelet aggregation, smooth-muscle contraction, neurite retraction, cell proliferation, and cell migration.[1,2] Further, LPA production and action has been implicated in pathophysiological events such as cancer, atherosclerosis, and altered blood pressure.[1,2] Most of these cellular events are transduced via signal transduction cascades downstream of three GPCRs belonging to the endothelial differentiation gene (EDG) family (LPA_1, LPA_2, and LPA_3, aka EDG2, EDG4, and EDG7, respectively). A fourth LPA receptor (LPA_4) more closely related to the purinergic family of GPCRs has been identified;[3] however, its functional role remains to be elucidated. LPA_1 and LPA_2 knockout mice reveal that LPA_1 has a crucial role in brain development.[4,5] The absence of LPA_1 expression results in craniofacial dysmorphism, semi-

Figure 1. Modifications of *sn*-1- and *sn*-2-acyl-LPA.

lethality due to defective suckling behavior, and generation of a small fraction of pups with frontal hematoma.[4] Although LPA_2 is not essential for normal mouse development, it acts redundantly with LPA_1 to mediate LPA responses in fibroblasts.[6] The physiological roles of LPA_3 and LPA_4 are still not known. LPA may have other targets in cells, based on the recent observations that LPA is a potential endogenous ligand for the nuclear hormone receptor PPARγ[7] and that LPA stimulates proliferation of rat hepatoma cells in an EDG-independent manner.[8] The question of which receptor type(s) are involved in the pleiomorphic effects of LPA in multiple cell lineages is largely unresolved in part because of the relative paucity of receptor subtype-selective agonists and antagonists. Such receptor subtype-selective agents would also be valuable tools in chemical genomics and would facilitate the development of therapeutic compounds for the manipulation of LPA responses.

* To whom correspondence should be addressed. Phone: +1-801-585-9051. Fax: +1-801-585-9053. E-mail: gprestwich@pharm.utah.edu.
[†] The University of Utah.
[‡] The University of Tokyo.
[§] M. D. Anderson Cancer Center.

10.1021/jm049186t CCC: $30.25
Published on Web 04/02/2005

Serum is the best characterized source of LPA. We recently showed that serum LPA is produced via multiple pathways requiring different phospholipases.[9] As a consequence of the reactions, LPA with various fatty acid species at either the *sn*-1 or *sn*-2 position is generated. Indeed, LPA species with saturated (16:0 and 18:0) or unsaturated (16:1, 18:1, 18:2, and 20:4) fatty acids were detected in serum[10] and activated human platelets.[11] Interestingly, these LPA species differentially activate the three LPA receptors. In particular, LPA_3 shows a relatively higher affinity for LPA species with unsaturated fatty acids.[12,13] This may explain the cellular responses selectively induced by unsaturated LPA, such as calcium mobilization in human A431 cells,[14] proliferation,[15] and dedifferentiation[16] of smooth muscle cells. LPA_1 and LPA_2 do not distinguish among different LPA species.[13] Thus, each receptor recognizes LPA differentially, which permits the identification of LPA receptor-specific agonists or antagonists.

In most glycerolphospholipids, the *sn*-1 position is occupied by saturated fatty acids whereas the *sn*-2 position is occupied by unsaturated fatty acids. This suggests that unsaturated LPA is initially produced as an *sn*-2-acyl-LPA and thus may be a potential ligand for LPA_3.[13] However, study of the 2-acyl-LPA isoform has been difficult because of its chemical lability resulting in intramolecular acyl chain migration. Thus, to explore the significance of the 2-acyl-LPA, analogues that are resistant to acyl chain migration are required. In addition, when applied to cells or tissues, LPA is readily degraded to monoacylglycerol by lipid phosphate phosphatases (LPPs), which complicates the determination of the nature and concentration of the activating ligand in studies of structure−activity relationships (SARs).

When compounds that have altered ligand specificity and stability are desired, the isosteric substitution of essential hydroxyl groups by fluorine has been a mainstay of analogue design.[17] This strategy has not been previously undertaken in a SAR study for LPA receptors. We therefore have developed a program to test the hypothesis that fluorinated analogues of LPA, particularly with fluorine in the *sn*-1 or *sn*-2 position, might mimic LPA as a biological ligand. Moreover, we sought a way to create phosphatase-resistant LPA analogues. Such stable LPA analogues could be useful in defining the regiochemical selectivity of LPA receptors for the acyl position and for identifying LPA receptor-selective agonists or antagonists. In this study, we describe the structure−activity study and receptor selectivity for 22 different fluorine-containing LPA analogues. In addition, we describe a more detailed evaluation of the enantiospecific response to a fluoromethylene phosphonate analogue **15**, which is a potent LPA_3-selective agonist.

Chemistry

The synthetic pathways to the LPA analogues in Figure 2 have already published.[18−21] The monofluorinated and difluorinated LPA analogues in which either the *sn*-1 or *sn*-2 hydroxy group was replaced by fluorine were prepared from (*R*)- or (*S*)-solketal.[18,21] The fluorine subsitution blocks acyl migration, effectively "freezing" them in the *sn*-1-*O*-acyl or *sn*-2-*O*-acyl forms. The

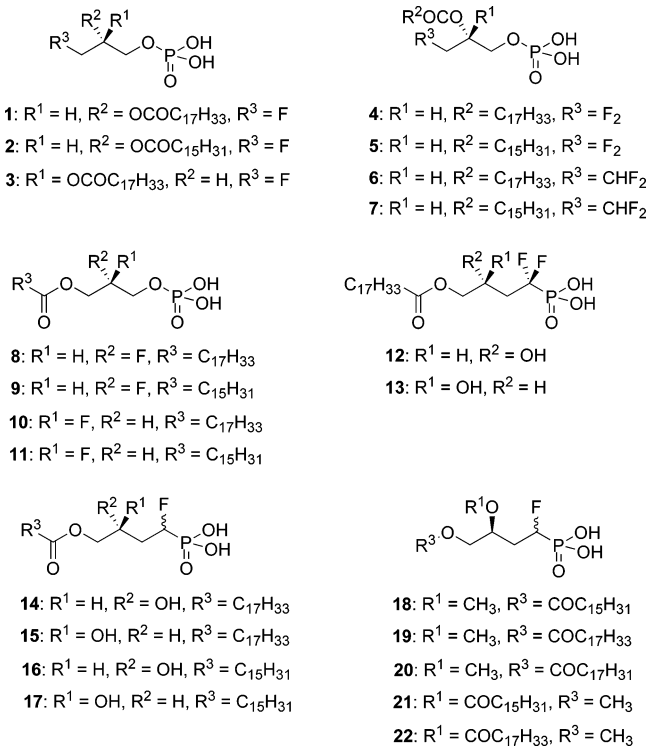

Figure 2. Structures of fluorinated LPA analogues.

fluoromethylene phosphonate LPA analogues were prepared from 3,4-epoxy butylfluorophosphonate using a chiral salen-Co catalyzed HKR (hydrolytic kinetic resolution) reaction[18,20] or using a fluorovinylphosphonate route.[19]

Biology

We have previously demonstrated that acyl chain length and saturation significantly alters the potency of LPA in a receptor subtype-specific manner.[12,13] LPA with oleic acid (18:1), linoleic (18:2), or linoleoic (18:3) at the *sn*-1 or *sn*-2 position efficiently activated all three receptors.[13] To further address how each LPA receptor recognizes LPA and to identify receptor-selective LPA analogues, a series of fluorinated LPA analogues were synthesized in which either the *sn*-1 or *sn*-2 hydroxyl group was replaced by fluorine or in which the bridging oxygen in the monophosphate was replaced by an α-monofluoromethylene (−CHF−) or α,α-fluoromethylene ($-CF_2-$) moiety; acyl chains were placed in either the *sn*-1 or *sn*-2 position (see Figures 1 and 2).[18−21] Since the *sn*-2 position of LPA is chiral, both enantiomers (2*R* and 2*S* forms) were prepared to probe receptor enantioselectivity. In addition, a series of difluorinated LPA analogues with either oleoyl (18:1) or palmitoyl (16:0) acyl chains was prepared to probe the role of different fatty acyl chains. The structures of LPA analogues are presented in Figure 2.

Analogue 15 Is a Potent Agonist for LPA_3. We tested 22 LPA analogues (Figure 2), 1-oleoyl-LPA, and 1-palmitoyl-LPA by determining the potency toward specific LPA receptors. Among the various common receptor assay techniques (ligand binding assay, adenylyl cyclase activation, GTP [γ^{35}S] binding, and calcium mobilization), we selected the calcium mobilization assay because changes in cytosolic calcium occur within seconds of addition, which precludes the stability of a

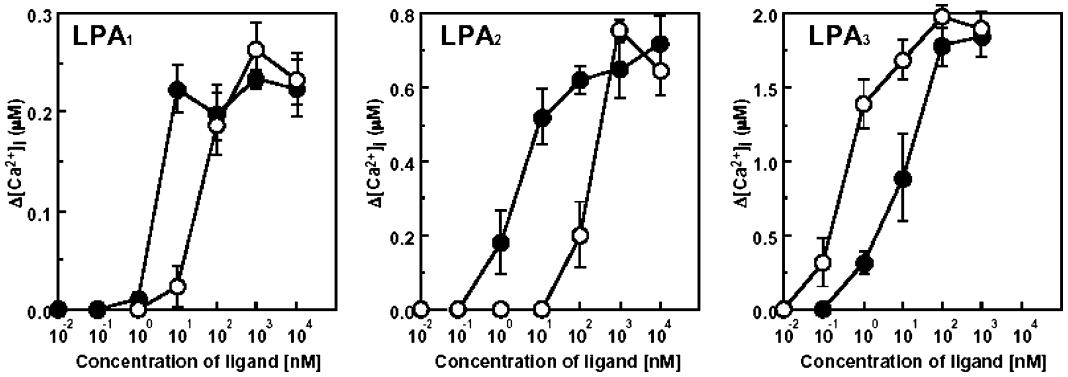

Figure 3. Induction of increases in intracellular calcium ($[Ca^{2+}]_i$) by 1-oleoyl LPA and **15** in LPA_1, LPA_2, or LPA_3 expressing Sf9 cells. Sf9 cells expressing LPA_1, LPA_2, or LPA_3 were loaded with Fura-2 AM and were stimulated with LPA (1-oleoyl) and **15**, and changes in $[Ca^{2+}]_i$ using various concentrations (10^{-2}−10^4 nM) were analyzed spectrofluorometrically: **15** (open circles); 1-oleoyl LPA (filled circles). Each point represents the mean ± SD for $n = 3$.

Table 1. EC_{50} Values of LPA Analogues for LPA_3 Receptor Activation

compd	EC_{50}	compd	EC_{50}
LPA		**10**	>10 μM
1-oleoyl	~10 nM	**11**	>10 μM
1-palmitoyl	>10 μM	**12**	~1 μM
analogues		**13**	~500 nM
1	~10 nM	**14**	~500 nM
2	~3 μM	**15**	~0.5 nM
3	~200 nM	**16**	>10 μM
4	>10 μM	**17**	~20 nM
5	>10 μM	**18**	>10 μM
6	>10 μM	**19**	~20 nM
7	>10 μM	**21**	~10 μM
8	~1 μM	**22**	~5 nM
9	>10 μM	OMPT	~5 nM

compound affecting its activity and limits the likelihood that observed effects are due to growth factors produced as a consequence of receptor ligation. The activation of LPA receptors was evaluated by measuring Ca^{2+} response in insect cells expressing each receptor after cells were stimulated with LPA analogues. Since insect cells lack endogenous LPA receptors, this permits independent assessment of each receptor. The analysis at each recombinant LPA receptor revealed striking differences in activity. Among the three LPA receptors, LPA_3 was found to be activated dramatically by several of the new synthetic LPA analogues. In contrast, none of the analogues were found to be more potent than 1-oleoyl-LPA for activation of LPA_1 and LPA_2 (not shown). The results of the LPA_3 activation are presented in Table 1 and Supporting Information Figure 1. Among the LPA analogues, **15** (Figure 2) was the most potent agonist for LPA_3. The rank order potencies of LPA analogues in LPA_3 activation was **15** > OMPT = **22** > **1** > **17** = **19** = 1-oleoyl-LPA > **3** > **13** = **14** > **8** = **12** > **21**. In contrast, analogues **2**, **4**, **5**, **6**, **9**, **10**, **11**, **16**, and **18** were very poor agonists for LPA_3. The EC_{50} value of **15** was approximately 0.5 nM (Table 1), while the EC_{50} value of 1-oleoyl-LPA was 10 nM. Thus, analogue **15** showed 20-fold higher potency as an LPA_3-selective agonist and essentially no activity for activation of either LPA_1 or LPA_2 at concentrations where it optimally activated LPA_3 (Figure 3).

We also tested whether analogue **15** acted specifically on LPA_3 naturally expressed in mammalian cells. For this purpose we chose two cancer cell lines, OVCAR-8 and HT-29. By real-time reverse transcription polymerase chain reaction (RT-PCR), it was found that OVCAR-8 dominantly expresses LPA_2 and LPA_3 and to a lesser extent of LPA_1. In contrast, HT-29 cells expressed almost exclusively LPA_2 mRNA. 1-Oleoyl-LPA induced a transient Ca^{2+} response in both cell lines. However, **15** induced potent Ca^{2+} response only in the LPA_3-expressing OVCAR-8 cells (Figure 4A). Activation of LPA_1 by **15** was also tested by another method. The dependence of LPA-induced cell migration on LPA_1 expression was recently documented.[22] We thus tested whether **15** could activate LPA_1 by examining cellular migration of three cancer cells that migrate in response to LPA in an LPA_1-dependent manner. As shown in Figure 4B, **15** did not stimulate significant migration of 203 glioma, PC-3, or MDA-MB-231 cells even at high concentrations, while 1-oleoyl-LPA induced significant cell migration in all three cells lines.

We determined the phosphorylation of Thr-473 of PKB/Akt and MAPK in signaling pathways downstream of LPA-activated GPCR. We used three different cancer cell lines: OVCAR-3 (predominantly LPA_3), SKOV-3 (LPA_2 > LPA_1 > LPA_3), and HT-29 (LPA_2 only, as assessed by quantitative PCR; see Figure 4A as an example). Figure 5 shows Western blots illustrating the dose-dependent phosphorylation of these protein kinases in OVCAR3 cells (predominantly LPA_3) in response to 1-oleoyl-LPA, racemic 1-oleoyl-2-*O*-methyl-rac-glycerophosphothionate (OMPT),[23] and analogues **14** and **15**. Consistent with the assays above, **15** was more active than its enantiomer **14**, the 1-oleoyl-LPA analogue, and the known LPA_3 agonist OMPT at inducing phosphorylation of MAPK. Figure 5 shows that at lower concentrations **14**, **15**, and OMPT were more potent than LPA for inducing phosphorylation of MAPK. However, at higher micromolar concentrations, the efficiency of the LPA analogues decreased, and LPA appeared to be the most potent. Figure 5 also shows that only 1-oleoyl-LPA activated AKT and MAPK signaling in HT-29 (LPA_2 only) cells. These data further confirm that **14**, **15**, and OMPT are selective LPA_3 agonists.

The stabilized phosphonate **15** was predicted to be dramatically more stable than 1-oleoyl-LPA. Figure 6 shows that following incubation with HeLaS3 cells for 15 h, less than 10% of 1-oleoyl-LPA remained, while 80% of **15** was still present. Thus, the half-life of LPA is about 1 h in the cell culture, while **15** is unchanged during the first hour of incubation.

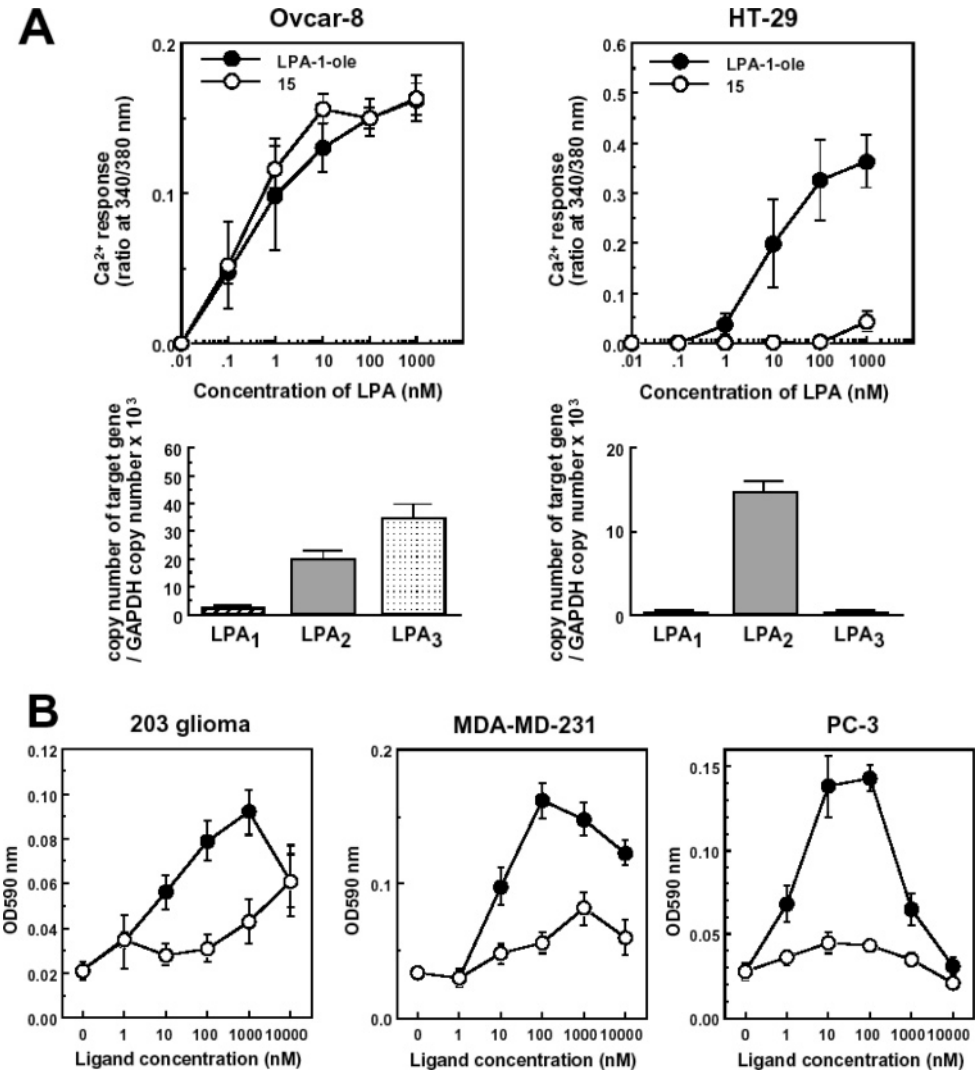

Figure 4. (A, top) Induction of increases in $[Ca^{2+}]_i$ by 1-oleoyl LPA and **15** in OVCAR-8 and HT-29 cells. Cells were loaded with Fura-2 AM and were stimulated with 1-oleoyl LPA and **15**. Changes in $[Ca^{2+}]_i$ resulting from various concentrations (10^{-2}–10^4 nM) were analyzed spectrofluorimetrically: **15** (open circles); 1-oleoyl LPA (filled circles). (A, bottom) Expression profiles of LPA_1, LPA_2, and LPA_3 GPCRs as judged by quantitative reverse transcriptase polymerase chain reaction (qRT-PCR) for these two cell lines. (B) Induction of cell migration by LPA (1-oleoyl) and **15** in 203 glioma, MDA-MD-231, and PC-3 cells. These cells all exhibit LPA_1-dependent cellular migration. Cell motility assay was performed using a Boyden chamber assay. Each point represents the mean ± SD for $n = 3$: **15** (open circles); 1-oleoyl LPA (filled circles).

Discussion

The SAR studies provided in Figure 2 enable us to address questions about the structural characteristics for activation of specific LPA receptors by comparing activities of pairs of analogues with subtle molecular differences. For example, we have tested enantiomers, compounds differing only by acyl subsituent, compounds differing by acyl regiochemistry, and compounds differing by a single functional group change. From these comparisons, we have defined key structural features that lead to potency and selectivity for LPA_3 receptor activation. Furthermore, detailed studies of signaling by analogue **15** and its enantiomer shed light on the downstream effects of activation of LPA_3 by analogues of LPA.

Acyl Chains: Oleoyl vs Palmitoyl Residues. We previously demonstrated that 1-oleoyl-LPA is a more potent ligand for LPA_3 than 1-palmitoyl-LPA.[12,13] When we compare the activity of each pair, **1** vs **2**, **6** vs **7**, **8** vs **9**, **14** vs **16**, **15** vs **17**, **22** vs **21**, those LPA analogues possessing an oleoyl residue (**1**, **6**, **8**, **14**, **15**, **22**) are more potent at LPA_3 by 1 log order or more than those with a palmitoyl residue (**2**, **7**, **9**, **16**, **17**, **21**) (Table 1 and Supporting Figure 1). Thus, independent of substitutions and alterations of the LPA glycerol backbone, 1-oleoyl-LPA is the preferred ligand for LPA_3.

Position of Acyl Chains: *sn*-1-Acyl vs *sn*-2-Acyl. The study of 2-acyl-LPA has been difficult because of its chemical lability; intramolecular acyl chain migration affords an equilibrium mixture of 1-acyl- and 2-acyl-LPA.[24] Thus, the resulting mixture does not allow accurate determination of the activity of the separate ligands in SAR studies. Analogues that lack either a 1- or 2-hydroxyl group are ideal compounds to evaluate the position of acyl chains in the SAR studies because they cannot undergo acyl migration. Compounds **1**, **3**, **8**, **10**, **19**, and **22** are such analogues. The enantiomeric *sn*-1-fluoro analogues **1** and **3** both have an oleoyl chain at the *sn*-2 position. These are more potent ligands for LPA_3 than **8** and **10**, which have the oleoyl chain in the

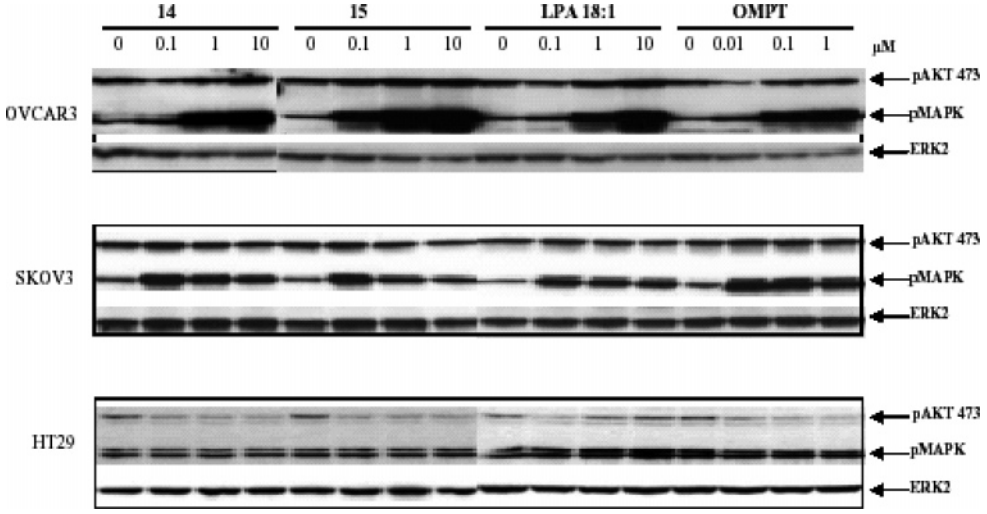

Figure 5. Induction of phosphorylation of AKT and MAPK in OVCAR-3, SKOV-3, and HT-29 cells by LPA analogues. Cells were lysed in SDS sample buffer or ice-cold X-100 lysis buffer. Total cellular protein was separated by SDS−PAGE, transferred to Immobilon, and immunoblotted with antibodies following the protocols provided. Immunocomplexes were visualized with an enhanced chemiluminescence detection kit using horseradish peroxidase conjugated secondary antibodies.

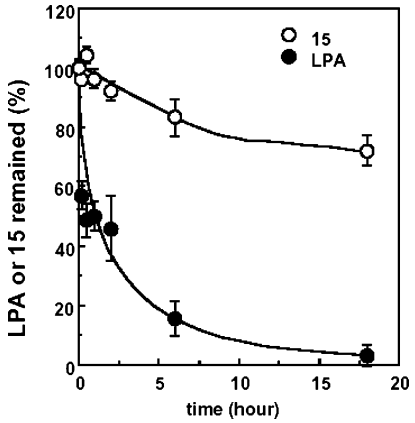

Figure 6. Stability of **15** and LPA in culture cells. Solutions of **15** and 1-oleoyl-LPA (both 20 μM final concentration) were added to HeLaS3 cells. After incubation for the indicated times, aliquots were taken and the concentrations of **15** and LPA were determined either by mass spectrometry (for **15**) or by an enzymatic coloriometric method (for LPA). Each point represents the mean ± SD for $n = 3$.

sn-1 position. Similarly, **22**, which has a 2-acyl group and a 1-*O*-methyl group to block migration, was more potent than the 1-acyl, 2-*O*-methyl analogue **19** (Table 1 and Supporting Information Figure 1). Analogue **1**, with its acyl chain in (2*S*)-configuration, was a slightly more potent ligand than its enantiomer **3**, having a (2*R*)-acyl chain (Table 1). Thus, LPA analogues with acyl chains in the *sn*-2 position with the unnatural (2*S*)-configuration appear to be the optimal ligands for LPA_3. It is noteworthy that we were unable to determine the importance of the acyl position of LPA analogues on activation of LPA_1 and LPA_2, since none of these 22 LPA analogues showed significant selectivity for these two receptor types.

Chirality of the *sn*-2 Hydroxy Group. Comparison of the activity of each pair of analogues, **12** and **13**, **14** and **15**, and **16** and **17** (Table 1 and Supporting Information Figure 1), enable us to evaluate the configuration of the hydroxy group at the *sn*-2 position of LPA. (Note: the IUPAC nomenclatural designation of *R* and *S* changes with the order of priority of the substituents; hence, we use the term "natural" and "unnatural" to clarify the absolute configuration of a given substituent relative to naturally occurring LPA.) In all cases, analogues with the same absolute configuration (**13**, **15**, and **17**, designated 2*S* in this case) as naturally occurring LPA were more potent than those with the unnatural configuration (**12**, **14**, **16**) (Table 1 and Supporting Information Figure 1). This illustrates that LPA analogues with the hydroxy group with the natural configuration are preferable ligands for LPA_3. Analogue **1**, with its acyl chain in the (2*R*)-configuration (note that the IUPAC priority has changed), was a slightly more potent ligand than its enantiomer **3**, having a (2*S*)-acyl chain (Table 1 and Supporting Information Figure 1). Thus, LPA analogues with acyl chains in the *sn*-2 position with the unnatural configuration appear to be the optimal ligands for LPA_3. The reason for the apparent "inverse" enantioselectivity remains to be elucidated. We have also demonstrated that the unnatural (2*S*)-isomer OMPT (the unnatural configuration for this substitution pattern) was more effective at activating LPA_3 and concomitant downstream signaling events than either (2*R*)-OMPT (natural configuration) or racemic OMPT. This result suggests that, relative to the native hydroxyl group, the 2-*O*-methoxy group is less well accommodated in the receptor binding site. Thus, we proposed that the natural (2*R*)-enantiomer of OMPT suffered a steric interference that could be avoided by the (2*S*)-enantiomer, leading to the apparent "inverse" enantioselectivity.[25] Whether this is also the case for the unnatural *sn*-2-LPA remains to be elucidated.

Replacement of Phosphate with Fluoromethylene Phosphonates. The metabolically stabilized analogue **15** features a monofluoromethylene phosphonate substituted for the bridging oxygen of the phosphate monoester. To further explore the molecular details that confer potency and selectivity of **15** for LPA_3 activation, several parameters were examined. First, the replacement of the phosphate oxygen with a monofluoromethylene (−CHF−) moiety occurs in two pairs: 1-oleoyl-LPA to **15** and 1-palmitoyl-LPA to **17**. In both cases,

the phosphonate derivative demonstrated a more than 100-fold increase in potency in the LPA_3 calcium release assay (Table 1 and Supporting Information Figure 1). In contrast, the enantiomeric phosphonates **12** and **13**, with a replacement of oxygen with a difluoromethylene ($-CF_2-$) moiety, were 2 orders of magnitude weaker LPA_3 agonists (compare **15** with **13**, and **14** with **12**). Both fluoromethylene phosphonate LPA analogues were poor ligands for both LPA_1 and LPA_2 (data not shown), suggesting that these two receptors may have a stricter requirement for the phosphate group than LPA_3.

Fluorination at the *sn*-1 Position. The effect of fluorine substitution at the *sn*-1 position can be evaluated by comparing the activity of **1** and **4**. Introduction of one fluorine residue (analogue **1**) did not substantially reduce agonist activity at LPA_3. However, introduction of two fluorines (analogue **4**) or a difluoromethyl group (analogue **6**) resulted in much weaker agonists at LPA_3. Thus, the $-CH_2OH$ group of an *sn*-1-OH-2-*O*-acyl-LPA could be replaced with $-CH_2F$ but not by $-CHF_2$ or $-CH_2CHF_2$.

Fluorination and Absolute Configuration at the *sn*-2 Position. Monofluorinated LPA analogues in which the central *sn*-2 position $-CHOH-$ was replaced by $-CHF-$ (**8**−**11**) were relatively poor agonists for all LPA receptor types (Figure 3, Table 1). However, a comparison of the activities of **8** and **10** enables us to evaluate the configuration of fluorine residue at the *sn*-2 position. The relatively higher potency of **8** relative to **10** indicates that the (2*S*)-configuration (in which the *sn*-2 fluorine occupies the position of the hydroxyl group in the natural enantiomer of LPA) is preferred by LPA_3.

O-Methylation at the *sn*-2 Position. The LPA_3-selective agonist OMPT has an oleoyl chain at the *sn*-1 position and *O*-methyl residues at the *sn*-2 position, in addition to the metabolically stabilized thiophosphate at the *sn*-3 position.[23] LPA_3 activation was enantioselective, with the unnatural (2*S*)-isomer showing higher potency than the (2*R*)-enantiomer.[25] This finding prompted us to synthesize **19** (see Figure 2), which has characteristics of both **15** (the monofluoromethylene phosphonate) and OMPT (the *O*-methyl group). However, as shown in Table 1 and Supporting Information Figure 1, **19** was found to be a less potent ligand for LPA_3 than either **15** or OMPT. It appears that simultaneous introduction of the *O*-methyl and monofluorophosphonate substitutions interferes with receptor recognition. In contrast, the regioisomer **22**, which has an oleoyl residue at the *sn*-2 position and the *O*-methyl group at the *sn*-1 position, was a more potent ligand than **19** (Table 1 and Supporting Information Figure 1). This provides further evidence that the LPA species possessing *sn*-2 acyl chains are generally more potent ligands for LPA_3.

Interpretation and Conclusions

In this study, we examined the potency of a wide variety of synthetic monofluorinated or difluorinated LPA analogues for activation of three LPA receptors belonging to the EDG family. Several of these analogues were shown to be potent agonists for LPA_3, and the combined data permitted dissection of the SAR for acyl regiochemistry and hydroxyl group configuration. We have also examined whether any of the weak LPA analogues might be antagonists. However, none of the LPA analogues described herein showed antagonism of LPA receptor activation by a receptor-selective LPA analogue (data not shown). The highly electronegative fluorine substituents can act as acceptors in forming intra- and intermolecular hydrogen bonds. These interactions will undoubtedly affect receptor−ligand interactions. Moreover, because these LPA analogues have sites of chirality at *sn*-2, both enantiomers were synthesized to determine what molecular features determine recognition by LPA receptors. Several patterns were revealed when we tested these LPA analogues at the three LPA receptors.

First, these LPA analogues showed higher preference to LPA_3 but not to LPA_1 or LPA_2 (Supporting Information Figure 1). Indeed, none of the LPA analogues were revealed to be potent agonists at LPA_1 and LPA_2. We obtained the same conclusion from the results using ovarian cancer cells that express multiple LPA receptors (Figure 3). In contrast, some analogues (**15**, **22**, and **1**) were much more potent than naturally occurring LPA at LPA_3. The affinities of the LPA receptors differ: LPA_1 and LPA_2 have relatively higher affinity for 1-palmitoyl-LPA than LPA_3 in several assay systems.[26] In contrast, LPA_3 prefers LPA with unsaturated acyl chains that have a more bulky structure than saturated acyl chains.[12,13] Therefore, the binding pocket of LPA_3 appears to be larger than those of LPA_1 and LPA_2. In other words, LPA_1 and LPA_2 may have less tolerance for modification of the basic LPA acylglycerophosphate features than LPA_3. This is consistent with our inability to develop potent LPA_1 or LPA_2 selective agonists in this study.

Second, substitution of the bridging oxygen in the monophosphate by a α-monofluoromethylene ($-CHF-$) moiety but not by difluoromethlene ($-CF_2-$) resulted in a potent and selective agonist for LPA_3. Originally, these phosphonates were designed to be resistant to degradation by LPPs. Indeed, experimentally analogue **15** was more stable than 1-oleoyl-LPA when co-incubated with cultured cells (Figure 6). Thus, the potency of **15** could be in part attributable to its metabolic stability, but this was not an issue in the calcium release assay employed. We showed that **15** is a potent agonist for LPA_3 but not for LPA_1 and LPA_2, again suggesting that the differential activity at LPA_3 was not due to increased stability. We also showed that the configuration of the hydroxyl residue at the *sn*-2 position is crucial for the activity (**15** vs **14**). In addition, we showed that replacement of the hydroxyl residue with fluorine substituents markedly decreased activity. Thus, the hydroxyl residue and the α-monofluoromethylene moiety in **15** seemed to be specifically recognized by LPA_3.

Third, in marked difference with the modification in the bridging oxygen in the monophosphate by an α-monofluoromethylene ($-CHF-$) moiety, modification of the hydroxyl residue at either *sn*-1 or *sn*-2 by mono- or difluoride did not allow potent agonist activity at all LPA receptors (**1**−**3**, **6**, **7**, and **11**). However, this strategy revealed several aspects of the SAR of LPA analogues for receptor activation. The activities of **1**, **3**, and **10** allow us to obtain evidence regarding the activity of 2-acyl-LPA, despite the fact that the lability of this species precludes assessment under cell culture condi-

tions. The 2-acyl-LPA analogues (**1**, **3**, and **22**) proved to be more potent at LPA_3 than their 1-acyl counterparts (**10** for **1** and **3**, and **19** for **22**). A fluorine modification of the *sn*-1 position is better tolerated than at the *sn*-2 position. For example, **1** and **3**, which are fluorinated at the *sn*-1 position, showed much higher activity than **8** and **10**, fluorinated at the *sn*-2 position. This suggests an important role for the hydroxyl group at the *sn*-2 position of 1-acyl-LPA for optimal activation of LPA_3.

Fourth, we prepared both the 18:1 and 16:0 acyl derivatives of each LPA analogue. LPA analogues with oleoyl chains were uniformly more potent than those with palmitoyl chains for activation of LPA_3. This is consistent with previous studies that showed that LPA with unsaturated fatty acyl chains were more effective ligands for LPA_3,[13] indicating that the (9*Z*)-olefin was preferred for LPA_3 activation.

Ligand recognition by GPCRs generally shows a preference for the naturally occurring enantiomer. However, recognition of LPA by its receptors can be viewed as an exception because both the natural L (*R*)- and unnatural D (*S*)-stereoisomers of LPA are equally active in some bioassays.[27] In contrast to the enantiomers of natural LPA, however, the activities of LPA analogues based on non-glycerol backbones show strong enantioselectivity. For example, analogues of *N*-acylethanolamine phosphoric acid (NAEPA) derivatives,[26] which contain a serine or an ethanolamine backbone in place of glycerol, analogues of *N*-palmitoyl-2-methylenehydroxyethanolamide phosphoric acid ((*R*)-MHEPA and (*S*)-MHEPA),[8] and analogues of carbohydrate scaffolds[28] are recognized in a stereoselective manner in which (2*R*)-enantiomers (natural configuration) are more potent than (2*S*)-enantiomers (unnatural configuration). This duality of response has been recently reviewed.[29] Moreover, OMPT and its alkyl analogues exhibit different enantioselectivities in SAR studies (unpublished results). For example, both (2*S*)-acyl-OMPT and (2*S*)-alkyl OMPT (unnatural configuration) have higher activity than their (2*R*)-enantiomers (natural configuration).[25] In this study, we showed that those fluorinated LPA analogues that have natural absolute configuration at the *sn*-2 position are more potent than their enantiomers. These results unambiguously indicate that LPA receptors exhibit enantioselective recognition of LPA analogues.

LPA and structural analogues all have a polar headgroup, a linker, and a hydrophobic tail.[30] As reported, of these three motifs, modifications to the polar headgroup may be the least well-tolerated, particularly at LPA_1 and LPA_2. Only the modifications of the phosphate headgroup that retain a negative charge under physiological conditions have been demonstrated to retain receptor activation. So far, α-methylene phosphonate,[31] α-hydroxyl phosphonate, α-ketone phosphonate,[32] and thiophosphate (OMPT)[23,25] have been reported to retain activity. However, the negligible activities of these analogues for activation of LPA_1 and LPA_2 suggested a greater dependence on the free phosphate for these receptors. Therefore, we have discovered and developed a new kind of stable LPA_3-selective analogue, α-fluoromethylene phosphonate. We have demonstrated that **15** is much more stable than 1-oleoyl-LPA in cell culture; however, because the selectivity of the fluoromethylene phosphonate analogues for LPA_3 was observed in cytosolic calcium assays, which are not dependent on ligand stability, the structure directly engenders selectivity for LPA_3. The increased stability of the fluoromethylene phosphonate analogues may have a much greater effect on activities when the analogues are evaluated in systems requiring longer incubation. The newly identified LPA_3-selective LPA analogue **15** will be a useful new reagent to characterize cellular and physiological roles of LPA_3 both in vitro and in vivo.

Experimental Section

The synthetic and analytical details for the LPA analogues herein were provided elsewhere.[18−21] The structure of each analogue was determined from NMR spectra recorded at 400 MHz (^{1}H), 101 MHz (^{13}C), 162 MHz (^{31}P), and 376 MHz (^{19}F) at 25 °C. 1-Oleoyl-LPA and 1-palmitoyl-LPA were obtained from Avanti Polar Lipids (Alabaster, AL). Fura-2 acetoxymethyl ester (Fura-2 AM) was purchased from Molecular Probes Inc., Eugene, OR. Biological results shown are representative of at least three independent experiments, and error bars indicate the standard deviation from the mean.

Evaluation of Receptor Activation by Ca^{2+} Assay. Assay for mobilization of intracellular Ca^{2+} was performed essentially as described.[12] Briefly, Sf9 insect cells infected with baculoviruses encoding human LPA_3, human LPA_2, or a human LPA_1−LPA_2 chimera were harvested 48 h after baculovirus infection, washed gently with a morpholinoethanesulfonic acid (MES) buffered saline (MBS) containing 10 mM NaCl, 60 mM KCl, 17 mM $MgCl_2$, 10 mM $CaCl_2$, 110 mM sucrose, 4 mM glucose, 0.1% fatty acid free bovine serum albumin (BSA) (Sigma), and 10 mM MES, pH-adjusted to 6.2 at room temperature with NaOH and loaded with 2 mM Fura-2 AM for 45 min. Free Fura-2 AM was washed out, and the cells were resuspended in the MBS buffer to produce a concentration of 10^6 cells/mL. Agonist-induced Fura-2 AM fluorescence of samples in quartz cuvettes kept at 27 °C was monitored at excitation wavelengths of 340 and 380 nm and an emission wavelength of 500 nm using a CAF-110 spectrofluorimeter (Japan Spectroscopy, Inc., Tokyo, Japan). Fluorescence was recorded before and after addition of ligands. The effects of LPA and LPA analogues on intracellular Ca^{2+} in HT-29 and OVCAR8 were performed as described following loading with the Fura-2 AM using a CAF-110 spectrofluorimeter.[23]

Chemotaxis Assay. Cancer cells were cultured in RPMI 1640 (Sigma) with 5% fetal bovine serume (FBS), plus 100 μg/mL streptomycin and 100 units/mL penicillin. Cell migration was measured in a modified Boyden chamber as described previously.[22] In brief, a polycarbonate filter with 8 μm pores for cancer cell lines (Neuro Probe, Inc., Gaithersburg, MD), which was coated with 0.001% of fibronectin (Sigma), was placed on a 96-blind-well chamber (Neuro Probe) containing the indicated amounts of LPA (18:1; Avanti Polar Lipids, Inc.) or LPA analogues, and cells (1×10^5 cells in 200 μL/well) were loaded into upper chambers. After incubation at 37 °C in 5% CO_2 for 3 h, the cells on the filter were fixed with methanol and stained with a Diff-Quik staining kit (International Reagents Corp., Kobe, Japan). The number of cells that migrated to the underside was determined by measuring optical densities at 590 nm using a 96-well microplate reader (Nalge Nunc International).

Downstream Signaling by Western Blot Analysis. Western blots were performed as described.[23] Briefly, cells were lysed in SDS sample buffer or ice-cold X-100 lysis buffer consisting of 1% Triton X-100, 50 mM Hepes, pH 7.4, 150 mM NaCl, 1.5 mM $MgCl_2$, 1 mM EGTA, 10% glycerol, 100 mM NaF, 10 mM sodium pyrophosphate, and protein inhibitor mixture (Roche). Total cellular protein was separated by SDS−PAGE, transferred to Immobilon [poly(vinylidene difluoride)], and immunoblotted with antibodies following the protocols provided. Immunocomplexes were visualized with an enhanced chemiluminescence detection kit (Amersham Pharmacia) using

horseradish peroxidase conjugated secondary antibodies (Bio-Rad, Richmond, CA). Antibodies against phospho Akt and total Akt were from New England Biolabs (Beverly, MA). The antibody against active phosphorylated MAPK was purchased from Promega (Madison, WI). Anti-Erk polyclonal antibody was from Santa Cruz Laboratories (Santa Cruz, CA).

Quantification of LPA and Analogue 15. To evaluate the stability of **15** in comparison to LPA, lipids were incubated with cultured HeLaS3 cells. We prepared 20 μM of each lipid in DMEM culture medium containing 0.1% BSA. After the indicated time, aliquots of the cultured medium were examined for LPA or **15** levels. LPA levels were determined by an enzyme-linked fluorometric assay previously established.[9] Analogue **15** was quantified using electrospray ionization mass spectrometry (ESI-MS) using a Quattro micro tandem quadrupole mass spectrometer (Micromass, Manchester, U.K.). After lipids were extracted from conditioned media, 2 μL aliquots dissolved in chloroform/methanol (2:1) were introduced by means of a flow injector into the ESI chamber at a flow rate of 2 μL/min. The eluting solvent was acetonitrile/methanol/water (2:3:1) containing 0.1% ammonium formate (pH 6.4). Under these conditions, **15** was detected as a parent ion of *m/z* 433.5 in the negative ion scan mode. In this system, we obtained linearity up to 50 μM **15**, and 200 nM was the lower limit of detectable **15**.

Acknowledgment. We thank the Utah Centers of Excellence Program, the Human Frontier Science Program (Grant RG0073-2000-B to G.D.P. and J.A.), Ministry of Education, Culture, Sports, Science and Technology of Japan (to J.A.), the NIH (Grant NS29632 to G.D.P., Grant NCI P01 CA64602, and Cancer Center Grant P30 CA16672 to G.B.M.), and the Department of Defense (Grant DAMD 17-02-1-0222 to G.B.M. and G.D.P.) for financial support of this work.

Appendix

Abbreviations. LPA, lysophosphatidic acid; EDG, endothelial differentiation gene; GPCR, G-protein-coupled receptor; HKR, hydrolytic kinetic resolution; LPP, lipid phosphate phosphatase; OMPT, 1-oleoyl-2-*O*-methyl-rac-glycerophosphothionate; RT-PCR, real time polymerase chain reaction; SAR, structure−activity relationship.

Supporting Information Available: A figure showing the activities of LPA and its analogues, a table showing references to the synthesis, characterization, and purity information of **1**−**22**, and a list of references. This material is available free of charge via the Internet at http://pubs.acs.org.

References

(1) Mills, G. B.; Moolenaar, W. H. The emerging role of lysophosphatidic acid in cancer. *Nat. Rev. Cancer* **2003**, *3*, 582−591.
(2) Feng, L.; Mills, G. B.; Prestwich, G. D. Modulators of lysophosphatidic acid signaling. *Expert Opin. Ther. Pat.* **2003**, *13*, 1619−1634.
(3) Noguchi, K.; Ishii, S.; Shimizu, T. Identification of p2y9/GPR23 as a novel G protein-coupled receptor for lysophosphatidic acid, structurally distant from the Edg family. *J. Biol. Chem.* **2003**, *278*, 25600−25606.
(4) Contos, J. J.; Ishii, I.; Chun, J. Lysophosphatidic acid receptors. *Mol. Pharmacol.* **2000**, *58*, 1188−1196.
(5) Contos, J. J.; Chun, J. The mouse LPA_3/Edg7 lysophosphatidic acid receptor gene: genomic structure, chromosomal localization, and expression pattern. *Gene* **2001**, *267*, 243−253.
(6) Contos, J. J.; Ishii, I.; Fukushima, N.; Kingsbury, M. A.; Ye, X.; Kawamura, S.; Brown, J. H.; Chun, J. Characterization of LPA_2 (Edg4) and LPA_1/LPA_2 (Edg2/Edg4) lysophosphatidic acid receptor knockout mice: signaling deficits without obvious phenotypic abnormality attributable to LPA_2. *Mol. Cell. Biol.* **2002**, *22*, 6921−6929.
(7) McIntyre, T. M.; Pontsler, A. V.; Silva, A. R.; St Hilaire, A.; Xu, Y.; Hinshaw, J. C.; Zimmerman, G. A.; Hama, K.; Aoki, J.; Arai, H.; Prestwich, G. D. Identification of an intracellular receptor for lysophosphatidic acid (LPA): LPA is a transcellular PPARγ agonist. *Proc. Natl. Acad. Sci. U.S.A.* **2003**, *100*, 131−136.
(8) Hooks, S. B.; Santos, W. L.; Im, D. S.; Heise, C. E.; Macdonald, T. L.; Lynch, K. R. Lysophosphatidic acid-induced mitogenesis is regulated by lipid phosphate phosphatases and is Edg-receptor independent. *J. Biol. Chem.* **2001**, *276*, 4611−4621.
(9) Aoki, J.; Taira, A.; Takanezawa, Y.; Kishi, Y.; Hama, K.; Kishimoto, T.; Mizuno, K.; Saku, K.; Taguchi, R.; Arai, H. Serum lysophosphatidic acid is produced through diverse phospholipase pathways. *J. Biol. Chem.* **2002**, *277*, 48737−48744.
(10) Baker, D. L.; Desiderio, D. M.; Miller, D. D.; Tolley, B.; Tigyi, G. J. Direct quantitative analysis of lysophosphatidic acid molecular species by stable isotope dilution electrospray ionization liquid chromatography−mass spectrometry. *Anal. Biochem.* **2001**, *292*, 287−295.
(11) Gerrard, J. M.; Robinson, P. Identification of the molecular species of lysophosphatidic acid produced when platelets are stimulated by thrombin. *Biochim. Biophys. Acta* **1989**, *1001*, 282−285.
(12) Bandoh, K.; Aoki, J.; Hosono, H.; Kobayashi, S.; Kobayashi, T.; Murakami-Murofushi, K.; Tsujimoto, M.; Arai, H.; Inoue, K. Molecular cloning and characterization of a novel human G-protein-coupled receptor, EDG7, for lysophosphatidic acid. *J. Biol. Chem.* **1999**, *274*, 27776−27785.
(13) Bandoh, K.; Aoki, J.; Taira, A.; Tsujimoto, M.; Arai, H.; Inoue, K. Lysophosphatidic acid (LPA) receptors of the EDG family are differentially activated by LPA species. Structure−activity relationship of cloned LPA receptors. *FEBS Lett.* **2000**, *478*, 159−165.
(14) Jalink, K.; Hengeveld, T.; Mulder, S.; Postma, F. R.; Simon, M. F.; Chap, H.; van der Marel, G. A.; van Boom, J. H.; van Blitterswijk, W. J.; Moolenaar, W. H. Lysophosphatidic acid-induced Ca^{2+} mobilization in human A431 cells: structure−activity analysis. *Biochem. J.* **1995**, *307*, 609−616.
(15) Tokumura, A.; Iimori, M.; Nishioka, Y.; Kitahara, M.; Sakashita, M.; Tanaka, S. Lysophosphatidic acids induce proliferation of cultured vascular smooth muscle cells from rat aorta. *Am. J. Physiol.* **1994**, *267*, C204−C210.
(16) Hayashi, K.; Takahashi, M.; Nishida, W.; Yoshida, K.; Ohkawa, Y.; Kitabatake, A.; Aoki, J.; Arai, H.; Sobue, K. Phenotypic modulation of vascular smooth muscle cells induced by unsaturated lysophosphatidic acids. *Circ. Res.* **2001**, *89*, 251−258.
(17) Patani, G. A.; LaVoie, E. J. Bioisosterism: A rational approach in drug design. *Chem. Rev.* **1996**, *96*, 3147−3176.
(18) Xu, Y.; Qian, L.; Prestwich, G. D. Synthesis of monofluorinated analogues of lysophosphatidic acid. *J. Org. Chem.* **2003**, *68*, 5320−5330.
(19) Xu, Y.; Qian, L.; Prestwich, G. D. Synthesis of α-fluorinated phosphonates from α-fluorovinylphosphonates: a new route to analogues of lysophosphatidic acid. *Org. Lett.* **2003**, *5*, 2267−2270.
(20) Xu, Y.; Prestwich, G. D. Synthesis of chiral (α,α-difluoroalkyl)-phosphonate analogues of (lyso)phosphatidic acid via hydrolytic kinetic resolution. *Org. Lett.* **2002**, *4*, 4021−4024.
(21) Xu, Y.; Prestwich, G. D. Concise synthesis of acyl migration-blocked 1,1-difluorinated analogues of lysophosphatidic acid. *J. Org. Chem.* **2002**, *67*, 7158−7161.
(22) Hama, K.; Aoki, J.; Fukaya, M.; Kishi, Y.; Sakai, T.; Suzuki, R.; Ohta, H.; Yamori, T.; Watanabe, M.; Chun, J.; Arai, H. Lysophosphatidic acid and autotaxin stimulate cell motility of neoplastic and non-neoplastic cells through LPA_1. *J. Biol. Chem.* **2004**, *279*, 17634−17639.
(23) Hasegawa, Y.; Erickson, J. R.; Goddard, G. J.; Yu, S.; Liu, S.; Cheng, K. W.; Eder, A.; Bandoh, K.; Aoki, J.; Jarosz, R.; Schrier, A. D.; Lynch, K. R.; Mills, G. B.; Fang, X. Identification of a phosphothionate analogue of lysophosphatidic acid (LPA) as a selective agonist of the LPA_3 receptor. *J. Biol. Chem.* **2003**, *278*, 11962−11969.
(24) Chevallier, J.; Sakai, N.; Robert, F.; Kobayashi, T.; Gruenberg, J.; Matile, S. Rapid access to synthetic lysobisphosphatidic acids using P(III) chemistry. *Org. Lett.* **2000**, *2*, 1859−1861.
(25) Qian, L.; Xu, Y.; Hasegawa, Y.; Aoki, J.; Mills, G. B.; Prestwich, G. D. Enantioselective responses to a phosphorothioate analogue of lysophosphatidic acid with LPA_3 receptor-selective agonist activity. *J. Med. Chem.* **2003**, *46*, 5575−5578.
(26) Heise, C. E.; Santos, W. L.; Schreihofer, A. M.; Heasley, B. H.; Mukhin, Y. V.; Macdonald, T. L.; Lynch, K. R. Activity of 2-substituted lysophosphatidic acid (LPA) analogs at LPA receptors: discovery of a LPA_1/LPA_3 receptor antagonist. *Mol. Pharmacol.* **2001**, *60*, 1173−1180.
(27) Yokoyama, K.; Baker, D. L.; Virag, T.; Liliom, K.; Byun, H. S.; Tigyi, G.; Bittman, R. Stereochemical properties of lysophosphatidic acid receptor activation and metabolism. *Biochim. Biophys. Acta* **2002**, *1582*, 295−308.

(28) Tamaruya, Y.; Suzuki, M.; Kamura, G.; Kanai, M.; Hama, K.; Shimizu, K.; Aoki, J.; Arai, H.; Shibasaki, M. Identifying specific conformations by using a carbohydrate scaffold: discovery of subtype-selective LPA-receptor agonists and an antagonist. *Angew Chem., Int. Ed.* **2004**, *43*, 2834−2837.

(29) Lynch, K. R.; Macdonald, T. L. Structure−activity relationships of lysophosphatidic acid analogs. *Biochim. Biophys. Acta* **2002**, *1582*, 289−294.

(30) Tigyi, G.; Parrill, A. L. Molecular mechanisms of lysophosphatidic acid action. *Prog. Lipid Res.* **2003**, *42*, 498−526.

(31) Heasley, B. H.; Jarosz, R.; Carter, K. M.; Van, S. J.; Lynch, K. R.; Macdonald, T. L. A novel series of 2-pyridyl-containing compounds as lysophosphatidic acid receptor antagonists: development of a nonhydrolyzable LPA_3 receptor-selective antagonist. *Bioorg. Med. Chem. Lett.* **2004**, *14*, 4069−4074.

(32) Santos, W. L.; Heasley, B. H.; Jarosz, R.; Carter, K. M.; Lynch, K. R.; Macdonald, T. L. Synthesis and biological evaluation of phosphonic and thiophosphoric acid derivatives of lysophosphatidic acid. *Bioorg. Med. Chem. Lett.* **2004**, *14*, 3473−3476.

JM049186T

Biol. Chem., Vol. 386, pp. 1137–1147, November 2005 • Copyright © by Walter de Gruyter • Berlin • New York. DOI 10.1515/BC.2005.130

Lysophosphatidic acid affinity chromatography reveals pyruvate kinase as a specific LPA-binding protein

Sophie Desmaret[1,a], Lian Qian[2,a], Berlinda Vanloo[1,a], Kris Meerschaert[1], Jozef Van Damme[1], Johan Grooten[3], Joël Vandekerckhove[1], Glenn D. Prestwich[2] and Jan Gettemans[1,*]

[1] Department of Medical Protein Research, Flanders Interuniversity Institute for Biotechnology (VIB), Ghent University, Faculty of Medicine and Health Sciences, Albert Baertsoenkaai 3, B-9000 Ghent, Belgium
[2] Department of Medicinal Chemistry, The University of Utah, 419 Wakara Way, Suite 205, Salt Lake City, UT 84108-1257, USA
[3] Department of Molecular Biomedical Research, Molecular Immunology Unit, VIB, Ghent University, B-9000 Ghent, Belgium

* Corresponding author
e-mail: jan.gettemans@ugent.be

Abstract

Lysophosphatidic acid is a pleiotropic lipid signaling molecule that evokes a broad array of cellular responses including proliferation, tumor cell invasion, neurite retraction, cytoskeletal rearrangements and smooth muscle contraction. Generally, lysophosphatidic acid triggers physiological responses through interaction with specific plasma membrane receptors called LPA 1–4. There is, however, increasing evidence in support of intracellular proteins that interact with LPA. We employed Affigel-immobilized LPA to isolate cytoplasmic proteins that interact with this lysophospholipid. Among the proteins retained by this affinity matrix, pyruvate kinase, clathrin heavy chain and heat shock protein 70 (Hsp70) were identified by mass spectrometry. Isothermal titration calorimetry showed that pyruvate kinase contains one binding site for LPA (K_a approx. 10^6 M^{-1}). Furthermore, LPA dissociates enzymatically active pyruvate-kinase tetramers into less active dimers, and is maximally active at concentrations close to its critical micelle concentration. These effects were not mimicked by other lysophospholipids. Co-immunoprecipitation experiments showed that pyruvate kinase interacts with clathrin, and confocal imaging revealed co-localization between clathrin and pyruvate kinase in the perinuclear region of cells. Our data suggest that pyruvate kinase partly exists in complex with clathrin in subcellular membranous areas, and that locally increased LPA levels can trigger inactivation of the metabolic enzyme.

Keywords: circular dichroism; enzymatic activity; gel filtration; isothermal calorimetry titration; mass spectrometry; phospholipid binding.

[a] These authors contributed equally to this work.

Introduction

Lysophosphatidic acid (LPA; 1-acyl-2 hydroxy-*sn*-glycero 3-phosphate) is one of the simplest natural phospholipids and a precursor in the *de novo* biosynthesis of phospholipids. In recent years, it has become clear that this lysophospholipid mediates various cellular processes, such as proliferation, differentiation, survival, migration, adhesion, invasion, and morphogenesis (Luquain et al., 2003; Mills and Moolenaar, 2003; Moolenaar et al., 2004).

Blood serum LPA is secreted by activated platelets, activated adipocytes, neuronal cells, and other cell types (Fukushima et al., 2001; Pages et al., 2001; Xie et al., 2002). Although mechanisms of LPA synthesis in individual cell types remain to be elucidated, serum LPA is produced by multiple enzymatic pathways that involve monoacylglycerol kinase, phospholipase A1, secretory phospholipase A2, and lysophospholipase D (lysoPLD), including autotaxin (Pages et al., 2001; Moolenaar, 2002; Xie and Meier, 2004).

Extracellular LPA evokes biological responses that are mediated through the activation of four G protein-coupled receptors (LPA1–4) (Ishii et al., 2004). In serum, LPA binds to gelsolin (Goetzl et al., 2000) and albumin (the main extracellular LPA-binding protein) with a nanomolar-range affinity for the phospholipid and a stoichiometry of ~3 mol LPA/mol albumin (Tigyi and Miledi, 1992; Thumser et al., 1994). Although important progress has been made in understanding the extracellular effects of LPA and its role in disease states such as cancer progression and atherosclerosis, the role of intracellular LPA has only recently been recognized. The role of intracellular LPA as an intermediate in the early steps of phospholipid biosynthesis is well established. This process occurs in the endoplasmic reticulum, where LPA is formed from glycerol-3-phosphate by a glycerophosphate acyltransferase and then further acylated to phosphatidic acid (PA), the precursor of all glycerophospholipids.

Weigert et al. (1999) showed that CtBP/BARS, a protein that is involved in Golgi tubule dynamics, is an essential component of the fission machinery operating at the Golgi tubular network. These authors found that CtBP/BARS uses acyl-CoA to selectively catalyze the acylation of LPA to PA both in pure lipidic systems and in Golgi membranes, and this reaction is essential for fission. Addition of LPA enhances the reaction and induces massive fission/defragmentation of the Golgi tubular networks, whereas other lysolipids have no effect. Lipid microdomains rapidly interconverting LPA, PA and diacylglycerol have the potential to facilitate the overall process of fission through coordinated changes in local membrane curvature. The lipid machinery probably involves other proteins. The best-characterized fission

protein so far is dynamin, which acts in concert with other proteins at the neck of endocytic vesicles. The dynamin binding protein endophilin is required for the formation of endocytic vesicles and has, like CtBP/BARS, LPA acyltransferase activity (Schmidt et al., 1999).

Intracellularly, LPA binds to fatty acid-binding proteins (FABP). Liver-type FABP (Thumser et al., 1994) exhibits micromolar-range affinity for LPA and allows the transport of mitochondrial LPA to microsomes in order to be acylated to PA (Vancura and Haldar, 1992). Gelsolin may also play an important role in LPA binding and transport. Cytoplasmic gelsolin binds, severs and caps actin filaments. LPA, as well as phosphoinositides containing D3 and D4 phosphate groups, binds to gelsolin, promoting actin filament uncapping and thus providing sites for actin assembly (Meerschaert et al., 1998). Recently, a role for intracellular LPA as a signaling molecule has been suggested by the finding that LPA (at relatively high doses) can compete with a synthetic ligand for binding to the nuclear transcription factor peroxisome proliferator-activated receptor γ (PPARγ). Extracellular LPA induces PPARγ-mediated reporter gene transcription in an LPA receptor-independent manner. It was also shown that LPA enhanced the expression of endogenous CD36 through PPARγ. CD36 is involved in internalizing oxidized low-density lipoprotein (LDL) in monocytes, leading to the formation of foam cells that are rich in cholesterol esters (McIntyre et al., 2003). This is an early event in the formation of atherosclerotic plaques, and Zhang et al. (2004) have indeed demonstrated that LPA activation of PPARγ can lead to accumulation of cells in the arterial wall. Intracellular LPA is also a potent regulator of the subfamily of mechano-gated K2P channels comprising TREK-1, TREK-2 and TRAAK. Channel mechano-sensitivity is drastically and reversibly altered by intracellular LPA (Chemin et al., 2005).

A recurring theme in studies on lipid mediators is their possible signaling role inside the cell. To identify intracellular LPA-binding proteins, we designed an affinity matrix consisting of an LPA analog covalently linked to Affigel-10. After incubation of cell extracts with this affinity matrix, several LPA-binding proteins were isolated and identified by mass spectrometry. As a proof-of-principle, validation and characterization of one of these LPA-binding proteins, pyruvate kinase, is described.

Results

LPA affinity matrix synthesis

To isolate novel LPA-binding proteins, we designed immobilized LPA as shown in Figure 1. An 11-aminoundecanoyl-linked LPA analog was synthesized for direct immobilization of LPA on Affigel-10 beads (Camus et al., 1987; Dingerdissen et al., 1987) as described in the materials and methods section. An additional control resin with no ligand was prepared by reaction of Affigel-10 with excess 2-aminoethanol.

Isolation and identification of cytosolic proteins that interact with LPA

We used HEK293T and MCF-7 cells as a source of material for isolation of LPA-binding proteins. After incubation with the LPA beads, unbound material was removed with several washes. The bound proteins were separated by SDS-PAGE and visualized by Coomassie Blue staining (Figure 2). It should be noted that the protein pattern of MCF-7 cells is very similar to the pattern of HEK293T cells. The identity of LPA-binding polypeptides was established by quadrupole time-of-flight (Q-TOF) mass spectrometry. In total, 12 polypeptides were identified. Among the candidate LPA interacting proteins, we further examined pyruvate kinase, clathrin heavy chain and heat shock protein 70 (Hsp70) because of their relatively high abundance. The identity of pyruvate kinase, clathrin heavy chain and Hsp70 was also confirmed by Western blotting (data not shown). To validate our method, commercially available pyruvate kinase M1 was further characterized with respect to its lipid-binding properties using isothermal titration calorimetry (ITC).

Binding of rabbit muscle pyruvate kinase to lysophospholipids

The interaction of pyruvate kinase with LPA (18:1) was studied by ITC. Figure 3 shows a typical experiment in which LPA solution was injected into the pyruvate kinase solution in the sample cell. Figure 3A shows the raw data and Figure 3B shows the integrated released heat as a function of the molar ratio of LPA/pyruvate kinase. After subtraction of the control (injection of LPA into buffer), the binding isotherm clearly shows an exothermic process with one binding site. The solid line represents the best fit of the data. The affinity of pyruvate kinase for LPA (18:1) is $\sim 3\times 10^{6}$ M^{-1} with a stoichiometry of about 1 mol LPA/mol pyruvate kinase and a reaction enthalpy of -12 kcal/mol. As pyruvate kinase exists as a tetramer in solution (Melamud and Mildvan, 1975), these data suggest that one tetramer of pyruvate kinase binds four LPA molecules. Titration of pyruvate kinase with lysophosphatidylcholine (LPC) or lysophosphatidylserine (LPS) showed no specific heat release after subtraction of the control (injection of the lysophospholipid into buffer) (data not shown).

Binding of pyruvate kinase to LPA is direct and specific

To examine the specificity of pyruvate kinase-LPA and clathrin-LPA interactions, we incubated MCF-7 cell lysate with Affigel-10 beads coupled to LPA, PA (Manifava et al., 2001) or phosphatidylinositol-4,5-bisphosphate (PIP_2). Western blot analysis showed that pyruvate kinase was strongly enriched by the LPA matrix, weak interaction occurred with the PA matrix, and no retention was observed on the PIP_2 matrix. Clathrin was also retained by the LPA beads (Figure 4A) but there was no significant signal following incubation with the PA beads. In both cases there was no interaction with Affigel beads. Furthermore, if binding of pyruvate kinase to immobilized

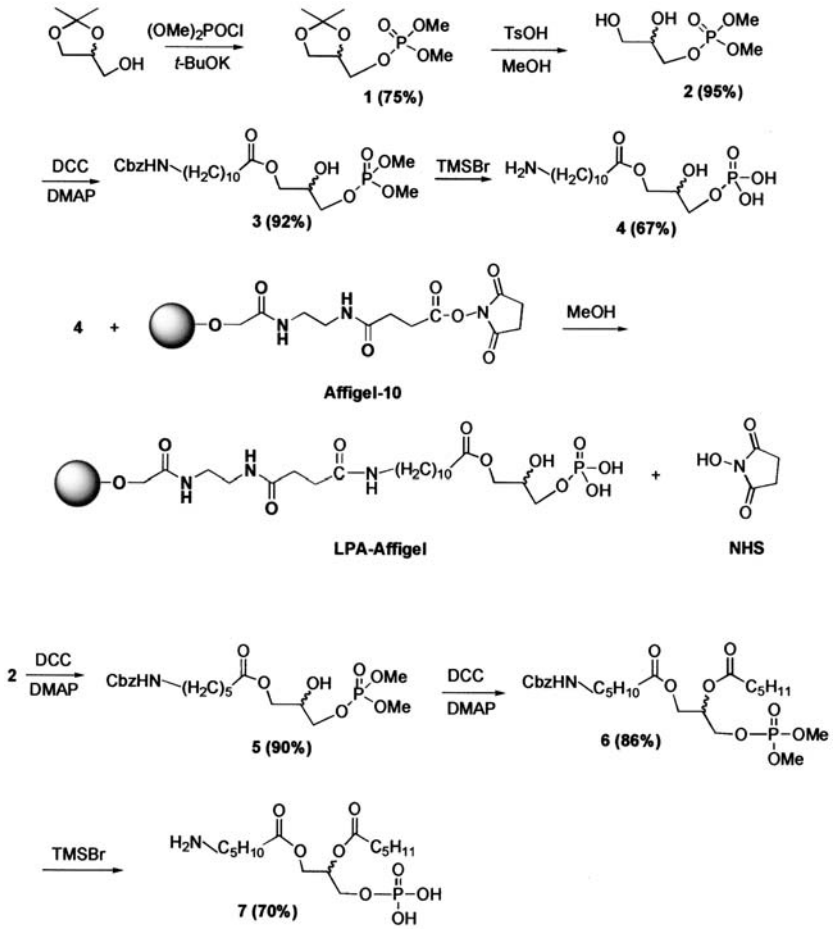

Figure 1 Synthesis of a derivatized LPA analog and coupling to Affigel-10.
The ω-amino functionalized lysophosphatidic acid was coupled to *N*-hydroxysuccinimide-activated ester resin, Affigel-10. The Affigel-10 bead is shown as a shaded sphere.

LPA is specific, then soluble LPA should compete and reduce the interaction between immobilized LPA and pyruvate kinase. We competed for binding of pyruvate kinase to Affigel-coupled LPA with hexanoyl LPA (6:0) or oleoyl LPA (18:1). When pyruvate kinase was preincubated with monomeric LPA (6:0), no competition was noted (Figure 4B, lanes 9–12), whereas preincubation with increasing concentrations of LPA (18:1) gradually abolished binding of pyruvate kinase to the LPA matrix (Figure 4B, lanes 1–8).

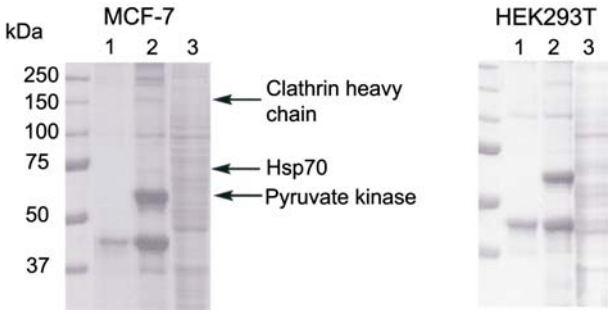

Figure 2 Coomassie-stained polyacrylamide gel (10%) revealing proteins retained by immobilized LPA.
Samples of 2 mg of cytosolic proteins (MCF-7 cells, left; HEK293T cells, right) were mixed with either control Affigel beads (lane 1) or LPA beads (lane 2). Lane 3 shows cytoplasmic proteins from MCF-7 or HEK293T cells. Proteins retained by the matrix were eluted with Laemmli sample buffer and separated by SDS-PAGE. Note the similar pattern between MCF-7 and HEK293T cells. Major bands are indicated by arrows. Molecular mass markers are shown on the left.

Effect of lysophospholipids on pyruvate kinase activity

The activity of pyruvate kinase was examined in the presence of hexanoyl LPA (6:0), myristoyl LPA (14:0) and oleoyl LPA (18:1) (Figure 5A). No effect was observed with hexanoyl LPA (6:0) over the entire concentration range (0–600 μM). With LPA (14:0) and LPA (18:1), the activity was reduced at concentrations higher than 400 and 50 μM, respectively. These concentrations are approximately the critical micellar concentration (CMC) of LPA (14:0) and LPA (18:1). Indeed, measurements with 2-(*p*-toluidinyl)-naphthalene-6-sodium sulfonate (TNS) yielded CMC values of ~370 and ~50 μM for LPA (14:0) and LPA (18:1), respectively (data not shown). At concentrations above the CMC of LPA (18:1), pyruvate kinase activity was almost completely abolished. Liposomes consisting of egg PC and LPA (18:1) (15% w/w) also significantly decreased the enzymatic activity of

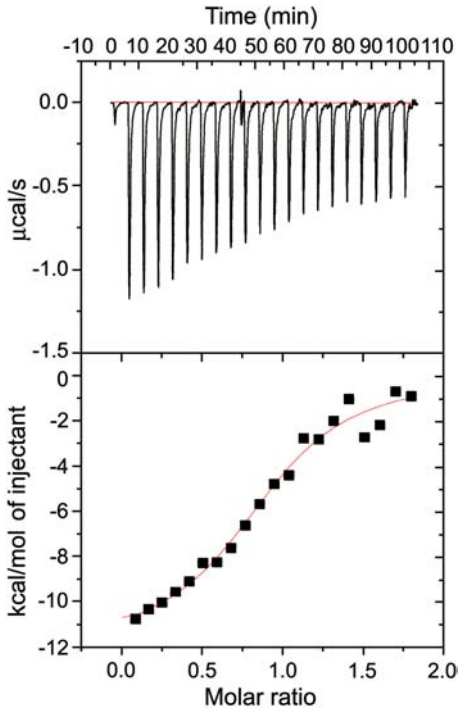

Figure 3 Lysophosphatidic acid-pyruvate kinase binding measured by isothermal titration calorimetry.
The top panel shows raw heat data obtained from 20 injections of LPA (18:1) into a cell containing 60 µM rabbit muscle pyruvate kinase (see the materials and methods section). The last six peaks correspond to heat of dilution and show that all of pyruvate kinase is saturated with LPA (18:1). Bottom panel: binding isotherm created by plotting areas under the peaks against the molar ratio of LPA (18:1) added to pyruvate kinase. The fit (line) corresponds with a model of four LPA molecules per tetramer of pyruvate kinase.

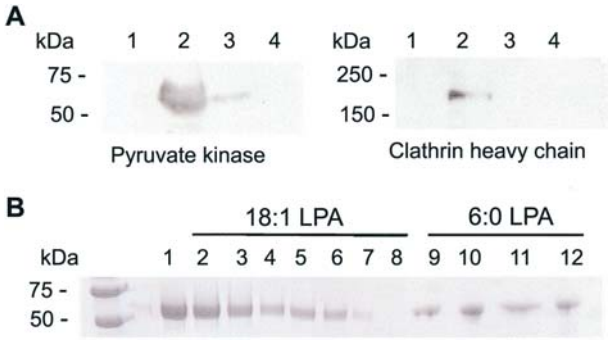

Figure 4 Specificity of clathrin and pyruvate kinase binding to LPA.
(A) MCF-7 cell lysate was incubated with control Affigel beads (lane 1), LPA beads (lane 2), PA beads (lane 3) or PIP2 beads (lane 4). Retained proteins were separated by SDS-PAGE, blotted and probed with anti-pyruvate kinase antibody (left) or anti-clathrin heavy chain antibody (right). (B) Purified pyruvate kinase (1 µM) was preincubated with 0 µM (lane 1), 5 µM (lane 2), 10 µM (lane 3), 20 µM (lane 4), 30 µM (lane 5), 40 µM (lane 6), 50 µM (lane 7) and 100 µM (lane 8) LPA (18:1) before incubation with LPA beads. To the left of lane 1, purified pyruvate kinase (1 µM) was incubated with control beads. Lanes 9–12: preincubation of 1 µM pyruvate kinase with 0 µM (lane 9), 50 µM (lane 10), 100 µM (lane 11) or 200 µM (lane 12) LPA (6:0) before incubation with LPA beads. Retained pyruvate kinase was visualized by SDS-PAGE and Coomassie Blue staining.

pyruvate kinase, whereas egg PC liposomes did not (data not shown). We also measured the activity of pyruvate kinase in the presence of different lysophospholipids (Figure 5B). LPC and LPS had no significant effect on pyruvate kinase activity, even at lipid concentrations exceeding their CMC. Lysophosphatidylinositol (LPI) only showed a minor effect at higher concentrations. We therefore conclude that LPA inhibits pyruvate kinase activity more specifically than other lysophospholipids. This finding was further supported by the lack of effect of different fatty acids (myristic and *cis*-parinaric acid) on the enzymatic activity (data not shown). Strong binding of LPA to pyruvate kinase at concentrations close to its CMC was also noted following non-denaturing gel electrophoresis (Figure 5C). A sharp decrease in lipid-free pyruvate configuration was observed at LPA concentrations of 50 µM and higher.

LPA dissociates active pyruvate kinase tetramers into inactive dimers

It has been documented that mammalian pyruvate kinase switches between a less active dimeric form and a highly active tetrameric form (Melamud and Mildvan, 1975). We investigated by gel filtration chromatography if the decrease in activity of pyruvate kinase upon incubation with LPA (18:1) was due to conversion of the tetrameric form to a dimeric form. Elution profiles of pyruvate kinase in buffer before and after incubation with lysophospholipids at a 1:100 pyruvate kinase/lipid molar ratio on a calibrated Superdex 200 PG column are shown in Figure 6. Pyruvate kinase in buffer eluted from the column as a tetramer with an apparent molecular weight of 233 kDa. Upon incubation with LPA (18:1) at a 1:100 molar ratio, two fractions eluted from the column with apparent molecular weights of 233 and 100 kDa, respectively. The second peak most likely corresponds to a dimer of pyruvate kinase. Pyruvate kinase activity in the top fraction of both peaks was measured: the first fraction retained full activity, whereas the second peak showed significantly decreased activity (data not shown). This effect was again specific for LPA, since LPC, LPS or LPI promoted no dissociation of pyruvate kinase at molar ratios similar to LPA.

Effect of lysophospholipids on the secondary structure of pyruvate kinase

The circular dichroism (CD) spectra of pyruvate kinase in phosphate buffer with or without LPA, LPC, LPS or LPI are shown in Figure 7. The CD spectrum of pyruvate kinase in phosphate buffer is indicative of an α-helical structure (Larsen et al., 1994) (characteristic minima at 208 and 222 nm). Upon incubation with LPA, the α-helicity increased from ~32% to ~36% at the expense of random coil. Incubation with LPC or LPS did not affect the secondary structure of pyruvate kinase, whereas LPI also slightly increased the α-helical structure. These data suggest that LPA does not unfold the enzyme, although it induces dissociation of the tetrameric configuration into a less active dimeric form.

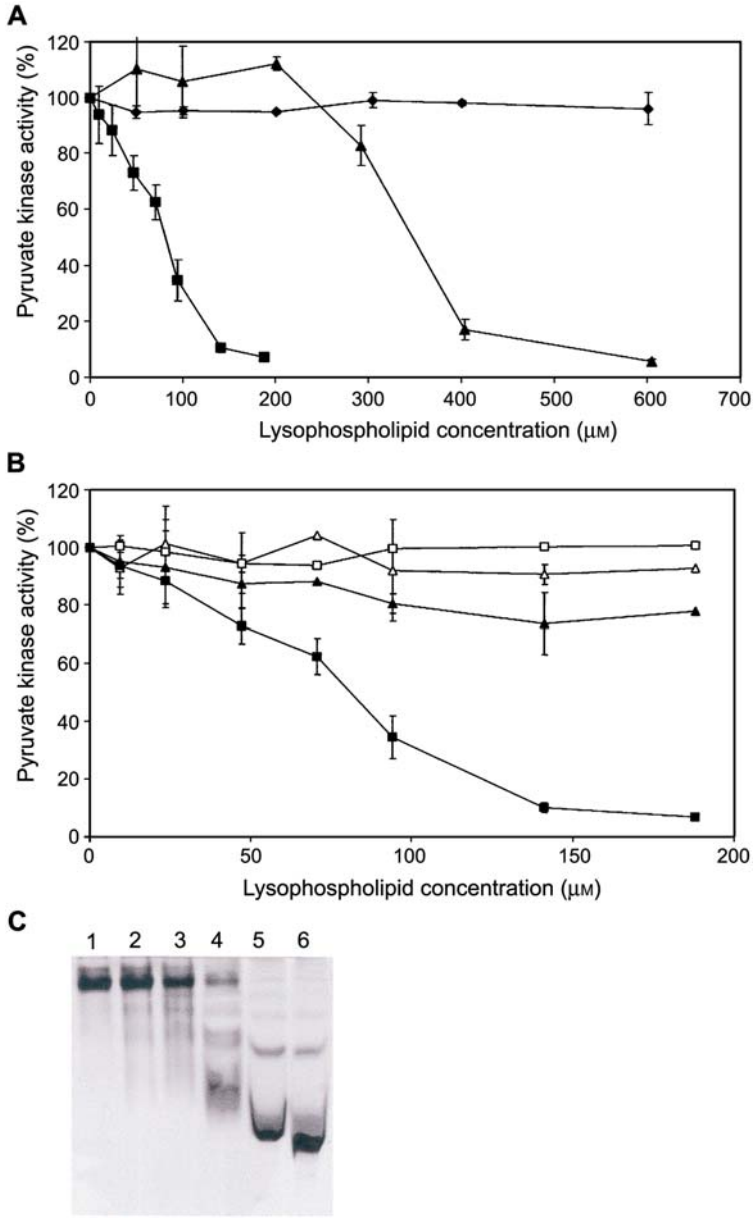

Figure 5 Effect of lysophosphatidic acid on pyruvate kinase activity.
(A) 0.5 μM pyruvate kinase was incubated at room temperature with increasing concentrations of LPA (18:1) (■); LPA (14:0) (▲) and LPA (6:0) (♦). (B) 0.5 μM pyruvate kinase was incubated at room temperature with increasing concentrations of LPA (18:1) (■); LPC (□); LPS (△) and LPI (▲). Activities are expressed relative to the activity of pyruvate kinase in buffer solution. None of these lysophospholipids had any effect on the LDH activity (data not shown). Symbols represent average±standard deviation for three experiments. (C) Non-denaturing polyacrylamide gel electrophoresis of pyruvate kinase without LPA (lane 1), or with increasing concentrations of LPA (18:1) at pyruvate kinase/LPA molar ratios of 1:10, 1:20, 1:50, 1:100 and 1:200, respectively (lanes 2–6).

Pyruvate kinase forms a complex with clathrin and Hsp70

Hsp70, clathrin heavy chain and pyruvate kinase were identified in this study as possible LPA-binding proteins. Pyruvate kinase has been reported to interact directly with HERC1 (Garcia-Gonzalo et al., 2003). HERC1 is a giant protein of almost 5000 amino acids long, is localized in inner cell membranes such as the Golgi apparatus, and purportedly plays a role in intracellular traffic (Rosa et al., 1996). Because HERC1 forms a cytoplasmic ternary complex with clathrin and Hsp70 (Rosa and Barbacid, 1997) we investigated whether pyruvate kinase could form a complex with clathrin and Hsp70 by co-immunoprecipitation assays. Immunoprecipitation of pyruvate kinase from MCF-7 cells with a polyclonal antibody followed by Western blotting showed co-precipitation of clathrin, but not of Hsp70 (Figure 8A, lane 1). Conversely, clathrin heavy chain immunoprecipitation with a monoclonal antibody revealed that both Hsp70 and pyruvate kinase are present in the complex (Figure 8B, lane 1). These findings suggest that clathrin heavy chain and Hsp70 may be retained by immobilized LPA through interaction with pyruvate kinase, although it does

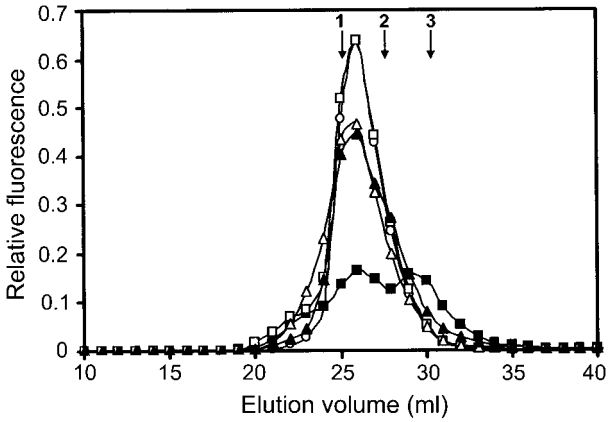

Figure 6 Dissociation of pyruvate kinase tetramers by LPA. Elution profiles of pyruvate kinase on a Superdex 200 PG column following 30-min pre-incubation with lysophospholipids at room temperature at a 1:100 molar ratio. Pyruvate kinase pre-incubated with buffer solution (○); LPA (18:1) (■); LPC (□); LPS (△) and LPI (▲). The fluorescence emission of tryptophan was used to monitor elution of the enzyme. The elution position of internal standards is indicated by arrows: catalase (1), lactate dehydrogenase (2), and ovalbumin (3).

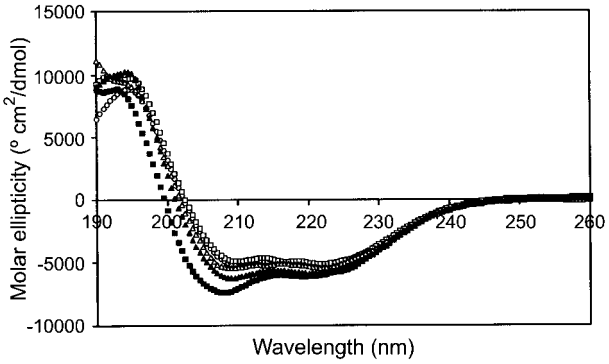

Figure 7 LPA increases α-helicity in pyruvate kinase. Circular dichroism spectra of pyruvate kinase after 30-min incubation with lysophospholipids at room temperature at a 1:100 molar ratio. Pyruvate kinase in buffer solution (○); LPA (18:1) (■); LPC (□); LPS (△) and LPI (▲). Protein concentration was 0.1 mg/ml and the cuvette path length was 0.1 cm.

not exclude a direct interaction between Hsp70 or clathrin with LPA.

Clathrin and pyruvate kinase partly co-localize in MCF-7 cells

The subcellular localization of endogenous clathrin and pyruvate kinase was studied by indirect immunofluorescence and confocal microscopy in MCF-7 cells (Figure 9). Both proteins displayed punctate staining. Whereas pyruvate kinase appeared to be distributed uniformly in the cytoplasm with occasional enrichment in particular areas, clathrin showed enrichment in the perinuclear area, in addition to a characteristic dot-like distribution in the cytoplasm. This punctate staining may suggest that these proteins interact with intracellular membranous structures (Wasiak et al., 2002; Garcia-Gonzalo et al., 2003). Of note, superposition of both images showed a partial overlap in distinct areas of the cell, particularly in the perinuclear region, with occasional co-localization in isolated cytoplasmic membranous compartments.

Discussion

Relatively few intracellular binding partners for LPA have been recognized in recent years. Proteins identified so far include CtBP/BARS (Weigert et al., 1999), L-FABP (Thumser et al., 1994) and gelsolin (Meerschaert et al., 1998; Goetzl et al., 2000). LPA is also a ligand for PPARγ (McIntyre et al., 2003) and was acknowledged more recently as a regulator of mechano-gated K2P channels comprising TREK-1, TREK-2 and TRAAK (Chemin et al., 2005).

For easier isolation and purification of novel LPA-binding proteins, we used a solid-phase approach involving Affigel-immobilized LPA. Here we describe the isolation of LPA-binding proteins from representative mammalian cells coupled to identification by mass spectrometry. Although several proteins were identified, the individual binding characteristics and affinity for the phosholipid have not been determined in each case. In addition, our

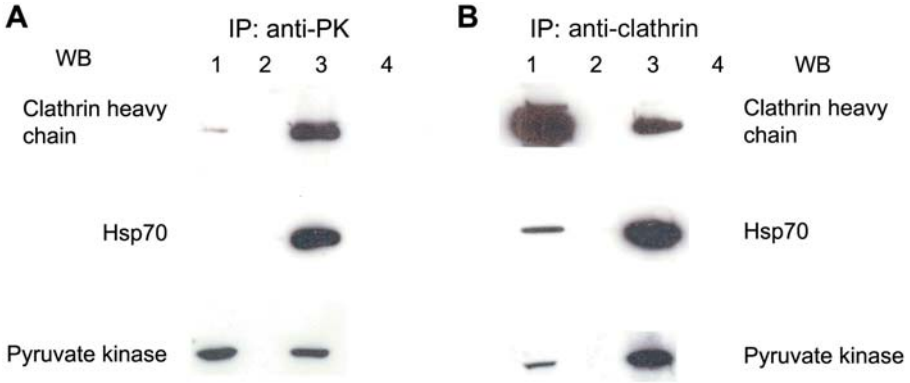

Figure 8 Pyruvate kinase occurs in a complex with clathrin heavy chain and Hsp70. MCF-7 cell lysates were immunoprecipitated with antibodies against pyruvate kinase (left) or against clathrin heavy chain (right) (lane 1). The immunoprecipitate was analyzed for the presence of pyruvate kinase, Hsp70 or clathrin heavy chain by immunoblotting with specific antibodies. Lanes 2–4 represent controls: non-specific rabbit IgG (lane 2) or mouse IgG (lane 2); crude cell lysate (lane 3) and protein G-Sepharose without antibodies (lane 4).

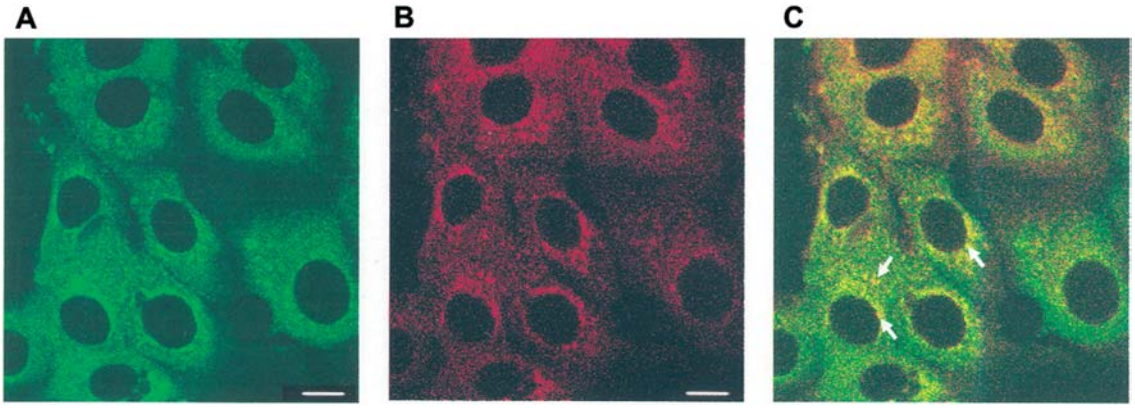

Figure 9 Co-localization of endogenous pyruvate kinase and clathrin.
MCF-7 cells were fixed and stained for pyruvate kinase or clathrin heavy chain and analyzed by confocal microscopy. (A) Staining of endogenous pyruvate kinase in MCF-7 cells (green). (B) Staining of endogenous clathrin heavy chain in MCF-7 cells (red). (C) Merged image. White arrows indicate co-localization between pyruvate kinase and clathrin heavy chain. The scale bar represents 10 μm.

approach does not rule out the possibility that some proteins bind indirectly to the LPA matrix through interaction with another polypeptide present in the sample. In fact, the association reported here between pyruvate kinase M (the M1 and M2 isozymes) and clathrin heavy chain/Hsp70 may well represent such an example.

We focused on pyruvate kinase given the relatively high abundance of peptides that were identified (this is also evident from the Coomassie-stained gel in Figure 2). To investigate if pyruvate kinase can bind directly to LPA, the interaction was measured in solution by ITC. The LPA/pyruvate kinase interaction proved to be an exothermic process with an affinity in the micromolar range. A number of reports have shown that pyruvate kinase and other glycolytic proteins can reversibly associate with subcellular membrane structures (reviewed in Gutowicz and Kosmiderschmidt, 1987). Local regulation of the glycolysis pathway in a cell and ATP compartmentation are hypothesized to be coupled to the function of organelles within the cell. Several studies have demonstrated that glycolytic enzymes (phosphoglycerate kinase, aldolase, phosphofructokinase, lactate dehydrogenase, glucose-3-phosphate dehydrogenase, hexokinase) can associate *in vitro* with phospholipid bilayers (Sidorowicz et al., 1986; Dabrowska et al., 1998). Most of the glycolytic enzymes studied are inactivated upon interaction with membranes or phospholipids (Karadsheh and Uyeda, 1977; Gutowicz and Kosmiderschmidt, 1987; Dabrowska and Czapinska, 1990; Masters, 1991; Michalak et al., 1992). However, Dabrowska et al. (1998) demonstrated that pyruvate kinase activity increases upon interaction with certain phospholipids, especially with phosphatidylserine incorporated in liposomes. Phosphatidylserine is an anionic phospholipid, like LPA; we therefore investigated if LPA could also affect the enzymatic activity of pyruvate kinase. Our data show that LPA (18:1) decreases pyruvate kinase activity, while other lysophospholipids (LPC, LPI and LPS) do not affect its activity. At concentrations above the CMC of LPA, pyruvate kinase activity is almost completely abolished. This is clearly demonstrated with LPA (18:1) and LPA (14:0), which have CMC values of 50 and 370 μM, respectively, whereas the short LPA (6:0), which does not form micelles, has no effect at all on the activity of pyruvate kinase. Moreover, we could show that incorporation of LPA (18:1) into liposomes also decreased the activity of pyruvate kinase. These results could indicate that an organized lipid structure is necessary for functional interaction between the enzyme and phospholipids. This was also claimed by Terlecki et al. (2002) for lactate dehydrogenase-phosphatidylserine interaction.

The mammalian M2-type pyruvate kinase isozyme can switch between a less active dimeric form and a highly active tetrameric form, which regulates the channeling of glucose carbons either to synthetic processes (dimeric form) or to glycolytic energy production (tetrameric form) (Michalak et al., 1992). Tumor cells are usually characterized by an overexpression of the dimeric form, leading to strong accumulation of all glycolytic phosphometabolites upstream of pyruvate kinase in the glycolysis pathway (Weernink et al., 1992; Oremek et al., 1999; Mazurek et al., 2002). On the other hand, LPA is also known to enhance tumorigenesis by increasing cellular motility and invasiveness (Xu et al., 1995; Gschwind et al., 2003, Mills and Moolenaar, 2003). We showed that LPA/pyruvate kinase interaction can lead to dimerization of the enzyme *in vitro*. Upon incubation with micellar LPA, the tetrameric pyruvate kinase dissociates into a less active dimer, as demonstrated by gel filtration chromatography. Mobility shifts observed in non-denaturing gel electrophoresis additionally suggest changes in pyruvate kinase configuration. The observed dissociation into dimers did not affect the secondary structure of the enzyme, as shown in the circular dichroic measurements. This dissociation into dimers was not observed with other lysophospholipids.

HERC proteins contain one or more RCC1-like domains and a C-terminal HECT domain (homologous to the E6-associated protein C-terminus). RCC1 is a guanine nucleotide exchange factor (GEF) for the small GTPase and nucleocytoplasmic shuttling protein Ran. Several HERC proteins have been recognized as ubiquitin ligases (Hochrainer et al., 2005). To identify proteins that interact with HERC1, Barbacid and coworkers (Rosa

et al., 1996; Rosa and Barbacid, 1997) used several HERC1 domains as baits in the yeast two-hybrid system. They found that HERC1 forms an ATP-dependent ternary complex with clathrin and Hsp70, and reported that the HECT domain of HERC1 interacts with M2-type pyruvate kinase. Since we identified pyruvate kinase, clathrin heavy chain and Hsp70 as possible LPA-binding proteins, we checked if these proteins could form a complex. Immunoprecipitation experiments with HEK293T or MCF-7 cell lysates indicated that pyruvate kinase is able to form a complex with clathrin. We did not, however, detect co-immunoprecipitation of Hsp70. This may be ascribed, in part, to overlap between protein interaction sites and polyclonal antibody recognition sites, because immunoprecipitation experiments with clathrin heavy-chain antibody did demonstrate interaction between clathrin heavy chain, Hsp70 and pyruvate kinase. These findings may suggest that clathrin, Hsp70, pyruvate kinase and HERC1 can form a complex involving LPA, or that the interaction is regulated by LPA. Endogenous pyruvate kinase and clathrin proteins were shown to display punctate cytosolic and perinuclear staining when their subcellular localization was analyzed by confocal microscopy. This presumably indicates that both proteins are associated with membranous compartments (Wasiak et al., 2002; Garcia-Gonzalo et al., 2003) and is in agreement with the data reporting pyruvate kinase activation by PS-containing liposomes (Dabrowska and Czapinska, 1990). LPA might thus also play a role in tethering pyruvate kinase to intracellular membrane structures.

Materials and methods

Chemicals and reagents

Rabbit-muscle pyruvate kinase was purchased from MP Biomedicals (Aurora, OH, USA). Lactate dehydrogenase was from Calbiochem (San Diego, CA, USA). Phosphoenolpyruvate, ADP, NADH, lysophosphatidylcholine, lysophosphatidylserine, lysophosphatidyinositol and clathrin heavy chain antibody were all purchased from Sigma (St. Louis, MO, USA). LPA (18:1), LPA (14:0) and LPA (6:0) were from Avanti Polar Lipids (Alabaster, AL, USA). PIP_2 beads were obtained from Echelon Research Laboratories (Salt Lake City, UT, USA). Alexa 594-conjugated goat anti-mouse and Alexa 488-conjugated rabbit anti-goat were obtained from Molecular Probes (Eugene, OR, USA). Molecular mass markers for SDS-PAGE were from Bio-Rad (Hercules, CA, USA). Phenylmethylsulfonyl fluoride was from Serva (Heidelberg, Germany). Other protease inhibitors were from Amersham Biosciences (Uppsala, Sweden). Antibodies against pyruvate kinase and Hsp70 were obtained from Abcam (Cambridge, UK).

Synthesis of tethered LPA ligand and preparation of the affinity matrices

An 11-aminoundecanoyl-linked LPA analog was synthesized for direct immobilization of LPA on Affigel-10 beads (Camus et al., 1987; Dingerdissen et al., 1987) (Figure 1). The synthesis started with the phosphorylation of *rac*-solketal using dimethyl chlorophosphate in the presence of potassium tertiary butanol (*t*-BuOK) (Xu et al., 1995). Hydrolysis of the acetal produced a diol, which was esterified with benzyloxycarbonyl (Cbz)-protected 11-aminoundecanoic acid selectively at *sn*-1 position at 0°C using dicyclohexylcarbodiimide and 4-(dimethylamino)pyridine (DCC/DMAP) to produce the protected 11-aminoundecanoyl-LPA analog (Chen and Prestwich, 1998). Trimethylsilyl bromide/methanol (TMSBr/MeOH) treatment resulted in elimination of the dimethyl phosphate and Cbz amino protecting groups at the same time, generating LPA-NH_2 (**4**), (Qian et al., 2003) which was then coupled to Affigel-10 in anhydrous methanol with a trace of triethylamine (TEA). The anhydrous organic solvent was used to minimize hydrolysis of NHS esters that occurs in aqueous solutions. Upon addition of (**4**), the NHS was displaced and a stable amide bond was formed. An excess of Affigel-10 was used to completely consume the aminoacyl LPA and to produce a loading of approximately 1–2 μmol/ml resin. This loading minimizes premature clogging of the resin by non-specific protein adsorption. Following overnight reaction with ligand, the reaction mixture was treated with a 50-fold excess of 2-aminoethanol to cap any remaining reactive ester groups. The reaction was monitored by the increase in UV absorption at 280 nm due to NHS release during coupling to the ligand. As the fatty acid at the *sn*-1 position anchors LPA to the Affigel-10 resin, the head group of the lysophospholipid is expected to be exposed to solvent, and thus available for binding. To prepare the control aminoacyl-linked PA affinity resin, an amino-acyl PA analog was coupled with Affigel-10 as described in Manifava et al. (2001).

Cell culture and fractionation, and lipid affinity chromatography

MCF7 cells were maintained in 1:1 (v/v) F12 nutrient mixture (Ham; Invitrogen, Merelbeke, Belgium) with L-glutamine and Dulbecco's modified Eagle medium (DMEM, Invitrogen), supplemented with 10% fetal bovine serum (Invitrogen), 100 U/ml penicillin and 0.1 mg/ml streptomycin. HEK293T cells were maintained in DMEM supplemented with 10% fetal bovine serum, 0.05% L-glutamine, 100 U/ml penicillin and 0.1 mg/ml streptomycin. Cells were washed twice with ice-cold phosphate-buffered saline (PBS) (2.7 mM KCl, 1.47 mM KH_2PO_4, 137 mM NaCl, 8.1 mM Na_2HPO_4, pH 7.4) and 1 ml of lysis buffer [50 mM Tris-HCl, pH 7.4, 150 mM NaCl, 2 mM EDTA, 50 mM sodium fluoride, 1 mM sodium orthovanadate, 0.1% Tween 20, 1 mM phenylmethylsulfonyl fluoride, and protease inhibitors (Roche, Basel, Switzerland)]. The mixture was sonicated and centrifuged at 20 000 *g* in a microcentrifuge for 10 min at 4°C to remove insoluble cell debris. LPA beads, stored in 20% ethanol, were equilibrated with three washes in lysis buffer. In a typical binding reaction, 1 ml of cytosol (containing 2 mg of total protein) was mixed with 5 μl of settled beads on ice. The tubes were put in a rotator at 4°C for 2 h. Following binding, the beads were quickly washed three times with lysis buffer and resuspended in Laemmli sample buffer, and bound proteins were analyzed by SDS-PAGE.

Identification of polypeptide bands by Q-TOF

Coomassie-stained gel bands from the LPA affinity chromatography were identified by mass spectrometry on a Q-TOF1 mass spectrometer (Waters-Micromass, Cheshire, UK) as described by Thomas et al. (2005).

Isothermal titration calorimetry

Microcalorimetric titration measurements were performed in a Microcal Omega isothermal titration calorimeter (Microcal, Northampton, MA, USA). All solutions were degassed under vacuum prior to use. In a typical experiment, 1.33 ml of 60 μM pyruvate kinase in 20 mM Tris-HCl, 150 mM NaCl, pH 7.5 was titrated by 20 15-μl injections of 400 μM LPA (18:1). During titration, the injection syringe was rotated at 250 rpm. Time between injections was set at 5 min. In a blank experiment, heat evolved

from dilution was measured by injecting the LPA (18:1) solution into the sample cell filled with 20 mM Tris-HCl, 150 mM NaCl, pH 7.5. This heat of dilution was subtracted from the corresponding LPA-binding data for pyruvate kinase. Data were integrated and fitted to an appropriate binding model using the ORIGIN software supplied by Microcal.

Enzyme activity measurements

The enzyme activity was measured at 25°C in a coupled system with lactate dehydrogenase (LDH) and NADH (Bücher and Pfleiderer, 1955). Standard assays were performed in the following medium: 1.5 mM ADP, 120 mM KCl, 62 mM $MgSO_4$, 1.5 mM phosphoenolpyruvate, 0.22 mM NADH and 4 U/ml LDH (which represented a large excess over pyruvate kinase) in 50 mM imidazole-HCl buffer at pH 7.6. The reaction was initiated by the addition of 5 μl of pyruvate kinase to a cuvette containing 0.5 ml of the above medium and was monitored by the decrease in absorbance at 340 nm for 5 min. The rate of reaction was measured from the initial linear region of the curve. Pyruvate kinase activity in the presence of different lysophospholipids was determined after 30-min incubation at room temperature. Pyruvate kinase concentration was determined by absorption measurements at 280 nm, using an extinction of 0.54 ml/mg cm (Boyer, 1962).

Gel filtration chromatography

Gel filtration chromatography was performed on a Waters Advanced Protein Purification System, using a precalibrated Superdex 200 PG 10/60 column (60×1.0 cm), and 0.05 M Tris-HCl, 0.15 M NaCl, pH 8.0 as running buffer. Reference markers were blue dextran (M_r 2 000 000), ferritin (M_r 450 000), catalase (M_r 240 000), LDH (M_r 140 000), bovine serum albumin (M_r 66 000), ovalbumin (M_r 45 000), chymotrypsinogen A (M_r 28 000), myoglobulin (M_r 17 000), vitamin B_{12} (M_r 1350) and dinitrophenylasparagine (M_r 298).

Non-denaturing polyacrylamide gel electrophoresis

Pyruvate kinase was incubated with or without increasing amounts of LPA (18:1) on ice for 30 min. Mixtures were loaded onto a 6% non-denaturing polyacrylamide gel and run at 4°C for 2 h at 90 V in a Tris-glycine buffer pH 8.6. Pyruvate kinase was visualized by Coomassie Brilliant Blue staining.

Circular dichroism measurements

Circular dichroism measurements were carried out at room temperature on a Jasco 710 spectropolarimeter between 190 and 260 nm in quartz cells with a path length of 0.1 cm. A total of 16 spectra were recorded and averaged. Pyruvate kinase was diluted to a concentration of 0.1 mg/ml in 10 mM sodium phosphate buffer. The CD spectra of pyruvate kinase in the presence of different lysophospholipids were recorded after 30-min incubation at room temperature of the enzyme with lipids at a molar ratio of 1:100. The spectra were corrected for minor contributions of lipids by subtracting the spectra measured for lipids alone. The secondary structure of pyruvate kinase was determined by curve fitting to reference protein spectra using the CDNN program (Bohm et al., 1992). The helicity of pyruvate kinase was determined from the mean residue ellipticity [θ] at 222 nm (Chen et al., 1972).

Immunoprecipitation experiments

Cells were washed twice in ice-cold PBS and lysed in PBS supplemented with 0.5% Nonidet P-40, 10 mM sodium fluoride, 8 mM sodium-β-glycerophosphate and a protease inhibitor cocktail mix (Roche). Cells were disrupted by sonication and centrifugation at 4°C for 10 min (20 000 *g*). Samples of 1 mg of protein were incubated overnight with affinity-purified antibodies against either pyruvate kinase, Hsp70 or clathrin heavy chain and subsequently with protein G-Sepharose (Amersham Pharmacia Biotech, Uppsala, Sweden) for 4 h. Pellets were washed three times with lysis buffer, boiled for 5 min in Laemmli sample buffer and fractionated by SDS-PAGE followed by Western blotting. Proteins were analyzed by enhanced chemiluminescence detection (ECL, Amersham Pharmacia Biotech).

Fluorescence microscopy and immunocytochemistry

The cells were fixed with 3% paraformaldehyde, permeabilized in 0.1% Triton X-100, washed in PBS, and incubated with primary antibody against pyruvate kinase for 1 h at 37°C. After several washes with PBS, the cells were incubated with Alexa 488-conjugated donkey anti-goat secondary antibody 30 min at room temperature. Clathrin staining was performed with a monoclonal antibody against clathrin heavy chain and Alexa 594-conjugated goat anti-mouse as secondary antibody. Photographs were taken with a Zeiss model LSM410 camera inverted on the base of a Zeiss Axiovert 100 microscope (Carl Zeiss B.V., Sliedrecht, The Netherlands).

Miscellaneous

Protein concentrations were determined by the method of Bradford (1976) using bovine serum albumin as a standard. We carried out SDS-PAGE according to Matsudaira and Burgess (1978). Western blotting was carried out according to the method of Towbin et al. (1979). The fluorescent probe 2-(*p*-toluidinyl)-naphthalene-6-sodium sulfonate (TNS) was used to determine the critical micelle concentration of LPA (18:1) and LPA (14:0). Upon mixing of TNS with the lysophospholipid, a large increase in fluorescence is observed if the lipid exceeds the critical micelle concentration (Cocera et al., 2001).

Acknowledgments

We thank Dr. Bart Christiaens for help with confocal microscopy and Hans Caster for help with gel filtration experiments. This work was supported by the Concerted Actions Program of Ghent University (GOA), the 'Belgische Federatie tegen Kanker', the Fund for Scientific Research-Flanders (FWO-Vlaanderen), by Fortis Bank Verzekeringen and by the IUAP program. K.M. is a Postdoctoral Fellow of the Fund for Scientific Research-Flanders (Belgium). G.D.P thanks the Human Frontier Science Program (RG0073-2000B) and the NIH (HL070231) for support at the University of Utah. We also thank Mr. T. Rose (University of Utah) for preparation of a batch of the LPA resin. G.B. Mills and G.D.P. thank the U.S. Department of Defense for award DAMD17-03-1-0222 for partial financial support of work at Utah University.

References

Bohm, G., Muhr, R., and Jaenicke, R. (1992). Quantitative analysis of protein far-UV circular dichroism spectra by neural networks. Protein Eng. *5*, 191–195.

Boyer, P.D. (1962). Pyruvate Kinase. The Enzymes, 2nd ed., Vol. 6 (New York, USA: Academic Press), pp. 95–113.

Bradford, M.M. (1976). Rapid and sensitive method for quantitation of microgram quantities of protein utilizing principle of protein-dye binding. Anal. Biochem. *72*, 248–254.

Bücher, T. and Pfleiderer, G. (1955). Pyruvate kinase from muscle. Methods Enzymol. *1*, 435–440.

Camus, D., Lyon, J.A., Reaudjareed, T., Haynes, J.D., and Diggs, C.L. (1987). Characterization of gp195 processed products purified from *Plasmodium falciparum* culture supernates. Mol. Biochem. Parasitol. *26*, 21–27.

Chemin, J., Patel, A., Duprat, F., Zanzouri, M., Lazdunski, M., and Honore, E. (2005). Lysophosphatidic acid-operated K^+ channels. J. Biol. Chem. *280*, 4415–4421.

Chen, J. and Prestwich, G.D. (1998). Asymmetric synthesis of water-soluble, nonhydrolyzable phosphonate analogue of phosphatidylinositol 4,5-bisphosphate. J. Org. Chem. *63*, 430–431.

Chen, Y.H., Yang, J.T., and Martinez, H.M. (1972). Determination of secondary structures of proteins by circular dichroism and optical rotatory dispersion. Biochemistry *11*, 4120–4131.

Cocera, M., Lopez, O., Estelrich, J., Parra, J.L., and de la Maza, A. (2001). Use of a fluorescence spectroscopy technique to study the adsorption of sodium dodecylsulfonate on liposomes. Chem. Phys. Lipids *110*, 19–26.

Dabrowska, A. and Czapinska, E. (1990). Limited proteolysis of bovine muscle and heart lactate dehydrogenase is inhibited by phospholipid liposome interaction. Biochim. Biophys. Acta *1027*, 301–303.

Dabrowska, A., Pietkiewicz, J., Dabrowska, K., Czapinska, E., and Danielewicz, R. (1998). Interaction of M1 and M2 isozymes pyruvate kinase from human tissues with phospholipids. Biochim. Biophys. Acta *1383*, 123–129.

Dingerdissen, J.J., Sitrin, R.D., Dephillips, P.A., Giovenella, A.J., Grappel, S.F., Mehta, R.J., Oh, Y.K., Pan, C.H., Roberts, G.D., Shearer, M.C., and Nisbet, L.J. (1987). Actinoidin-A2, a novel glycopeptide: production, preparative HPLC separation and characterization. J. Antibiot. (Tokyo) *40*, 165–172.

Fukushima, N., Ishii, I., Contos, J.J.A., Weiner, J.A., and Chun, J. (2001). Lysophospholipid receptors. Annu. Rev. Pharmacol. Toxicol. *41*, 507–534.

Garcia-Gonzalo, F.R., Cruz, C., Munoz, P., Mazurek, S., Eigenbrodt, E., Ventura, F., Bartrons, R., and Rosa, J.L. (2003). Interaction between HERC1 and M2-type pyruvate kinase. FEBS Lett. *539*, 78–84.

Goetzl, E.J., Lee, H., Azuma, T., Stossel, T.P., Turck, C.W., and Karliner, J.S. (2000). Gelsolin binding and cellular presentation of lysophosphatidic acid. J. Biol. Chem. *275*, 14573–14578.

Gschwind, A., Hart, S., Fischer, O.M., and Ullrich, A. (2003). TACE cleavage of proamphiregulin regulates GPCR-induced proliferation and motility of cancer cells. EMBO J. *22*, 2411–2421.

Gutowicz, J. and Kosmiderschmidt, A. (1987). Fluorescence investigation on conformational state of rabbit muscle aldolase interacting with phosphatidylinositol liposomes. Biophys. Chem. *27*, 97–102.

Hochrainer, K., Mayer, H., Baranyi, U., Binder, B.R., Lipp, J., and Kroismayr, R. (2005). The human HERC family of ubiquitin ligases: novel members, genomic organization, expression profiling, and evolutionary aspects. Genomics *85*, 153–164.

Ishii, I., Fukushima, N., Ye, X.Q., and Chun, J. (2004). Lysophospholipid receptors: signaling and biology. Annu. Rev. Biochem. *73*, 321–354.

Karadsheh, N.S. and Uyeda, K. (1977). Changes in allosteric properties of phosphofructokinase bound to erythrocyte membranes. J. Biol. Chem. *252*, 7418–7420.

Larsen, T.M., Laughlin, L.T., Holden, H.M., Rayment, I., and Reed, G.H. (1994). Structure of rabbit muscle pyruvate kinase complexed with Mn^{2+}, K^+, and pyruvate. Biochemistry (Mosc.) *33*, 6301–6309.

Luquain, C., Sciorra, V.A., and Morris, A.J. (2003). Lysophosphatidic acid signaling: how a small lipid does big things. Trends Biochem. Sci. *28*, 377–383.

Manifava, M., Thuring, J.W.J.F., Lim, Z.Y., Packman, L., Holmes, A.B., and Ktistakis, N.T. (2001). Differential binding of traffic-related proteins to phosphatidic acid- or phosphatidylinositol (4,5)-bisphosphate-coupled affinity reagents. J. Biol. Chem. *276*, 8987–8994.

Masters, C. (1991). Cellular differentiation and the microcompartmentation of glycolysis. Mech. Ageing Dev. *61*, 11–22.

Matsudaira, P.T. and Burgess, D.R. (1978). SDS microslab linear gradient polyacrylamide-gel electrophoresis. Anal. Biochem. *87*, 386–396.

Mazurek, S., Grimm, H., Boschek, C.B., Vaupel, P., and Eigenbrodt, E. (2002). Pyruvate kinase type M2: a crossroad in the tumor metabolome. Br. J. Nutr. *87*, S23–S29.

McIntyre, T.M., Pontsler, A.V., Silva, A.R., St Hilaire, A., Xu, Y., Hinshaw, J.C., Zimmerman, G.A., Hama, K., Aoki, J., Arai, H., and Prestwich, G.D. (2003). Identification of an intracellular receptor for lysophosphatidic acid (LPA): LPA is a transcellular PPARγ agonist. Proc. Natl. Acad. Sci. USA *100*, 131–136.

Meerschaert, K., De Corte, V., De Ville, Y., Vandekerckhove, J., and Gettemans, J. (1998). Gelsolin and functionally similar actin-binding proteins are regulated by lysophosphatidic acid. EMBO J. *17*, 5923–5932.

Melamud, E. and Mildvan, A.S. (1975). Magnetic resonance studies of interaction of Co^{2+} and phosphoenolpyruvate with pyruvate kinase. J. Biol. Chem. *250*, 8193–8201.

Michalak, K., Gutowicz, J., and Modrzycka, T. (1992). Temperature studies of glyceraldehyde-3-phosphate dehydrogenase binding to liposomes using fluorescence technique. Gen. Physiol. Biophys. *11*, 545–554.

Mills, G.B. and Moolenaar, W.H. (2003). The emerging role of lysophosphatidic acid in cancer. Nat. Rev. Cancer *3*, 582–591.

Moolenaar, W.H. (2002). Lysophospholipids in the limelight: autotaxin takes center stage. J. Cell Biol. *158*, 197–199.

Moolenaar, W.H., van Meeteren, L.A., and Giepmans, B.N.G. (2004). The ins and outs of lysophosphatidic acid signaling. Bioessays *26*, 870–881.

Oremek, G.M., Teigelkamp, S., Kramer, W., Eigenbrodt, E., and Usadel, K.H. (1999). The pyruvate kinase isoenzyme tumor M2 (tu M2-PK) as a tumor marker for renal carcinoma. Anticancer Res. *19*, 2599–2601.

Pages, C., Simon, M.F., Valet, P., and Saulnier-Blache, J.S. (2001). Lysophosphatidic acid synthesis and release. Prostaglandins Lipid Mediat. *64*, 1–10.

Qian, L., Xu, Y., Arai, H., Aoki, J., McIntyre, T.M., and Prestwich, G.D. (2003). Synthesis of migration-resistant hydroxyethoxy analogues of lysophosphatidic acid. Org. Lett. *5*, 4685–4688.

Rosa, J.L. and Barbacid, M. (1997). A giant protein that stimulates guanine nucleotide exchange on ARF1 and Rab proteins forms a cytosolic ternary complex with clathrin and hsp70. Oncogene *15*, 1–6.

Rosa, J.L., CasaroliMarano, R.P., Buckler, A.J., Vilaro, S., and Barbacid, M. (1996). p619, a giant protein related to the chromosome condensation regulator RCC1, stimulates guanine nucleotide exchange on ARF1 and Rab proteins. EMBO J. *15*, 4262–4273.

Schmidt, A., Wolde, M., Thiele, C., Fest, W., Kratzin, H., Podtelejnikov, A.V., Witke, W., Huttner, W.B., and Soling, H.D. (1999). Endophilin I mediates synaptic vesicle formation by transfer of arachidonate to lysophosphatidic acid. Nature *401*, 133–141.

Sidorowicz, A., Golebiowska, J., and Siemieniewski, H. (1986). Interaction of phosphoglycerate kinase with phosphatidylserine liposomes. Gen. Physiol. Biophys. *5*, 307–313.

Terlecki, G., Czapinska, E., and Gutowicz, J. (2002). The role of lipid phase structure in the interaction of lactate dehydrogenase with phosphatidylserine activity studies. Cell. Mol. Biol. Lett. *7*, 895–903.

Thomas, A., Leprince, P., Dizier, I., Ball, H., Gevaert, K., Vandamme, J., Mainil, J., and Linden, A. (2005). Identification by two-dimensional electrophoresis of a new adhesin expressed by a low passaged strain of *Mycoplasma bovis*. Res. Microbiol. *156*, 713–718.

Thumser, A.E.A., Voysey, J.E., and Wilton, D.C. (1994). The binding of lysophospholipids to rat liver fatty acid binding protein and albumin. Biochem. J. *301*, 801–806.

Tigyi, G. and Miledi, R. (1992). Lysophosphatidates bound to serum albumin activate membrane currents in *Xenopus* oocytes and neurite retraction in PC12 pheochromocytoma cells. J. Biol. Chem. *267*, 21360–21367.

Towbin, H., Staehelin, T., and Gordon, J. (1979). Electrophoretic transfer of proteins from polyacrylamide gels to nitrocellulose sheets – procedure and some applications. Proc. Natl. Acad. Sci. USA *76*, 4350–4354.

Vancura, A. and Haldar, D. (1992). Regulation of mitochondrial and microsomal phospholipid synthesis by liver fatty acid binding protein. J. Biol. Chem. *267*, 14353–14359.

Wasiak, S., Legendre-Guillemin, V., Puertollano, R., Blondeau, F., Girard, M., de Heuvel, E., Boismenu, D., Bell, A.W., Bonifacino, J.S., and McPherson, P.S. (2002). Enthoprotin: a novel clathrin-associated protein identified through subcellular proteomics. J. Cell Biol. *158*, 855–862.

Weernink, P.A.O., Rijksen, G., Mascini, E.M., and Staal, G.E.J. (1992). Phosphorylation of pyruvate kinase type K is restricted to the dimeric form. Biochim. Biophys. Acta *1121*, 61–68.

Weigert, R., Silletta, M.G., Spano, S., Turacchio, G., Cericola, C., Colanzi, A., Senatore, S., Mancini, R., Polishchuk, E.V., Salmona, M. et al. (1999). CtBP/BARS induces fission of Golgi membranes by acylating lysophosphatidic acid. Nature *402*, 429–433.

Xie, Y.H. and Meier, K.E. (2004). Lysophospholipase D and its role in LPA production. Cell. Signal. *16*, 975–981.

Xie, Y.H., Gibbs, T.C., and Meier, K.E. (2002). Lysophosphatidic acid as an autocrine and paracrine mediator. Biochim. Biophys. Acta *1582*, 270–281.

Xu, Y., Fang, X.J., Casey, G., and Mills, G.B. (1995). Lysophospholipids activate ovarian and breast cancer cells. Biochem. J. *309*, 933–940.

Zhang, C.X., Baker, D.L., Yasuda, S., Makarova, N., Balazs, L., Johnson, L.R., Marathe, G.K., McIntyre, T.M., Xu, Y., Prestwich, G.D., et al. (2004). Lysophosphatidic acid induces neointima formation through PPARγ activation. J. Exp. Med. *199*, 763–774.

Received June 16, 2005; accepted August 16, 2005

CHEMMEDCHEM

DOI: 10.1002/cmdc.200500042

Phosphorothioate Analogues of Alkyl Lysophosphatidic Acid as LPA_3 Receptor-Selective Agonists

Lian Qian,[a] Yong Xu,[a] Ted Simper,[a] Guowei Jiang,[a] Junken Aoki,[b] Makiko Umezu-Goto,[b] Hiroyuki Arai,[b] Shuangxing Yu,[c] Gordon B. Mills,[c] Ryoko Tsukahara,[d] Natalia Makarova,[d] Yuko Fujiwara,[d] Gabor Tigyi,[d] and Glenn D. Prestwich*[a]

*The metabolically stabilized LPA analogue 1-oleoyl-2-O-methyl-rac-glycerophosphorothioate (OMPT) was recently shown to be a potent subtype-selective agonist for LPA_3, a G-protein-coupled receptor (GPCR) in the endothelial differentiation gene (EDG) family. Further stabilization was achieved by replacing the sn-1 O-acyl group with an O-alkyl ether. A new synthetic route for the enantiospecific synthesis of the resulting alkyl LPA phosphorothioate analogues is described. The pharmacological properties of the alkyl OMPT analogues were characterized for subtype-specific agonist activity using Ca^{2+}-mobilization assays in RH7777 cells expressing the individual EDG family LPA receptors. Alkyl OMPT analogues induced cell migration in cancer cells mediated through LPA_1. Alkyl OMPT analogues also activated Ca^{2+} release through LPA_2 activation but with less potency than sn-1-oleoyl LPA. In contrast, alkyl OMPT analogues were potent LPA_3 agonists. The alkyl OMPTs **1** and **3** induced cell proliferation at submicromolar concentrations in 10T 1/2 fibroblasts. Interestingly, the absolute configuration of the sn-2 methoxy group of the alkyl OMPT analogues was not recognized by any of the LPA receptors in the EDG family. By using a reporter gene assay for the LPA-activated nuclear transcription factor PPARγ, we demonstrated that phosphorothioate diesters have agonist activity that is independent of their ligand properties at the LPA-activated GPCRs. The availability of new alkyl LPA analogues expands the scope of structure–activity studies and will further refine the molecular nature of ligand–receptor interactions for this class of GPCRs.*

Introduction

Lysophosphatidic acid (LPA, 1-radyl-*sn*-glycerol-3-phosphate) has been shown to elicit growth-factor-like effects, including cell proliferation, cell survival, Ca^{2+} mobilization, and changes in cell shape and motility in a variety of cell types.[1–4] Based on animal experiments, LPA is implicated in complex physiological responses that include immunological competence, brain development, wound healing, coagulation, and regulation of blood pressure.[5,6] The physiological functions of LPA suggest that LPA could contribute to a number of pathophysiological states including cancer, autoimmunity, immunodeficiency, atherosclerosis, and ischemia reperfusion injury.[7] LPA elicits its effects by binding to G-protein-coupled receptors (GPCRs) with subsequent activation of multiple heterotrimeric G-protein-linked downstream events.[7–9] Four different LPA GPCR types on mammalian cell surfaces have been characterized so far, including three members of the Edg family (LPA_1, LPA_2, and LPA_3, previously known as Edg 2, Edg 4, and Edg 7, respectively). A purinergic receptor family GPCR (GPR23/P2Y9) was recently identified as a putative LPA receptor.[10] LPA also activates the nuclear transcription factor peroxisome proliferator-activated receptor γ (PPARγ). Through activation of these GPCRs and PPARγ, LPA induces multiple physiological and pathological responses. Our understanding of these complex responses at the present time is limited by the lack of specific probes for the receptor types and subtypes.

Under normal circumstances, the production and degradation of LPA is tightly regulated to maintain a concentration range of 50–100 nM for LPA bound to carrier proteins. LPA levels are elevated during blood clotting, wound healing, and

[a] *Dr. L. Qian, Dr. Y. Xu, T. Simper, G. Jiang, Prof. Dr. G. D. Prestwich*
Department of Medicinal Chemistry, The University of Utah
419 Wakara Way, Suite 205
Salt Lake City, Utah 84108-1257 (USA)
Fax: (+1) 801-585-9053
E-mail: gprestwich@pharm.utah.edu

[b] *Prof. Dr. J. Aoki, Dr. M. Umezu-Goto, Prof. Dr. H. Arai*
Graduate School of Pharmaceutical Sciences, The University of Tokyo
7-3-1, Hongo Bunkyo-ku, Tokyo, 113-0033 (Japan)

[c] *Dr. S. Yu, Dr. G. B. Mills*
Department of Molecular Therapeutics, M.D. Anderson Cancer Center
1515 Holcombe Boulevard, Houston, Texas 77030 (USA)

[d] *Dr. R. Tsukahara, Dr. N. Makarova, Dr. Y. Fujiwara, Prof. Dr. G. Tigyi*
Department of Physiology, College of Medicine
University of Tennessee Health Science Center
Memphis, Tennessee 38163 (USA)

Supporting information for this article is available on the WWW under http://www.chemmedchem.org or from the author.

in a number of biological fluids such as saliva and ovarian cyst fluid.[7] Although the underlying mechanisms remain elusive, aberrations in the production and degradation of LPA have been identified in cancer cells as well as in cancer patients.[7] Markedly elevated levels of LPA have been found in the ascitic fluid of ovarian cancer patients and in autocrine activation loops in ovarian and prostate cancer.[3] In combination with alterations in LPA receptor expression and potentially receptor function, LPA appears to be an important mediator in the pathophysiology of cancer.[6,7,11] Therefore, LPA receptors have emerged as highly attractive targets for therapeutic intervention.

As with many other GPCRs, LPA receptors should be amenable to the development of highly specific and potent agonists or antagonists that have favorable pharmacokinetic, bioavailability, and metabolic characteristics. Currently available compounds represent a promising start to the development of useful chemical tools, although none can be considered definitive in determining receptor selectivity or biological functions, especially for studies in vivo. Several groups have reported the characterization of LPA agonists and antagonists. A partial list of compounds with reported LPA_1 receptor selectivity includes the ethanolamide phosphate and phosphorothioate derivatives,[12,13] 3-(4-[4-([1-(2-chlorophenyl)-ethoxy]carbonylamino)-3-methyl-5-isoxazolyl] benzylsulfanyl)propanoic acid (Ki16425),[14] and additional ethanolamide derivatives.[13,15] Compounds with LPA_2 agonist activity are less common but include the decyl and dodecyl fatty alcohol phosphates (FAP-10 and FAP-12).[16] Most common are the LPA_3 agonists, including OMPT, a phosphorothioate analogue of LPA,[17] a monofluorophosphonate analogue of LPA,[18] phosphates and phosphorothioates based on a carbohydrate scaffold,[19] and several ethanolamide derivatives.[15] Appropriately validated compounds are essential to advance in vivo studies, particularly in view of potential off-target effects. The development of more selective, more stable, more potent, and more druglike agonists and antagonists is eagerly awaited.

The metabolically stabilized LPA analogue 1-oleoyl-2-*O*-methylglycerophosphorothioate (OMPT) is a potent agonist for the LPA_3 receptor that shows enantioselective action.[17,20] Subsequently, we showed that alkyl LPA analogues were equipotent to natural acyl LPAs as LPA receptor agonists for each receptor isoform (Figure 1).[21] Catabolism of LPA proceeds by three principal pathways.[7] First, phosphate hydrolysis to form monoacylglycerol is catalyzed by phosphatase (LPP) or phosphohydrolase enzymes. Second, conversion into PA is mediated by LPA acyltransferases (LPAATs). Third, LPA-specific lysophospholipases hydrolyze the *sn*-1 acyl chain to form the corresponding glycerol phosphate. Alkyl substitution may introduce unexpected biological activities, as ether analogues are selectively phospholipase-resistant[22] and might be strong activators of PPARγ as a result of their unique properties.

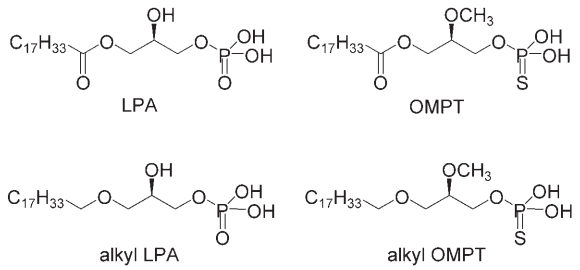

Figure 1. Structures of LPA, OMPT, and the corresponding *O*-alkyl analogues.

The alkyl OMPT analogues described herein are threefold metabolically stabilized with a phospholipase-resistant *sn*-1 ether chain, a migration and acyltransferase-resistant *sn*-2 *O*-methoxy group, and the less-readily hydrolyzed phosphorothioate head group.[20] To further elucidate the structural features of OMPT that determine agonist activity, we designed compounds **1**–**7** (Figure 2). Each analogue contains an *sn*-1 alkyl hydrophobic chain, an *sn*-2 methoxy group, and an anionic phosphorothioate group. To investigate the importance of absolute configuration of the *sn*-2 *O*-methoxy group for GPCR and PPARγ activity, we designed two pairs of enantiomers: **1** and **3**, plus **2** and **4**. Herein, we describe a convenient enantioselective synthetic approach to make these LPA analogues, and we describe cell-based assays for structure–activity relationships (SARs) for transfected human LPA receptors in the context of cell proliferation and migration, and for the activation of PPARγ.

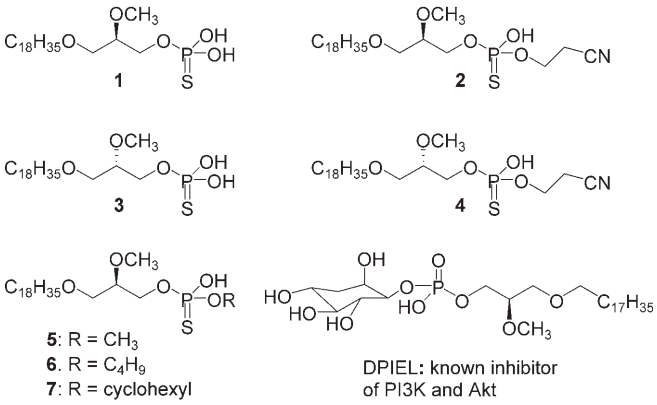

Figure 2. LPA analogues designed as LPA receptor agonists and antagonists.

Results

Chemistry

The enantioselective synthesis of OMPT involved the use of 2-cyanoethyl (CE) phosphate protecting groups, which can be removed under mild basic conditions.[17] For the synthesis of phosphorothioate analogues **1**–**7**, we used a common synthetic approach. Scheme 1 shows the concise conversion of the *p*-toluenesulfonyl (Ts) derivative of (*R*)-glycidol **8** to both enantiomerically pure phosphorothioates **1** and **2**. The key carbon–oxygen bond-forming step was a regio- and stereospecific nucleophilic opening of (*R*)-glycidyl tosylate **8** with a long-chain alcohol using BF_3 etherate as a catalyst.[23,24] As reported by

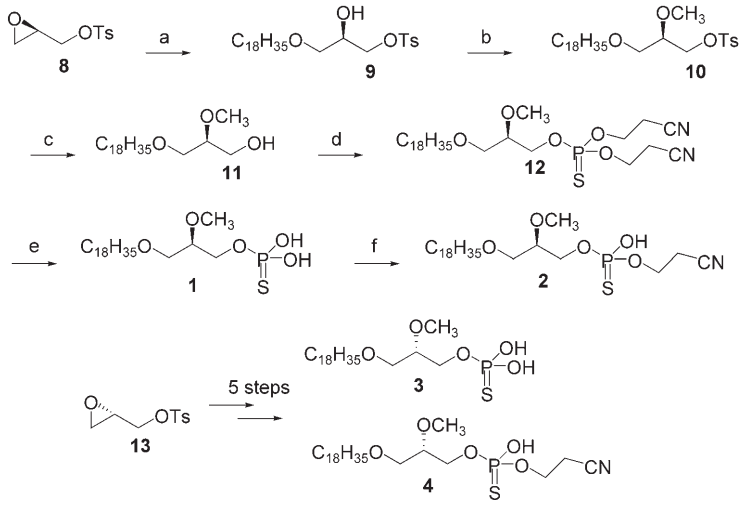

Scheme 1. Reagents and conditions for the synthesis of analogues **1**–**4**: a) (*Z*)-9-octadecen-1-ol, BF_3-$(C_2H_5)_2O$, CH_2Cl_2, 95%; b) CH_3OTf, 2,6-di-*t*Bu-4-MePy, CH_2Cl_2, 73%; c) Mg, CH_3OH, 91%; d) di-(2-cyanoethyl)-*N*,*N*-diisopropylphosphodiamidite, 1*H*-tetrazole; S, CS_2, Py, 86%; e) *t*$BuNH_2$, BTMSA, 72 h, 84%; f) *t*$BuNH_2$, BTMSA, 10 h, 84%. BTMSA = bis(trimethylsilyl)acetamide, Tf = trifluoromethanesulfonyl (triflate).

Guivisdalsky and Bittman, epoxide opening of (*R*)- or (*S*)-glycidol toluenesulfonate with oleyl alcohol occurred exclusively at the C3 position, stereospecifically affording the ring-opened product in very high enantiomeric excess (97–99% *ee*) as determined by HPLC on a chiral stationary phase.[25,26] Therefore, there is no loss of optical purity during the synthesis of the phosphorothioate LPA analogues. Mild conditions were required for the conversion of ring-opened product **9** into *O*-methyl compound **10** to avoid epoxide formation by intramolecular nucleophilic displacement. Methylation of the *sn*-2 hydroxy group was carried out by using methyl triflate in the presence of the hindered 2,6-di-*tert*-butyl-4-methylpyridine in dichloromethane at reflux, to generate **10** in good yield.[25] It was important to use the bulky and non-nucleophilic base 2,6-di-*tert*-butyl-4-methylpyridine to avoid the unwanted methylation of the base. Tosylate **10** was converted into alcohol **11** in high yield by using magnesium[27] in methanol instead of potassium superoxide with 18-crown-6.[25] Alcohol **11** was then phosphorylated with phosphoramidite methodology. The resulting phosphoramidite triester was oxidized with elemental sulfur to yield the corresponding phosphorothioate triester **12**.[17] Finally, one cyanoethyl ester group was removed under aprotic basic conditions (*tert*-butyl amine in acetonitrile) for 10 h to yield the desired phosphorothioate diester **2**. After 72 h, both cyanoethyl groups were removed to give phosphorothioate monoester **1**. The analogues **3** and **4** were prepared by using the analogous procedures starting from (*S*)-glycidyl tosylate **13** (Supporting Information). All compounds were characterized by ^1H, ^{13}C, and ^{31}P NMR spectroscopy and by MS.

To investigate the steric effect of the ester group of the phosphorothioate diester analogues, we synthesized analogues **5**–**7**, which are similar to the phosphorothioates **2** and **4**. The butyl side chain in **6** approximates the physical size of the cyanoethyl group, whereas the methyl group in **5** is smaller, and the cyclohexyl group in **7** is bulkier. These structures were selected based on the observed antagonist effect of DPIEL[28] toward LPA receptor activation (Y. Hasegawa, G. Mills, unpublished results), and allowed us to probe the relationship between the bulk of the phosphorothioate ester side chain and its biological effect in receptor activation or antagonism.

Thus, three phosphoramidite reagents **15a**, **15b**, and **15c** were prepared by the reaction of 2-cyanoethyl-*N*,*N*-diisopropylchlorophosphoramidite with methanol, butanol, or cyclohexanol, respectively, with diethylisopropylamine (DIPEA) as the base (Scheme 2).[29] The air-sensitive phosphoramidites were purified by rapid flash chromatography with a basic solvent system. The phosphoramidites were then condensed with primary alcohol **11** in the presence of 1*H*-tetrazole to yield the phosphoramidite intermediates. Sulfurization with S_8 in CS_2/pyridine (1:1 *v*/*v*) gave the corresponding phosphorothioate diesters **16a**–**c**. The final reaction included deprotection of the cyanoethyl group on the phosphorothioate by the addition of triethylamine (TEA), combined with bis(trifluoromethylsilyl)acetamide (BTFSA). BTFSA was added to prevent the phosphorothioate anion from undergoing re-alkylation. Compounds **2** and **4**–**7** all contain a chiral phosphorothioate phosphorus atom; the ^{31}P NMR of these compounds indicates that each analogue is, as anticipated, a 1:1 mixture of the resulting diastereomers.

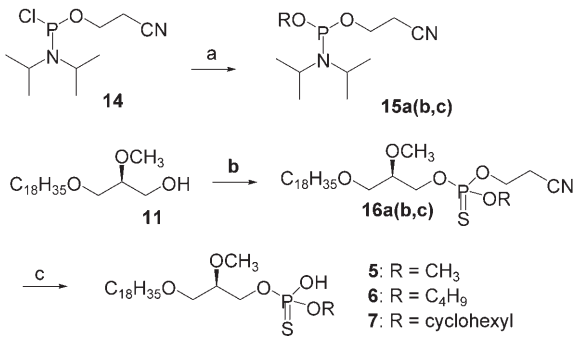

Scheme 2. Reagents and conditions for the synthesis of analogues **5**–**7**: a) ROH, DIPEA, 43–64%; b) phosphodiamidite **15**, 1*H*-tetrazole; S, CS_2, Py, 60–68%; c) triethylamine, BTFSA, 72 h, 59–65%.

Biology

The ligand properties of the compounds were first evaluated on the activation of LPA_1, LPA_2, and LPA_3 by the mobilization of Ca^{2+} in Sf9 or RH7777 cells expressing LPA_1, LPA_2, and LPA_3 receptors, with a FlexStation II automated fluorometer (Molecular Devices, Sunnyvale, CA).[16] In a biological context, the activation of LPA_1 was evaluated with a cell-migration assay with

203G murine glioma cells, MDA-MD-231 human breast cancer cell lines, and PC-3 prostate cancer cells.[30]

The enantiomers of alkyl OMPTs **1** and **3** induced cell migration, but with lower potency than 1-oleoyl LPA (Supporting Information Fig. 1). As LPA-induced cell migration in various cell types is LPA_1-dependent, the cell migration assay was found to be more sensitive than the system using LPA_1–LPA_2 chimeric receptor calcium assay, and was thus employed for comparing the biological activities of the synthetic analogues toward the LPA_1 receptor.[21] Therefore, **1** and **3** were weak agonists for the LPA_1 receptor.

Supporting Information Fig. 1 also illustrates calcium responses elicited through the activation of human LPA_1, LPA_2, and LPA_3 receptors.[16,31] In these experiments, RH7777 cells, which are intrinsically unresponsive to LPA,[16,31] were transfected with human LPA_1, LPA_2, and LPA_3, respectively. Both **1** and **3** are weak LPA_2 receptor agonists. Importantly, both **1** and **3** are potent agonists for LPA_3 subtypes, with higher potency than 1-oleoyl-LPA. The phosphorothioate diesters **2** and **4** (Supporting Information Fig. 2) showed the same activities as **1** and **3**. Similar to the activity of **1** and **3**, analogues **2** and **4** are LPA_3-selective agonists. However, the phosphorothioate diesters **5**–**7** did not show any activity toward LPA receptors, with the exception that **5** showed weak LPA_3 agonist activity (Supporting Information Fig. 3).

Alkyl OMPT **1** and **3** are LPA_3-selective agonists in one assay system using RH7777 cells expressing the human LPA_3 receptor. These independent assay results with RH7777 cells confirm that alkyl OMPT analogues are LPA_3 agonists and that the monoester alkyl OMPT analogue **2** is a weak LPA_3 agonist (Table 1). Interestingly, among the monoester alkyl OMPTs **5**–**7**, only the methyl phosphodiester **5** showed weak agonist activity, whereas the butyl phosphodiester **6** and the cyclohexyl phosphodiester **7** slightly inhibited LPA activation in this assay system.

Table 1. Effects of LPA analogues on RH7777 cells transfected with LPA_1 and LPA_3.[a]

	LPA_1		LPA_3	
Compd	E_{max} [%]	EC_{50} [nM]	E_{max} [%]	EC_{50} [nM]
1	79.7	790	130	62
2	123	3880	123	817
3	74.2	571	ND[c]	ND[c]
4	116	2720	124	207
5	73.9	13500	100	4840
6	NE[b]	ND[c]	51[d]	inhibited
7	NE[b]	ND[c]	68[d]	inhibited
18:1 LPA	100	17	100	263

[a] Intracellular Ca^{2+} transients were measured in response to the application of increasing concentrations of LPA analogues and compared with transients elicited by 1-oleoyl (18:1) LPA; results represent the average of four measurements. [b] NE = no effect. [c] ND = not determined. [d] Inhibition of 200 nM LPA response.

LPA is a member of the phospholipid growth factor family and exerts pleiotropic effects that include enhancement of cell survival and cell proliferation. In vitro, LPA has been shown to function as a growth and survival factor for renal proximal tubular cells, inhibiting apoptosis induced by growth factor deprivation.[7] To further examine the potential biological activities of the analogues, we used an MTT assay to analyze effects on cell proliferation. We found that starting at a concentration of 100 nM, compounds **1** and **3** stimulated the growth of 10T 1/2 cells in a dose-dependent manner with a robust induction shown by **3** at 10 μM (Figure 3). No significant difference was

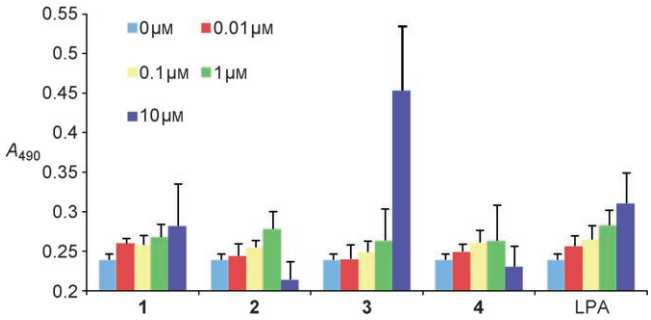

Figure 3. Stimulation of DNA synthesis in 10T 1/2 cells by LPA and analogues **1**–**4** as determined by MTT assay.

observed between compounds **1**, **3** and natural LPA within the concentration range of 0.01–1 μM. At the higher concentrations, the 2*S* enantiomer **3** was more effective than either the 2*R* enantiomer **1** or natural LPA toward the proliferation of 10T 1/2 cells. This result is consistent with previous reports of the enantioselectivity of OMPT, in which (2*S*)-OMPT was threefold to eightfold more active than (2*R*)-OMPT in activating cytosolic calcium release, downstream kinase activation, and production of the potent neovascularizing factor IL-6.[17] In the present case, the enantioselectivity of compounds **1** and **3** was revealed at a much higher concentration (10 μM) than was that of the enantiomers of OMPT (0.1 μM).

In addition to LPA plasma membrane receptors, LPA was found to activate the nuclear transcription factor PPARγ.[32] Many agents have been reported to be agonists of the nuclear transcription factor PPARγ including members of the thiazolidinedione family represented by rosiglitazone (Rosi) as well as oxidized phospholipids, fatty acids, eicosanoids, and oxidized LDL. LPA and the alkyl ether analogue of LPA directly bind to the ligand-binding domain of PPARγ. The activation of PPARγ is direct, and is enhanced when LPA entry into cells is facilitated by carrier amine sulfonamides capable of increasing the transmembrane movement of LPA.[32] Compounds **1**, **3**, **5**, **6**, and **7** were tested for PPARγ activation in CV1 cells that had been transfected with an acyl-coenzyme A oxidase–luciferase (PPRE-Acox-Rluc) reporter gene construct as previously reported.[33] The results are illustrated in Figure 4. Interestingly, the phosphorothioate diesters **5**–**7**, which are inactive or have low activity toward LPA receptors, can nonetheless activate the PPRE-Acox-Rluc reporter more robustly than can arachidonoyl LPA and alkyl OMPT **1** and **3**. These results are consistent with our previously reported observations, in that LPA analogues

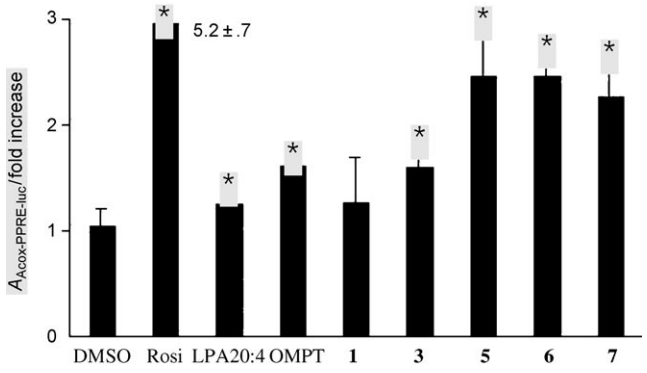

Figure 4. Results of in vitro activation of PPARγ by selected compounds in CV1 cells transfected with PPARγ and the PPRE-Acox-Rluc reporter gene. Rosiglitazone, a known PPARγ agonist, was used as the positive control. CV1 cells were treated with DMSO (1%) or test compound (10 μM in DMSO) for 20 h. Luciferase and β-galactosidase activities (reported as mean ± SE) were measured in the cell lysate ($n = 4$); *$p < 0.05$, significant differences over vehicle control.

that lack the ability to activate GPCRs for LPA receptors may still be potent activators of PPARγ.

Discussion

Ligand recognition by GPCRs generally shows a preference for the naturally occurring enantiomer. However, recognition of LPA by its receptors can be viewed as an exception, as both the natural L (*R*) and unnatural D (*S*) stereoisomers of LPA are equally active in some bioassays.[34] The lack of stereoselectivity of the LPA GPCRs distinguishes them from PPARγ, which shows enantioselective activation.[33] In contrast to the enantiomers of acyl and alkyl LPA, however, the activities of LPA analogues based on non-glycerol backbones show strong enantioselectivity. For example, analogues of *N*-acylethanolamine phosphoric acid (NAEPA) derivatives[13] (which contain a serine or an ethanolamine backbone in place of glycerol), analogues of *N*-palmitoyl-2-methylenehydroxyethanolamide phosphoric acid ((*R*)-MHEPA and (*S*)-MHEPA),[35] and analogues of carbohydrate scaffolds[19] are recognized in a stereoselective manner, in which the 2*R* enantiomers (natural configuration) are more potent than the 2*S* enantiomers (unnatural configuration). This duality of responses has been recently reviewed.[34,36] It appears that OMPT and its alkyl analogues further reinforce this duality of enantioselective recognition. At different concentration ranges, both (2*S*)-acyl OMPT and (2*S*)-alkyl OMPT (the unnatural configuration) show higher activity than their 2*R* enantiomer (natural configuration) counterparts in bioassays. This result further confirms that relative to other kinds of LPA analogues, OMPT and its analogues may interact with LPA receptors through a different orientation than does natural LPA. Furthermore, enantioselective degradation by lipid phosphatases and other metabolic enzymes might also be responsible for differences observed in cellular assays.

As expected, 1-oleoyl LPA stimulated cell survival in 10T 1/2 cells at all concentrations tested (Figure 3). Compounds **1** and **3** stimulated cell viability in a dose-dependent manner, with a robust induction exhibited by **3** at 10 μM. Phosphorothioate diesters **2** and **4** increased cell viability at low concentrations (0.01–1 μM), but functioned as inhibitors at 10 μM, with **2** showing a more prominent effect. These data prompted us to further assess whether compounds **2** and **4** are potential antagonists for LPA signaling. For this purpose, we evaluated these compounds on LPA receptors. However, we could not confirm antagonist activity after the evaluation of all of these compounds. It is thus possible that the inhibitory effect on cell viability arose from the cytotoxicity of cyanoethanol resulting from phosphodiester hydrolysis.

To investigate the function of the ester group on the alkyl OMPT analogues, we prepared phosphorothioate diester compounds **5**–**7**, each with the natural 2*R* configuration at the *sn*-2 position. Among these three analogues, only methyl phosphodiester **5** had agonist activity toward the LPA_3 receptor after biological evaluation. The butyl and cyclohexyl phosphodiesters failed to activate the LPA receptors. Although analogues **2**, **4**, and **5** have similar steric sizes, their activities are quite different. It appears that the polar cyanoethyl group may explain this biological activity.

LPA and its structural analogues all have a polar head group, a linker, and a hydrophobic tail. As reported, of these three motifs, modifications to the polar head group may be the least tolerated. Only modifications of the phosphate head group that retain a negative charge under physiological conditions have been found to retain receptor activation. So far, only two classes of phosphate mimics are good LPA agonists. One class are the phosphonate derivatives, such as α-hydroxymethylene phosphonate, α-ketomethylene phosphonate[35] and α-fluoromethylene phosphonate.[18] The second class includes the phosphorothioate analogues such as OMPT. Therefore, comparison of analogues **1**–**4** with **4**–**6**, switching phosphorothioate monoester to phosphorothioate diester decreases and even deletes agonistic activity. Recently, different substituents at the *sn*-2 position of the *N*-acylethanolamide phosphate backbone were explored.[13] Compounds with smaller substituents at the *sn*-2 position were more potent and efficacious agonists; indeed, in some cases, these compounds are more potent and efficacious than LPA. The fact that efficacy decreased sharply with the bulk of hydrophobic substituents at position 2 led to the discovery of a dual LPA_1/LPA_3 competitive antagonist, VPC12249.[13] This observation further demonstrates that agonists and antagonists might have similar molecular structures, and that small changes can convert an LPA agonist to an antagonist. An excellent LPA agonist can potentially be used as a good lead compound for design of antagonists, because agonists and antagonists may share common features for binding with LPA receptors.

McIntyre and colleagues provided the first evidence that the transcription factor PPARγ can function as an intracellular LPA receptor.[32] The authors showed that oleoyl LPA, palmitoyl LPA, and hexadecyl glycerol phosphate competitively displaced rosiglitazone and hexadecyl azelaic phosphatidylcholine, previously identified ligands of PPARγ. The authors provided conclusive evidence that LPA activates the transcription of genes that contain the peroxisomal proliferator responsive element (PPRE)

including the scavenger receptor CD36. Subsequently, the unsaturated and alkyl ether analogues of LPA were found to induce neointima formation, an early step leading to the development of atherogenic plaques, through PPARγ activation. The SAR of neointima formation by LPA analogues in vivo was identical to PPARγ activation in vitro and was clearly different from the SAR for LPA GPCRs.[33] In the PPARγ activation assays reported herein, both alkyl OMPT (**1** and **3**) and phosphorothioate diesters **5**–**7** activated PPARγ.[33] In contrast to their activities on LPA receptors, the phosphorothioate diesters were more potent than alkyl OMPT and natural LPA. This result strengthens the point that the SAR for PPARγ activation is different from that for GPCR activation.

In summary, an initial SAR analysis of alkyl-chain-substituted OMPT analogues was described, and these alkyl OMPTs were found to be selective agonists of LPA_3. We also found that switching the phosphorothioate monoester to a phosphorothioate diester changed their activities sharply. This study has resulted in the discovery of a new series of agonists for the LPA receptors through the use of an in vitro cell viability assay. The discovery of LPA receptor-specific agonists and antagonists that have favorable properties will facilitate the understanding of the physiological and pathophysiological roles played by single LPA receptor subtypes, which is a major current challenge for LPA biology. Effective LPA subtype-specific agonists will be important for understanding the fundamental biology of LPA receptors and for the development of human therapies based on targeting LPA receptors and components of their signaling pathways. The findings presented herein provide a useful platform for further optimization of OMPT-type analogues, both for agonists and antagonists.

Experimental Section

Chemicals were purchased from Aldrich and Acros Chemical Corporation and were used without prior purification. Solvents were reagent grade and distilled before use; CH_2Cl_2 was distilled from CaH_2 and THF was distilled from sodium wire. TLC: precoated silica gel aluminum sheets (EM SCIENCE silica gel $60F_{254}$). Flash Chromatography (FC): Silica gel Whatman 230–400 mesh ASTM. NMR spectra were recorded on a Varian INOVA 400 at 400 MHz (^{1}H), 101 MHz (^{13}C), or 162 MHz (^{31}P) at 25 °C. Chemical shifts are given in ppm with TMS as internal standard ($\delta = 0.00$); ^{31}P, 85% H_3PO_4 ($\delta = 0.00$). Low- and high-resolution mass spectra were obtained on HP5971A MSD and Finnigan MAT95 double focusing mass spectrometer instruments, respectively.

1-*O*-(9*Z*-octadecen-1-yl)-2(*R*)-*sn*-glycerol-3-*O*-*p*-toluenesulfonate (9): Freshly distilled BF_3 etherate (50 μL) was added to (2*R*)-glycidyl tosylate (200 mg, 0.88 mmol) and 9*Z*-octadecen-1-ol (330 mg, 1.23 mmol) in 4 mL anhydrous CH_2Cl_2. The mixture was stirred at room temperature for 24 h under argon. The solvent was removed under decreased pressure to give a residue. FC (EtOAc/hexane 1:5 *v*/*v*, $R_f = 0.36$) gave **9** (320 mg) as a colorless oil (0.642 mmol, 73%). ^{1}H NMR ($CDCl_3$): $\delta = 0.88$ (t, $J = 8.0$ Hz, 3H), 1.26 (br s, 24H), 1.51 (t, $J = 6.8$ Hz, 2H), 2.01 (m, 4H), 2.04 (s, 1H), 2.45 (s, 3H), 3.37–3.48 (m, 4H), 3.97 (m, 1H), 4.01–4.15 (m, 2H), 5.35 (m, 2H), 7.35 (d, $J = 8.4$ Hz, 2H), 7.80 ppm (d, $J = 8.8$ Hz, 2H); ^{13}C NMR: $\delta = 14.11$, 21.65, 22.68, 26.00, 27.18, 29.24, 29.31, 29.41, 29.47, 29.51, 29.69, 29.75, 31.89, 68.28, 70.39, 70.54, 71.74, 127.99, 129.79, 129.89, 129.97, 132.63, 144.99 ppm; MS (CI) *m*/*z* 497.3 [M^++H−OH]; HRMS [M^++H−OH] calcd for $C_{28}H_{49}SO_5$: 497.3301, found: 497.3344.

3-*O*-(9*Z*-octadecen-1-yl)-2(*S*)-*O*-methyl-*sn*-glycerol-1-*O*-*p*-toluenesulfonate (10): A solution of **9** (2.74 g, 5.50 mmol) and 2,6-di-*tert*-butyl-4-methylpyridine (7.76 g, 37.8 mmol) in dry dichloromethane (50 mL) was treated with methyl triflate (4.28 mL, 37.8 mmol). After the mixture was heated at reflux for 16 h under nitrogen, the solvents were evaporated. EtOAc (500 mL) and 2 N HCl (100 mL) were added to the residue. The organic phase was isolated and washed again with 2 N HCl (30 mL). To recover the excess hindered pyridine, the combined aqueous phase was neutralized with 20% aqueous NaOH, and 2,6-di-*tert*-butyl-4-methylpyridine was extracted into dichloromethane. The EtOAc phase was washed with water, saturated $NaHCO_3$ and water, and then dried (Na_2SO_4). Removal of the solvents gave a residue that was purified by FC (hexane/EtOAc 9:1 *v*/*v*, $R_f = 0.18$) to give 2.10 g of **10** as a colorless oil (3.99 mmol, 73%). ^{1}H NMR ($CDCl_3$): $\delta = 0.85$ (t, $J = 7$ Hz, 3H), 1.28 (br s, 22H), 1.45 (t, $J = 6.4$ Hz, 2H), 1.97 (m, 3H), 2.42 (s, 3H), 3.32 (m, 5H), 3.37 (m, 2H), 3.50 (m, 1H), 5.32 (m, 2H), 7.28 (d, $J = 8.0$ Hz, 2H), 7.77 ppm (d, $J = 8.0$ Hz, 2H); ^{13}C NMR: $\delta = 14.11$, 21.64, 22.67, 25.99, 27.20, 29.25, 29.31, 29.42, 29.48, 29.51, 29.69, 29.75, 31.89, 58.11, 68.92, 69.15, 71.82, 127.99, 129.80, 129.95 ppm; MS (CI) *m*/*z* 527.3 [M^++H]; HRMS [M^++H] calcd for $C_{29}H_{51}SO_6$: 527.3406, found: 527.3272.

1-*O*-(9*Z*-octadecen-1-yl)-l-2(*S*)-*O*-methyl-*sn*-glycerol (11): Dry methanol (15 mL) was added to **10** (1.4 g, 2.66 mmol) and magnesium (650 mg, 26.6 mmol) in a flask fitted with a condenser and a calcium chloride guard tube. The solution was stirred at room temperature, with the flask kept in a water bath overnight. When the reaction was complete, the reaction mixture was neutralized with cold 1 N HCl and extracted with diethyl ether (3×20 mL). The combined organic layers were washed with water and brine, dried over Na_2SO_4, and concentrated. The residue was purified by chromatography (hexane/EtOAc 3:1 *v*/*v*) to afford 860 mg of **11** as a colorless oil (2.41 mmol, 91%). ^{1}H NMR ($CDCl_3$): $\delta = 0.88$ (t, $J = 7.2$ Hz, 3H), 1.26 (br s, 24H), 1.56 (m, 2H), 2.01 (m, 4H), 3.44 (m, 3H), 3.46 (s, 3H), 3.54 (m, 2H), 3.62–3.77 (m, 2H), 5.34 ppm (m, 2H); ^{13}C NMR: $\delta = 14.09$, 22.67, 26.05, 27.18, 27.19, 29.23, 29.31, 29.41, 29.46, 29.51, 29.56, 29.64, 29.68, 29.75, 31.89, 57.76, 62.67, 70.61, 71.90, 79.81, 129.81, 129.93 ppm; MS (CI) *m*/*z* 357.3 [M^++H]. HRMS [M^++H] calcd for $C_{22}H_{45}O_3$: 357.3369, found: 357.3369.

3-*O*-bis-(2-cyanoethoxy)thiophosphoryl-1-*O*-(9*Z*-octadecen-1-yl)-2(*R*)-*O*-methyl-*sn*-glycerol (12): Di(2-cyanoethyl) diisopropylphosphorodiamidite (32 mg, 0.12 mmol) was added under an argon atmosphere to a solution of **11** (14 mg, 0.04 mmol) and 1H-tetrazole (8.4 mg, 0.12 mmol) in 1 mL dry CH_2Cl_2. After stirring for 1 h, sulfur (10 mg, 0.2 mmol) and CS_2/pyridine (10 μL, 1:1 *v*/*v*) were added. After stirring at room temperature for 2 h, the reaction mixture was filtered and the filtrate was washed with brine, dried over Na_2SO_4, and concentrated. FC (EtOAc/hexane/CH_2Cl_2 1:2:2 *v*/*v*/*v*) gave 20 mg of **12** as a colorless oil (0.109 mmol, 91%). ^{1}H NMR ($CDCl_3$): $\delta = 0.87$ (t, $J = 7.2$ Hz, 3H), 1.28 (br s, 24H), 1.56 (m, 2H), 2.00 (m, 4H), 2.76 (m, 4H), 3.44 (m, 2H), 3.46 (s, 3H), 3.50 (m, 2H), 3.55 (m, 1H), 4.14 (m, 2H), 4.25–4.33 (m, 5H), 5.34 ppm (m, 2H); ^{13}C NMR: $\delta = 14.09$, 19.36, 19.43, 22.57, 22.54, 22.64, 26.03, 27.17, 29.09, 29.23, 29.28, 29.41, 29.47, 29.54, 29.61, 29.66, 29.73, 31.86, 58.01, 62.43 (t, $J = 4.6$ Hz), 67.95 (d, $J = 6.2$ Hz), 68.99, 71.87, 78.44 (d, $J = 7.6$ Hz), 116.34, 116.38, 129.79, 129.92 ppm; ^{31}P NMR: $\delta = 68.91$ ppm (s); MS (CI) *m*/*z* 559.3 [M^++H]; HRMS [M^++H] calcd for $C_{28}H_{52}PSN_2O_5$: 559.3334, found: 559.3365.

1-*O*-(9*Z*-octadecen-1-yl)-2(*R*)-*O*-methyl-*sn*-glycero-3-phosphothionate (1): *tert*-Butylamine (1 mL) was added to a solution of compound **12** (28 mg, 0.05 mmol) in CH_3CN (1 mL) under N_2 followed by the addition of bistrimethylsilylacetamide (43 μL, 0.175 mmol). After 72 h, the reaction mixture was concentrated and the residue was purified by chromatography (EtOAc/MeOH 8:1→1:1 *v/v*) to afford 18 mg of **1** as a light yellow oil (0.041 mmol, 84%). ^{1}H NMR (CD_3OD): $\delta = 0.78$ (t, $J = 7.2$ Hz, 3H), 1.23 (m, 24H), 1.45 (m, 2H), 1.91 (m, 4H), 3.35 (m, 3H), 3.50 (m, 3H), 3.85 (m, 2H), 5.22 ppm (m, 2H); ^{13}C NMR: $\delta = 13.42$, 15.52, 22.60, 25.13, 25.29, 26.07, 26.99, 27.02, 29.19, 29.31, 29.47, 29.59, 31.91, 37.48, 57.20, 58.12, 65.08, 65.14, 71.85, 72.56, 80.78, 80.86, 118.07, 130.73 ppm; ^{31}P NMR: $\delta =$ 52.18 ppm (s); MS (CI) *m/z* 453.3 [M^++H]; HRMS [M^++H] calcd for $C_{22}H_{46}PSO_5$: 453.2804, found: 453.2822.

3-*O*-mono-(2-cyanoethoxy)thiophosphoryl-1-*O*-(9*Z*-octadecen-1-yl)-2(*R*)-*O*-methyl-*sn*-glycerol (2): *tert*-Butylamine (1 mL) was added to a solution of compound **12** (28 mg, 0.05 mmol) in CH_3CN (1 mL) under N_2 followed by the addition of bistrimethylsilylacetamide (43 μL, 0.175 mmol). After 10 h, the reaction mixture was concentrated and the residue was purified by chromatography (EtOAc/MeOH 8:1 *v/v*) to afford 21 mg of **2** as a light yellow oil (0.042 mmol, 84%). ^{1}H NMR (CD_3OD): $\delta = 0.78$ (t, $J = 7.2$ Hz, 3H), 1.23 (m, 24H), 1.45 (m, 2H), 1.91 (m, 4H), 2.69 (t, $J = 6.4$ Hz, 2H), 3.46 (m, 6H), 3.60 (m, 2H), 3.95 (m, 2H), 4.12 (m, 2H), 5.22 ppm (m, 2H); ^{13}C NMR: $\delta = 13.39$, 15.49, 22.57, 25.06, 25.26, 26.04, 26.96, 26.98, 29.16, 29.28, 29.44, 29.56, 31.88, 37.45, 54.76 (m), 57.17, 58.09, 62.07 (m), 65.05, 65.11, 71.82, 72.53, 80.75, 80.83, 116.34 (s), 118.04, 129.73 (s), 129.83 (s),130.70 ppm; ^{31}P NMR: $\delta = 58.64$ (s), 58.57 ppm (s); MS (CI) *m/z* 506.3 [M^++H]; HRMS [M^++H] calcd for $C_{25}H_{49}NO_5PS$: 506.3069, found: 506.3081.

Ca^{2+} mobilization assay for receptor activation: The assay for mobilization of intracellular Ca^{2+} was performed as described.[16,30,31] Briefly, RH7777 cells stably expressing human LPA_1, LPA_2, or LPA_3 were loaded with Fura-2 AM. Changes in the intracellular Ca^{2+} concentration were monitored by determining the ratio of emitted light intensities at $\lambda = 520$ nm in response to excitation at $\lambda = 340$ and 380 nm. Responses were monitored for 80–120 s. Ca^{2+} transients were quantified automatically by calculating the difference between maximum and baseline ratio values for each sample. To determine antagonist properties, varying concentrations of the compounds were mixed with LPA (200 nM, 18:1) and responses were recorded. Each test was performed in quadruplicate.

Chemotaxis assay: Cancer cells (203G, MDA-MD-231, and PC-3) that each exhibit LPA_1-dependent cellular migration were used. Cells were cultured in RPMI 1640 (Sigma) with 5% fetal bovine serum (FBS) plus streptomycin (100 μg mL^{-1}) and penicillin (100 U mL^{-1}). Cell migration was measured in a modified Boyden chamber as described previously.[30] The number of cells that migrated to the underside was determined by measuring optical densities at $\lambda = 590$ nm using a 96-well microplate reader (Nalge Nunc International).

MTT assay for cell viability: 10T 1/2 cells were plated into 96-well plates at a density of 5000 cells per 100 μL^{-1}well^{-1} in Basal Medium Eagle Medium containing 10% FBS for one day. Cells were starved in serum-free medium for 24 h prior to stimulation with different compounds for 48 h. At this time, 20 μL well^{-1} of MTS/PMS solution was added to the cells and incubated for an additional 1–4 h at 37 °C. The amount of soluble formazan produced by cellular reduction of MTS was measured at $\lambda = 490$ nm by using a plate reader. MTT = 3-(4,5-dimethylthiazol-2-yl)-2,5-diphenyltetrazolium bromide.

PPARγ activation assay: PPARγ activation using CV1 cells transfected with an acyl-coenzyme A oxidase–luciferase (PPRE-Acox-Rluc) reporter gene construct was performed as previously reported. Briefly, CV-1 cells were plated in 96-well plates at a density of 5×10^3 cells well^{-1} in Dulbecco's modified Eagle's medium supplemented with 10% FBS. The next day, the cells were transiently transfected with 125 ng pGL3-PPRE-Acox-Rluc, 62.5 ng pcDNAI-PPARγ, and 12.5 ng pSV-β-galactosidase (Promega, Madison, WI, USA) by using LipofectAMINE 2000 (Invitrogen). Twenty-four hours after transfection, cells were treated with OptiMEMI (Invitrogen) supplemented with 1% FBS, containing DMSO or 10 μM test compound dissolved in DMSO for 20 h. Luciferase and β-galactosidase activities were measured with Steady-Glo Luciferase Assay system (Promega) and the Galacto-Light Plus system (Applied Biosystems, Foster City, CA, USA), respectively. Samples were run in quadruplicate and the mean ± SE were calculated. Data are representative of at least two independent transfections.

Acknowledgement

We thank the Utah Centers of Excellence Program (to G.D.P.), the Human Frontier Science Program (RG0073-2000-B to G.D.P.), the NIH (NS29632 to G.D.P., HL070231 to G.D.P., HL61469 and CA921160 to G.T., and NCI P01 CA64602 and Cancer Center Grant P30 CA16672 to G.B.M), the Ministry of Education, Science, Sports and Culture Japanese government (to J.A.), and the Department of Defense (DAMD 17-02-1-0222 to G.B.M. and G.D.P.) for financial support of this work.

Keywords: calcium · cell migration · EDG receptors · PPARγ · synthetic methods

[1] W. H. Moolenaar, O. Kranenburg, F. R. Postma, G. C. M. Zondag, *Curr. Opin. Cell Biol.* **1997**, *9*, 168.
[2] D. A. Fishman, Y. Y. Liu, S. M. Ellerbroek, M. S. Stack, *Cancer Res.* **2001**, *61*, 3194.
[3] X. Fang, M. Schummer, M. Mao, S. Yu, F. H. Tabassam, R. Swaby, Y. Hasegawa, J. L. Tanyi, R. LaPushin, A. Eder, R. Jaffe, J. Erickson, G. B. Mills, *Biochim. Biophys. Acta* **2002**, *1582*, 257.
[4] Y. Xu, Y.-J. Xiao, K. Zhu, L. M. Baudhuin, J. Lu, G. Hong, K.-S. Kim, K. L. Cristina, L. Song, F. S. Williams, P. Elson, M. Markman, J. Belinson, *Curr. Drug Targets: Immune Endocr. Metab. Disord.* **2003**, *3*, 23.
[5] X. Fang, D. Gaudette, T. Furui, M. Mao, V. Estrella, A. Eder, T. Pustilnik, T. Sasagawa, R. Lapushin, S. Yu, R. B. Jaffe, J. R. Wiener, J. R. Erickson, G. B. Mills, *Ann. N. Y. Acad. Sci.* **2000**, *905*, 188.
[6] G. B. Mills, A. Eder, X. Fang, Y. Hasegawa, M. Mao, Y. Lu, J. Tanyi, F. H. Tabassam, J. Wiener, R. Lapushin, S. Yu, J. A. Parrott, T. Compton, W. Tribley, D. Fishman, M. S. Stack, D. Gaudette, R. Jaffe, T. Furui, J. Aoki, J. R. Erickson, *Cancer Treat. Res.* **2002**, *107*, 259.
[7] G. B. Mills, W. H. Moolenaar, *Nat. Rev. Cancer* **2003**, *3*, 582.
[8] C. Luquain, V. A. Sciorra, A. J. Morris, *Trends Biochem. Sci.* **2003**, *28*, 377.
[9] M. Umezu-Goto, J. Tanyi, J. Lahad, S. Liu, S. Yu, R. Lapushin, Y. Hasegawa, Y. Lu, R. Trost, T. Bevers, E. Jonasch, K. Aldape, J. Liu, R. D. James, C. G. Ferguson, Y. Xu, G. D. Prestwich, G. B. Mills, *J. Cell. Biochem.* **2004**, *92*, 1115.
[10] K. Noguchi, S. Ishii, T. Shimizu, *J. Biol. Chem.* **2003**, *278*, 25600.
[11] L. Feng, G. B. Mills, G. D. Prestwich, *Expert Opin. Ther. Pat.* **2003**, *13*, 1619.
[12] W. L. Santos, B. H. Heasley, R. Jarosz, K. M. Carter, K. R. Lynch, T. L. Macdonald, *Bioorg. Med. Chem. Lett.* **2004**, *14*, 3473.
[13] C. E. Heise, W. L. Santos, A. M. Schreihofer, B. H. Heasley, Y. V. Mukhin, T. L. Macdonald, K. R. Lynch, *Mol. Pharmacol.* **2001**, *60*, 1173.
[14] H. Ohta, K. Sato, N. Murata, A. Damirin, E. Malchinkhuu, J. Kon, T. Kimura, M. Tobo, Y. Yamazaki, T. Watanabe, M. Yagi, M. Sato, R. Suzuki,

H. Murooka, T. Sakai, T. Nishitoba, D. S. Im, H. Nochi, K. Tamoto, H. Tomura, F. Okajima, *Mol. Pharmacol.* **2003**, *64*, 994.
[15] R. H. Heasley, R. Jarosz, K. R. Lynch, T. L. Macdonald, *Bioorg. Med. Chem. Lett.* **2004**, *14*, 2735.
[16] T. Virag, D. B. Elrod, K. Liliom, V. M. Sardar, A. L. Parrill, K. Yokoyama, G. Durgam, W. Deng, D. D. Miller, G. Tigyi, *Mol. Pharmacol.* **2003**, *63*, 1032.
[17] L. Qian, Y. Xu, Y. Hasegawa, J. Aoki, G. B. Mills, G. D. Prestwich, *J. Med. Chem.* **2003**, *46*, 5575.
[18] Y. Xu, L. Qian, G. D. Prestwich, *Org. Lett.* **2003**, *5*, 2267.
[19] Y. Tamaruya, M. Suzuki, G. Kamura, M. Kanai, K. Hama, K. Shimizu, J. Aoki, H. Arai, M. Shibasaki, *Angew. Chem.* **2004**, *116*, 2894; *Angew. Chem. Int. Ed.* **2004**, *43*, 2834.
[20] Y. Hasegawa, J. R. Erickson, G. J. Goddard, S. Yu, S. Liu, K. W. Cheng, A. Eder, K. Bandoh, J. Aoki, R. Jarosz, A. D. Schrier, K. R. Lynch, G. B. Mills, X. Fang, *J. Biol. Chem.* **2003**, *278*, 11962.
[21] Y. Xu, M. Tanaka, H. Arai, A. J. , G. D. Prestwich, *Bioorg. Med. Chem. Lett.* **2004**, *14*, 5323.
[22] S. R. Tyagi, D. N. Burnham, J. D. Lambeth, *J. Biol. Chem*. **1989**, *264*, 12977.
[23] S. Ali, R. Bittman, *Biochem. Cell Biol.* **1990**, *68*, 360.
[24] J. Lindberg, J. Ekeroth, P. Konradsson, *J. Org. Chem.* **2002**, *67*, 194.
[25] P. N. Guivisdalsky, R. Bittman, *J. Org. Chem.* **1989**, *54*, 4637.
[26] P. N. Guivisdalsky, R. Bittman, *J. Org. Chem.* **1989**, *54*, 4643.
[27] M. Sridhar, B. A. Kumar, R. Narender, *Tetrahedron Lett.* **1998**, *39*, 2847.
[28] L. Qiao, F. Nan, M. Kunkel, A. Gallegos, G. Powis, A. P. Kozikowski, *J. Med. Chem.* **1998**, *41*, 3303.
[29] E. Uhlman, J. Engels, *Tetrahedron Lett.* **1986**, *27*, 1023.
[30] K. Hama, J. Aoki, M. Fukaya, Y. Kishi, T. Sakai, R. Suzuki, H. Ohta, T. Yamori, M. Watanabe, J. Chun, H. Arai, *J. Biol. Chem.* **2004**, *279*, 17634.
[31] D. J. Fischer, N. Nusser, T. Virag, K. Yokoyama, D. A. Wang, D. L. Baker, D. Bautista, A. L. Parrill, G. Tigyi, *Mol. Pharmacol.* **2001**, *60*, 776.
[32] T. M. McIntyre, A. V. Pontsler, A. R. Silva, A. St. Hilaire, Y. Xu, J. C. Hinshaw, G. A. Zimmerman, K. Hama, J. Aoki, H. Arai, G. D. Prestwich, *Proc. Natl. Acad. Sci. USA* **2003**, *100*, 131.
[33] C. Zhang, D. L. Baker, S. Yasuda, N. Makarova, L. Balazs, L. R. Johnson, G. K. Marathe, T. M. McIntyre, Y. Xu, G. D. Prestwich, H. S. Byun, R. Bittman, G. Tigyi, *J. Exp. Med.* **2004**, *199*, 763.
[34] K. Yokoyama, D. L. Baker, T. Virag, K. Liliom, H. S. Byun, G. Tigyi, R. Bittman, *Biochim. Biophys. Acta* **2002**, *1582*, 295.
[35] S. B. Hooks, W. L. Santos, D. S. Im, C. E. Heise, T. L. Macdonald, K. R. Lynch, *J. Biol. Chem.* **2001**, *276*, 4611.
[36] K. R. Lynch, T. L. Macdonald, *Biochim. Biophys. Acta* **2002**, *1582*, 289.

Received: September 8, 2005
Revised: November 14, 2005
Published online on January 10, 2006

Functional Lipidomics: Lysophosphatidic Acid as a Target for Molecular Diagnosis and Therapy of Ovarian Cancer

Janos L. Tanyi[1], David Croetzer[2], Judith Wolf[2], Shuangxing Yu[1], Yutaka Hasegawa[1], John Lahad[1], Kwai Wa Cheng[1], Makiko Umezu-Goto[1], Glenn D. Prestwich[3], Andrew Morris[6], Robert A. Newman[5], Edward A. Felix[5], Rose Lapis[6,] and Gordon B. Mills[1]

[1] Department of Molecular Therapeutics, The University of Texas M. D. Anderson Cancer Center, Houston, TX 77030

[2] Department of Gynecologic Oncology, The University of Texas M. D. Anderson Cancer Center, Houston, TX 77030

[3]Department of Medicinal Chemistry, The University of Utah, Salt Lake City, UT 84108

[4] Department of Cell and Developmental Biology, University of North Carolina, Chapel Hill, NC 27599-7090

[5] Department of Experimental Therapeutics, The University of Texas M. D. Anderson Cancer Center, Houston, TX 77030

[6]Texas Children's Hospital-Texas Children's Pediatric Associates, Baylor College of Medicine, Houston, TX 77054

Corresponding author: Janos L. Tanyi M.D.,

Department of Molecular Therapeutics, Unit 184,

The University of Texas M.D. Anderson Cancer Center,

7777 Knight Road, Houston, TX 77057.

Tel: 713-563-4225;

Fax: 713-745-1184.

e-mail: jtanyi@mdanderson.org

Keywords: ovarian cancer, molecular therapy, lysophosphatidic acid, lipid phosphate phosphatases, lipidomics

Summary

Epithelial ovarian cancer has the highest mortality rate of all gynecologic malignancies owing to late diagnosis and a lack of effective tumor-specific therapeutics. Ovarian carcinogenesis and metastasis occurs as a consequence of an orchestrated cascade of genetic, molecular, and biochemical events. Indeed, over the last several years, an extensive array of aberrations have been identified in this tumor, however, their roles in the pathophysiology of ovarian cancer remain to be elucidated. Abnormal lysophosphatidic acid (LPA) production, receptor expression, and signaling are frequently found in ovarian cancers, suggesting that LPA plays a role in the pathophysiology of the disease. Although LPA is the simplest lipid found in nature, it contains a number of structure components providing important informational content. High affinity LPA receptors of the G protein coupled receptor family provide evidence for the importance of the molecule in normal cellular functions. LPA levels and levels of related lysopholipids have been reported to be elevated in patient fluids including ascites and peripheral blood. The recent identification of the enzymes that mediate the degradation and production of LPA and the development of receptor-selective analogs may lead to new approaches in the treatment of this deadly disease. Thus, the LPA pathway may contain novel molecular targets, illustrating the potential role of functional lipidomics in the development of new therapeutic and diagnostic strategies for disease management.

I. Introduction

Ovarian cancer has the highest mortality rate of all gynecologic cancers. This gloomy prognosis results from an inability to diagnose the tumor at an early, curable stage because there is no well-established screening method. Although current therapeutic approaches, which consist of a wide variety of chemotherapeutic regimens preceded by radical debulking surgery, radiation therapy, or both result in high response rates that translate into modest increases in survival time and improvement in quality of life, no notable increase in the cure rate has occurred in the last 25 years (Penson et al, 1998; Greenlee et al, 2001). Most patients rapidly develop resistance to chemotherapy and eventually die of their disease. The overall 5-year survival rate in patients with advanced disease remains less than 30% (Penson et al, 1998; Greenlee et al, 2001). Ovarian cancer genomes are remarkably unstable; an advanced cancer usually harbors multiple genomic changes, an unknown fraction of which influence biologic and clinical behavior (Mills et al, 2003a; Suzuki et al, 2003; Gray et al, 2003). This genomic variability, both within and between tumors, likely contributes to drug resistance and the lack of effective therapeutic approaches that can convert the high response rate into a high cure rate. The outcomes of ongoing genomic analyses may improve ovarian cancer management by revealing early events in ovarian cancer oncogenesis and progression that can be investigated as markers for early detection and by identifying specific genetic aberrations that can be targeted therapeutically. Alternatively, global genomic analysis

may identify patterns of genetic aberrations that predict outcome or response to particular therapies, allowing tailoring of disease management to the specific genetic aberrations in the tumor -- individualized molecular medicine.

Regional delivery of gene therapy constructs was heralded as an attractive alternative for the treatment of ovarian cancer because ovarian cancer tends to remain localized in the peritoneal cavity, with local tumor growth contributing to morbidity and mortality. However, most gene therapy approaches currently use non-specific and non-selective prokaryotic promoters (eg, CMV and SV40) that allow a high expression of the gene in normal cells, potentially limiting the therapeutic index due to toxicity to normal tissues. Further, it has proven difficult to introduce target genes into all tumor cells, and the long-hoped-for "bystander effect," in which non-transfected cells die because of interactions with their neighbors, has not proven to be sufficiently effective to alter patient outcomes. Additional studies are needed to clarify optimal gene therapy targets and to identify effective methods for tumor-selective delivery, such as tumor-specific promoters or cell surface markers to deliver gene therapy preferentially and effectively to tumor cells (Tanyi et al, 2002; Lee et al, 2004; Bao et al, 2002).

Lysophosphatidic acid (LPA), which was originally considered a precursor and component of lipid remodeling, is now know to constitute an important extracellular bioactive lipid, mediating cell proliferation, migration, and survival in almost every cell type, both normal and malignant (Mills and Moolenaar, 2003b). In this review, we summarize recent studies demonstrating a key role of LPA in ovarian carcinogenesis,

supported by our recent findings of the therapeutic potential of LPA and its function and metabolism in this deadly disease. In the context of functional lipidomics, the biosynthesis, metabolism, and receptor-mediated interactions of LPA constitute an excellent case study of how disorders of lipid metabolism may offer important therapeutic targets (Feng et al, 2003).

II. Physiologic role of LPA

Despite being one of the simplest of all serum phospholipids, LPA exerts pleomorphic effects on many cell lineages (Mills and Moolenaar, 2003b). LPA and its actions are highly conserved through ontogeny, and affect diverse organisms (Moolenaar et al, 1992). Yeast and insect cells, which lack functional receptors for LPA, have proven to be powerful models for understanding the mechanisms by which LPA mediates its effects (Hu et al, 2001). Although LPA induces cellular proliferation and survival in most cell lineages, it can induce differentiation or death in some. For example, in neurons, LPA can induce necrosis and apoptosis (Nietgen and Durieux, 1998). LPA also induces a number of early cellular responses, such as motility, chemotaxis, gap-junction opening, and invasion and morphologic changes that do not require new protein synthesis. Longer-term effects such as changes in cellular shape, increased cell viability, improved wound healing, and production of endothelin and proangiogenic factors, may require, at least in part, new gene transcription (Mills and Moolenaar, 2003b). LPA may additionally function as part of an autocrine signaling loop by increasing the secretion or activation of multiple peptide growth factors, including transforming growth factors α and β,heparin-

binding epidermal growth factor, insulin-like growth factor II, and endothelin 1 (Nakano et al, 1994; Pustilnik et al, 1999; Laffargue et al, 1999; Fang et al, 2000a). LPA also induces the production of several paracrine growth factors active on blood vessel endothelial cells, such as interleukin-6, interleukin-8, gro-alpha, and vascular endothelial growth factor, and increasing neovascularization in physiologic (wound healing) and pathologic (tumor) environments (Jalink et al, 1994; Xu et al, 1995a; Levine et al, 1997, Fang et al, 2004). LPA exerts multiple other vascular effects, including alteration of monocyte attachment to blood vessel walls, plaque formation, increased endothelial permeability, and vascular smooth muscle cell contraction. These changes can alter blood pressure in animal model and humans and may also play a role in the development of atherosclerosis (Shulcze et al, 1997; van Nieuw Amerongen et al, 2000). Further, LPA is a precursor for other, more complex lipid syntheses, some of which may also function as bioactive mediators. For example, conversion of LPA to phosphatidic acid by endophilin and lysophospholipid acyltransferase is known to influence membrane curvature and the process of endocytosis (Schmidt, 1999). Most of the signaling effects of LPA appear to be due to binding to specific cell surface receptors, but intracellular LPA has been demonstrated to activate the peroxisome proliferating activating receptor, potentially contributing to atherosclerosis, adipogenesis, and insulin signaling (McIntyre et al, 2003).

III. LPA receptors

The extracellular activities of LPA are mediated by its binding to a group of G-protein-coupled receptors on the surface of mammalian cells. The first three members of

the LPA receptor family are members of the endothelial differentiation gene (EDG) family (An et al, 1998; Bandoh et al, 1999). The EDG2, EDG4, and EDG7 LPA receptors were recently renamed LPA1, LPA2, and LPA3, respectively. A fourth LPA receptor, LPA4, a member of the purinergic family of protein-coupled receptors, was recently identified (Noguchi et al, 2003). The roles of specific LPA receptors in the outcomes of extracellular LPA remain complex and elusive. The frequently contradictory results likely represent the spectrum of LPA receptors on the cell surface, the cell lines and potentially lineages studied and the interaction of LPA receptors with other receptors and intracellular signaling molecules.

LPA1, which is widely expressed in the placenta, brain, small intestine, and colon, has a lower level of expression in pancreatic and normal ovarian tissue (Hecht et al, 1996). In some cell lineages, LPA1 is a major regulator of cellular motility by initiating Rho-dependent changes in cytoskeletal function, including cell rounding and stress fiber formation (Fukushima et al, 1998; Van Leeuwen et al, 2003). LPA2, however clearly mediates motility in at least some cellular lineages. LPA2 and LPA3 have more constrained distribution patterns than LPA1 does in terms of normal tissues. LPA1 and LPA2 are aberrantly expressed in prostatic and ovarian cancer (Fang et al, 2002) and in other cancer lineages, suggesting that they may be appropriate targets for therapy. LPA2 exhibits a higher affinity than the other family members for LPA, suggesting that it is a major contributor to the functions of LPA, particularly at the low levels of LPA that are present in normal tissues and plasma. LPA2 appears to be a major regulator of the production of vasculogenic factors (Fang et al, 2003; Huang et al, 2004). The lower-

affinity LPA receptors may function in pathologic or stress states, such as those following cellular injury. These include, for example, wound healing, reperfusion after ischemia, and blood clotting (Okusa et al, 2003). The receptors by which LPA mediates cellular proliferation and viability remain controversial, although LPA3 remain a strong candidate because LPA3-selective LPA homologs are potent activators of proliferation and viability (Hasegawa et al, 2003). LPA4 is expressed at a very low level in most human tissues, but a substantial level of expression has been detected in normal ovarian tissue (Noguchi et al, 2003). The role of LPA4 in physiologic and pathologic states has not been elucidated.

LPA activates at least three different G proteins via the LPA receptors, which can, in turn, stimulate multiple intracellular signal transduction systems. How the integration of these signaling events leads to the functional outcome of LPA receptor ligation remains to be fully determined. Activation of G_q leads to activation of phospholipase C, producing diacylglycerol and inositol triphosphate, second messengers that contribute to the activation of protein kinase C and increases in cytosolic calcium level, respectively. Activation of G_i feeds into three different and important signaling pathways: adenylate cyclase by increasing CAMP levels and activating protein kinase A; RAS and the mitogen-activated protein kinase cascade; and activation of the phosphatidylinositol 3-kinase (PI3K) pathway (Van Leeuwen et al, 2003; Fang et al, 2000a; Fang et al, 2000b). LPA also activates $G_{12/13}$, contributing to activation of the small GTPase RhoA, which leads to cell rounding and cytoskeletal contraction (Etienne-Manneville and Hall, 2002).

IV. LPA Metabolism

The concentration of LPA in plasma is normally low (100-200 nM), suggesting that the production, metabolism, and clearance of LPA are strictly controlled in vivo (Xu et al, 1998). LPA can be produced by activated platelets, adipocytes, leukocytes, fibroblasts, endothelial cells, during clotting and, of particular importance, by ovarian cancer cells (Moolenaar et al, 1992; Goetzl et al, 1998; Fang et al, 2000b; Eder et al, 2000; Sano et al, 2002; Aoki et al, 2002.). The primary pathway for extracellular LPA production is the activity of autotaxin/lysophospholipase D (ATX/lysoPLD), which removes a choline from lysophosphatidylcholine (LPC) (Sano et al, 2002; Aoki et al, 2002; Umezu-Goto et al; 2002; Tokumura et al, 2002). LPC is produced by the removal of a fatty acyl chain from phosphatidylcholine (PC) by phospholipase A1 (PLA1) or A2 (PLA2). PLA2 has limited ability to hydrolyze lipids in intact membranes, suggesting that the major source of LPA production may be vesicles or apoptotic cells in which normal membrane structure is compromised. In addition, LPC is generated by the lecithine cholesterol acyltransferase pathway in which cholesteryl esters are generated by acyl transfer from PC. PC secreted by the liver and bound to albumin or low-density lipoproteins could be hydrolyzed by the sequential activity of PLA2 and ATX/lysoPLD, producing bioactive LPA (Croset et al, 2000). LPA also can be produced by the removal of a fatty acyl chain from PA by PLA1 or PLA2 (Aoki et al, 2002; Sano et al, 2002), however, the physiological relevance of this pathway remains to be determined.

ATX/LysoPLD was originally identified as a major regulator of motility, metastasis, and tumor aggressiveness (Nam et al, 2000; Nam et al, 2001; Yang et al, 2002); however, the mechanism by which it mediates these processes was unknown. The

discovery that ATX and lysoPLD were encoded by the same molecule resulted in a convergence of these two major areas of research (Umezu-Goto et al, 2002; Tokumura et al, 2002). ATX/lysoPLD is widely expressed, with the highest mRNA levels in the ovary, intestine, lung, and brain (Bachner et al, 1998). The fact that ATX/lysoPLD levels are markedly increased in multiple different cancers supports the idea that it has a role in the pathophysiology of malignant disease (Umezu-Goto et al, 2004).

LPA is efficiently metabolized, being maintained at low levels under physiologic conditions. A family of lipid phosphate phosphohydrolases (LPPs) dephosphorylates LPA, decreasing the duration of LPA-mediated signaling events (Imai et al, 2000; Tanyi et al, 2003a; Tanyi et al, 2003b). This family consists of three members LPP-1 (PAP2A), LPP-2 (PAP2C), and LPP-3 (PAP2B) (Hu et al, 2001). Other routes of LPA metabolism include acylation by lysophospholipid acyltransferase or endophilin to create phosphatidic acid and deacylation by lysophospholipases to produce glycerol phosphate (Wang and Dennis, 1999). In addition to its metabolism, LPA is cleared rapidly from the circulation, potentially contributing to its maintenance at appropriately low levels under physiologic conditions.

V. Pathophysiology of LPA in ovarian cancer

Ascitic fluid from patients with ovarian cancer frequently contains elevated concentrations of LPA (up to 80 μM) (Eder et al, 2000; Xu et al, 2003). This suggests that ovarian cancer cells are exposed to an LPA-rich environment in vivo. Because ovarian cancer cells can produce LPA (Eder et al, 2000; Sengupta et al, 2003; Shen et al,

1998; Luquain et al, 2003), the cancer cells themselves are potential sources of the elevated concentrations of LPA. LPA can increase the proliferation of ovarian cancer cells (Xu et al, 1995b), and it contributes to the multistep process of metastasis and invasion by increasing the production of urinary plasminogen activator (Pustilnik et al, 1999). Furthermore, LPA markedly decreases anoikis (a form of apoptosis) in ovarian cancer cell lines, suggesting that it plays a role in preventing anoikis and increasing metastasis in vivo. LPA also is a potent inducer of neovascularizing factors, vascular endothelial growth factor, and production of interleukin 6 and 8 by ovarian cancer cells, potentially contributing to neovascularization and the aggressiveness of ovarian cancer (Hu et al, 2001; Fang et al, 2004; Schwartz et al, 2001) and to the elevated levels of these factors in ovarian cancer (Zebrowski et al, 1999).

LPA is not produced in notable amounts by normal ovarian surface epithelial cells but is produced at considerable levels by some ovarian cancer cell lines (Eder et al, 2000; Sengupta et al, 2003; Shen et al, 1999; Luquain et al, 2003). The levels of ATX/lysoPLD mRNA and protein levels are modestly elevated in malignant disease. In at least half of ovarian cancers, patients exhibit at least a 2-fold increase, and one quarter exhibit up to a 3-fold increase (Umezu-Goto et al, 2004). The production of LPA by ovarian cancer cells can be increased by phorbol esters, nucleotides, laminin, and even LPA itself (Eder et al, 2000; Sengupta et al, 2003; Shen et al, 1999; Luquain et al, 2003). In addition to increased rates of LPA production, LPA metabolism is decreased, with LPP-1 mRNA levels and activity consistently being consistently in ovarian cancer samples as compared to normal ovarian epithelium (Tanyi et al, 2003a). The decreased LPA inactivation, the

increased levels of ATX/lysoPLD protein, and the LPA autocrine loop likely contribute to the increased levels of LPA in the ascitic fluid.

LPA has modest activity on normal ovarian surface epithelium, which expresses predominantly LPA1. Overexpression of LPA1 in ovarian cancer cell lines decreases cellular proliferation and increases apoptosis, suggesting that LPA1 can act as a negative regulator (Furui et al, 1999). In contrast, both LPA2 and LPA3 are aberrantly overexpressed in ovarian cancer cells, suggesting that LPA plays an important role in the pathophysiology of this cancer (Furui et al, 1999; Goetzl et al, 1999; Eder et al, 2000; Fang et al, 2002). Expression of LPA2 and LPA3 receptors in ovarian cancer cells greatly increases their ability to proliferate, form colonies, grow under anchorage independent conditions and to grow in vivo (unpublished data), compatible with a role for receptor overexpression in the pathophysiology of ovarian cancer.

In addition to increased LPA production and receptor expression, the genetic aberrations in ovarian cancer cells may contribute to increased responsiveness to LPA receptor ligation. Both the PI3K and Ras/Erk pathways are stimulated by LPA receptors in ovarian cancer cells (Xu et al, 1995c; Fang et al, 2000b), and contribute to LPA-induced cell proliferation and survival. It is intriguing that the p110β catalytic subunit of PI3K is selectively activated by LPA in ovarian cancer cells (Roche et al, 1998). Both the PI3K and Ras/Erk pathways are highly activated in ovarian cancer cells, at least in part because of the presence of LPA in ascitic fluid. A recent review highlighted the importance of the PI3K pathway as a second target of lipidomics in developing new

targeted signal transduction or targeted therapeutics for the treatment of ovarian cancer (Drees et al, 2004).

If LPA is present at an increased concentration in ascitic fluid, it could diffuse into the systemic blood circulation, where it could serve as a tumor marker for early disease detection. Indeed, plasma levels of LPA from patients with ovarian cancer are lower than they are in matched samples of ascitic fluid, a finding that is compatible with the levels of LPA in plasma representing diffusion from the peritoneal cavity (Eder et al, 2000). High LPA levels have been reported in the plasma of approximately 90% of patients with ovarian cancer (Xu et al, 1998). Similarly, aberrations of particular phosphatidylcholine isoforms have been detected in the plasma of patients with ovarian cancer (Okita et al, 1997). However, considerable controversy exists about whether LPA levels are elevated in the plasma of patients with ovarian cancer and whether such elevations can predict of the presence of ovarian cancer (Xiao et al, 2000; Baker et al, 2002; Yoon et al, 2003, Sutphen et al 2004)

VI. LPA production or "activity" as a target for therapy of ovarian cancer

Elevated LPA concentrations in ascites could be a consequence of altered levels or activity of enzymes involved in LPA production, increased numbers of LPA-producing cells (ie, tumor cells), or altered clearance. Using public transcriptional profiling databases, the CGAP SAGE database, and our own transcriptional profiling databases, we analyzed the transcriptional profiles of genes involved in LPA production and

metabolism in ovarian cancer tissue samples and cell lines and compared them with those of normal ovarian surface epithelium and cell lines. We found marked increases in levels of ATX/lysoPLD, the key enzyme regulating LPA production (Umezu-Goto et al, 2002; Tokumura et al, 2002). ATX/lysoPLD mRNA levels were elevated up to 200 times in a proportion of ovarian cancer cell preparations obtained directly from patients (Umezu-Goto et al, 2004). These increases were concurrent with decreases in the levels of LPPs (Tanyi et al, 2003a), which degrade LPA in ovarian cancer. The expected combined effects of the changes in these enzymes in ovarian cancer would be to increase LPA levels in the local tumor environment.

It is important to note, however, that approximately 40% of ovarian cancer samples do not express markedly elevated levels of ATX/lysoPLD mRNA. Compatible with the increase in mRNA levels, ATX/lysoPLD activity is increased in ascitic fluid of patients with ovarian cancer, compared with normal plasma (12.6 units vs. 6.9 units; $p<0.01$), albeit at a lower level than mRNA levels. As with mRNA levels, ATX/lysoPLD activity was markedly elevated in a subset of patients; approximately 20% of patients did not demonstrate alterations in ATX/lysoPLD activity, compared with plasma (Umezu-Goto, 2004).

In contrast to ATX/lysoPLD and compatible with the increased LPA levels in ascitic fluid, the overall total levels of all three LPP mRNA's were lower in ovarian cancer tissue samples and cell lines than they were in normal ovarian epithelial tissues and cell lines (Tanyi et al, 2003a). Most of the difference in total LPP mRNA levels could be

attributed to the decreased concentration of LPP-1, which was, on average, five times lower in ovarian cancers than in normal epithelial tissues. Again, it is important to note that only some patients' samples demonstrated marked aberrations in LPP-1 mRNA levels. In contrast to LPP-1, LPP-2 and LPP-3 expression was similar in ovarian cancer and normal epithelium. The same pattern of enzyme expression (ie, decreased LPP-1 with normal LPP-2 and LPP-3 levels) was observed in the HEY, OVCAR-3, and SKOV3 ovarian cancer cell lines (Tanyi et al, 2003a).

Together, these data suggest that ovarian cancer cells, compared with normal ovarian epithelium, have an increased ability to produce LPA. This is indeed the case with ovarian cancer cells producing high levels of LPA constitutively or in response to stimuli such as LPA itself, phorbol esters, laminin, and nucleotides (Eder et al, 2000; Sengupta et al, 2003; Shen et al, 1999; Luquain et al, 2003). The ability of ovarian cancer cell lines to produce LPA constitutively or inducibly depends on the action of PLA isozymes and PLD (Eder et al, 2000; Sengupta et al, 2003; Shen et al, 1999; Luquain et al, 2003). Whether the levels and activity of these enzymes are aberrant in ovarian cancer and contribute to elevated levels of LPA in the tumor microenvironment remains to be elucidated. Secretory PLA2 (sPLA2) has a limited ability to hydrolyze lipids in intact cell membranes but is highly efficient at hydrolyzing lipids in vesicles and apoptotic cells (Fourcade et al, 1998; Kudo et al, 1993; Fourcade et al, 1995). Ovarian cancer ascitic fluid contains elevated levels of vesicles accessible to sPLA2, potentially increasing the amount of substrate available for ATX/lysoPLD (Ginestra et al, 1999; Andre et al, 2002).

In addition to alterations in the production or action of enzymes involved in LPA production, even a modest ability of ovarian cancer cells to produce LPA could result in marked aberrations in levels of LPA in patients with ovarian cancer. It is not unusual for these patients to present with more than 1 kg of tumor in the peritoneal cavity and several liters of ascitic fluid, which can contain up to 10^8 tumor cells per mililiter. Thus, the initial numbers of ovarian cancer tumor cells in patients can be very high. Together, these studies suggest that the ovarian cancer environment is LPA-rich because of aberrations in both LPA production and metabolism.

We have begun to explore the LPA transcriptome in model systems and have identified a number of genes regulated by LPA. It is important that many of the LPA-regulated genes are coordinately altered in patients with ovarian cancer, compatible with the ovarian cancer microenvironments being LPA-rich and with LPAs playing a role in the pathophysiology of ovarian cancer. In this regard, the availability of LPA affinity reagents from one of our laboratories (G.D.P.) and from Echelon Biosciences, (Salt Lake City UT) will facilitate the discovery of LPA-binding proteins and physically associated proteins that constitute an essential part of the signaling complexes.

Combined with the observations described above, that the expression of LPA receptors is aberrant in ovarian cancer, the evidence that LPA levels and metabolizing enzymes are aberrant in ovarian cancer suggests that LPA production or activity could provide novel effective targets for therapy. We have validated LPA production, metabolism and action as potential therapeutic targets in ovarian cancer both in vitro and

in vivo by evaluating the effects of decreasing LPA production by ovarian cancer cells by transfecting them with LPP. Ovarian cancer cell lines and normal control epithelial cells were transiently and stably transfected with LPP-1- and LPP-3-expressing vectors, and enzyme overexpression was confirmed by semiquantitative reverse transcriptionase polymerase chain reaction, immunoprecipitation and western blotting and immunofluorescence (Figure 1) (Tanyi et al, 2003a; 2003b). Overexpression of either LPP-1 or LPP-3 isozymes decreased proliferation and survival as indicated by the colony-forming activity of ovarian cancer cells and by MTT dye reduction (Figure 2). The ability of LPP-3 and LPP-1 to decrease the colony-forming activity of ovarian cancer cells depended on LPA degradation because mutant, biologically inactive LPP-3 had no effect on colony-forming activity (unpublished data).

To further determine whether the effects of LPP-3 on the growth of ovarian cancer cells were due to hydrolysis of extracellular LPA, we assessed the ability of a non-hydrolyzable LPA3 receptor-selective agonist OMPT (Hasegawa et al, 2003), to reverse the effects of LPP-3 expression. OMPT substantially reversed the inhibition of both colony-forming activity and apoptosis by LPP-3 (Tanyi et al, 2003b). To determine whether OMPT was acting as an agonist for LPA receptors or inhibiting LPP activity, we assessed the OMPT's ability to inhibit LPP-mediated LPA hydrolysis. High concentrations of OMPT (>10 μM) can inhibit LPPs, but the concentrations used in these studies (100 nM) failed to alter LPP activity. Recently, the activity of OMPT on LPA3 was shown to be enantioselective, with the "unnatural" (2S) enantiomer being 4-fold to 8-fold more potent than the 2R isomer (Qian et al, 2003). The ability of exogenous OMPT

to reverse the effects of LPP-3 suggests that the major effect of hLPP-3 on the growth of ovarian cancer cells is due to hydrolysis of extracellular LPA. LPP-1 and LPP-3 overexpression markedly increased the apoptosis rate in ovarian carcinoma cell lines, with lesser effects on cell cycle progression, suggesting that the decreased growth rate was a consequence of both decreased proliferation and increased cell death. However, the recent demonstration that XY-14, a difluorophosphonate analog of PA (Xu et al, 2002), acts as a submicromolar inhibitor of LPP-1 (Smyth et al, 2003), but has no activity on the LPA G protein coupled receptors offers an additional tool for determining the importance of LPA metabolism and signaling in tumorigenesis.

The amount of LPA produced by ovarian cancer cells depends on the rates of production and catabolism. ATX/lysoPLD and LPPs appear to be the major contributors to this process (Umezu-Goto et al, 2003; Imai et al, 2000), which suggests that overexpression of ATX/lysoPLD could potentially increase LPA production to levels sufficient to overcome the effects of LPP transfection. Indeed, ATX/lysoPLD reversed the growth - inhibitory (Figure 3) and apoptosis-inducing effects (Figure 4) of LPP-3 overexpression in ovarian carcinoma cell lines, This suggests that high levels of LPA production can override the effects of LPP expression. We evaluated the role of ATX/lysoPLD in tumorigenesis by increasing expression through transfection or decreasing expression through the use of RNAi in cancer cell lines. ATX/lysoPLD RNAi markedly decreased cell proliferation and survival in model systems (Umezu-Goto et al, 2004). Conversely, overexpression of ATX/lysoPLD can increase colony-forming cell activity and anchorage-independent growth (unpublished data). Together, these findings suggest that

autocrine loops involving LPA play a critical role in the proliferation and survival of ovarian cancer cells.

LPA has been shown to markedly increase cellular migration, which could contribute to tumor aggressiveness or metastasis (Van Leeuwen et al, 2003b; Stahle et al, 2003). We thus assessed whether overexpression of LPP-1 in ovarian cancer cells would alter LPA-induced migration. LPA (10 μM) stimulated migration of control-transfected SKOV3 cells in a trans-well assay. In contrast, LPA failed to induce migration in LPP-1-overexpressing SKOV3 ovarian cancer cells. (data not shown), indicating that the increased extracellular hydrolysis of LPA by LPP-1 is translated into alterations of cellular motility and proliferation, colony formation, and survival. These findings are compatible with the hypothesis that decreases in LPP-1 levels and activity in ovarian cancer cells contribute to the pathophysiology of ovarian cancer through increased local LPA levels and subsequence increases in proliferation, survival and activation of the metastatic cascade. This was also supported by previous study results indicating that LPA increased the activity and amount of a number of proteases involved in invasion and metastasis (Pustilnik et al, 1999; Fishman et al, 2001).

LPP-1 and LPP-3 are transmembrane enzymes whose catalytic surface is on the exterior side of the cell membrane. Thus, overexpression of these enzymes should decrease LPA concentrations in cell culture medium. Compatible with this hypothesis, we demonstrated that cells transfected with LPPs had an increased ability to hydrolyze radiolabeled LPA (Tanyi et al, 2003a). To confirm this ability to hydrolyze extracellular LPA, we determined the concentration of LPA isoforms in supernatants of transfected

and nontransfected cells using a MicroMass QuattroUltima triple quadrapole mass spectrometer (Waters, Milford, MA). Non-transfected SKOV3 cells induced moderate hydrolysis of extracellular LPA: LPA levels decreased to 76% of the original concentration at the end of the first hour. In contrast, transfection of LPP-1 and LPP-3 into SKOV3 cells resulted in decreases in the extracellular concentration of LPA to 52% and 28%, respectively, of the original concentrations after 1 hour.

If expression of LPP-1 and LPP-3 decreases extracellular LPA, then overexpression of LLP-1 and LLP-3 in one population of ovarian cancer cells should also influence the colony-forming ability of non-transfected tumor cells. This might prove very important in gene therapy approaches because LPP-1 or LPP-3 could then induce the death of nontransfected bystander cancer cells. To evaluate this hypothesis, we mixed LPP-1- and LPP-3-transfected cells with an equal number of parental cells (Tanyi et al, 2003a,b). Both types of transfected cells decreased the proliferation of non-transfected tumor cells, a finding compatible with the hypothesis that the effect of LPP-1 or LPP-3 is related to degradation of an extracellular mediator, likely LPA. This also suggests that LPP-mediated gene therapy could result in effective bystander activity.

Overexpression of LPP isoenzymes appears to alter cellular function through degradation of LPA and limitation of LPA-induced signaling. LPA induces changes in cytosolic calcium within seconds of its addition to the medium. In contrast, other signaling events such as phosphorylation of Erk kinases are delayed and prolonged. If the effects of LPPs primarily result from degradation of LPA, LPP overexpression should not

alter changes in cytosolic calcium which occur prior to LPA degradation but in contrast LPP overexpression would be expected to decrease Erk phosphorylation. In contrast, if LPPs alter LPA receptor function directly as has been suggested, then both responses should be inhibited. As indicated in **Figure 5**, there was no difference in the ability of LPA to induce increases in intracellular calcium mobilization in parental or LPP transfected cells. In contrast, transfection of LPP-3 resulted in a decrease in maximal levels of Erk phosphorylation, and further in a more rapid decline in Erk phosphorylation levels to baseline. The differential rate of decline in Erk phosphorylation was compatible with the rate of degradation of LPA by LPP transfected and parental cells (Tanyi et al, 2003a).

The ability of LPPs to decrease cellular proliferation and apoptosis in vitro was reflected by a marked decrease in tumor "take" rates and growth rates in vivo. After subcutaneous injection of SKOV3 cells, tumors developed in 90% of mice compared with only 40% of mice injected with LPP-3-expressing SKOV3 cells. Thus, the take rate of tumors expressing LPP-3 was markedly less than that of the parental line. In addition, the growth rate of the hLPP-3-expressing SKOV3 tumor cells was markedly less than that of the parental cell lines (Tanyi et al, 2003b). At the termination of the study (mandated by tumor size and Association for Assessment and Accreditation of Laboratory Animal Care guidelines), the average weight of SKOV3 parental tumors was four times higher than that of hLPP-3-expressing SKOV3 tumors. When SKOV3 cells were injected into the orthotopic site for ovarian cancer (the peritoneal cavity), LPP-3 expression decreased the take rate to 20% in the injected mice, whereas all parental cell

injections resulted in tumor growth. LPP-3 expression decreased intraperitoneal growth, as assessed by both weigh and abdominal circumference of the animals (Tanyi et al, 2003b).

Thus, LPP-3 resulted in a marked decrease in tumor take rates and a decrease in growth rates in those cases in which tumors formed. However, after a delay in growth, the LPP-3-expressing tumors appeared to enter a more rapid growth phase. Because the hLPP-3 construct was not under selective pressure in vivo, it was possible that the eventual increase in the growth rate was due to loss of LPP-3. It was striking that when the rapidly growing tumors were excised and assessed for the presence of the LPP-3 transgene, LPP-3 levels in the transfected cell lines were markedly decreased. Furthermore, LPP-3 levels were decreased in the parental lines in vivo (Tanyi et al, 2003b). It therefore appears that in vivo growth of SKOV3 cells is associated with downregulated expression of transfected LPP-3. This suggests that a very strong negative selection exists against LPP-3 expression in ovarian cancer cells in vivo.

Together, these studies suggest that an autocrine LPA loop is critical for the proliferation, survival, motility, and in vivo growth of ovarian cancer cells. A similar autocrine loop appears to be present in prostate cancer (Xie et al, 2002) and renal cell carcinoma (Umezu-Goto et al, 2004). Further, the results suggest that this autocrine loop is a potential target for therapy of ovarian and probably other cancer cell lineages.

VII. Targeting LPA function in patients

A wide variety of LPA receptor-selective agonists and antagonists have been investigated (Fischer et al, 1998; Bandoh et al, 1999; Fischer et al, 2001; Okusa et al, 2003; Lynch et al, 2002; Hasegawa et al, 2003; Feng et al, 2003), but a highly effective therapeutic agent with drug-like characteristics that could be used in the treatment of ovarian cancer is not yet available. It is not yet clear whether a pan-LPA receptor inhibitor would be toxic, precluding its utility and thus whether LPA receptor selective analogs would be required (Feng et al, 2003). However, mice lacking specific LPA receptors are viable, albeit with variable adult phenotypes, and LPP-overexpressing mice are also viable (Yang et al, 2002; Contos et al, 2002; Yue et al, 2004). The effects of altering the expression of LPA receptor or LPP on tumorigenesis remain to be determined. The structural basis of LPA receptor selectivity is beginning to be determined through structure-activity relationships and molecular modeling, suggesting that rational drug design could contribute to the creation of new and more-selective receptor agonists and antagonists to serve as therapeutic mediators (Feng et al, 2003; Tigyi et al, 2003; Virag et al, 2003; Sardar et al 2002; Wang et al, 2001).

ATX/lysoPLD is a particularly attractive target for therapy. Its enzyme face is external and should be accessible to small-molecule drugs or inhibitory antibodies. Its role in cancer, both before it was found to be a lysoPLD and through studies of LPA in cancer is well validated. Indeed, RNAi to ATX/lysoPLD potently downregulates cellular proliferation and survival (Umezu-Goto et al, 2004). We are currently exploring preclinical gene therapeutic approaches using LPPs on the basis of the effects of overexpressing these moieties in cells. We have developed a series of adenoviral vectors

with broadly active promoters and with ovarian cancer-specific promoters such as telomerase, survivin, and ceruloplasm (Tanyi et al, 2002; Bao et al, 2002; Lee et al, 2004) and are also exploring liposomal delivery approaches. Preliminary data indicates marked effects on tumor growth supporting the potential of gene therapy targeting the LPA pathway.

VIII. Conclusions

Understanding the physiologic aberrations that originate from genetic alterations of ovarian cancer will lead to the development of new therapeutic approaches for treating the disease. Functional lipidomics is an essential part of developing signal transduction modifiers suited to improvement of patient outcomes. Through its production, metabolism, and receptors, LPA may provide an excellent target for the development of molecular therapeutics, and the early detection of molecular forms of LPA and, other lysolipids and the activities of LPA pathway receptors and enzymes may facilitate both diagnosing and monitoring patients' responses to therapy. The impressive development of knowledge about the pathway that regulates LPA production and the identification of selective LPA receptor agonists suggest that targeting the LPA cascade could be a valuable approach to the management and treatment of this still-deadly disease. Additional studies of the LPA cascade and other phospholipids in ovarian cancer are essential to further elucidate their critical roles in ovarian cancer.

Acknowledgements The authors acknowledge support from DAMD17-03-1-0409, DMAD 17-03-1-0222, and NIH PPG CA64602

References

1. An S, Bleu T, Hallmark OG, and Goetzl EJ **(1998)** Characterization of novel subtype of human G protein-coupled receptor for lysophosphatidic acid. **J Biol Chem** 273, 7906-7910.
2. Andre F, Schartz NE, Movassagh M, Flament C, Pautier P, Morice P, Pomel C, Lhomme C, Escudier B, Le Chevalier T, Tursz T, Amigorena S, Raposo G, Angevin E, and Zitvogel L **(2002)** Malignant effusions and immunogenic tumour-derived exosomes. **Lancet** 360, 295-305.
3. Aoki J, Taira A, Takanezawa Y, Kishi Y, Hama K, Kishimoto T, Mizuno K, Saku K, Taguchi R, and Arai H **(2002)** Serum lysophosphatidic acid is produced through diverse phospholipase pathways. **J Biol Chem** 277, 48737-48744.
4. Bachner D, Ahrans M, Schroder D, Hoffmann A, Lauber J, Batat N, Steinert P, Flohe L, and Gross G **(1998)** Bmp-2 downstream targets in mesenchymal development identified by subtractive cloning from recombinant mesenchymal progenitors (C3H10T1/2). **Dev Dyn** 213, 398-411.
5. Bandoh K, Aoki J, Hosomo H, Kobayashi T, Murakami-Murofushi K, Tsujimoto M, Arai H, and Inoue K **(1999)** Molecular cloning and characterization of a novel human G-protein-coupled receptor, Edg-7, for lysophosphatidic acid. **J Biol Chem** 274, 27776-27785.

6. Bandoh K, Aoki J, Taira A, Tsujimoto M, Arai H, and Inoue K **(2000)** Lysophosphatidic acid (LPA) receptors of the Edg family are differentially activated by LPA species. Structure-activity relationship of cloned LPA receptors. **FEBS Lett** 478, 159-165.
7. Baker DL, Morrison P, Miller B, Riely CA, Tolley B, Westermann AM, Bonfrer JM, Bais E, Moolenaar WH and Tigyi G **(2002)** Plasma lysophosphatidic acid concentration and ovarian cancer. **JAMA** 287:3081-3082.
8. Bao R, Connolly DC, Murphy M, Green J, Weinstein JK, Pisarcik DA, and Hamilton TC **(2002)** Activation of cancer-specific gene expression by the survivin promoter. **J Natl Cancer Inst** 94, 522-528.
9. Contos JJ, Ishii I, Fukushima N, Kingsbury MA, Ye X, Kawamura S, Brown JH, and Chun J **(2002)** Characterization of lpa(2) (Edg4) and lpa(1)/lpa(2) (Edg2/Edg4) lysophosphatidic acid receptor knockout mice: signaling deficits without obvious phenotypic abnormality attributable to lpa(2). **Mol Cell Biol** 22, 6921-6929.
10. Croset M, Brossard N, Polette A, and Lagarde M **(2000)** Characterization of plasma unsaturated lysophosphatidylcholine in human and rat. **Biochem J** 345, 61-67.
11. Eder AM, Sasagawa T, Mao M, Aoki J, and Mills GB **(2000)** Constitutive and lysophosphatidic acid (LPA)-induced LPA production: role of phospholipase D and phospholipase A2. **Clin Cancer Res** 6, 2482-2491.
12. Etienne-Manneville S, and Hall A **(2002)** RhoGTPases in cell biology. **Nature** 420, 629-635.

13. Fang X, Yu S, Lapushin R, Lu Y, Furui T, Pena LZ, Stokor D, Erickson J, Bast RC Jr, and Mills GB **(2000a)** Lysophosphatidic acid prevents apoptosis in fibroblast via G(i) protein-mediated activation of mitogen activated protein kinase. **Biochem J** 352, 135-143.
14. Fang X, Gaudette D, Furui T, Mao M, Esterella V, Eder AM, Pustilnik T, Sasagawa T, Lapushin R, Yu S, Jaffe R, Wiener J, Erickson J, and Mills GB **(2000b)** Lysophospholipid growth factor in the initiation, progression, metastasis, and management of ovarian cancer. **Ann N Y Acad Sci** 905, 188-208.
15. Fang X et al. Mechanism of lysophosphatidic acid induced cytokine production in ovarian cancer cells. **J Biol Chem** (in press).
16. Fang X, Schummer M, Mao M, Yu S, Tabassam FH, Swaby R, Hasegawa Y, Tanyi JL, Lapushin R, Eder A, Jaffe R, Erickson J, and Mills GB **(2002)** Lysophosphatidic acid is a bioactive mediator in ovarian cancer. **Biochim Biophys Acta** 1582, 257-264.
17. Fang X, Yu S, Bast RC, Liu S, Lapushin R, Claret FX, Aggarwal BB, Lu Y, and Mills GB **(2004)** Mechanisms of lysophosphatidic acid-induced cytokine production in ovarian cancer cells. **J Biol Chem** 279, 9653-9661.
18. Feng L, Mills GB, and Prestwich, GD **(2003)** Modulators of lysophosphatidic Acid Signaling **Expert Opinions on Therapeutic Patents** 13, 1619-1634.
19. Fishman DA, Liu Y, Ellerbroek SM, and Stack MS **(2001)** Lysophosphatidic acid promotes matrix metalloproteinase (MMP) activation and MMP-dependent invasion in ovarian cancer cells. **Cancer Res** 61, 3194-3199.

20. Fischer DJ, Liliom K, Guo Z, Nusser N, Virag T, Murakami-Murofushi K, Kobayashi S, Erickson J, Sun G, Miller DD, and Tigyi G **(1998)** Naturally occurring analogs of lysophosphatidic acid elicit different cellular responses through selective activation of multiple receptor subtypes. **Mol Pharmacol** 54, 979-988.
21. Fischer DJ, Nusser N, Virag T, Yokohama K, Wang DA, Baker DL, Bautista D, Parril AL, and Tigyi G **(2001)** Short-chain phosphatidates are subtype selective antagonists of lysophosphatidic acid receptors. **Mol Pharmacol** 60, 776-784.
22. Fourcade O, Le Balle F, Fauvel J, Simon MF, and Chap H. (1998) Regulation of secretory type-II phospholipase A2 and of lysophosphatidic acid synthesis. **Adv Enzyme Regul** 38, 99-107.
23. Fourcade O, Simon MF, Viode C, Rugani N, Leballe F, Ragab A, Fournie B, Sarda L, and Chap H (1995) Secretory phospholipase A2 generates the novel lipid mediator lysophosphatidic acid in membrane microvesicles shed from activated cells. **Cell** 80, 919-27.
24. Fukushima N, Kimura Y, and Chun J **(1998)** A single receptor encoded by vzg-1/LPA1/Edg-2 couples to G proteins and mediates multiple cellular responses to lysophosphatic acid. **Proc Natl Acad Sci U S A** 95, 6151-6156.
25. Furui T, Lapushin R, Mao M, Khan H, Watt SR, Watt MA, Lu Y, Fang X, Tsutsui S, Siddik ZH, Bast RC Jr, and Mills GB **(1999)** Overexpression of Edg-2/vzg-1 induces apoptosis and anoikis in ovarian cancer cells in a lysophosphatidic acid-independent manner. **Clin Cancer Res** 5, 4308-4318.

26. Frisch SM, and Rouslahti E **(1997)** Integrins and anoikis. **Curr Opin Cell Biol** 9, 701-706.

27. Gijsberg R, Aoki J, Arai H, and Bollen M **(2003)** The hydrolysis of lysophospholipids and nucleotides by autotoxin (NPP-2) involves a single catalytic site. **FEBS Lett** 538, 60-64.

28. Ginestra A, Miceli D, Dolo V, Romano FM, and Vittorelli ML **(1999)** Membrane vesicles in ovarian cancer fluids: a new potential marker. **Anticancer Res** 19, 3439-3445.

29. Goetzl EJ, and An S **(1998)** Diversity of cellular receptors and functions for the lysophospholipid growth factor lysophosphatidic acid and sphingosine 1-phosphate. **FASEB J** 12, 1589-1598.

30. Goetzl EJ, Dolezalova H, Kong Y, Hu YL, Jaffe RB, Kalli KR, and Conover CA **(1999)** Distinctive expression and function of the type 4 endothelial differentiation gene-encoded G protein coupled receptor for lysophosphatidic acid in ovarian cancer. **Cancer Res** 59, 5370-5375.

31. Gray JW, Suzuki S, Kuo WL, Polikoff D, Smith McCune K, Berchuck A, Pinkel D, Albertson D, and Mills GB **(2003)** Genome copy number abnormalities in ovarian cancer. **Gynecol Oncol** (**suppl**) S16-S21, 88.

32. Greenlee RT, Hill-Harmon MB, Murray T, and Thun M **(2001)** Cancer statistics 2001. **CA Cancer J Clin** 51, 15-36.

33. Hasegawa Y, Erickson JR, Goddard GJ, Yu S, Liu S, Cheng KW, Eder A, Bandoh K, Aoki J, Jarosz R, Schrier AD, Lynch KR, Mills GB, and Fang X

(2003) Identification of phosphothionate analogue of lysophosphatidic acid (LPA) as a selective agonist of the LPA3 receptor. **J Biol Chem** 278, 11962-11969.

34. Haserueck N, Erl W, Pandey D, Tigyi G, Ohlmann P, Ravanat C, Gachet C, and Siess W **(2003)** The plaque lipid lysophosphatidic acid stimulates platelet activation and platelet-monocyte aggregate formation in whole blood: involvement of P2Y1 and P2Y12 receptors. **Blood** (in press).
35. Hecht JH, Weiner JA, Post SR, and Chun J **(1996)** Ventricular zone gene-1 (vzg-1) encodes a lysophosphatidic acid receptor expressed in neurogenic regions of the developing cerebral cortex. **J Cell Biol** 135, 1071-1083.
36. Hu YL, Tee MK, Goeztl EJ, Auersperg N, Mills GB, Ferrara N, and Jaffe RB **(2001)** Lysophosphatidic acid induction of vascular endothelial growth factor expression in human ovarian cancer cells. **J Natl Cancer Inst** 93, 762-768.
37. Huang MC, Lee HY, Yeh CC, Kong Y, Zaloudek CJ, and Goetzl EJ **(2004)** Induction of protein growth factor systems in the ovaries of transgenic mice overexpressing human type 2 lysophosphatidic acid G protein-coupled receptor (LPA2). **Oncogene** 23, 122-129.
38. Imai A, Furui T, Tamaya T, and Mills GB **(2000)** A gonadotropin-releasing hormone-responsive phosphatase hydrolyses lysophosphatidic acid within the plasma membrane of ovarian cancer cells. **J Clin Endocrinol Metab** 85, 3370-3375.
39. Jalink K, Hordijk PL, and Moolenaar WH **(1994)** Growth factor like effect of lysophosphatidic acid, a novel lipid mediator. **Biochim Biophys Acta** 1198, 185-196.

40. Kudo I, Murakami M, Hara S, and Inoue K **(1993)** Mammalian non-pancreatic phospholipases A2. **Biochim Biophys Acta** 1170, 217–231.

41. Laffargue M, Raynal P, Yart A, Peres C, Wetzker R, Roche S, Payraste B, and Chap H **(1999)** An epidermal growth factor receptor/Gab1 signaling pathway is required for activation of phosphoinositide 3-kinase by lysophosphatidic acid. **J Biol Chem** 274, 32835-32841.

42. Lee CM, Lo HW, Shao RP, Wang SC, Xia W, Gershenson DM, and Hung MC **(2004)** Selective activation of ceruloplasmin promoter in ovarian tumors: potential use for gene therapy. **Cancer Res** 64, 1788-1793.

43. Levine JS, Koh JS, Triaca V, and Lieberthal W **(1997)** Lysophosphatidic acid a novel growth and survival factor for renal proximal tubular cells. **Am J Physiol** 273, 6575-6585.

44. Lynch KR, and Macdonald TL (**2002**) Structure-activity relationships of lysophosphatidic acid analogs. **Biochim Biophys Acta** 1582, 289-294.

45. Luquain C, Singh A, Wang L, Natarajan V, and Morris AJ **(2003)** Role of phospholipase D in agonist-stimulated lysophosphatidic acid synthesis by ovarian cancer cells. **J Lipid Res** 44, 1963-1975.

46. Yang SY, Lee J, Park CG, Kim S, Hong S, Chung HC, Min SK, Han JW, Lee HW and Lee HY, **(2002)** Expression of autotaxin (NPP-2) is closely linked to invasiveness of breast cancer cells. **Clin Exp Metastasis** 19, 603-608.

47. Yang AH, Ishii I, and Chun J **(2002)** In vivo roles of lysophospholipid receptors revealed by gene targeting studies in mice. **Biochim Biophys Acta** 1582, 197-203.

48. Yoon HR, Kim H, and Cho SH **(2003)** Quantitative analysis of acyl-lysophosphatidic acid in plasma using negative ionization tandem mass spectrometry. **J Chromatogr B Analyt Technol Biomed Life Sci** 788, 85-92.
49. Yue J, Yokoyama K, Balazs L, Baker DL, Smalley D, Pilquil C, Brindley DN, and Tigyi G **(2004**) Mice with transgenic overexpression of lipid phosphate phosphatase-1 display multiple organotypic deficits without alteration in circulating lysophosphatidate level. **Cell Signal** 16, 385-399.
50. McIntyre TM, Pontler AV, Silva AR, St Hilaire A, Xu Y, Hinshaw JC, Zimmerman GA, Hana K, Aoki J, Arai H, and Prestwich GD **(2003)** Identification of intracellular receptor for lysophosphatidic acid (LPA): LPA is a transcellular PPARgamma agonist. **Proc Natl Acad Sci U S A** 100, 131-136.
51. Mills GB, Bast RC, and Srivastava S **(2001)** Future for ovarian cancer screening: novel markers for emerging technologies of transcriptional profiling and proteomics. **J Natl Cancer Inst** 93, 1437-1439.
52. Mills GB, May C, McGill M, Roifman C, and Mellors A **(1988)** A putative new growth factor in ascetic fluid from ovarian cancer patients: identification, characterization and mechanism of action. **Cancer Res** 48, 1066-1071.
53. Mills GB, Fang X, Lu Y, Hasegawa Y, Eder A, Tanyi J, Tabassam FH, Mao M, Wang H, Cheng KW, Nakayama Y, Kuo W, Erickson J, Gershenson D, Kohn EC, Jaffe R, Bast RC Jr, and Gray J **(2003)** Specific keynote: Molecular therapeutics in ovarian cancer. **Gynecol Oncol** 88 (Suppl), S88-S92.
54. Mills GB, and Moolenar WH **(2003)** The emerging role of lysophosphatidic acid in cancer. **Nat Rev** 3, 582-591.

55. Moolenaar W, Jalink K, and Van Corven E **(1992)** Lysophosphatidic acid: a bioactive phospholipid with growth factor-like properties. **Rev Physiol Biochem Pharmacol** 119, 7-65.

56. Nakano T, Raines EW, Abraham JA, Klagsburn M, and Ross R **(1994)** Lysophosphatidylcholine upregulates the level of heparin-binding epidermal growth factor-like growth factor mRNA in human monocytes. **Proc Natl Acad Sci U S A** 91, 1069-1073.

57. Nam SW, Clair T, Campo CK, Lee HY, Liotta LA, and Stracke ML **(2000)** Autotaxin (ATX), a potent tumor mitogen, augments invasive and metastatic potential of ras-transformed cells. **Oncogene** 19, 241-247.

58. Nam SW, Clair T, Kim YS, McMarlin A, Schiffmann E, Liotta LA, and Stracke ML **(2001)** Autotaxin (NPP-2), a metastasis-enhancing mitogen, is an angiogenic factor. **Cancer Res** 61, 6938-6944.

59. Nietgen GW, and Durieux ME **(1998)** Intercellular signaling by lysophosphatide, recent developments. **Cell Adhes Commun** 5, 221-235.

60. Noguchi K, Ishii S, and Shimizu T **(2003)** Identification of P2y9/GPR23 as a novel G protein-coupled receptor for lysophosphatidic acid, structurally distant from the Edg family. **J Biol Chem** 278, 25600-25606.

61. Okita M, Gaudette DC, Mills GB, and Holub BJ **(1997)** Elevated levels and altered fatty acid composition of plasma lysophosphatidylcholine (lysoPC) in ovarian cancer patients **Int J Cancer** 71, 31-34.

62. Okusa MD, Ye H, Huang L, Sigismund L, Macdonald T, and Lynch KR **(2003)** Selective blockade of lysophosphatidic acid LPA3 receptors reduces murine renal ischemia-reperfusion injury. **Am J Physiol Renal Physiol** 285, F565-574.

63. Penson RT, Shannon NE, and Seiden MV **(1998)** Ovarian cancer: an update of genetics and therapy. **Compr Ther** 24, 477-487.

64. Pustilnik TB, Esterella V, Wiener J, Mao M, Eder A, Watt MAV, Bast RC, and Mills GB **(1999)** Lysophosphatidic acid induces urokinase secretion in ovarian cancer cells. **Clin Cancer Res** 5, 3704-3710.

65. Qian L, Xu Y, Hasegawa Y, Aoki J, Mills GB, and Prestwich GD (**2003**) Enantioselective responses to a phosphorothioate analogue of lysophosphatidic acid with LPA_3 receptor-selective agonist activity. **J Med Chem** 46, 5575-5578.

66. Roche S, Downward J, Raynal P, and Courtneidge SA **(1998)** A function of phosphatidylinositol 3-kinase (p85–p110) in fibroblast during mitogenesis: requirement for insulin- and lysophosphatidic acid-mediated signal transduction. **Mol Cell Biol** 18, 7119-7129.

67. Sano T, Baker D, Virag T, Wada A, Yatomi Y, Kobayashi I, Igarashi Y, and Tigyi G **(2002)** Multiple mechanisms linked to platelet activation result in lysophosphatidic acid and sphingosine 1-phosphate generation in blood. **J Biol Chem** 277, 21197-21206.

68. Sardar VM, Bautista DL, Fischer DJ, Yokoyama K, Nusser N, Virag T, Wang DA, Baker DL, Tigyi G, and Parrill AL **(2002)** Molecular basis for lysophosphatidic acid receptor antagonist selectivity. **Biochim Biophys Acta** 1582, 309-317.

69. Schmidt A, Wolde M, Thiele C, Fest W, Kratzin H, Rodtelejnikov AV, Witke W, Huttner WB, and Boling HD **(1999)** Endophilin I mediates synaptic vesicle formation by transfer of arachidonate to lysophosphatidic acid. **Nature** 401, 133-141.

70. Schwartz BM, Hong G, Morrison BH, Wu W, Baudhuin LM, Xiao YJ, Mok SC and Xu Y **(2001)** Lysophospholipids increase interleukin-8 expression in ovarian cancer cells. **Gynecol Oncol** 81, 291-300.

71. Sengupta S, Xiao YJ and Xu Y **(2003)** A novel laminin-induced LPA autocrine loop in the migration of ovarian cancer cells. **FASEB J** 17, 1570-1572.

72. Shen Z, Belinson J, Morton RE, Xu Y, and Xu Y **(1998)** Phorbol 12-myristate 13-acetate stimulates lysophosphatidic acid secretion from ovarian and cervical cancer cells but not from breast cancer or leukemia cells. **Gynecol Oncol** 71, 364-368.

73. Shulcze C, Smales C, Rubin LL, and Staddon JM **(1997)** Lysophosphatidic acid increases tight junction permeability in cultured brain endothelial cells. **J Neurochem** 68, 991-1000.

74. Sutphen R, Xu Y, Wilbanks GD, Fiorica J, Grendys EC Jr, LaPolla JP, Arango H, Hoffman MS, Martino M, Wakeley K, Griffin D, Blanco RW, Cantor AB, Xiao YJ, Krischer JP. **(2004)** Lysophospholipids are potential biomarkers of ovarian cancer. **Cancer Epidemiol Biomarkers Prev**. 13:1185-91.

75. Suzuki S, Moore D II, Ginzinger D, Godfrey T, Barclay J, Powell B, Pinkel D, Zaloudek C, Lu K, Mills GB, Berchuck A and Gray JW **(2000)** An approach to

analysis of large-scale correlations between genome changes and clinical endpoints in ovarian cancer **Cancer Res** 60: 5382-5385.

76. Smyth SS, Sciorra VA, Sigal YJ, Wang Z, Xu Y, Prestwich GD, and Morris AJ **(2003)** Lipid phosphate phosphatase 1 (LPP1) regulates lysophosphatidic acid signaling in platelets. **J Biol Chem** 278, 43214-43223.
77. Stahle M, Veit C, Bachfischer U, Schierling K, Skripczynski B, Hall A, Gierschik P, and Giehl K **(2003)** Mechanisms in LPA-induced tumor cell migration: critical role of phosphorylated ERK. **J Cell Sci** 116, 3835-3846.
78. Tanyi J, Lapushin R, Eder A, Auersperg N, Tabassam FH, Roth JA, Gu J, Fang B, Mills GB, and Wolf J (**2002**) Identification of tissue- and cancer-selective promoters for the introduction of genes into human ovarian cancer cells. Gynecol Oncol, 85, 451-458.
79. Tanyi JL, Hasegawa J, Lapushin R, Morris AJ, Wolf JK, Berchuk A, Lu K, Smith DJ, Kalli K, Hartmann LC, McCune K, Fishman D, Broaddus R, Cheng KW, Atkinson EN, Yamal JM, Bast RC Jr, Felix EA, Newman RA, and Mills GB **(2003a)** Role of decreased level of LPP-1 in accumulation of lysophosphatidic acid (LPA) in ovarian cancer. **Clin Cancer Res** 9, 3534-3545.
80. Tanyi J, Morris AJ, Wolf JK, Fang X, Hasegawa J, Lapushin R, Auersperg N, Sigal YJ, Newman RA, Felix AE, Atkinson EN, and Mills GB **(2003b)** The human lipid phosphate phosphatase-3 decreases the growth, survival and tumorigenesis of ovarian cancer cells: validation of the lysophosphatidic acid signaling cascade as a target for therapy in ovarian cancer. **Cancer Res** 63, 1073-1082.

81. Tigyi G, and Parrill AL **(2003)** Molecular mechanisms of lysophosphatidic acid action. **Prog Lipid Res** 42, 498-526.

82. Tokumura A, Majima E, Kariya Y, Tominaga K, Kogure K, Yasuda K, and Fukuzawa K **(2002)** Identification of human plasma lysophospholipase D, a lysophosphatidic acid-producing enzyme, as autotaxin, a multifunctional phosphodiesterase. **J Biol Chem** 277, 39436-39442.

83. Van Nieuw Amerongen GP, Wermeer MA, and van Hinsberg VW **(2000)** Role of RhoA and Rho-kinase in lysophosphatidic acid-induced endothelial barrier dysfunction. **Thromb Vasc Biol** 20, 127-133.

84. Van Leeuwen FN, Olivo C, Grivell S, Griepnans BN, Collard JG, and Moolenaar WH **(2003a)** Rac activation by lysophosphatidic acid LPA1 receptors through the guanine nucleotide exchange factor Tiam 1. **J Biol Chem** 278, 400-406.

85. Van Leeuwen FN, Giepmans BN, van Meeteren LA, and Moolenaar WH **(2003b)** Lysophosphatidic acid: mitogen and motility factor. **Biochem Soc Trans** 31, 1209-1212.

86. Virag T, Elrod DB, Liliom K, Sardar VM, Parrill AL, Yokoyama K, Durgam G, Deng W, Miller DD, and Tigyi G (**2003**) Fatty alcohol phosphates are subtype-selective agonists and antagonists of lysophosphatidic acid receptors. **Mol Pharmacol** 63, 1032-1042.

87. Wang A, and Dennis EA **(1999)** Review: mammalian lysophospholipases. **Biochim Biophys Acta** 1001, 282-285.

88. Xiao Y, Chen Y, Kennedy AW, Belinson J, and Xu Y **(2000)** Evaluation of plasma lysophospholipids for diagnostic significance using electrospray

ionization mass spectrometry (ESI-MS) analyses. **Ann N Y Acad Sci** 905, 242-259.

89. Wang DA, Lorincz Z, Bautista DL, Liliom K, Tigyi G, and Parrill AL **(2001)** A single amino acid determines lysophospholipid specificity of the S1P1 (EDG1) and LPA1 (EDG2) phospholipid growth factor receptors. **J Biol Chem** 276, 49213-49220.
90. Xie Y, Gibbs TC, Mukhin YV, and Meier KE **(2002)** Role for 18:1 lysophosphatidic acid as an autocrine mediator in prostate cancer cells. **J Biol Chem** 277, 32516-32526.
91. Xu Y, Casey G, and Mills GB **(1995a)** Effects of lysophospholipids on signaling in the human Jurkat T cell line. **J Cell Physiol** 163, 441-450.
92. Xu Y, Gaudette D, Boynton JD, Frankel A, Fang XJ, Sharma A, Hurteau J, Casey G, Goodbody A, Mellors A, Holub B, and Mills GB **(1995b)** Characterization of an ovarian cancer activating factor (OCAF) in ascites from ovarian cancer patients. **Clin Cancer Res** 1, 1223-1232.
93. Xu Y, Fang XF, Casey G, and Mills GB **(1995c)** Lysophospholipids activate ovarian and breast cancer cells. **Biochem J** 309, 933-940.
94. Xu Y, Shen Z, Wiper DW, Wu M, Morton RE, Elson P, Kennedy AW, Belinson J, Markman M, and Casey G **(1998)** Lysophosphatidic acid as a potential biomarker for ovarian and other gynecologic cancer. **JAMA** 280, 719-723.
95. Xu Y, and Prestwich GD **(2002)** Synthesis of chiral (α,α-difluoroalkyl)phosphonate analogues of (lyso)phosphatidic acid *via* hydrolytic kinetic resolution. **Org Lett** 4, 4021-4024.

96. Xu Y, Xiao YJ, Zhu K, Baudhuin LM, Lu J, Hong G, Kim KS, Cristina KL, Song L, Williams F, Elson P, Markman M, and Belinson J **(2003)** Unfolding the pathophysiological role of bioactive lysophospholipids. **Curr Drug Targets Immune Endocr Metabol Disord** 3, 23-32.

97. Zhang C, Baker DL, Yasuda S, Makarova N, Balazs L, Johnson LR, Marathe GK, McIntyre TM, Xu Y, Prestwich GD, Byun HS, Bittman R, and Tigyi G **(2004)** Lysophosphatidic acid induces neointima formation through PPAR (gamma) activation. **J Exp Med** 199, 763-774.

98. Zebrowski BK, Liu W, Ramirez K, Akagi MD, Mills GB, and Ellis LM **(1999)** Markedly elevated levels of vascular endothelial growth factor in malignant ascites. **Ann Surg Oncol** 6, 373-378.

99. Umezu-Goto M, Kishi Y, Taira A, Hama K, Dohmae N, Takio K, Yamori T, Mills GB, Inoue K, Aoki J, and Arai H **(2002)** Autotaxin has lysophospholipase D activity leading to tumor cell growth and motility by lysophosphatidic acid production. **J Cell Biol** 158, 227-233.

100. Umezu-Goto M, Tanyi JL, Lahad J, Liu S, Yu S, Lapushin R, Hasegawa Y, Lu Y, Trost R, Bevers T, Jonasch E, Aldape K, Liu J, James RA, Ferguson CG, Xu Y, Prestwich GD, and Mills GB, **(2004)** Lysophosphatidic acid production and action: validated targets in cancer. **J Cell Biochem** (in press).

Figure Legends

Figure 1: LPP-3 overexpression in the stably transfected SKOV3 ovarian carcinoma cell line. (A) Parental SKOV3 cells and (B) LPP-3 enzyme-overexpressing stably transfected SKOV3 cells were fixed and stained with antibodies against LPP-3. Immunoreactive proteins were visualized using a fluorescein-conjugated secondary antibody as described by Smyth et al (2003).

Figure 2: LPP-3 inhibits cell proliferation in stably transfected SKOV3 ovarian cancer cells Different units (U) of cells (1 U = 2 x 10^3) from stably hLPP-3-transfected SKOV3 cells (LPP-3) and SKOV3 parental cells (pc) were seeded onto 96-well plates and cultured for 24 hours in RPMI 1640 medium. Thereafter, the cells were starved for 48 hours. Cell proliferation induced by 0.1% bovine serum albumin containing mixed LPA was evaluated by MTT hydrolysis. The predicted value is the sum of the absorption values when the control and LPP-3-expressing cell lines were seeded separately. The actual value is that obtained when the control cells and hLPP-3-expressing cells were plated together.

Figure 3: Growth-inhibitory effects of LLP-3 overexpression after transfection of hLPP-3 are opposed by ATX/lysoPLD transient transfection. Two days after transfection, the cells were trypsinized, washed twice in PBS, and counted. Cells (3 x 10^4) were seeded into 30-mm six-well plates. Selection medium supplemented with G418 was changed every third day. Two weeks later, colonies were stained with 0.1% Coomassie blue

(Serva, Heidelberg, Germany) in 30% methanol and 10% acetic acid. The mean number of colonies per dish is shown. The data represent the means ± standard error of three samples in three separate experiments.

Figure 4: Transient transfection of hLPP-3 increases apoptosis, but transient transfection with ATX/lysoPLD opposes this effect. Forty-eight hours after transient transfection with LPP and a green fluorescent protein-containing vector, cells were harvested and fixed with 0.25% paraformaldehyde in PBS solution followed by propidium iodide (10 μg/ml) DNA staining. Two-color cytometric analysis was performed, and the percentages of hypodiploid cells as an indication of apoptosis were determined CellQuest software; Becton Dickinson, Franklin Lakes, NJ). The data shown are the means ± standard error of three separate experiments.

Figure 5: LPA induces intracellular calcium mobilization independently of LPP-3 expression. Parental and LPP-3-overexpressing SKOV3 ovarian cancer cell lines were grown to subconfluence, starved in serum-free medium, and harvested for cytoplasmic $[Ca^{2+}]_I$ assay. Cytoplasmic $[Ca^{2+}]_I$ was determined at an excitation wavelength of 331 nm and an emission wavelength of 410 nm using a fluorescence spectrophotometer (F-4000, Hitachi, Tokyo Japan). Approximately 3 x 10^6 cells were used for $[Ca^{2+}]_I$ determination, stirred in a quartz cuvette and kept at 37 ºC as detailed by Hasegawa et al (2003).

Validation of an anti-sphingosine-1-phosphate antibody as a potential therapeutic in reducing growth, invasion, and angiogenesis in multiple tumor lineages

Barbara Visentin,[1,5] John A. Vekich,[1,5] Bradley J. Sibbald,[1] Amy L. Cavalli,[2] Kelli M. Moreno,[2] Rosalia G. Matteo,[2] William A. Garland,[2] Yiling Lu,[3,5] Shuangxing Yu,[3,5] Hassan S. Hall,[3] Vikas Kundra,[4] Gordon B. Mills,[3] and Roger A. Sabbadini[1,2,*]

[1] Department of Biology, San Diego State University, San Diego, California 92182
[2] Lpath, Inc., San Diego, California 92121
[3] Departments of Molecular Therapeutics and Radiation Oncology, M.D. Anderson Cancer Center, Houston, Texas 77054
[4] Departments of Radiology and Experimental Diagnostic Imaging, University of Texas M.D. Anderson Cancer Center, Houston, Texas 77054
[5] These authors contributed equally to this work.
*Correspondence: rsabba@sunstroke.sdsu.edu

Summary

S1P has been proposed to contribute to cancer progression by regulating tumor proliferation, invasion, and angiogenesis. We developed a biospecific monoclonal antibody to S1P to investigate its role in tumorigenesis. The anti-S1P mAb substantially reduced tumor progression and in some cases eliminated measurable tumors in murine xenograft and allograft models. Tumor growth inhibition was attributed to antiangiogenic and antitumorigenic effects of the antibody. The anti-S1P mAb blocked EC migration and resulting capillary formation, inhibited blood vessel formation induced by VEGF and bFGF, and arrested tumor-associated angiogenesis. The anti-S1P mAb also neutralized S1P-induced proliferation, release of proangiogenic cytokines, and the ability of S1P to protect tumor cells from apoptosis in several tumor cell lines, validating S1P as a target for therapy.

Introduction

The identification of signaling components that promote tumor growth represents an important step toward discovering new therapies to reduce the morbidity and mortality of cancer. In this regard, the bioactive lysolipid signaling molecule sphingosine-1-phosphate (S1P) is a little-explored target for antitumor treatment. Evidence suggests that S1P may play a major regulatory role in tumor biology by having direct effects both on tumor-associated angiogenesis and on the tumor cells themselves (Ogretmen and Hannun, 2004).

S1P is a mediator of tumor cell proliferation and protects tumor cells from apoptosis through the activation of survival pathways (Maceyka et al., 2002; Spiegel and Milstien, 2003; Radeff-Huang et al., 2004). The balance between S1P and ceramide/sphingosine (CER/SPH) levels, the upstream precursors of S1P, is believed to provide a rheostat mechanism that determines whether a cell proliferates or undergoes apoptosis (Kwon et al., 2001; Maceyka et al., 2002). The key regulatory enzyme of the rheostat mechanism is sphingosine kinase (SPHK), whose role is to convert the death-promoting sphingolipids (CER/SPH) into the growth-promoting S1P (Bektas et al., 2005). Indeed, SPHK1 transfectants produced tumors when injected into mice (Xia et al., 2000). Furthermore, cells overexpressing SPHK escape contact inhibition, a property commonly exhibited by transformed cells. The reported loss of contact inhibition is consistent with reports suggesting that S1P production correlates with the metastatic potential of selected human cancer cell lines (Takuwa, 2002; Yamaguchi et al., 2003). Additionally, high levels of SPHK1 expression in certain tumor tissues correlate with lower patient survival, thus suggesting a connection between SPHK1 and the aggressiveness of these tumors (Van Brocklyn et al., 2005).

S1P contributes to angiogenesis (Allende and Proia, 2002; Argraves et al., 2004) by stimulating DNA synthesis, chemotactic motility, and capillary tube formation of endothelial cells (ECs)

SIGNIFICANCE

The data suggest that S1P is required for the neovascularizing activity of VEGF and bFGF as well as angiogenesis induced by multiple cytokines. Thus, neutralizing S1P with anti-S1P monoclonal antibodies has the potential to block neovascularization in multiple tumor lineages and is less likely to be bypassed by production of multiple factors than are other approaches to targeting tumor vessels. Further, the data suggest that S1P is required for proliferation and invasion of multiple tumor lineages. Thus, the anti-S1P mAb warrants clinical evaluation to determine its efficacy in reducing cancer progression by neutralizing the proliferative, invasive, and angiogenic effects of S1P. Thus, the anti-S1P mAb may represent a noncancer type-specific therapy for use in humans.

and bone marrow-derived EC precursors, processes that contribute to early blood vessel formation (Lee et al., 1999). The capillary tube formation induced by S1P is comparable to that of the well-known proangiogenic mediators basic fibroblastic growth factor (bFGF) and vascular endothelial growth factor (VEGF) (Lee et al., 1999). Furthermore, S1P elicits synergistic effects with these growth factors to promote development of vascular networks in vivo (Wang et al., 1999). Recently, crosstalk between S1P and other proangiogenic growth factors such as VEGF, EGF, PDGF, bFGF, and IL-8 has been reported (Schwartz et al., 2001; Spiegel and Milstien, 2003). Importantly, bevacizumab (Avastin), a monoclonal antibody that selectively absorbs VEGF from the extracellular fluid (Ferrara, 2004), demonstrated efficacy in limiting the progression of three major types of human cancer. The success of Avastin has stimulated an exploration for similar and more efficacious targets to block tumor-associated angiogenesis. Since S1P is required for the optimal activity of multiple proangiogenic factors, S1P is a promising target for novel therapeutic approaches.

These findings indicate that lowering the interstitial concentration of S1P in tumors could provide a less favorable growth environment for cancer cells by decreasing angiogenesis, while decreasing proliferation and metastatic potential and increasing sensitivity to apoptosis. For this reason, we have produced a monoclonal antibody against S1P (anti-S1P mAb) that is specific to S1P and can bind and neutralize extracellular S1P at its physiologically relevant concentrations. In addition to providing a sensitive probe of the in vivo function of S1P, we hypothesize that this antibody could prove useful as a therapeutic molecular sponge to selectively absorb S1P, thus lowering effective extracellular concentrations of this tumor growth factor.

In this study, we demonstrate that neutralization of S1P results in the reduction of tumor growth through multiple mechanisms including reduced tumor proliferation, cell survival, and metastatic potential concurrently with reduced vessel formation and function. The efficacy of the molecular absorption of S1P in these models suggests that treatment with a humanized version of the murine anti-S1P antibody may provide an innovative and useful approach to cancer therapeutics.

Results

Characteristics of the anti-S1P mAb

Competitive ELISA was used to determine the specificity and sensitivity of the anti-S1P mAb. Figure 1A shows that the anti-S1P mAb was capable of recognizing S1P over the range of S1P concentrations used in the cell-based experiments described below. The anti-S1P mAb was unable to recognize the structurally related bioactive lysolipid lysophosphatidic acid (LPA) or the bioactive precursor to S1P, SPH. Other lysolipids and phospholipids including CER, ceramide-1-phosphate (C1P), and phosphatidyl ethanolamine (PE) were tested without observing appreciable antibody crossreactivity with the exception of the fully saturated form of S1P,DH-S1P, and modest crossreactivity with sphingosylphosphoryl choline (SPC). Neutralizing SPC as well as S1P with the antibody could be advantageous because SPC itself is tumorigenic (Beil et al., 2003). However, extracellular levels of SPC are low, likely due to the presence of autotoxin which has recently been shown to convert SPC to S1P (Clair et al., 2003).

A study utilizing BIAcore demonstrated that the anti-S1P mAb has an affinity for S1P of 99.7 ± 14.4 pM (SD; n = 3). This affinity is over 100-fold higher than the reported affinity of S1P receptors for S1P and much higher than the nonspecific binding sites on serum proteins (Richieri et al., 1993).

To determine the dosing for subsequent in vivo experiments, the in vivo $t_{1/2}$ of the anti-S1P mAb was determined. A competitive ELISA was used to determine the pharmacokinetics of the anti-S1P mAb in blood. Figure 1B shows the time course of the anti-S1P mAb elimination with the dosing of 25 mg/kg. Using a standard two compartment model calculation in WinNonlin, a $t_{1/2}$ (elimination) of 20–26 hr was determined. This $t_{1/2}$ is consistent with the pharmacokinetic profiles of other therapeutic antibodies (Ignoffo, 2004). A simulation of dosing of 25 mg/kg anti-S1P mAb every 2 days demonstrated the concentrations of antibody in the mouse that did not significantly accumulate over time (Figure S1 in the Supplemental Data available with this article online). Intraperitoneal injection of a bolus dose of the anti-S1P mAb revealed that over 95% of the antibody appeared in the bloodstream after 20 min, suggesting that mice could effectively be dosed either intraperitoneally (i.p.) or intravenously (i.v.). We have calculated that the molar ratio of anti-S1P mAb to plasma S1P is ~3:1 at the 25 mg/kg dose injected into a 20 g mouse and assuming a plasma volume of 1.4 ml with a S1P concentration (total) of 2.45 μM.

We conducted a 7 day toxicology study to determine how the antibody was tolerated. Mice were administered (by tail vein injection) 1, 3, 10, 30, or 50 mg/kg of the anti-S1P mAb or vehicle for 7 consecutive days. Figure 1C demonstrates a few selected parameters for the 50 mg/kg and saline dosing. All biochemical and CBC panel analyses were within normal ranges. Histopathological examination revealed no lesions or other pathological changes in the liver, kidney, heart, lungs, skeletal muscle, or spleen of mice in any dosing group. Mice in all treatment groups consumed food and water and socialized similarly to control animals. In one of the xenograft studies described below, mice were administered i.p. 25 mg/kg of the anti-S1P mAb every other day for up to 6 weeks. Even though this was not a bona fide toxicology study, mice in this study exhibited no prominent abnormalities of the major organs upon sacrifice.

Anti-S1P antibodies slow tumor progression in multiple murine models

The ability of the anti-S1P mAb to inhibit cancer progression was tested in three orthotopic models using the breast carcinoma cells MDA MB-231 and MDA MB-468, and the ovarian cancer cell line SKOV3. The anti-S1P mAb was also tested in a subcutaneous xenograft model using lung adenocarcinoma A549 cells.

Figures 2A and 2B show the effects of the systemic anti-S1P mAb treatment on MDA MB-231 multidrug-resistant breast carcinomas orthotopically placed in the mouse mammary fat pads (Figure 2A). The ability of the anti-S1P mAb to reduce tumor volumes was most apparent after the tumors reached approximately 400 mm^3, where tumors of the anti-S1P mAb-treated animals nearly stopped growing. At the end of the study, MDA MB-231 tumor volumes and weights were reduced by 62% and 40% (Figure 2A; *$p < 0.001$), respectively. The anti-S1P mAb was as effective as weekly paclitaxel in decreasing tumor volume in these mice (data not shown).

In a similar orthotopic breast cancer study (Figure S2), MDA MB-468 tumor volumes were reduced by 40% with respect to

A

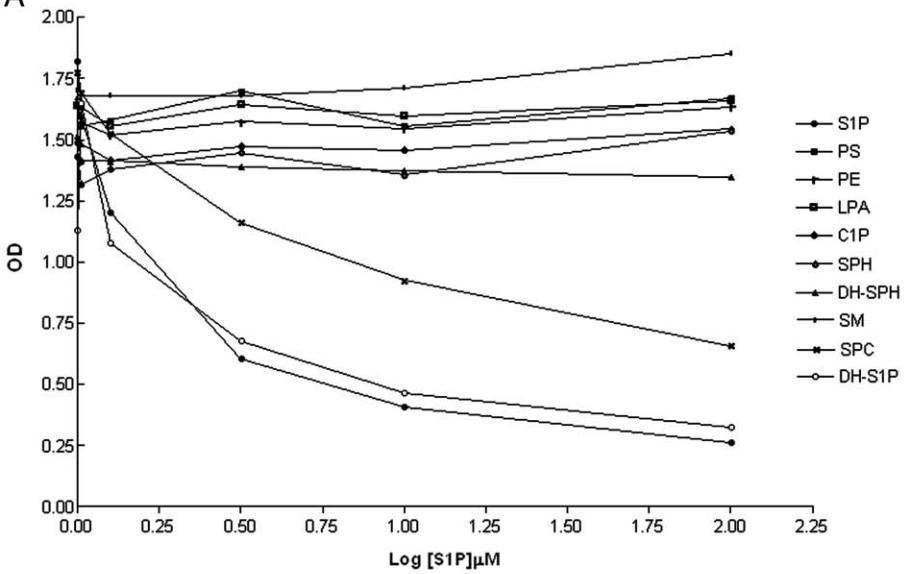

B

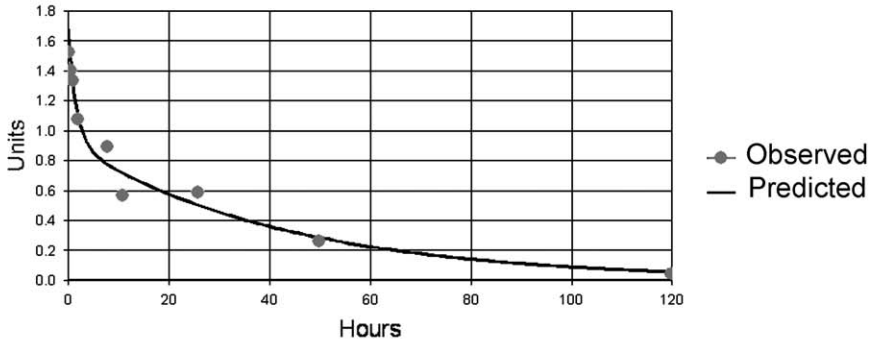

C

Selected Toxicological Results: Mean ± SD.		
Selected Parameters	**Control**	**50mg/kg Anti-S1P mAb**
Weight on day 1 (g)	18.6 ± 0.4	19.1 ± 0.7
Weight on day 7 (g)	19.6 ± 0.6	20.6 ± 0.8
Food Intake (pellets/day)	1.08 ± 0.2	1.11 ± 0.1
WBC (thou/μL)	5.87 ± 2.6	3.43 ± 0.3
RBC (mil/μL)	8.83 ± 0.3	9.34 ± 0.5
Alk Phosphatase (IU/L)	94.5 ± 36.1	58.0 ± 35.4
CK (IU/L)	5154 ± 1765	6906 ± 5023
Albumin (g/dL)	3.3 ± 0.01	3.1 ± 0.3
Total Bilirubin (mg/dL)	≤0.3	≤0.3
BUN (mg/dL)	22.5 ± 2.1	23.7 ± 1.5

Figure 1. Characteristics of the anti-S1P mAb

A: Competitive ELISA demonstrating the ability of the anti-S1P mAb to recognize S1P but not LPA, SPH, or other related lipids.

B: Mice were treated with a bolus dose of 25 mg/kg of the anti-S1P mAb. The elimination $t_{1/2}$ of the antibody, as determined by the concentration of mAb in the serum at designated time points using a competitive ELISA, was calculated to be 22–26 hr.

C: Represented toxicological data from mice (four in each group) dosed i.v. every day with 50 mg/kg anti-S1P mAb. Values are means ± SD and demonstrate the lack of adverse effects elicited by the anti-S1P mAb.

saline controls (*$p < 0.05$). These data confirm the efficacy of the anti-S1P mAb against two human multidrug-resistant orthotopic breast cancer models.

We next evaluated the ability of the anti-S1P mAb to alter the progression of larger and very well-established tumors (Figure 2). In the orthotopic MDA MA-231 model, tumors were allowed to establish until they reached an approximate volume of 700–800 mm^3 (10-fold larger than those used in Figure 2A) before antibody (specific or nonspecific) treatments were commenced. As shown, the anti-S1P mAb-treated animals exhibited significantly reduced tumor volumes. By the 14th day, the final tumor volumes from the anti-S1P mAb-treated mice were reduced by over 58% (*$p < 0.001$) by comparison to tumors from control mice. After 2 weeks, the treatment was ceased in half of the mice receiving the anti-S1P mAb, and the progression of the tumors was evaluated for 12 additional days. After a delay of 3 days, tumors from the mice no longer receiving the anti-S1P mAb once again started to grow compared to tumors from

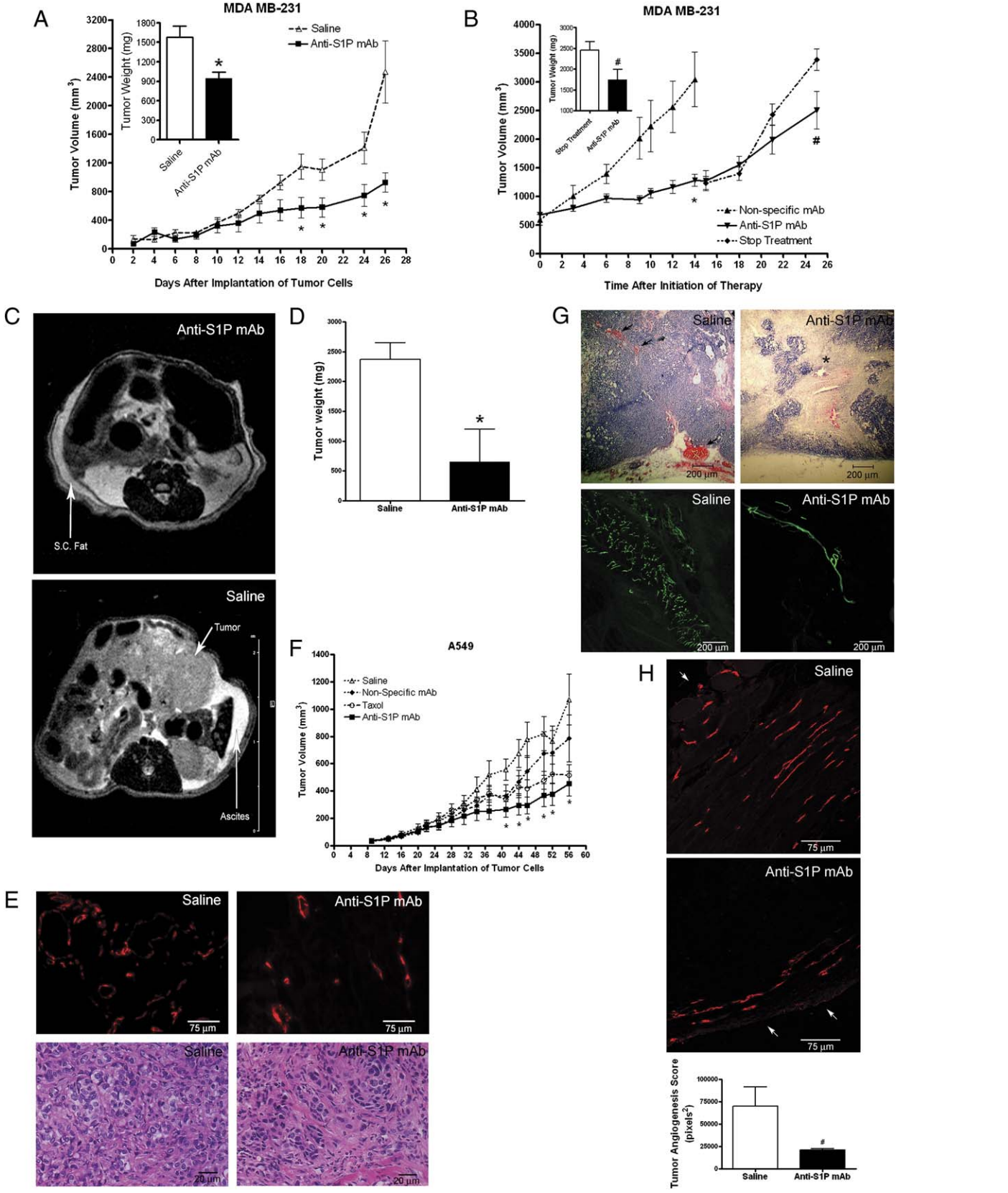

Figure 2. The anti-S1P mAb reduces tumor progression in multiple models

Orthotopically placed MDA MB-231 (**A** and **B**), SKOV3 (**C**–**E**), and s.c. A549 (**F**) tumors were established to volumes of 75–100 mm^3 (**A**, **C**, and **E**) or 700–800 mm^3 (**B**) in nude mice. Treatments consisted of 25 mg/kg of the anti-S1P mAb, 25 mg/kg of nonspecific mAb, saline administrated every 3 days i.p., and 10 mg/kg of Taxol administrated once a week. In all tested xenografts, the anti-S1P mAb reduced significantly final tumor volumes (mm^3) by 62% (**A**), by 58% (**B**), and by 42%

animals maintained on antibody treatment. This lag suggests that the $t_{1/2}$ of 26 hr (see Figure 1B) was likely an underestimate of the physiological half-life of the effective antibody dose.

Figures 2C–2E demonstrates that the anti-S1P mAb was efficacious in inhibiting the progression and, in some cases, eliminating orthotopic SKOV3 tumors in nude mice. MRI analysis revealed that all saline control mice contained large tumors throughout the peritoneal cavity and that these mice had accumulated observable amounts of ascites. Conversely, in two out of the five animals treated with the anti-S1P mAb, no tumors or ascites were detected by MRI analysis or upon postmortem dissection of the peritoneal cavity. Three out of the five animals treated with the anti-S1P mAb had detectable tumors; significantly, these tumors were 68% smaller (750 mg versus 2300 mg) than tumors from the saline-treated animals (*$p < 0.05$). These results compare favorably to a very similar study showing that mouse anti-human VEGF mAb (A.4.6.1) produced a 47% reduction in the size of SKOV3 tumors by MRI (Gossmann et al., 2000). The SKOV3 intraperitoneal model was also assessed for CD31 and H&E staining (Figure 2E). Anti-CD31-labeled sections (upper panel) showed a marked decrease in EC staining of tumor vessels in the anti-S1P mAb-treated mice (representative mouse of five analyzed). Further, H&E staining (lower panel) revealed evidence of increased fibrosis in anti-S1P mAb-treated mice.

Figure 2F shows data using xenografted A549 lung carcinoma cells where the A549 tumor volumes were significantly (*$p < 0.05$) reduced in the antibody-treated animals when compared to animals treated with saline as a control (58% reduction) or animals treated with the nonspecific antibody (42% reduction). The ability of the anti-S1P mAb to retard tumor growth was equivalent to mice treated with Taxol as a positive control. The excised tumors were evaluated for histopathological features in order to determine the full extent of the anti-S1P effects on the viability of remaining tumor cells. H&E-stained sections of the A549 tumors revealed that the tumors from the anti-S1P mAb-treated animals exhibited larger necrotic cores as well as extensive fibrosis (Figure 2G, top panel). Only the tumor peripheries showed appreciable numbers of viable tumor cells. Histological examination indicated that the measurements of gross tumor volumes seen in Figure 2F may have underestimated the actual antitumorigenic effects of the anti-S1P mAb, considering that gross tumor volumes also take into account the volume occupied by dead cells and fibrotic tissue (as also seen in the SKOV3 tumors; Figure 2E). In both control and anti-S1P mAb-treated animals, the vascularization within each tumor was largely confined to the viable regions of the tumor at the periphery rather than in the necrotic core. The extent of tumor-associated angiogenesis was largely mitigated by the anti-S1P mAb treatment, as evidenced by the overall lack of robust microcapillary staining with the isolectin (Figure 2G, bottom panel). In parallel experiments, EC staining with anti-CD31 revealed substantial (3.3-fold) and significant ($^{\#}p < 0.05$) reductions in EC presence in the A549 tumors of anti-S1P mAb-treated animals (Figure 2G), similar to the CD31 staining of the SKOV3 tumors (Figure 2E).

Taken together, these in vivo xenograft models demonstrate that the observed antitumor effects of the anti-S1P mAb were not cancer type specific. Furthermore, the efficacy of the anti-S1P mAb in slowing tumor progression was not dependent on the size of the tumors at the initiation of treatment. Thus, S1P appears to play a major role in tumorigenesis and vascularization in multiple tumor lineages.

The anti-S1P mAb inhibits the release of proangiogenic growth factors in vitro and in vivo

Figure 3A demonstrates that 1 μM S1P induced substantial (2- to 4-fold) increases in IL-6, IL-8, and VEGF release from MDA MB-231 cells in vitro. Figure 3A also demonstrates that treatment of cells with S1P after preincubation with the anti-S1P mAb caused a reduction in the extent of cytokine release to basal levels or less. Secreted VEGF levels were nearly undetectable after antibody treatment, suggesting a potential autocrine stimulatory loop in MDA MB-231. S1P also elicited significant release of IL-8 into the cell-conditioned media from cultured SKOV3 and OVCAR3 cells, and addition of the anti-S1P mAb reduced IL-8 release from all tumor types in a concentration-dependent manner (Figure S3).

Figure 3B demonstrates that serum from MDA MB-231 and SKOV3 xenografted animals displayed substantial levels of the three human cytokines, IL-6, IL-8, and VEGF. Consistent with the in vitro observations of Figure 3A, animals treated with the anti-S1P mAb had significantly reduced (2- to 4-fold) levels of all circulating proangiogenic cytokines tested. Both the in vitro and in vivo data demonstrate that one of the effects of S1P on angiogenesis may be its ability to induce the release of a variety of other proangiogenic compounds.

The anti-S1P mAb blocks the function of proangiogenic growth factors in vivo

Figure 4 compares the proangiogenic activities of S1P, bFGF, or VEGF in vivo when added to the Matrigel plugs. Figure 4A shows that all three growth factors induced substantial evidence of vascularization compared to control animals whose plugs were lacking the growth factors. Notably, S1P was as potent as VEGF and bFGF used at their optimum concentrations in the Matrigel plug assay.

Endogenous S1P has been shown to act synergistically with other growth factors such as bFGF and VEGF in stimulating angiogenesis (Licht et al., 2003). We hypothesized that endogenous S1P from the blood and surrounding tissue may represent an additional proangiogenic factor to supplement plugs containing either VEGF or bFGF. To evaluate these hypotheses, mice implanted with plugs containing VEGF or bFGF received injections of the anti-S1P mAb. Figure 4B shows representative examples of plugs where the neovascularization effects of either

and 58% (**F**). Inset figures represent final tumor weights (mg). **C** shows MRI images of animals bearing SKOV3 tumors, demonstrating substantial absence of tumors and lack of ascites production in animals treated with the anti-S1P mAb. SKOV3 tumor weights were reduced 68% (**D**). For **A** and **C** n = 5 and 5, for **B** n = 10 and 15, and for **F** n = 8 and 9 mice treated with control (saline vehicle or nonspecific mAb, as indicated) and anti-S1P mAb, respectively. CD31 and H&E staining of ECs in the SKOV3 tumors (**E**) show that the anti-S1P mAb reduced tumor-associated angiogenesis and increased fibrosis. H&E staining of A549 tumors (**G**) also demonstrates that the anti-S1P mAb increased central necrosis (asterisk). In A549 tumors, isolectin staining of developed microcapillaries (**G**) and CD31 staining of ECs (**H**) both show that the anti-S1P mAb reduced tumor-associated angiogenesis (white arrows indicate tumor margins). *$p < 0.01$ for the anti-S1P mAb versus saline- or nonspecific mAb-treated mice and $^{\#}p < 0.05$ for the anti-S1P mAb versus the stop treatment. All data are represented as the mean ± SEM.

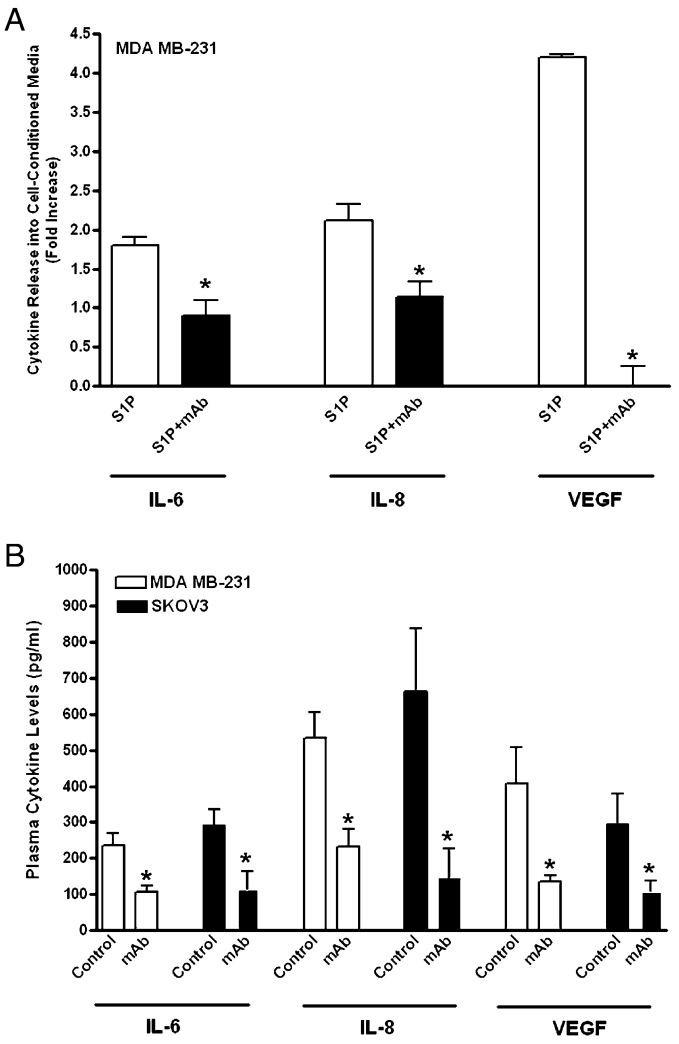

Figure 3. The anti-S1P mAb inhibits the release of proangiogenic growth factors from tumor cells in vitro and in vivo

A: Representative data demonstrating that S1P increases the release of IL-6, IL-8, and VEGF from MDA MB-231 tumor cells into the cell-conditioned media. The release is completely neutralized by incubation with 1 μg/ml of the anti-S1P mAb, in vitro.

B: Serum from MDA MB-231 and SKOV3 xenografted animals reveals the ability of the anti-S1P to reduce plasma levels of IL-6, IL-8, and VEGF. *$p < 0.05$ for the anti-S1P mAb versus saline- or nonspecific mAb-treated mice. All data are represented as the mean ± SEM.

VEGF or bFGF were mitigated by systemic treatment with the anti-S1P mAb. Quantification of data from all mice in the study (Figure 4C) shows that the VEGF- or bFGF-containing plugs from mice treated with 25 mg/kg of the anti-S1P mAb exhibited substantial reductions (82% and 89%, respectively) in blood vessel formation compared to VEGF- or bFGF-containing plugs from mice that did not receive the anti-S1P mAb. In the bFGF-containing plugs, the reduction in vascularization were dose dependent, as 1 mg/kg or 25 mg/kg of anti-S1P mAb reduced the bFGF-dependent vascularization by 32% and 89%, respectively. The ability of the anti-S1P mAb to block these effects suggests that endogenous S1P present in plasma and tissues or produced in the Matrigel plug has the ability to enhance microvascularization induced by other key proangiogenic growth factors.

The anti-S1P mAb inhibits tumor vascularization by directly influencing ECs in vitro and in vivo

Enhanced EC survival is a critical component of angiogenesis. The ability of ECs to survive depends upon circumventing cell death induced by hypoxia as well as chemotherapy. Accordingly, the ability of S1P to protect human umbilical vein endothelial cells (HUVECs) from apoptosis induced by two clinically relevant chemotherapeutic agents, doxorubicin and paclitaxel, was investigated. Figure 5A shows that HUVECs were sensitive to doxorubicin (4.4-fold increase in caspase activity after 24 hr of treatment) and, to a lesser extent, paclitaxel (2.2-fold increase). S1P induced a statistically significant reduction of caspase-3 activation in HUVECs exposed to both of the chemotherapeutic drugs (31% and 33%, respectively, for doxorubicin and paclitaxel). As expected, the addition of the anti-S1P mAb completely abolished the protective, antiapoptotic effects of S1P. Thus, S1P has the ability to protect HUVECs from the toxicity of chemotherapy agents.

The ability of ECs to migrate to the site of a tumor is also an important part of tumor-associated angiogenesis. Figure 5B shows a substantial HUVEC migration response following exposure to S1P. The addition of 1 μg/ml anti-S1P mAb to the media blocked S1P-induced migration of HUVECs by 70%.

In vitro studies have shown that S1P not only stimulates HUVEC chemotactic motility but also induces HUVEC differentiation into multicellular structures suggestive of early blood vessel formation even in the absence of growth factors (Lee et al., 1999). Figure 5C shows that serum-deprived HUVECs placed on growth factor-reduced (GFR) Matrigel failed to form capillary-like structures in the absence of S1P. Upon the addition of 1 μM S1P, HUVECs formed elongated tube-like structures after only 6 hr. The addition of the anti-S1P mAb substantially blocked the formation of the typical capillary-like structures for the duration of the experiment.

A critical stem in tumor vascularization is the infiltration and proliferation of ECs into the tumor as a consequence of the tumor-associated release of angiogenic factors. Accordingly, the ability of S1P to promote the infiltration of ECs into plugs was evaluated in vivo using the Matrigel plug assay (Figure 5D). Animals that were injected with Matrigel containing 5 μM S1P showed a substantial (>6-fold) and significant (*$p < 0.001$) increase in the density of ECs compared to those injected with Matrigel lacking S1P. The administration of anti-S1P mAb completely neutralized the ability of S1P-saturated plugs to promote cell infiltration, as no significant differences were found between antibody-treated animals and controls not treated with S1P.

Considering that the anti-S1P mAb may neutralize S1P's ability to induce the release of proangiogenic growth factors (Figure 3) and to promote de novo blood vessel formation in vivo (see Figures 2E, 2G, and 2H), one may speculate that tumor growth may depend on S1P-mediated angiogenesis, which could account for the ability of the anti-S1P mAb to retard tumor growth (Figures 2A–2D and 2F). The ability of the anti-S1P mAb to block angiogenesis was evaluated in the murine melanoma (B16-F10) allograft model. B16-F10 cells are known to be unresponsive to S1P in terms of proliferation, protection from doxorubicin-induced apoptosis, and promotion of cell migration (see below) (Arikawa et al., 2003; Yamaguchi et al., 2003). Therefore, if one were to observe an effect of the anti-S1P mAb on B16-F10 tumor growth in vivo, one could argue that this would be due to an antiangiogenic effect from the antibody rather than a direct

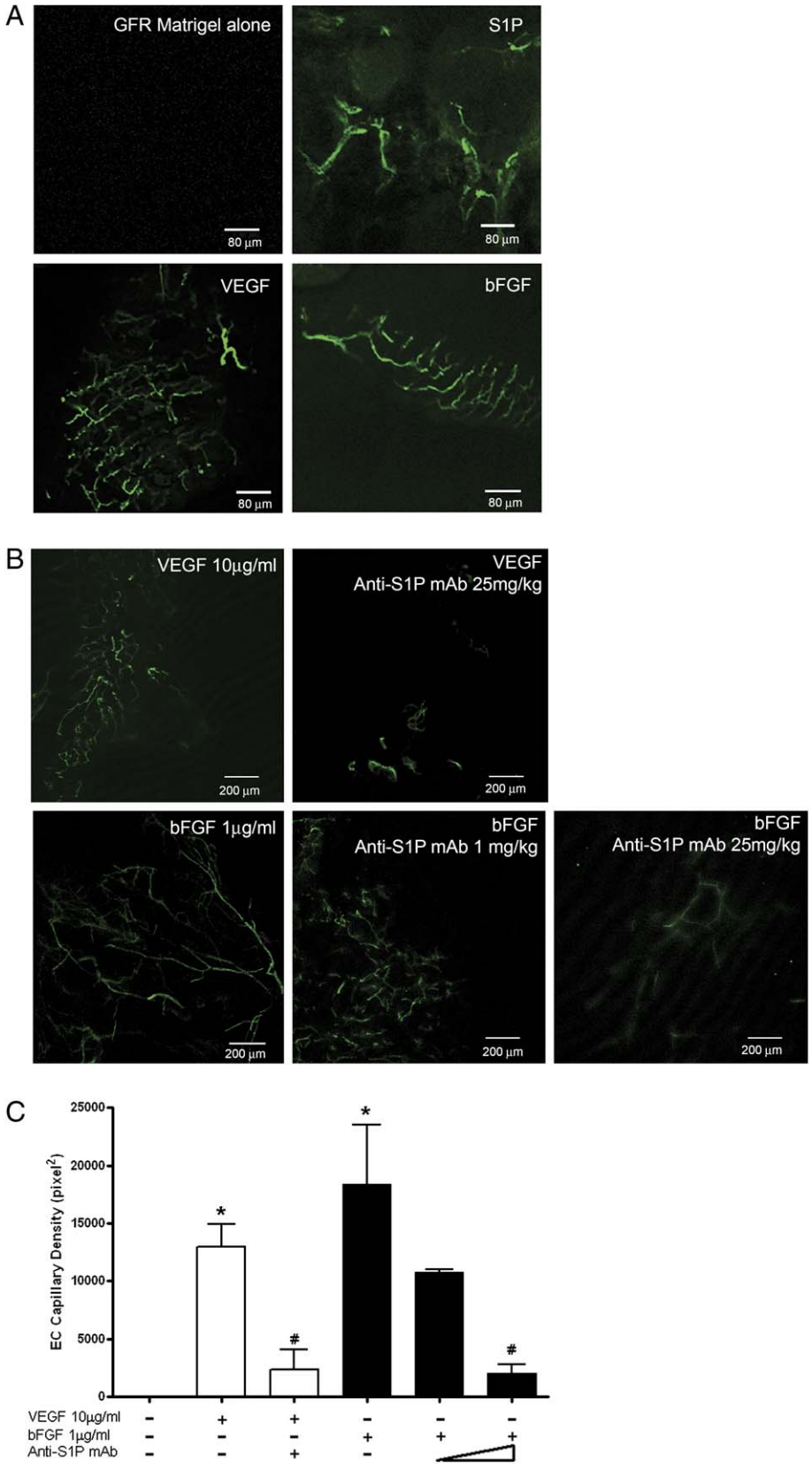

Figure 4. The anti-S1P mAb inhibits the proangiogenic effects of bFGF and VEGF in vivo

GFR Matrigel containing bFGF, VEGF, S1P, or saline was implanted into mice. Selected animals received 1 or 25 mg/kg of the anti-S1P mAb or saline every 48 hr, starting a day prior to matrix implantation. After 10 days, the plugs were harvested and analyzed for microvascular density by FITC-isolectin staining functional vessels. In **A** are representative images (scale 80 μm) showing the neovascularization effects of S1P (5 μM) compared to optimum concentrations of VEGF (10 μg/ml) and bFGF (500 ng/ml) all mixed with the GFR Matrigel prior to implantation. **B** shows representative images (scale 200 μm) of plugs premixed with either VEGF (10 μg/ml) or bFGF (1 μg/ml) prior to implantation in mice that were treated systemically with the anti-S1P mAb. **C** is a quantification of data from all treatment groups (n = 3–4 per group). Animals bearing VEGF and bFGF plugs and in treatment with 25 mg/kg of the anti-S1P mAb showed 82% and 89% reduction in tumor vasculature compared to control groups. $p < 0.001$ for *VEGF or bFGF versus saline (Matrigel alone) and $^{\#}$VEGF or bFGF versus VEGF or bFGF plus anti-S1P mAb. All data are represented as the mean ± SEM.

effect of the antibody on tumor cells. Accordingly, animals were implanted with B16-F10 melanoma cells and treated with the anti-S1P mAb. Figure 5E shows that animals treated with anti-S1P mAb exhibited on average a 57% reduction in tumor volume (and a 53% reduction in tumor weight) compared to control animals treated with saline or the nonspecific antibody. To

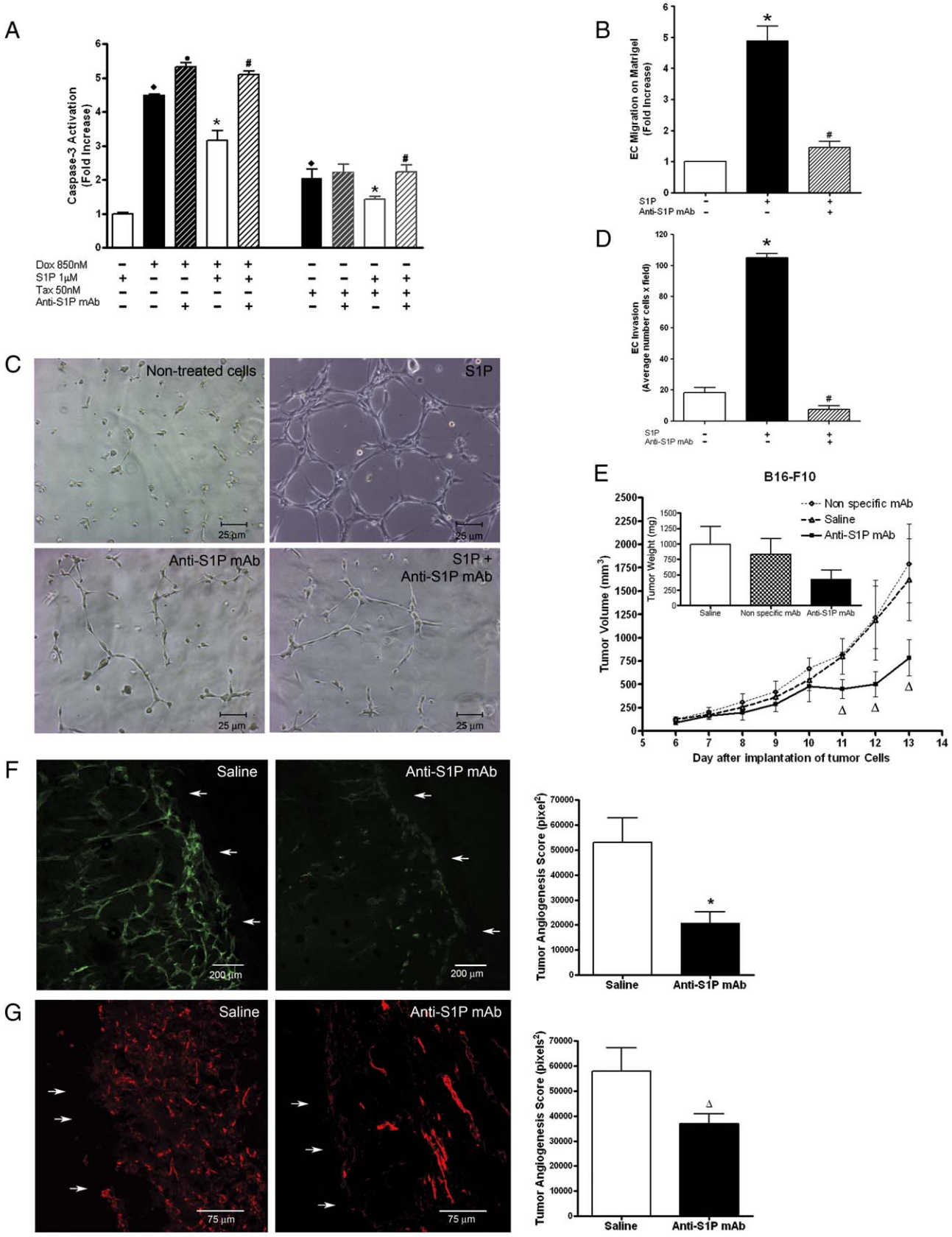

Figure 5. The anti-S1P mAb inhibits vascularization in vitro and in vivo

The anti-S1P mAb (1 μg/ml) reduced HUVEC survival against standard chemotherapeutics, doxorubicin (850 nM; Dox) or Taxol (50 nM; Tax) (**A**), migration (**B**), and the formation of capillary-like structures (**C**) when exposed to 1 μM S1P. Data are expressed as fold increases of caspase-3 activation or migrating cells

assess tumor angiogenesis after treatment with the anti-S1P mAb, we examined excised B16-F10 tumors for isolectin and CD31 staining. As Figure 5F demonstrates, treatment with the anti-S1P mAb resulted in a substantial (61%) and significant (*$p = 0.023$) reduction in tumor microcapillary density after staining with the isolectin. Similarly, Figure 5G shows that the anti-S1P mAb significantly ($^{\triangle}p < 0.05$) reduces the presence of EC density as quantified by anti-CD31 staining.

Anti-S1P mAb's direct effects on tumor cells

A variety of human tumor cell lines as well as the mouse-derived B16-F10 cells were tested in vitro for the ability of S1P to stimulate invasion, proliferation, and protection from cytotoxic agents. The in vitro Matrigel cell invasion assay was employed to evaluate cellular invasion as an indicator of metastatic potential for several cell lines (A549, HT-29, MCF-7, and B16-F10). As shown in Figure 6A, treatment with S1P induced a substantial (6- to 7-fold) increase in invasion through the Matrigel matrix in multiple tumor cell lines when compared to nontreated control cells. Only the B16-F10 cells were not stimulated by S1P in this assay. Addition of anti-S1P mAb reduced the chemotactic migration of S1P-responsive cells into the Matrigel matrix to control levels regardless of the concentration of S1P used. The dose dependence of S1P-induced invasion in the Matrigel matrix was evaluated for the A549 cell line where 1 μg/ml anti-S1P mAb neutralized all of the S1P concentrations tested (Figure S4). These results suggest that this concentration of antibody was sufficient to absorb up to 1 μM S1P as a result of the higher affinity of the antibody for S1P compared to S1P receptors on the A549 cell surfaces.

The ability of the anti-S1P mAb to neutralize S1P-induced stimulation of cellular proliferation in multiple cell lines was also evaluated. Figure 6B demonstrates the ability of S1P to increase [^{3}H]-thymidine incorporation in cells treated with 100 nM S1P when compared to nontreated control cells. The increase in DNA synthesis produced by S1P was completely mitigated by the addition of 1 μg/ml of the anti-S1P mAb.

The ability of the anti-S1P mAb to alter tumor cell survival under the stress of chemotherapeutic agents was accessed by exposing multiple tumor cell lines to 1 μM doxorubicin. Tumor cell death was assessed by the activation of the apoptotic executioner caspase-3 or H/PI (Figure 6C). As shown, S1P was able to decrease doxorubicin-induced caspase-3 activation and/or cell death to control, nontreated levels in almost all of cell types tested. With the exception of the B16-F10 cells, caspase-3 activation was increased by the anti-S1P mAb in the presence of S1P, suggesting that the protective antiapoptotic effect of S1P was eliminated by selective absorption of the lysolipid by the antibody. The ability of the anti-S1P mAb to neutralize the antiapoptotic effects of S1P depended on the dose tested

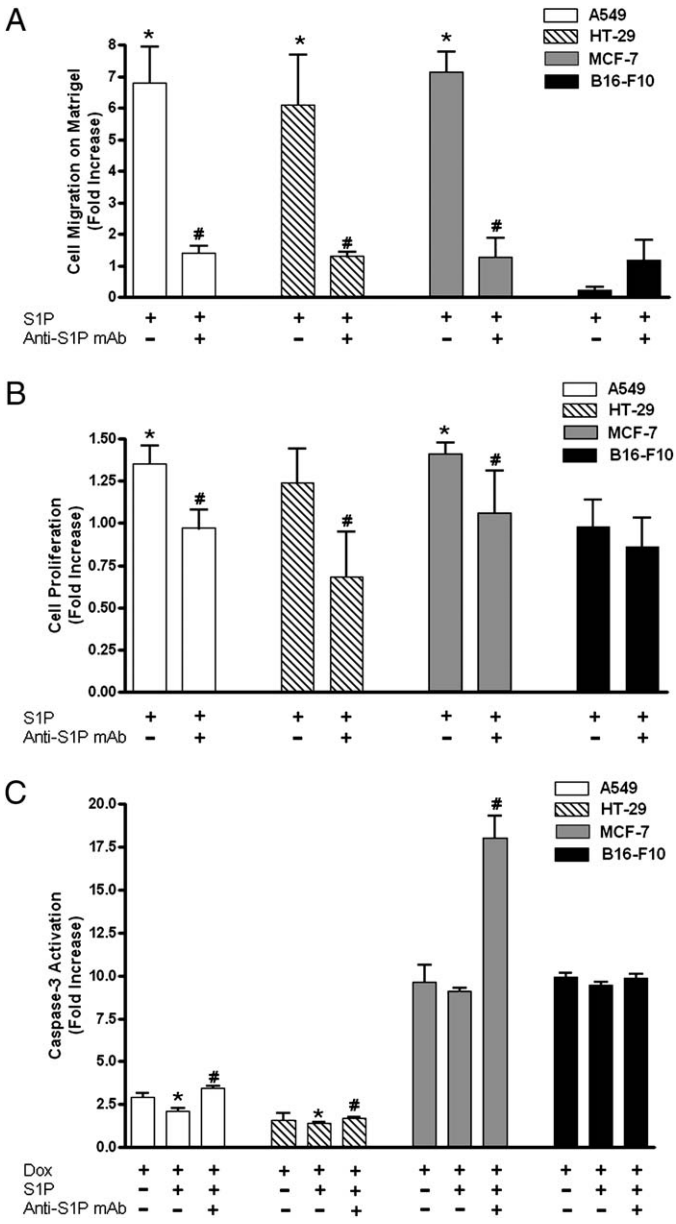

Figure 6. The anti-S1P mAb inhibits many of the protumorigenic processes

The anti-S1P mAb (1 μg/ml) mitigated S1P-induced migration (**A**), tumor cell proliferation (**B**), and cell survival against doxorubicin (Dox) (**C**) in all the tumor cell lines tested with the exception of B16-F10 cells. Data are expressed as fold increases of migrating cells, proliferation, or caspase-3 activation with respect to the control cells, in at least three independent experiments performed in triplicate. $p < 0.01$ for *S1P versus control or S1P + Dox versus Dox, and $^{\#}$S1P or S1P + Dox versus S1P + mAb or S1P + Dox + mAb. All data are represented as the mean ± SEM.

with respect to the control (taken as 1), in at least three independent experiments performed in duplicate. Matrigel plugs containing saline or 5 μM S1P were quantified for EC invasion after 10 days with Masson Trichrome (**D**). Selected animals received the anti-S1P mAb (25 mg/kg, every 48 hr). In the B16-F10 allograft model, mice bearing murine melanoma tumors were treated with saline, 25 mg/kg of the nonspecific mAb, and 25 mg/kg of the anti-S1P mAb (**E**). Data represent tumor volumes and tumor weights (inset) from nine mice per group. Animals treated with the anti-S1P mAb showed 57% and 53% reductions in tumor volumes and weights, respectively. **F** and **G** show representative images and graphic quantification of tumors stained with isolectin or CD31, respectively. White arrows indicate tumor margins. $p < 0.01$ for $^{\blacklozenge}$Dox/Tax versus saline, *S1P + Dox/Tax versus Dox/Tax, and $^{\#}$S1P + Dox/Tax versus S1P + Dox/Tax + mAb; or $p < 0.05$ for $^{\triangle}$anti-S1P mAb versus saline/nonspecific mAb and for *anti-S1P mAb versus control. All data are represented as the mean ± SEM.

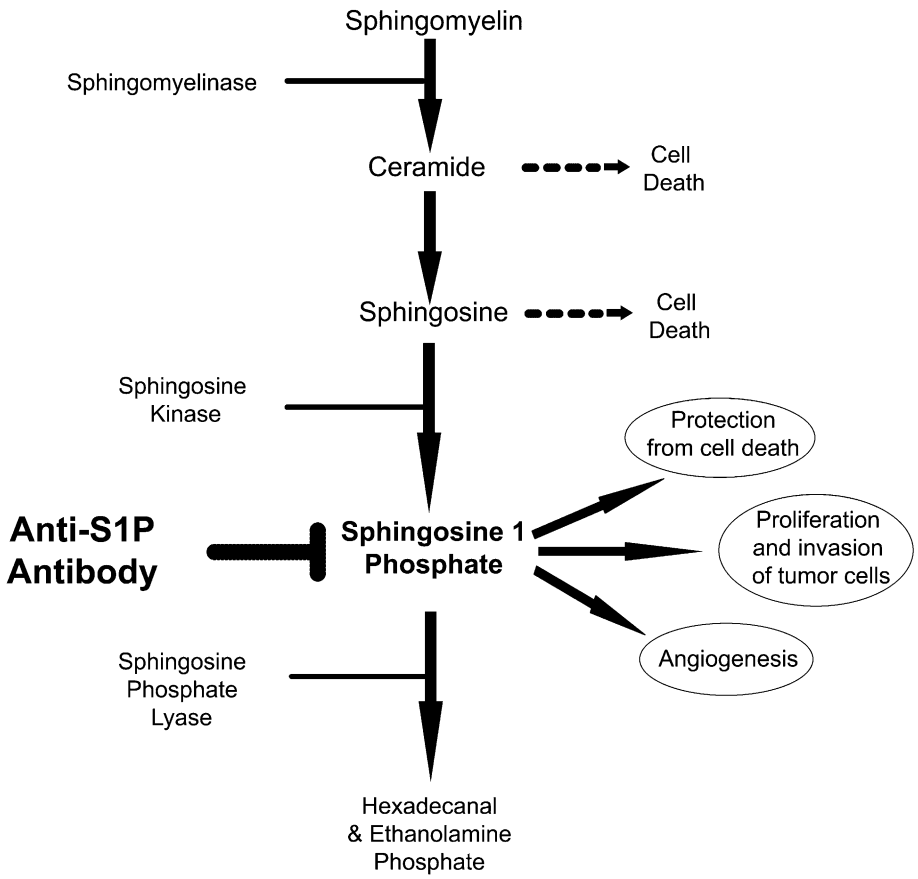

Figure 7. The sphingolipid signaling cascade

The molecular sponge concept proposed here envisions that the antibody will neutralize S1P and prevent its cancer growth-promoting effects. We also propose that the resulting decrease in the effective extracellular concentration of the protective S1P would alter the rheostat in cancer cells in favor of ceramide and sphingosine, two well-known proapoptotic signaling molecules that can be activated in cancer cells by radiation and chemotherapeutic agents. Thus, we propose that a S1P molecular sponge would have multiple mechanisms of antitumor action when used as an adjunct to standard chemotherapy or radiation therapy.

(0.001–1.0 μg/ml) (Figure S5), while the nonspecific antibody completely lacked the ability to reduce S1P-protective affects against doxorubicin-induced cell death (Figure S6).

The ability of the anti-S1P mAb to mitigate the effects of S1P in these in vitro assays suggests that (1) the mAb can effectively neutralize the direct protumorigenic effects of S1P on tumor cells; and (2) the affinity of the mAb for S1P was higher than that of the S1P receptors expressed by the tumor cells. In addition, the lack of responsiveness of the B16-F10 mouse melanoma cells to the direct actions of S1P supports the data in Figure 5F and demonstrates that S1P has a profound angiogenic effect on tumor progression.

Discussion

In this study, we used a highly specific monoclonal antibody against S1P as a molecular sponge to selectively absorb and neutralize this bioactive lipid mediator in in vitro and in vivo models designed to evaluate potential angiogenic and tumorigenic effects of S1P. The anti-S1P mAb blocked both S1P's prosurvival and angiogenic actions and has proved to be a useful tool in evaluating the actions of S1P. The ability of the anti-S1P mAb to significantly retard the progression, and in some cases eliminate established tumors of human and mouse origins, was consistent with the profound proangiogenic effects of S1P. Taken together, these data imply that the anti-S1P mAb warrants evaluation in human clinical trials.

The studies presented here suggest that a principal mechanism of the anti-S1P mAb in blocking tumor progression is through the neutralization of the proangiogenic effects of the blood-borne lipid mediator S1P. The proangiogenic effects of S1P were demonstrated in an in vivo allograft tumor model using the B16-F10 cells, in vivo with the Matrigel plug assay as well as in in vitro studies using HUVECs. Unexpectedly, the anti-S1P mAb also inhibited the release of proangiogenic cytokines in vitro and in vivo, while also potently blocking the function of VEGF and bFGF in vivo. The effects of anti-S1P mAb on VEGF and bFGF suggest either that S1P is permissive for the angiogenic effects of VEGF and bFGF or that S1P acts as the ultimate downstream mediator of VEGF and bFGF. A central and obligatory role for S1P on VEGF action, as suggested by our data, is in agreement with published results showing that VEGF receptors are transactivated by S1P (Igarashi et al., 2003). Regardless, these data confirm and validate the important role of S1P during vascularization and further suggest that the anti-S1P mAb may exhibit a wide spectrum of activity considering the complexity of the tumor environment.

In addition to the antiangiogenic effect of the anti-S1P mAb, the antibody inhibited tumor cell proliferation, invasion, and survival against standard chemotherapeutics. The reduction of tumor vasculature along with the neutralization of the prosurvival effects of S1P on tumor cells suggests that this antibody could be used as a clinical adjunct to conventional chemotherapy by sensitizing tumor cells to anticancer agents and possibly reducing the effective dose of cytotoxic chemotherapeutic agents.

The mechanism for the antitumorigenic effects of the anti-S1P mAb is simple neutralization of S1P by selective absorption. In addition to the endogenous plasma S1P, new sources of S1P in a tumor-bearing mouse could include S1P produced by tumor

cells themselves as a consequence of the upregulation of the SPHK oncogene (French et al., 2003; Johnson et al., 2005) or from stromal and inflammatory cells or other components attracted to the tumor. Regardless of the S1P source, the efficacy of anti-S1P mAb action demonstrates the importance of S1P in tumor aggressiveness and also validates the anti-S1P mAb as a potential therapeutic agent. Figure 7 shows how this strategy may be useful in cancer treatment and compares S1P as a cancer target to other key components of the sphingolipid signaling cascade. This molecular sponge concept is similar to the mechanism of action of Avastin, a humanized mAb directed against the proangiogenic growth factor VEGF (Ferrara, 2004). In contrast to the anti-VEGF strategy of neutralizing tumorigenic growth factors, most anticancer therapeutic antibodies are directed against tumor-selective antigens expressed on the surfaces of transformed cells. These therapeutic antibodies are often conjugated to radionuclides or other toxic payloads and deliver the materials to tumors by molecular targeting. The efficacy of this treatment depends, in part, on the accessibility of the antibodies to the tumor cells. As is the case for Avastin, the anti-S1P mAb used here may not suffer from this limitation in that the target, S1P, is circulating in the same compartment (i.e., blood) as is the antibody. Further, S1P is a small molecule (MW = 379 Da) and a lipid target that is thought to freely cross cell and compartment boundaries more easily than protein targets like VEGF. An additional potential advantage of an anti-S1P mAb is that the target is not species specific, as is the case with cancer targets of protein origin. S1P has the same chemical composition not only across species, but also across phyla, and it is not susceptible to mutation as a means of escaping the therapeutic.

An additional potential benefit of reducing the effective extracellular S1P concentration with the anti-S1P mAb may be in altering the sphingolipid signaling rheostat in favor of CER and SPH as it neutralizes S1P (Figure 7). CER and SPH are well-known proapoptotic intracellular signaling molecules that can be activated in cancer cells by radiation and chemotherapeutic agents (Gouaze et al., 2001; Kolesnick and Fuks, 2003) and can promote apoptosis in tumor cells (Kurinna et al., 2004), in contrast to S1P, which largely serves a protective function for cancer cells. Altering the rheostat in favor of CER would augment the anticipated ability of the anti-S1P mAb to serve as an adjunct to standard chemotherapy or radiation therapy.

Taken together, the selective absorption of S1P by a neutralizing antibody could represent a promising approach to cancer therapy. This approach may have advantages over other targets in the sphingolipid signaling cascade, such as targeting key enzymes of the S1P biosynthetic pathway responsible for S1P production (Figure 7). The pleiotropic effects of S1P in promoting tumor growth, metastasis, and angiogenesis make S1P a robust target for anticancer therapy because S1P has several mechanisms of action. Thus, the anti-S1P mAb could sensitize cancer cells to anticancer agents while exerting antiproliferative, antiangiogenic, and antimetastatic effects. The molecular sponge approach for neutralizing S1P, coupled to the finding that antibodies have favorable pharmacokinetic features and high therapeutic indices, suggest that an anti-S1P antibody may provide therapeutic benefits in treating a broad range of cancers. However, clinical trials with a humanized version of the mouse antibody will be needed to confirm this contention.

Experimental procedures

Materials

S1P, LPA, SPH, and other lipids were obtained from Avanti Polar Lipids or from Calbiochem. S1P, LPA, and SPH were complexed with fatty acid-free BSA (1 mg/ml in PBS) as a solvent-free carrier. Dulbecco's modified Eagle's medium (DMEM) and fetal bovine serum (FBS) were purchased from Invitrogen. EMB-2 medium and Bullet Kit were purchased from Cambrex. GFR and Matrigel basement membrane matrix were purchased from BD BioSciences. Anti-mouse CD31 primary antibody was obtained from Chemicon. Horseradish peroxidase (HRP)-conjugated goat anti-mouse secondary antibody and the rhodamine red-X-conjugated rabbit anti-mouse CD31 was purchased from Jackson Immunoresearch. [^{3}H]-thymidine was from Amersham Bioscience. Recombinant murine VEGF was obtained from PeproTech. Fluorescein Griffonia (Bandeiraea) Simplicifolia Lectin I, Isolectin B-4 was obtained from Vector Laboratories. High-sensitivity ELISA-based kits for cytokine determinations were purchased from R&D Systems. All other reagents were purchased from Sigma. An IgG_1 isotype-matched mouse mAb directed against a plant antigen was obtained from Strategic BioSolutions and used as a control antibody.

Cell culture

Human lung carcinoma (A549), human breast adenocarcinoma (MCF-7), human colorectal adenocarcinoma (HT-29), and the mouse melanoma (B16-F10) cell lines were obtained from American Type Culture Collections. SKOV3, MDA MB-231, and MDA MB-468 cells were obtained from the M.D. Anderson Cancer Center (Houston, TX). Cells were subcultured twice a week as per care instructions and did not exceed passage 10. HUVECs were obtained from Cambrex, maintained in EGM-2 media supplemented with EGM-2 Bullet Kit, and used between passages 3 and 8. Tumor cells were maintained in DMEM supplemented with 10% FBS, unless otherwise stated, at 37°C in a humidified 5% CO_2 atmosphere.

Animals

Four- to six-week-old female C57BL/6 and athymic nude (Ncr Nu/Nu) mice were obtained from Harland. All experiments were performed in accordance with NIH guidelines for the humane use of animals. All protocols involving the use of animals were approved by the IACUC committees at M.D. Anderson Cancer Center and San Diego State University (SDSU; protocol numbers: 04-04-010S, 04-08-020S) and conformed to all regulatory standards (NIH assurance #A3728-01 and USDA Veterinary Permit #7793).

Production of the anti-S1P mAb

For immunization, S1P was conjugated to KLH. Swiss Webster mice were immunized four times over a 2 month period with 50 μg immunogen per injection. Serum samples were collected 2 weeks after the second, third, and fourth immunizations and were screened by ELISA for the presence of anti-S1P antibodies. Spleens from animals that displayed high titers of the antibody were subsequently used to generate hybridomas using standard fusion procedures. The resulting hybridomas were grown to confluency, after which cell supernatants were collected for ELISA analysis to identify positive hybridoma clones. For ascites production, SCID mice were injected i.p. with the positive clonal cells. Monoclonal antibodies were purified by Protein A and were >95% pure by HPLC. Endotoxin levels were <3 EU/mg. The antibody was prepared in 20 mM sodium phosphate with 150 mM sodium chloride (pH 7.2) and stored at −80°C.

ELISA

Ninety-six-well high binding ELISA plates (Costar) were coated overnight with S1P diluted in PBS (137 mM NaCl, 2.68 mM KCl, 10.1 mM Na_2HPO_4, 1.76 mM KH_2PO_4; pH 7.4) containing 1% BSA at 4°C. Plates were washed with PBS and blocked with PBS/BSA for 1 hr. For the primary incubation, 0.1 μg/ml anti-S1P mAb and designated amounts of S1P, LPA, phosphatidyl serine (PS), PE, CER, C1P, SPH, dihydrosphingosine (DH-SPH), sphingomyelin (SM), SPC, and dihydrosphingosine-1-phosphate (DH-S1P) were added to wells of the ELISA plates. Plates were washed and incubated with 100 μl per well of 0.1 μg/ml HRP-conjugated goat anti-mouse secondary for 1 hr at room temperature. Plates were then exposed to tetramethylbenzidine for 1–10 min. The detection reaction was stopped by the addition of an

equal volume of 1 M H_2SO_4. Optical density of the samples was determined by measurement at 450 nm using a Thermo Multiskan EX.

Pharmacokinetic experiments

Eight-week-old C57/Bl mice were dosed with 25 mg/kg of the anti-S1P mAb i.v. and bled at designated time points. A competitive ELISA using a biotin-labeled anti-S1P mAb was used to determine the concentration of antibody remaining in the mouse blood between 20 and 120 min after the bolus dose. A standard two compartment model calculation in WinNonlin was used to determine the $t_{1/2}$ of the antibody. The experiment was repeated three times with three animals per group each time.

Toxicology study

Eight- to twenty-week-old female and male C57/Bl mice were treated with 1, 3, 10, 30, or 50 mg/kg of the anti-S1P mAb or vehicle (sterile saline) for 7 consecutive days by tail vein injection. Solutions for injection were made daily. Twenty-four hours after the final treatment, the mice were sacrificed, blood was collected by venous puncture, and organs were harvested. Whole blood and serum were sent to a veterinary testing laboratory (IDEXX Laboratories) for standard CBC and biochemical panel analysis. Tissue samples were stored in 10% formalin and shipped to a board-certified pathologist (Comparative Biosciences) for evaluation.

Cell proliferation assays

Cells were seeded onto 12-well tissue culture plates (1×10^5 cells per well) in DMEM containing 10% FBS. During treatment, cells were incubated in 10% FBS DMEM, containing either 1 mg/ml BSA in PBS as a vehicle control or various concentrations of S1P. The cells were incubated with or without anti-S1P mAb (1 μg/ml). For S1P plus antibody treatments, S1P was incubated with the anti-S1P mAb (1 μg/ml) in the media for 1 hr prior to addition to the cells. After 24 hr, cells were labeled with 1 μCi/ml [^{3}H]-thymidine and incubated for an additional 6 hr at 37°C. Labeled cells were fixed with ice-cold 10% TCA for 30 min at 4°C and then washed three times with ice-cold 10% TCA to removed unincorporated [^{3}H]-thymidine. The cells were then lysed in 1 N NaOH, and the radioactivity was counted.

Chemoinvasion assay

Cells (5×10^4 cells per well) were suspended in DMEM with 0.1% FBS and added to the top chamber of a BD BioCoat TM Invasion Systems (BD Biosciences). FBS media (10%) were used as a chemoattractant in the bottom chamber. The anti-S1P mAb (0.01, 0.1, or 1 μg/ml), and various concentrations of S1P (100 nM, 500 nM, 1 μM, and 2 μM) were preincubated for 1 hr and then added to cells in the top chamber. Tumor cells were allowed to migrate for 22 hr, at 37°C.

EC migration assays were performed using modified Boyden chambers (Corning Constar) coated with Matrigel matrix (500 μg/ml). Serum-deprived HUVECs (5×10^4 cells per well) were resuspended in minimum media (2% FBS) and added to the top chambers. S1P (100 nM) with or without the anti-S1P mAb (1 μg/ml) was added to the bottom chambers, and HUVECs were allowed to migrate for 6 hr at 37°C. After treatment, migrating cells were stained with HEMA 3 stain set (Fisher Scientific) as per the manufacturer's protocol. Five fields per filter were counted at 40× (Nikon Labophot-2). Data are expressed as the fold increases of cell invasion with respect to the nontreated control cells for at least four independent experiments performed in duplicate.

Cell death assays

Cells ($2–2.5 \times 10^5$ cells per well) were seeded into 6-well plates and allowed to grow to 80% confluence prior to treatment. The cells were then treated with and without 0.5–1 μM doxorubicin (Andriamycin) hydrochloride, 50–500 nM paclitaxel (Taxol), 0.1–1 μM S1P, and 1 μg/ml of the anti-S1P mAb, in 10% FBS DMEM for 48 hr. Treated media were replaced with fresh media after 24 hr. After 48 hr, the cells were washed twice with PBS and lysed in 85 μl of caspase assay buffer (0.5 M HEPES [pH 7.4], 10% Chaps, 0.5 M EDTA). Samples were then centrifuged at 14,000 rpm in an Eppendorf Centrifuge 5417C for 5 min to discard cellular debris. Caspase-3 activity in the supernatant was measured by caspase-3 assay kit (A.G. Scientific) according to the manufacturer's protocol and was standardized by protein determination with a BCA detection kit (Pierce). Caspase-3 activity is expressed as the fold increase in fluorescence signal with respect to nontreated cells. For the MCF-7 cells that do not express caspase-3, Hoechst/propidium iodide staining was used to evaluate cell death. At least three independent experiments were performed with triplicate runs of each condition.

EC tube-like formation assay

The formation of vascular-like structures was assessed on GFR Matrigel matrix. Tissue culture plates were coated with 300 μl of GFR Matrigel diluted 1:2 with serum-free media (0% FBS, 1 mg/ml of BSA). Matrigel was allowed to polymerize for 2 hr at 37°C. Serum-deprived HUVECs (5×10^5 cells per well) were suspended in serum-free media, seeded onto the polymerized matrix, treated with 1 μM of S1P with or without the anti-S1P mAb (1 μg/ml), and incubated at 37°C for 6 hr. Tubular networks were visualized after 6 hr at 10× (Olympus IX-70) and visualized using PhotoShop 6.0.

Cytokine release assay

Cells were starved of serum and treated with the indicated concentrations of S1P and/or the anti-S1P mAb for 22 hr. Cell-conditioned media were collected and assessed for IL-6, IL-8, and VEGF by ELISA as suggested by the manufacturer (R&D Systems). Data are presented as the fold increase with respect to nontreated cells.

In vivo matrigel plug assay

Angiogenesis in vivo was performed using the Matrigel plug assay (Staton et al., 2004). Anesthetized C56BL/6 mice were injected in the left flank with 500 μl of ice-cold GFR Matrigel. The GFR Matrigel was injected either alone (nontreated group) or with 0.5–1 μg/ml bFGF, 10 μg/ml VEGF, or 5 μM S1P. Each treatment group consisted of a minimum of three mice. Subsets of animals were treated with the anti-S1P mAb (either 1 or 25 mg/kg). Dosing of the anti-S1P mAb was initiated 1 day prior to the implantation of Matrigel, and each dose was administrated i.p. every 48 hr for the duration of the experiments. After 10 days, the mice were heparinized (12.8 mg/ml) and then injected i.v. with 200 μl of Fluorescein Griffonia (Bandeiraea) Simplicifolia I, Isolectin B-4 (0.5 mg/ml) 15 min prior to sacrifice. The plugs were excised, immediately embedded in OCT, frozen in isopentane/dry ice, sectioned (80 μm), and then mounted with coverslips using antifade mounting medium (VectaShield, Vector). Microvascular density was visualized using a Leica TCS SP2 inverted confocal microscope. Digital images were acquired using Leica Analysis Software, and the fluorescence was then quantified by PhotoShop 6.0 program and expressed as capillary density (pixel^2) by ImageJ. Selected sections (10 μm) from each treatment were also analyzed by Masson Trichrome staining. ECs infiltrating (and/or proliferating) into the plugs were counted at 100× resolution in five fields from nine sections per plug.

Xenograft and allograft mouse models

Nude mice were implanted s.c. with 2.5×10^6 A549 cells on the left flank, orthotopically into the mammary fat pads with 1×10^7 MDA MB-231 or MDA MB-468 cells or i.p. with 1×10^7 SKOV3 cells. Alternatively, 5×10^5 B16-F10 cells were implanted s.c. into the flanks of C57/Bl6 mice. Tumors were allowed to establish (75–200 or 700–800 mm^3), and then the mice were randomly divided into treatment groups (5 to 20 mice per group). Treatment groups were as follows: vehicle (saline) control, 20 mg/kg isotype-matched nonspecific mAb, 10–20 mg/kg anti-S1P mAb, and 10 mg/kg Taxol diluted to 2 mg/ml with saline. Taxol was administered once per week while all other treatments (antibodies or saline) were administered every 3 days. Measurements of tumor volume were made using calipers every 3 days by two blinded individuals and averaged. The study was terminated when the first mouse reached a maximum average volume as per IACUC standards. At the end of the study, final volumes were taken, and tumors were collected for histology. Histological features and microcapillary density were assessed by H&E, FITC-isolectinB4, and CD31 staining of vessels, respectively. For the FICT-isolectinB4 staining in the B16-F10 model, tumors from saline- and anti-S1P mAb-treated animals were sectioned (80 μm), and four sections from different regions of each tumor were selected and assessed by isolectin staining by confocal microscopy (10×). For the CD31 staining in the B16-F10, SKOV3, and A549 models, tumor sections (10 μm) were blocked overnight and stained with rat anti-mouse CD31 (1:50 dilution) and then with rhodamine red-X-conjugated rabbit anti-rat antibody (1:500 dilution), for 1 hr at room temperature each. Selected sections of each tumor were assessed by the rhodamine-X staining (40×). Each section was expressed as sum of capillary density (pixel^2) in six random fields (two in the tumor center and four in the

periphery), and values of the sections derived from each tumor were averaged. Final tumor vasculature score was expressed as the average of capillary vessel density present in the two treatment groups (n = 3/4 animals per group). Studies were completely blinded to all those collecting and analyzing the data until all data were finalized.

Magnetic resonance imaging

Animals anesthetized with inhaled isoflurane were imaged with a 4.7 T small animal MR (Bruker) axially (TE 60 ms, TR 5700 ms, 4 Nex, field of view 3.5 cm, slice thickness 1 mm with 0.3 mm skip, matrix 256 × 256, in plane resolution 150 μm) and sagittally (TE 80 ms, TR 4500 ms, 4 Nex, field of view 3.5 cm, slice thickness 1 mm with 0.3 mm skip, matrix 256 × 256, in plane resolution 230 μm) using a T2-weighted fast spin echo (FSE) sequence.

Statistical analysis

Data are presented as means ± SEM except for those shown in Figure 1C. Statistical significance of the differences between experimental groups was calculated by one-way ANOVA and an unpaired Student's t test using Graphpad software.

Supplemental data

The Supplemental Data include six supplemental figures and can be found with this article online at http://www.cancercell.org/cgi/content/full/9/3/225/DC1/.

Acknowledgments

This work was supported by NIH R43 CA110298-01 (A.L.C, R.A.S.); PO1 CA64602 and DAMD 17-02-1-0222 (G.B.M.); an International Research Doctorate on Molecular and Cellular Pharmacology (B.V.); and Lpath, Inc. R.A.S., A.L.C., W.A.G., B.J.S, B.V., K.M.M., J.A.V., and G.B.M. have stock options in Lpath, Inc.

Received: August 16, 2005
Revised: December 30, 2005
Accepted: February 23, 2006
Published: March 13, 2006

References

Allende, M.L., and Proia, R.L. (2002). Sphingosine-1-phosphate receptors and the development of the vascular system. Biochim. Biophys. Acta *1582*, 222–227.

Argraves, K.M., Wilkerson, B.A., Argraves, W.S., Fleming, P.A., Obeid, L.M., and Drake, C.J. (2004). Sphingosine-1-phosphate signaling promotes critical migratory events in vasculogenesis. J. Biol. Chem. *279*, 50580–50590.

Arikawa, K., Takuwa, N., Yamaguchi, H., Sugimoto, N., Kitayama, J., Nagawa, H., Takehara, K., and Takuwa, Y. (2003). Ligand-dependent inhibition of B16 melanoma cell migration and invasion via endogenous $S1P_2$ G protein-coupled receptor. Requirement of inhibition of cellular RAC activity. J. Biol. Chem. *278*, 32841–32851.

Beil, M., Micoulet, A., von Wichert, G., Paschke, S., Walther, P., Omary, M.B., Van Veldhoven, P.P., Gern, U., Wolff-Hieber, E., Eggermann, J., et al. (2003). Sphingosylphosphorylcholine regulates keratin network architecture and visco-elastic properties of human cancer cells. Nat. Cell Biol. *5*, 803–811.

Bektas, M., Jolly, P.S., Muller, C., Eberle, J., Spiegel, S., and Geilen, C.C. (2005). Sphingosine kinase activity counteracts ceramide-mediated cell death in human melanoma cells: role of Bcl-2 expression. Oncogene *24*, 178–187.

Clair, T., Aoki, J., Koh, E., Bandle, R.W., Nam, S.W., Ptaszynska, M.M., Mills, G.B., Schiffmann, E., Liotta, L.A., and Stracke, M.L. (2003). Autotaxin hydrolyzes sphingosylphosphorylcholine to produce the regulator of migration, sphingosine-1-phosphate. Cancer Res. *63*, 5446–5453.

Ferrara, N. (2004). Vascular endothelial growth factor as a target for anticancer therapy. Oncologist Suppl. *9*, 2–10.

French, K.J., Schrecengost, R.S., Lee, B.D., Zhuang, Y., Smith, S.N., Eberly, J.L., Yun, J.K., and Smith, C.D. (2003). Discovery and evaluation of inhibitors of human sphingosine kinase. Cancer Res. *63*, 5962–5969.

Gossmann, A., Helbich, T.H., Mesiano, S., Shames, D.M., Wendland, M.F., Roberts, T.P., Ferrara, N., Jaffe, R.B., and Brasch, R.C. (2000). Magnetic resonance imaging in an experimental model of human ovarian cancer demonstrating altered microvascular permeability after inhibition of vascular endothelial growth factor. Am. J. Obstet. Gynecol. *183*, 956–963.

Gouaze, V., Mirault, M.E., Carpentier, S., Salvayre, R., Levade, T., and Andrieu-Abadie, N. (2001). Glutathione peroxidase-1 overexpression prevents ceramide production and partially inhibits apoptosis in doxorubicin-treated human breast carcinoma cells. Mol. Pharmacol. *60*, 488–496.

Igarashi, J., Erwin, P.A., Dantas, A.P., Chen, H., and Michel, T. (2003). VEGF induces $S1P_1$ receptors in endothelial cells: implications for cross-talk between sphingolipid and growth factor receptors. Proc. Natl. Acad. Sci. USA *100*, 10664–10669.

Ignoffo, R. (2004). Overview of bevacizumab: a new cancer therapeutic strategy targeting vascular endothelial growth factor. Am. J. Health Syst. Pharm. *61*, S21–S26.

Johnson, K.R., Johnson, K.Y., Crellin, H.G., Ogretmen, B., Boylan, A.M., Harley, R.A., and Obeid, L.M. (2005). Immunohistochemical distribution of sphingosine kinase 1 in normal and tumor lung tissue. J. Histochem. Cytochem. *59*, 1159–1166.

Kolesnick, R., and Fuks, Z. (2003). Radiation and ceramide-induced apoptosis. Oncogene *22*, 5897–5906.

Kurinna, S.M., Tsao, C.C., Nica, A.F., Jiffar, T., and Ruvolo, P.P. (2004). Ceramide promotes apoptosis in lung cancer-derived A549 cells by a mechanism involving c-Jun NH2-terminal kinase. Cancer Res. *64*, 7852–7856.

Kwon, Y.G., Min, J.K., Kim, K.M., Lee, D.J., Billiar, T.R., and Kim, Y.M. (2001). Sphingosine 1-phosphate protects human umbilical vein endothelial cells from serum-deprived apoptosis by nitric oxide production. J. Biol. Chem. *276*, 10627–10633.

Lee, O.H., Kim, Y.M., Lee, Y.M., Moon, E.J., Lee, D.J., Kim, J.H., Kim, K.W., and Kwon, Y.G. (1999). Sphingosine 1-phosphate induces angiogenesis: its angiogenic action and signaling mechanism in human umbilical endothelial cells. Biochem. Biophys. Res. Commun. *264*, 743–750.

Licht, T., Tsirulnikov, L., Reuveni, H., Yarnitzky, T., and Ben-Sasson, S.A. (2003). Induction of pro-angiogenic signaling by a synthetic peptide derived from the second intracellular loop of S1P3 (EDG3). Blood *102*, 2099–2107.

Maceyka, M., Payne, S.G., Milstien, S., and Spiegel, S. (2002). Sphingosine kinase, sphingosine-1-phosphate, and apoptosis. Biochim. Biophys. Acta *1585*, 193–201.

Ogretmen, B., and Hannun, Y.A. (2004). Biologically active sphingolipids in cancer pathogenesis and treatment. Nat. Rev. Cancer *4*, 604–616.

Radeff-Huang, J., Seasholtz, T.M., Matteo, R.G., and Brown, J.H. (2004). G protein mediated signaling pathways in lysophospholipid induced cell proliferation and survival. J. Cell. Biochem. *92*, 949–966.

Richieri, G.V., Anel, A., and Kleinfeld, A.M. (1993). Interactions of long-chain fatty acids and albumin: determination of free fatty acid levels using the fluorescent probe ADIFAB. Biochemistry *32*, 7574–7580.

Schwartz, B.M., Hong, G., Morrison, B.H., Wu, W., Baudhuin, L.M., Xiao, Y.J., Mok, S.C., and Xu, Y. (2001). Lysophospholipids increase interleukin-8 expression in ovarian cancer cells. Gynecol. Oncol. *81*, 291–300.

Spiegel, S., and Milstien, S. (2003). Sphingosine-1-phosphate: an enigmatic signalling lipid. Nat. Rev. Mol. Cell Biol. *4*, 397–407.

Staton, C.A., Stribbling, S.M., Tazzyman, S., Hughes, R., Brown, N.J., and Lewis, C.E. (2004). Current methods for assaying angiogenesis in vitro and in vivo. Int. J. Exp. Pathol. *85*, 233–248.

Takuwa, Y. (2002). Subtype-specific differential regulation of Rho family G proteins and cell migration by the Edg family sphingosine-1-phosphate receptors. Biochim. Biophys. Acta *1582*, 112–120.

Van Brocklyn, J.R., Jackson, C.A., Pearl, D.K., Kotur, M.S., Snyder, P.J., and Prior, T.W. (2005). Sphingosine kinase-1 expression correlates with poor survival of patients with glioblastoma multiforme: roles of sphingosine kinase isoforms in growth of glioblastoma cell lines. J. Neuropathol. Exp. Neurol. *64*, 695–705.

Wang, F., Van Brocklyn, J.R., Hobson, J.P., Movafagh, S., Zukowska-Grojec, Z., Milstien, S., and Spiegel, S. (1999). Sphingosine 1-phosphate stimulates cell migration through a G(i)-coupled cell surface receptor. Potential involvement in angiogenesis. J. Biol. Chem. *274*, 35343–35350.

Xia, P., Gamble, J.R., Wang, L., Pitson, S.M., Moretti, P.A., Wattenberg, B.W., D'Andrea, R.J., and Vadas, M.A. (2000). An oncogenic role of sphingosine kinase. Curr. Biol. *10*, 1527–1530.

Yamaguchi, H., Kitayama, J., Takuwa, N., Arikawa, K., Inoki, I., Takehara, K., Nagawa, H., and Takuwa, Y. (2003). Sphingosine-1-phosphate receptor subtype-specific positive and negative regulation of Rac and haematogenous metastasis of melanoma cells. Biochem. J. *374*, 715–722.

Carba Analogs of Cyclic Phosphatidic Acid Are Selective Inhibitors of Autotaxin and Cancer Cell Invasion and Metastasis

Daniel L. Baker[1,2,3,5,*], Yuko Fujiwara[4,*], Kathryn R. Pigg[2], Ryoko Tsukahara[4], Susumu Kobayashi[6], Hiromu Murofushi[7], Ayako Uchiyama[8], Kimiko Murakami-Murofushi[8], Eunjin Koh[9], Russell W. Bandle[9], Hoe-Sup Byun[10], Robert Bittman[10], Dominic Fan[11], Mandi Murph[12], Gordon B. Mills[12] and Gabor Tigyi[4,5,†]

Department of Medicine[1] and the Vascular Biology[2] and Genomics & Bioinformatics[3] Centers of Excellence, and Department of Physiology[4], The University of Tennessee Health Science Center, Memphis, TN 38163, The University of Tennessee Cancer Institute[5], Memphis, TN 38163, Department of Medicinal Chemistry[6], Faculty of Pharmaceutical Sciences, Science University of Tokyo, Chiba 278-8510, Japan, Department of Biological Science[7], Faculty of Natural Sciences, Yamaguchi University, Yamaguchi 753-8511, Japan, Department of Biology[8], Faculty of Science, Ochanomizu University, Tokyo 112-8610, Japan, Laboratory of Pathology[9], National Cancer Institute, NIH, Bethesda, MD 20892, Department of Chemistry and Biochemistry[10], Queens College of the City University of New York, Flushing, NY 11367, Departments of Cancer Biology[11] and Molecular Theraputics[12], M.D. Anderson Cancer Center, The University of Texas, Houston, TX 77030

Running Title: Cyclic Phosphatidic Acid Analogs Inhibit Autotaxin

[*]These authors contributed equally

[†]Corresponding Author, Department of Physiology, The University of Tennessee Health Science Center, 894 Union Avenue, Memphis TN, 38163, Tel: (901) 448-4793, Fax: (901) 448-7126, email: gtigyi@utmem.edu

Autotaxin (ATX, nucleotide pyrophosphate/phosphodiesterase-2, NPP2) is an autocrine motility factor initially characterized from melanoma cell conditioned medium. ATX is known to contribute to cancer cell survival, growth, and invasion. Recently ATX was shown to be responsible for the lysophospholipase D activity that generates lysophosphatidic acid (LPA). Production of LPA is sufficient to explain the effects of ATX on tumor cells. Cyclic phosphatidic acid (cPA) is a naturally occurring analog of LPA in which the *sn*-2 hydroxy group forms a 5-membered ring with the *sn*-3 phosphate. Cellular responses to cPA generally oppose those of LPA despite activation of apparently overlapping receptor populations, suggesting that cPA also activates cellular targets distinct from LPA receptors. cPA has previously been shown to inhibit tumor cell invasion *in vitro* and cancer cell metastasis *in vivo*. However, the mechanism governing this effect remains unresolved. Here we show that 3-carba analogs of cPA lack agonist activity at LPA receptors yet are potent inhibitors of ATX activity, LPA production, and A2058 melanoma cell invasion *in vitro* and B16F10 melanoma cell metastasis *in vivo*.

INTRODUCTION

Autotaxin (ATX‡, nucleotide pyrophosphate/ phosphodiesterase-2, NPP2) was initially purified and characterized as an autocrine motility factor from A2058 melanoma cell conditioned medium nearly 15 years ago (1). ATX has been shown to be an important mediator in cancer cell survival, growth, migration, invasion, and metastasis (2-6). Until recently, ATX was merely thought to be a nucleotide phosphodiesterase (7); however, the apparent central role of ATX in cancer cell biology, owing to its numerous effects on tumor cells, was difficult to reconcile with this singular activity. In 2002, two independent groups showed that ATX was responsible for the long elusive lysophospholipase D activity that generates lysophosphatidic acid (LPA) (6,8). It is now fully appreciated that ATX is a multifunctional phosphodiesterase that hydrolyzes both nucleotides and

lysophospholipids (6,8,9) using a single active site (10).

LPA (1-acyl-2-hydroxy-*sn*-glycero-3-phosphate) is the prototype member of a family of phospholipid growth factors. LPA elicits numerous biological effects including the promotion of cellular survival, mitogenesis, angiogenesis, migration, and invasion that are mediated by cell surface G protein-coupled receptors (GPCR) (11-14) and the intracellular nuclear hormone receptor PPARγ (15). LPA has long been associated with ovarian and breast cancers (16) but its production by ATX means it likely plays some role in many, if not all, metastatic cancers (17). ATX expression positively correlates with the metastatic and invasive properties of human tumors including melanoma (1,18), breast cancer (19,20), renal cell cancer (21), lung cancer (22,23), neuroblastoma (24), hepatocellular carcinoma (25), and glioblastoma multiforme (26). Euer *et al.* reported compatible results, using Affymetrix gene chip assays, in which ATX was among the 40 most upregulated genes associated with highly metastatic cancers (27).

Although many questions were answered when the biology associated with ATX was linked to the generation of LPA; one significant question remained, namely how are plasma LPA levels maintained in the low nanomolar range (28)? ATX is a ubiquitous plasma protein (8,29) and its substrate, lysophosphatidylcholine (LPC), is abundantly present in the 100-200 μM range in plasma (30,31), a concentration equivalent to the K_m for ATX hydrolysis (9,32). Therefore, why are plasma LPA levels only ~100 nM? van Meeteren and colleagues recently showed that ATX is subject to inhibition by its hydrolysis products LPA and sphingosine-1-phosphate (32). This phenomenon is the likely explanation for low plasma LPA levels and has provided insight into modulation of ATX activity.

Cyclic phosphatidic acid (1-acyl-*sn*-glycero-2,3-cyclic-phosphate, cPA) was initially isolated as a eukaryotic DNA polymerase inhibitor from slime mold (33). cPA is known to be generated via phospholipase D catalyzed transphosphatidylation of LPC (34) and has been shown to be present in mammalian plasma bound to albumin (35). cPA partially desensitizes LPA responses in NIH3T3 cells and *Xenopus* oocytes, suggesting activation of at least partially overlapping receptor populations (36,37). Despite this apparent overlap in receptor targets, cPA and LPA elicit very distinct cellular effects. Unlike LPA, cPA is antimitogenic (36,38) and prevents cancer cell invasion *in vitro* (39) and metastasis *in vivo* (40,41). Analogs of cPA, in which a methylene (CH_2, carba) group replaces either the *sn*-1 or *sn*-2 oxygen within the cyclic phosphate have been prepared by total chemical synthesis (See Figure 1 for structures) (42) and were shown to be more potent than the parent compounds as inhibitors of tumor cell invasion *in vitro* (41).

Here we show that carba analogs of cPA are (A) poor activators of LPA GPCR, (B) highly potent inhibitors of ATX activity and LPA production and (C) inhibitors of ATX-mediated invasion of melanoma cells *in vitro* and *in vivo*.

EXPERIMENTAL PROCEDURES

Materials

1-Oleoyl-2-hydroxy-*sn*-glycero-3-phosphocholine (LPC 18:1) was obtained from Avanti Polar Lipids (Alabaster, AL). 1-Palmitoleoyl-*sn*-glycero-2,3-cyclic-phosphate (cPA 16:1), 1-oleoyl-*sn*-glycero-2,3-cyclic-phosphate (cPA 18:1) and stabilized cPA analogs, in which the phosphate oxygen was replaced with a methylene group at either the *sn*-2 (2ccPA 16:1 and 2ccPA 18:1) or the *sn*-3 position (3ccPA 16:1 and 3ccPA 18:1) position were synthesized as described previously (42,43). Bis-(*p*-nitrophenyl) phosphate (BPNPP) was purchased from Sigma-Aldrich (St Louis, MO).

Spectrophotometric ATX Inhibition Assay

This assay utilizes BPNPP as substrate and recombinant ATX expressed in conditioned media isolated from transiently transfected HEK293T cells (32). Briefly, 4 x 10^6 HEK293 cells were plated in 10-cm dishes and allowed to attach and recover overnight. On day 2, the cells were transfected with an expression plasmid generated by Clair and

colleagues (9) using Effectene (Qiagen, Valencia, CA) according to the manufacturer's protocol. After 24 h, the transfection medium was replaced with serum-free DMEM and the cells were cultured at 37º C and 5% CO_2 for an additional 30 h (32). Conditioned medium was collected and centrifuged at 3000xg for 10 min at 4º C. The clarified medium was stored at –20º C in aliquots until used. For analysis, 50 µl of conditioned medium was added to 100 µl of BPNPP, 1 mM final concentration in assay buffer (Tris 50 mM, pH 8.0, NaCl 150 mM, KCl 5mM, $CaCl_2$ 1 mM, $MgCl_2$ 1 mM) and 50 µl of test compound in assay buffer containing 1:1 bovine serum albumin in 96-well plates. The absorbance at 405 nm was measured at time zero and after 4 hours of incubation at 37º C using a Molecular Devices $Versa_{max}$ (Sunnyvale, CA) plate reader. Data were normalized to the corresponding vehicle control and the mean and standard deviations of triplicate wells were expressed as percent ATX inhibition.

Purification of Recombinant ATX

ATX-HIS^6 (generously provided by Drs. Mary Stracke and Tim Clair, NCI), lacking the 31 N-terminal amino acids of ATX but containing the honeybee melittin secretion sequence at the N-terminus and a HIS^6 epitope tag at the C-terminus, was purified by Con-A and Ni-NTA chromatography from media conditioned by stably expressing HighFive cells as previously described (9).

Full-length ATX cDNA possessing a C-terminal HA epitope tag (ATX-HA) was generated and cloned into pcDNA3.1(+) (Invitrogen, Carlsbad, CA). ATX-HA was immuno-purified by anti-HA affinity matrix (Covance Research Products, Berkeley, CA) from media conditioned by stably expressing COS-1 cells. A detailed description of ATX-HA production and purification will be published elsewhere (Bandle *et al.*, manuscript in preparation).

Synthesis of fluorescent LPC analog (ADMAN-LPC)

The fluorescent LPC analog 1-(7'-(dimethylamino)-3'-(pentadecanoyl)-1-naphthyl)-2-*O*-methyl-*sn*-glycero-3-phosphocholine (3-acyl-7-dimethylaminonaphthyl-1-LPC (ADMAN-LPC), for structure see Figure 3) was synthesized in 9 steps using 3-pentadecanoyl-7-(dimethylamino)-1-naphthol and (*S*)-3-iodo-2-*O*-methyl-3-(*O*-*tert*-butyldiphenylsilyl)propane-1,2-diol as the key intermediates. After deprotection of the silyl group from the resulting coupling product, a phosphocholine moiety was incorporated at the *sn*-3 position as described previously (44) to generate the desired reagent. A detailed description of the synthesis and characterization of ADMAN-LPC will be published elsewhere (Byun *et al.*, manuscript in preparation). This compound was readily visualized using long wavelength UV for detection following TLC as described below.

Fluorescent ATX Inhibition Assay

This method is a modification of that reported by van Meteeren *et al*. (32). ADMAN-LPC (2.5 µM) was dried and resuspended by sonication in assay buffer (Tris 50 mM, pH 8.0, NaCl 150 mM, KCl 5mM, $CaCl_2$ 1 mM, $MgCl_2$ 1 mM) containing 2 mg/ml BSA in the presence and absence of the individual cPA analogs (1µM). Recombinant ATX-HA (1 µl) was added and the reaction was allowed to proceed for 4 h at 37º C. Lipids were extracted using a modification of the Bligh and Dyer protocol that utilized 3.5 volumes of citrate phosphate buffer (pH 4) prior to chloroform and methanol addition. Extracted lipids were dried *in vacuo*, resuspended in 25 µl of chloroform/ methanol (1:1 v/v), and separated by TLC on silica gel using chloroform/ methanol/ ammonium hydroxide (60:35:8 v/v) (45). Fluorescent LPC and LPA species were visualized by UV trans-illumination.

In vitro Invasion Assay

A-2058 melanoma cells (a generous gift from Drs. Mary Stracke and Tim Clair, NCI) were maintained in DMEM + 10% FBS. Invasion of these cells across a Matrigel™-coated membrane was assessed using Fluoroblok™ 24-well plates (BD Biosciences, Oxford, UK, 8-µm pore size) according to the manufacturer's protocol. Briefly, cell suspensions ($1x10^5$ cells/ml) were prepared by trypsinizing and resuspending A2058 cells in DMEM containing 0.1% BSA. The plate inserts were prepared by rehydrating the

matrix coating with PBS for 2 h at 37°C. The PBS was then carefully removed and 0.75 ml of DMEM/BSA containing chemoattractant (recombinant ATX-HIS^6 + 1 μM LPC 18:1) in the presence or absence of cPA analogs was added to the lower well, and 0.5 ml of the cell suspension in DMEM + 0.1% BSA was added to each upper well insert. Plates were incubated for 22 h at 37°C. Following incubation, the medium was removed from the upper chamber and the entire insert was transferred to a 24-well plate containing 2 μg calcein AM (Molecular Probes, Eugene, OR) in 0.5 ml Hank's balanced salt solution (Na_2HPO_4 0.34 mM, KH_2PO_4 0.44 mM, pH 7.4, NaCl 138 mM, KCl 5.3 mM, $NaHCO_3$ 4.17 mM, D-glucose 5.56 mM). The plates were incubated for 1 h at 37°C and bottom read in a FLEXstation fluorescence plate reader (Molecular Devices, Sunnyvale, CA) at excitation and emission wavelengths of 485 and 530 nm, respectively. Data are presented as the mean and standard deviation of triplicate wells.

LPA GPCR Activation Assay

This method measures real-time, transient increases in intracellular Ca^{2+} to determine LPA GPCR activation. The rat hepatoma (RH7777) cell lines used here stably express $LPA_{1/2/3}$ G protein-coupled receptors and have been used extensively to examine the pharamacology of natural LPA isoforms and synthetic LPA analogs (46-48). CHO cells that stably express LPA_4 were a generous gift of Dr. Takao Shimizu (Tokyo University). The procedure of cell labeling and monitoring has been described previously (49,50). The mean ± standard deviation of triplicate wells was determined. Curves were fitted and EC_{50} values were calculated using KaleidaGraph (Synergy Software, Reading, PA).

In vivo Metastasis Assay

This model utilizes highly metastatic B16F10 melanoma cells to examine the therapeutic effect of metastasis blockers *in vivo*. PBS (vehicle control), 3ccPA 16:1 or 3ccPA 18:1 were delivered as intraperitoneal injections (250 μg/kg, 5 μg per dose) 15 min and 48 h after the intravenous injection of 5 x 10^5 melanoma cells per mouse via the tail vein. Three weeks post inoculation, animals were euthanized, the lungs were washed, fixed with formalin, and the number of lung metastases was determined. No tumors were noted in tissues other than the lungs in animals treated with ccPA.

RESULTS

cPA has previously been shown to block the invasion and migration of cancer cells *in vitro* (39) and *in vivo* (40); however, the cellular targets and mechanisms governing this effect remain unresolved. Recently, van Meeteren *et al.* showed that ATX is subject to feedback inhibition by LPA and S1P, the products of ATX-mediated hydrolysis of lysophosphatidylcholine and sphingosylphosphorylcholine, respectively (32). These results led us to hypothesize that cyclic phosphatidic acids, naturally occurring analogs of LPA, might achieve their anti-invasive effect through inhibition of ATX-mediated LPA production. In this study we examined six cPA analogs (for structures see Figure 1). First, we examined the effect of these analogs on ATX activity by measuring ATX-mediated hydrolysis of BPNPP spectrophotometrically (Figure 2). The cPA analogs containing a natural 2,3-cyclic phosphate group (cPA 16:1 and cPA 18:1) were poor inhibitors of ATX; cPA 16:1 and 18:1 showed maximum ATX inhibitions of 45% and 22% respectively. Conversely, stabilized cPA analogs containing an isosteric replacement of the *sn*-2 oxygen with a methylene group (2ccPA 16:1 and 2ccPA 18:1) were highly effective ATX inhibitors. 2ccPA 16:1 blocked ATX activity by 91% with an IC_{50} of 140 nM, whereas 2ccPA 18:1 blocked ATX activity by 90% with an IC_{50} of 370 nM. Stabilized cPA analogs containing a methylene unit in place of the *sn*-3 oxygen (3ccPA 16:1 and 3ccPA 18:1) were intermediately potent inhibitors of ATX. 3ccPA 18:1 blocked ATX activity by 70% with an IC_{50} of 294 nM, whereas 3ccPA 16:1 blocked 67% of ATX activity with an IC_{50} of 620 nM. All forms of ccPA tested were highly potent inhibitors of ATX with IC_{50} values in the nanomolar range.

Following initial screening using BPNPP as the ATX substrate, we conducted

secondary screening of the effect of 1 μM cPA on ATX-mediated production of LPA via the hydrolysis of a synthetic LPC substrate (Figure 3). The synthetic, fluorescent LPC analog ADMAN-LPC was hydrolyzed to a fluorescent analog of LPA by ATX (compare lanes 1 and 2). Both cPA 16:1 and 18:1 modestly inhibited ATX-mediated LPC hydrolysis (compare lanes 3 and 6 to lane 2). In contrast, 2ccPA 16:1 was a highly effective inhibitor of LPA production (compare lanes 4 and 2). 3ccPA 16:1, 2ccPA 18:1 and 3ccPA 18:1 were intermediate in their ability to inhibit ATX-mediated LPA production (compare lanes 5, 7 and 8 to lane 2). Similar results were obtained when a combination of 1 μM LPC 18:1 and [^{14}C]-LPC 16:0 were used as substrate (data not shown).

We have previously described the pharmacology of natural cPA analogs with respect to activation of the LPA_1, LPA_2 and LPA_3 receptors (51). Here we expand our understanding of this structure-activity relationship to include the 2 and 3ccPA analogs. Knowledge of the activation profiles of these reagents is critically important given the role of LPA GPCR in cancer cell migration associated with LPA produced via ATX (5). Table 1 summarizes the results of the pharmacological screening of the six cPA analogs with respect to activation of all four known LPA GPCR. cPA 16:1 activates $LPA_{1/2/4}$ and cPA 18:1 activates $LPA_{1/2/3/4}$ both with significantly higher (>10-fold) EC_{50} concentrations than LPA 18:1. The 2-carba analog of cPA 16:1 is a weak agonist (24% efficacy as compared to LPA 18:1) of LPA_3, whereas the 2-carba form of cPA 18:1 is a partial agonist of both LPA_1 (54% efficacy) and LPA_3 (46% efficacy). 3-Carba cPA 16:1 and 18:1 activate LPA_2 at EC_{50} concentrations ~1000-fold greater than LPA 18:1. Both compounds failed to elicit significant activation of the other LPA receptors tested.

In order to characterize the functional effect of the cPA analogs on an ATX-mediated cellular endpoint, we examined the invasion of A2058 melanoma cells using a modified Boyden chamber assay in the presence and absence of the test compounds. ATX, LPC, and cPA analogs were all applied in the lower chamber, whereas cells in DMEM + 0.1% BSA were plated in the upper chamber containing a Matrigel-coated membrane bearing 8-μm pores. First, we examined assay conditions to optimize concentrations of recombinant ATX, LPC 18:1, and cPA analogs (Figure 4A). In our hands, purified recombinant ATX-HIS^6 (100-fold dilution), in the presence of 1 μM LPC, elicited a 5.6-fold increase in the number of invading A2058 cells as compared to cells exposed to LPC in the absence of ATX. Exposure of cells to ATX without LPC resulted in a modest (1.6-fold) increase in invading cells. Increasing the dilution of recombinant ATX to 300 fold significantly reduced the number of invading cells in both the presence and absence of LPC, demonstrating the importance of ATX activity in this effect. In this assay, invasion of A2058 cells was significantly attenuated (81%) by co-application of 3 μM 3ccPA 16:1. Next, the effect of all 6 cPA analogs was examined using a 100-fold dilution of recombinant ATX-HIS^6, 1 μM exogenous LPC 18:1, and 3 μM of the test compound (Figure 4B). Treatment with ATX and LPC without the test lipid resulted in an 8-fold increase in the number of A2058 cells that invaded the lower chamber. Co-administration of 3 μM cPA 16:1 or cPA 18:1 with ATX and LPC resulted in modest 40 and 51% decreases in the number of invading cells, respectively. In contrast, co-application of 2ccPA 16:1 or 2ccPA 18:1 with ATX and LPC significantly attenuated the number of invading cells by 84 and 90%, respectively. Co-treatment with 3ccPA 16:1 or 3ccPA 18:1 plus ATX and LPC resulted in intermediate inhibitions of ~68% each.

B16F10 mouse melanoma cells are widely used as a model to assess the therapeutic effect of anti-metastatic compounds *in vivo* (52,53). We used this model to examine the therapeutic effect of 3ccPA 16:1 and 3ccPA 18:1, delivered as intraperitoneal injections (250 μg/kg, 5 μg per dose), 15 min and 48 h after the intravenous injection of 5 x 10^5 cells per mouse. Three weeks post inoculation, animals were euthanized and the number of lung metastases was determined (Figure 5). Treatment with

PBS (vehicle control) resulted in animals bearing 57 ± 14 tumors (range 44-80, n = 6). In contrast, animals treated with 3ccPA 16:1 contained 37 ± 10 tumors (range 27-50, n = 5, $p < 0.01$ ANOVA), whereas those treated with 3ccPA 18:1 had only 24 ± 8 tumors (range 16-40, n = 5, $p < 0.01$, ANOVA). 3ccPA 18:1 was significantly more effective at blocking lung metastasis than was 3ccPA 16:1 ($p < 0.01$).

DISCUSSION

Here we have shown that carba-cPA analogs, in particular the 3ccPA (16:1 and 18:1) forms, are potent inhibitors of ATX that lack the ability to activate LPA GPCR. This ATX inhibitory activity was correlated with the inhibition of LPA-dependent invasion of A2058 cells and the inhibition of pulmonary metastasis of B16 melanoma in mice. This is the second report describing ATX inhibition mediated by naturally occurring lysophospholipids. van Meeteren *et al.* first showed that LPA and S1P blocked ATX activity with nanomolar potency and the mechanism of this inhibition was deemed mixed type as both K_M and V_{max} were both reduced (32). In our hands, LPA and S1P blocked ATX activity with IC_{50} values of 2.2 μM and 280 nM, respectively. These concentrations are significantly higher than the previously reported values (32). The reasons for these differences are not clear but could be the result of differences in the ATX construct, substrate, or assay conditions used. Nonetheless, under identical assay conditions, the 2ccPA 16:1 and 2ccPA 18:1 analogs were 15- and 6-fold more potent inhibitors of ATX than was LPA. We have previously shown that cPA 18:1 is stable in neutral buffered aqueous medium for up to 24h using LC-MS (51). The modest drop in cPA concentration over this time frame was not accompanied by a significant increase in LPA levels (51). This suggests that cPA analogs may be more effective ATX inhibitors *in vivo* due to their increased stability. Detailed analysis of the pharmacokinetics of cPA analogs is currently ongoing. The findings that 3ccPA analogs show a significantly lower IC_{50} for ATX inhibition than does LPA, and that cPA analogs are stable under assay conditions ((51) and Figure 3, lane 1), suggest that ccPA analogs are themselves novel, potent ATX inhibitors with promising *in vivo* activity.

Previous reports on the anti-invasive properties of cPA implicated increased cellular cAMP levels (39,54) and subsequent RhoA inactivation (39) in this effect. This implicated cell surface GPCR activation in the response. We have previously shown that natural cPA isoforms are poor activators of the LPA_1, LPA_2, and LPA_3 receptors (51). In the course of this study, we have shown that natural cPA analogs are also poor activators of LPA_4 (Table 1), a recently identified LPA GPCR that shares sequence homology with the purinergic receptor family (50). We have now extended the pharmacological knowledge of this structural family to include the 16:1 and 18:1 forms of 2ccPA and 3ccPA. The 2ccPA and 3ccPA 16:1 analogs and 3ccPA 18:1 were all poor activators of $LPA_{1/2/3/4}$ (Table 1). On the other hand, 2ccPA 18:1 was a partial agonist of $LPA_{1/2/3/4}$ (Table 1). It is worth noting that the invasion of PC3 prostate cancer cells was blocked by 2ccPA 16:1, 3ccPA 16:1, and 3ccPA 18:1 but was unaffected by 2ccPA 18:1 (data not shown). This lack of effect by 2ccPA 18:1 in PC3 cells is in stark contrast to the significant inhibition of A2058 cell invasion (Figure 4B). 2ccPA 18:1 is the only ccPA analog that possesses significant agonist activity, albeit as a significantly less potent, partial agonist as compared with LPA 18:1 at LPA_1 (Table 1). PC3 cells express significant levels of LPA_1 (~125 copies/ GAPDH x 10^3), whereas A2058 express 10-fold lower levels (~12 copies/ GAPDH x 10^3) (5). These results suggest that GPCR activation is not likely to explain the anti-invasive properties of cPA analogs. Likewise, the cPA analogs tested did not antagonize LPA-mediated GPCR activation (data not shown). Therefore, cPA does not seem to inhibit invasion via direct LPA GPCR effects. These data also show the importance of designing/ identifying ATX inhibitors that do not activate LPA GPCR.

Two previous studies reported the anti-metastatic potential of cPA *in vivo* using

injected B16 melanoma cells (41) and azoxymethane-induced intestinal tumors (40) in mice. In the first study cPA analogs were delivered as single doses intravenously (4 or 8 μg) mixed with $1x10^6$ tumor cells (41). This protocol resulted in an 88% decrease in B16 derived lung metastases at the highest concentration (41). The second study delivered cPA analogs (3 and 6 mg/kg) subcutaneously in olive oil every other day for 30 weeks (40). cPA blocked bombesin-enhanced metastasis by up to 95% in this model (40). Here we show that 3ccPA 16:1 and 3ccPA 18:1 were able to block B16F10 tumor cell-derived lung metastasis by 35 and 57%, respectively, following only two 5 μg doses (250 µg/kg) 15 min and 48 h after inoculation. This decrease in metastatic potential resulted from intraperitoneal injections applied during the earliest phase of the metastatic process, suggesting that ccPA acted by inhibiting the formation of metastatic foci. We are currently working to optimize delivery and dosing of these reagents in an effort to maximize the anti-metastatic effect.

In this study we have described a novel role of cPA analogs as potent, natural ATX inhibitors. These are the most potent inhibitors we have identified to date. The 3ccPA 16:1 and 3ccPA 18:1 analogs are attractive lead compounds since they block ATX at nanomolar levels, yet they fail to significantly activate LPA GPCR at these concentrations. These compounds blocked cancer cell invasion *in vitro* and tumor cell metastasis *in vivo* without evidence of toxicity. Our results further validate ATX activity as a viable target of future cancer chemotherapeutics. These results also show proof of principle that compounds can be designed that selectively block LPA effects, via inhibition of LPA production, without the need for specific subtype selective LPA receptor antagonists.

ACKNOWLEDGEMENTS

This research was supported, in part, by a University of Tennessee Cancer Institute Pilot Grant (DLB); the Intramural Research Program of the NIH, National Cancer Institute, Center for Cancer Research (RWB); PO1 CA64602 and DAMD 17-03-1-0222 (GBM); and USPHS grants CA92160, HL61469 and HL79004 (GT).

REFERENCES

1. Stracke, M. L., Krutzsch, H. C., Unsworth, E. J., Arestad, A., Cioce, V., Schiffmann, E., and Liotta, L. A. (1992) *J Biol Chem* **267**, 2524-2529
2. Murata, J., Lee, H. Y., Clair, T., Krutzsch, H. C., Arestad, A. A., Sobel, M. E., Liotta, L. A., and Stracke, M. L. (1994) *J Biol Chem* **269**, 30479-30484
3. Nam, S. W., Clair, T., Campo, C. K., Lee, H. Y., Liotta, L. A., and Stracke, M. L. (2000) *Oncogene* **19**, 241-247
4. Nam, S. W., Clair, T., Kim, Y. S., McMarlin, A., Schiffmann, E., Liotta, L. A., and Stracke, M. L. (2001) *Cancer Res* **61**, 6938-6944
5. Hama, K., Aoki, J., Fukaya, M., Kishi, Y., Sakai, T., Suzuki, R., Ohta, H., Yamori, T., Watanabe, M., Chun, J., and Arai, H. (2004) *J Biol Chem* **279**, 17634-17639
6. Umezu-Goto, M., Kishi, Y., Taira, A., Hama, K., Dohmae, N., Takio, K., Yamori, T., Mills, G. B., Inoue, K., Aoki, J., and Arai, H. (2002) *J Cell Biol* **158**, 227-233
7. Clair, T., Lee, H. Y., Liotta, L. A., and Stracke, M. L. (1997) *J Biol Chem* **272**, 996-1001
8. Tokumura, A., Majima, E., Kariya, Y., Tominaga, K., Kogure, K., Yasuda, K., and Fukuzawa, K. (2002) *J Biol Chem* **277**, 39436-39442

9. Clair, T., Aoki, J., Koh, E., Bandle, R. W., Nam, S. W., Ptaszynska, M. M., Mills, G. B., Schiffmann, E., Liotta, L. A., and Stracke, M. L. (2003) *Cancer Res* **63**, 5446-5453
10. Gijsbers, R., Aoki, J., Arai, H., and Bollen, M. (2003) *FEBS Lett* **538**, 60-64
11. Contos, J. J., Ishii, I., and Chun, J. (2000) *Mol Pharmacol* **58**, 1188-1196
12. Anliker, B., and Chun, J. (2004) *Semin Cell Dev Biol* **15**, 457-465
13. Tigyi, G., and Parrill, A. L. (2003) *Prog Lipid Res* **42**, 498-526
14. Tigyi, G. (2001) *Prostaglandins Other Lipid Mediat* **64**, 47-62
15. McIntyre, T. M., Pontsler, A. V., Silva, A. R., St Hilaire, A., Xu, Y., Hinshaw, J. C., Zimmerman, G. A., Hama, K., Aoki, J., Arai, H., and Prestwich, G. D. (2003) *Proc Natl Acad Sci U S A* **100**, 131-136
16. Fang, X., Schummer, M., Mao, M., Yu, S., Tabassam, F. H., Swaby, R., Hasegawa, Y., Tanyi, J. L., LaPushin, R., Eder, A., Jaffe, R., Erickson, J., and Mills, G. B. (2002) *Biochim Biophys Acta* **1582**, 257-264
17. Mills, G. B., and Moolenaar, W. H. (2003) *Nat Rev Cancer* **3**, 582-591
18. Kohn, E. C., Hollister, G. H., DiPersio, J. D., Wahl, S., Liotta, L. A., and Schiffmann, E. (1993) *Int J Cancer* **53**, 968-972
19. Debies, M. T., and Welch, D. R. (2001) *J Mammary Gland Biol Neoplasia* **6**, 441-451
20. Yang, S. Y., Lee, J., Park, C. G., Kim, S., Hong, S., Chung, H. C., Min, S. K., Han, J. W., Lee, H. W., and Lee, H. Y. (2002) *Clin Exp Metastasis* **19**, 603-608
21. Stassar, M. J., Devitt, G., Brosius, M., Rinnab, L., Prang, J., Schradin, T., Simon, J., Petersen, S., Kopp-Schneider, A., and Zoller, M. (2001) *Br J Cancer* **85**, 1372-1382
22. Yang, Y., Mou, L., Liu, N., and Tsao, M. S. (1999) *Am J Respir Cell Mol Biol* **21**, 216-222
23. Klominek, J., Robert, K. H., Bergh, J., Hjerpe, A., Gahrton, G., and Sundqvist, K. G. (1998) *Anticancer Res* **18**, 759-767
24. Deissler, H., Blass-Kampmann, S., Bruyneel, E., Mareel, M., and Rajewsky, M. F. (1999) *Faseb J* **13**, 657-666
25. Zhang, G., Zhao, Z., Xu, S., Ni, L., and Wang, X. (1999) *Chin Med J (Engl)* **112**, 330-332
26. Hoelzinger, D. B., Mariani, L., Weis, J., Woyke, T., Berens, T. J., McDonough, W. S., Sloan, A., Coons, S. W., and Berens, M. E. (2005) *Neoplasia* **7**, 7-16
27. Euer, N., Schwirzke, M., Evtimova, V., Burtscher, H., Jarsch, M., Tarin, D., and Weidle, U. H. (2002) *Anticancer Res* **22**, 733-740
28. Sano, T., Baker, D., Virag, T., Wada, A., Yatomi, Y., Kobayashi, T., Igarashi, Y., and Tigyi, G. (2002) *J Biol Chem* **277**, 21197-21206
29. Tokumura, A., Yamano, S., Aono, T., and Fukuzawa, K. (2000) *Ann N Y Acad Sci* **905**, 347-350
30. Okita, M., Gaudette, D. C., Mills, G. B., and Holub, B. J. (1997) *Int J Cancer* **71**, 31-34
31. Croset, M., Brossard, N., Polette, A., and Lagarde, M. (2000) *Biochem J* **345 Pt 1**, 61-67

32. van Meeteren, L. A., Ruurs, P., Christodoulou, E., Goding, J. W., Takakusa, H., Kikuchi, K., Perrakis, A., Nagano, T., and Moolenaar, W. H. (2005) *J Biol Chem* **280**, 21155-21161
33. Murakami-Murofushi, K., Shioda, M., Kaji, K., Yoshida, S., and Murofushi, H. (1992) *J Biol Chem* **267**, 21512-21517
34. Friedman, P., Haimovitz, R., Markman, O., Roberts, M. F., and Shinitzky, M. (1996) *J Biol Chem* **271**, 953-957
35. Kobayashi, T., Tanaka-Ishii, R., Taguchi, R., Ikezawa, H., and Murakami-Murofushi, K. (1999) *Life Sci* **65**, 2185-2191
36. Fischer, D. J., Liliom, K., Guo, Z., Nusser, N., Virag, T., Murakami-Murofushi, K., Kobayashi, S., Erickson, J. R., Sun, G., Miller, D. D., and Tigyi, G. (1998) *Mol Pharmacol* **54**, 979-988
37. Liliom, K., Murakami-Murofushi, K., Kobayashi, S., Murofushi, H., and Tigyi, G. (1996) *Am J Physiol* **270**, C772-777
38. Murakami-Murofushi, K., Kaji, K., Kano, K., Fukuda, M., Shioda, M., and Murofushi, H. (1993) *Cell Struct Funct* **18**, 363-370
39. Mukai, M., Imamura, F., Ayaki, M., Shinkai, K., Iwasaki, T., Murakami-Murofushi, K., Murofushi, H., Kobayashi, S., Yamamoto, T., Nakamura, H., and Akedo, H. (1999) *Int J Cancer* **81**, 918-922
40. Ishihara, R., Tatsuta, M., Iishi, H., Baba, M., Uedo, N., Higashino, K., Mukai, M., Ishiguro, S., Kobayashi, S., and Murakami-Murofushi, K. (2004) *Int J Cancer* **110**, 188-193
41. Murakami-Murofushi, K., Uchiyama, A., Fujiwara, Y., Kobayashi, T., Kobayashi, S., Mukai, M., Murofushi, H., and Tigyi, G. (2002) *Biochim Biophys Acta* **1582**, 1-7
42. Kobayashi, S., Murofushi, H., and Murakami-Murofushi, K. (2004), International Patent
43. Kobayashi, S., Tokunoh, R., Shibasaki, M., Shinagawa, R., and Murakami-Murofushi, K. (1993) *Tetrahedron Letters* **34**, 4047-4050
44. Erukulla, R. K., Byun, H.-S., and Bittman, R. (1994) *Tetrahedron Letters* **35**, 5783-5784
45. Tokumura, A., Kanaya, Y., Kitahara, M., Miyake, M., Yoshioka, Y., and Fukuzawa, K. (2002) *J Lipid Res* **43**, 307-315
46. Fischer, D. J., Nusser, N., Virag, T., Yokoyama, K., Wang, D., Baker, D. L., Bautista, D., Parrill, A. L., and Tigyi, G. (2001) *Mol Pharmacol* **60**, 776-784
47. Ohta, H., Sato, K., Murata, N., Damirin, A., Malchinkhuu, E., Kon, J., Kimura, T., Tobo, M., Yamazaki, Y., Watanabe, T., Yagi, M., Sato, M., Suzuki, R., Murooka, H., Sakai, T., Nishitoba, T., Im, D. S., Nochi, H., Tamoto, K., Tomura, H., and Okajima, F. (2003) *Mol Pharmacol* **64**, 994-1005
48. Virag, T., Elrod, D. B., Liliom, K., Sardar, V. M., Parrill, A. L., Yokoyama, K., Durgam, G., Deng, W., Miller, D. D., and Tigyi, G. (2003) *Mol Pharmacol* **63**, 1032-1042
49. Durgam, G. G., Virag, T., Walker, M. D., Tsukahara, R., Yasuda, S., Liliom, K., van Meeteren, L. A., Moolenaar, W. H., Wilke, N., Siess, W., Tigyi, G., and Miller, D. D. (2005) *J Med Chem* **48**, 4919-4930
50. Noguchi, K., Ishii, S., and Shimizu, T. (2003) *J Biol Chem* **278**, 25600-25606

51. Fujiwara, Y., Sardar, V., Tokumura, A., Baker, D. L., Murakami-Murofushi, K., Parrill, A. L., and Tigyi, G. (2005) *J Biol Chem*
52. Qian, F., Zhang, Z. C., Wu, X. F., Li, Y. P., and Xu, Q. (2005) *Biochem Biophys Res Commun* **333**, 1269-1275
53. Yamaguchi, H., Kitayama, J., Takuwa, N., Arikawa, K., Inoki, I., Takehara, K., Nagawa, H., and Takuwa, Y. (2003) *Biochem J* **374**, 715-722
54. Mukai, M., Nakamura, H., Tatsuta, M., Iwasaki, T., Togawa, A., Imamura, F., and Akedo, H. (2000) *FEBS Lett* **484**, 69-73

‡ABBREVIATIONS

ATX, autotaxin; cPA, 1-acyl-*sn*-glycero-2,3-cyclic-phosphate; 2ccPA, 2-carba-cyclic phosphatidic acid, 3ccPA 3-carba-cyclic phosphatidic acid; GPCR, G protein-coupled receptor; LPA, 1-acyl-2-hydroxy-*sn*-glycero-3-phosphate; LPA_1, LPA receptor type 1 (EDG2); LPA_2, LPA receptor type 2 (EDG4); LPA_3, LPA receptor type 3 (EDG7); LPA_4, LPA receptor type 4 (P2Y9).

FIGURE LEGENDS

Figure 1 Structures of the cPA analogs tested.

Figure 2 Inhibition of ATX-mediated hydrolysis of BPNPP by cPA analogs. Conditioned media from HEK293 cells transiently transfected with an ATX-HIS^6 construct was incubated with 1 mM BPNPP in presence of increasing amounts of individual cPA analogs complexed in a 1:1 molar ratio with BSA. Data were normalized to the appropriate BSA control and are reported as percent ATX inhibition.

Figure 3 Inhibition of ATX-mediated LPA production by cPA analogs. Purified, recombinant ATX-HA (1:100 dilution) was incubated with 2.5 μM ADMAN-LPC, a synthetic, fluorescent LPC analog (upper panel) in the absence or presence of 1 μM individual cPA analogs for 4 h. Lipids were extracted using a modified Bligh-Dyer protocol, separated by TLC (chloroform/ methanol/ ammonium hydroxide, 65:30:8 v/v/v), and visualized by UV transillumination.

Figure 4 Inhibition of cell invasion by cPA analogs. Optimization of *in vitro* invasion assay conditions (A). The invasive potential of A2058 melanoma cells was determined using a modified Boyden chamber assay. The effect of varying amounts of purified, recombinant ATX-HA (100 or 300 fold dilution), LPC 18:1 (0 or 1 μM) and 3ccPA (0 and 3 μM) was assessed. Data are means of duplicate wells. Optimized conditions were used to assess the inhibition of individual cPA analogs on melanoma cell invasion (B). The data are means ± standard deviations of triplicate wells and are representative of 3 separate experiments (* $p < 0.01$).

Figure 5 Inhibition of melanoma cell metastasis *in vivo*. B16F10 melanoma cells (5×10^5) were injected in the tail vein of C57BL/6 mice, followed by i.p. injections of PBS (vehicle control) or 3ccPA 16:1 or 3ccPA 18:1 (250 μg/kg, 5 μg per dose) 15 min and 48 h after inoculation. Animals were sacrificed 3 weeks later and lungs were washed, fixed in formalin, and lung nodules were counted. The data are means ± standard deviations from groups of 6 (PBS) or 5 (3ccPA 16:1 and 3ccPA 18:1) animals (* $p < 0.01$ ANOVA).

Table 1 Summary of pharmacological evaluation of cPA analogs in RH7777 cells stably expressing individual LPA GPCR.

Compound	EC_{50} [μM] (Efficacy)§			
	LPA_1	LPA_2	LPA_3	LPA_4
LPA 18:1	0.20 ± 0.068 (100%)	0.007 ± 0.001 (100%)	0.26 ± 0.023 (100%)	0.50 ± 0.027 (100%)
cPA 16:1	NS¶ (99%)	0.18 ± 0.04 (121%)	NS (19%)	NS (70%)
2ccPA 16:1	NS (34%)	NA‖	0.17 ± 0.10 (24%)	NA
3ccPA 16:1	NA	NS (95%)	NA	NA
cPA 18:1	1.7 ± 0.23 (66%)	0.085 ± 0.011 (140%)	1.0 ± 0.62 (61%)	NS (100%)
2ccPA 18:1	1.7 ± 0.89 (54%)	NS (68%)	0.17 ± 0.073 (46%)	NS (90%)
3ccPA 18:1	NA	NS (35%)	NA	NA

§ Normalized to the maximum LPA 18:1 effect

¶ Nonsaturable activation up to the highest concentration tested (10 μM for $LPA_{1/3/4}$ and 3 μM for LPA_2)

‖ No activation up to the highest concentration tested (10 μM for $LPA_{1/3/4}$ and 3 μM for LPA_2)

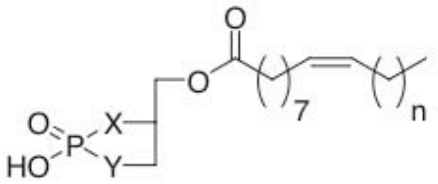

cPA 16:1	n=5	X=O	Y=O
2ccPA 16:1	n=5	X=CH_2	Y=O
3ccPA	n=5	X=O	Y=CH_2
cPA 18:1	n=7	X=O	Y=O
2ccPA 18:1	n=7	X=CH_2	Y=O
3ccPA 18:1	n=7	X=O	Y=CH_2

Baker et al. Figure 1.

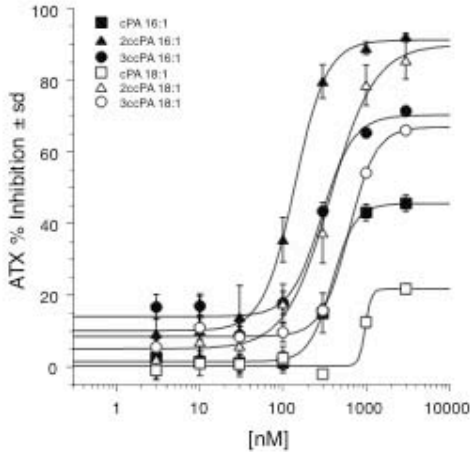

Baker et al. Figure 2.

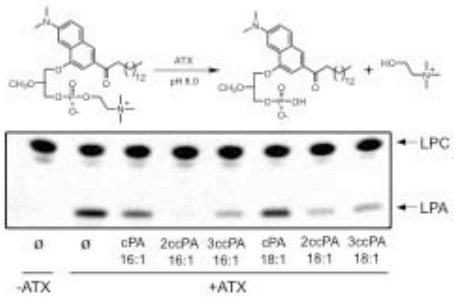

Baker et al. Figure 3

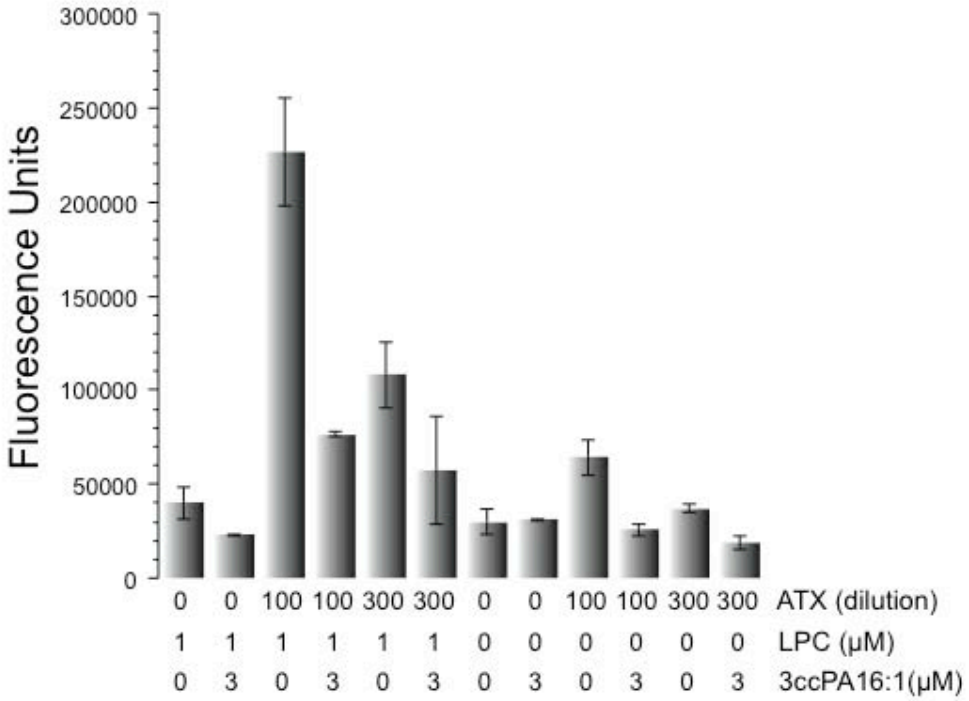

Baker et al. Figure 4A.

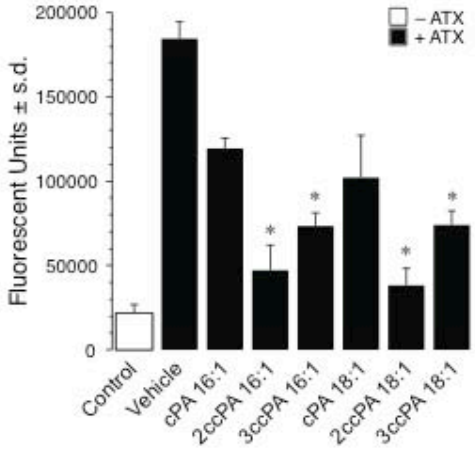

Baker et al. Figure 4B

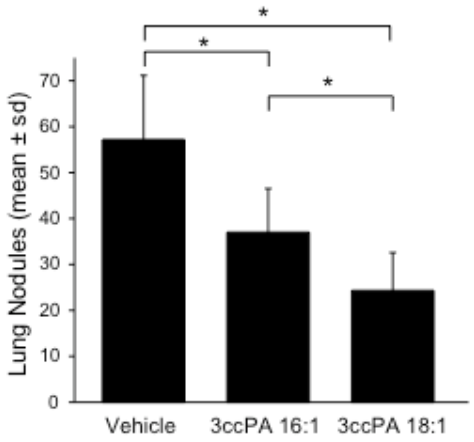

Baker et al. Figure 5.